ZooKeys 825: 1–24 (2019)
doi: 10.3897/zookeys.825.32271
http://zookeys.pensoft.net

RESEARCH ARTICLE

A peer-reviewed open-access journal
ZooKeys
Launched to accelerate biodiversity research

Three new species and a new genus of majoid crabs from the eastern Pacific (Decapoda, Brachyura)

Jessica Colavite[1,2], Amanda Windsor[3], William Santana[1,2]

1 *Universidade do Sagrado Coração, Pró-Reitoria de Pesquisa e Pós-Graduação, Laboratório de Sistemática Zoológica, 10-50, Irmã Arminda st., Jd. Brasil, Bauru, SP 17011-160, Brazil* **2** *Departamento de Zoologia, Instituto de Biociências, Universidade do Estado de São Paulo (UNESP), Botucatu, SP 18618-970, Brazil* **3** *Department of Invertebrate Zoology, National Museum of Natural History, Smithsonian Institution, Museum Support Center, 4210 Silver Hill Road, Suitland, MD 20746-2863, USA*

Corresponding author: *William Santana* (willsantana@gmail.com)

Academic editor: *S. De Grave* | Received 8 December 2018 | Accepted 18 January 2019 | Published 18 February 2019

http://zoobank.org/38503135-C971-4A5A-99FB-E9CB8814AF1D

Citation: Colavite J, Windsor A, Santana W (2019) Three new species and a new genus of majoid crabs from the eastern Pacific (Decapoda, Brachyura). ZooKeys 825: 1–24. https://doi.org/10.3897/zookeys.825.32271

Abstract

Three new species and a new genus of majoid crabs from deep waters in the eastern Pacific are described and illustrated using morphological and molecular data. A new species of inachoidid, *Collodes anartius* **sp. n.** is described from Peru, which resembles *C. tenuirostris* Rathbun, 1893, in the general appearance of the carapace, but is distinguished by the details of tubercles on the carapace and thoracic sternum, proportions of the pereopod articles, and bathymetric distribution. A new epialtid, *Nibilia machala* **sp. n.**, is described from Ecuador; *Nibilia* A Milne-Edwards, 1878 has, until now, been considered to be monotypic, occurring only in the western Atlantic. This new species, from the eastern Pacific, closely resembles *N. antilocapra* (Stimpson, 1871) in the general morphology, but can be distinguished by the number of spines on the carapace and pereopods. Another epialtid, *Solinca aulix* **gen. n. et sp. n**, is establish for material collected from Ecuador and Peru, and can be easily identified from other taxa by the presence of a deep furrow between the very inflated branchial regions.

Keywords

Biodiversity, Epialtidae, Inachoididae, Pisinae, spider crab

Copyright *Jessica Colavite et al.* This is an open access article distributed under the terms of the Creative Commons Attribution License (CC BY 4.0), which permits unrestricted use, distribution, and reproduction in any medium, provided the original author and source are credited.

Introduction

The Southeast Pacific Biological Oceanographic Project (SEPBOP) comprised several cruises of the R/V Anton Bruun, between October 1965 and September 1966 (Child 1992; Garth and Haig 1971). Examination of unidentified majoids from this expedition in the National Museum of Natural History, Smithsonian Institution (USNM) Crustacea Collection revealed the existence of three new species and a new genus of spider crabs from southeast Pacific Ocean. Material from this cruise were found to be viable for DNA sequencing so, in addition to morphological analyses, we constructed a multi-locus molecular phylogeny of these three new taxa to place them within the context of other members of their respective genera and within the superfamily Majoidea.

The amphi-American inachoididae *Collodes* Stimpson, 1860, currently comprises 15 species, four of which are known from the eastern Pacific, inhabiting waters up to 700 m deep (Santana and Tavares 2017). The new species, *Collodes anartius* sp. n., is described from the northwest of Peru, based on 118 specimens.

The second new species described herein belongs to the epialtid *Nibilia* A Milne-Edwards, 1878. *Nibilia machala* sp. n. is described from a single female collected in waters off Machala, Ecuador. Until now, *Nibilia antilocapra* (Stimpson, 1871) was considered to be the only species of the genus, which is found in waters between 71–342 m on muddy and sandy bottoms with broken shells, corals, and rocks in the western Atlantic (Melo 1996, Hernández-Ávila et al. 2008, Carmona-Suárez and Poupin 2016).

A new genus, *Solinca* gen. n. established for *Solinca aulix* gen. n. et sp. n. is based on morphological analysis of 28 specimens from three different localities between Ecuador and Peru. *Solinca aulix* gen. n. et sp. n. is phylogenetically allied to Epialtidae crabs *Scyra acutifrons* Dana, 1851, *Pugettia nipponensis* Rathbun, 1932, *Pugettia quadridens* (De Haan, 1839) and *Chorilia longipes* Dana, 1851. *Solinca aulix* gen. n. et sp. n. shares the distinct, sculpted chelipeds with these allied species. *Solinca aulix* gen. n. et sp. n., nevertheless, can be easily distinguished by a unique set of characters.

Materials and methods

Holotype and paratype specimens were deposited in the National Museum of Natural History, Smithsonian Institution, Washington, DC, USA (**USNM**). Additional paratype specimens of *Collodes anartius* sp. n. and *Solinca aulix* gen. n. et sp. n. are deposited in the Museum of Zoology at the University of São Paulo (**MZUSP**). Comparative material for both morphological and molecular assessments was obtained from the University of Louisiana at Lafayette Zoological Collection (**ULLZ**), Museu de Oceanografia Prof. Petrônio Alves Coelho (**MOUFPE**), MZUSP, and USNM. The terminology used follows Davie et al. (2015). Abbreviations used:

cl carapace length, taken along the dorsal midline from the base of the rostral sinus to the posterior margin of the carapace;

cw carapace maximum width, taken at the level of its widest point, branchiostegal spines excluded;
G1 first gonopod or male pleopod 1;
G2 second gonopod or male pleopod 2;
P2–P5 pereopods 2 to 5 (P1 is the cheliped).
R/V research vessel.

DNA extraction, PCR, and sequencing

Total genomic DNA was extracted from muscle tissue using either the Qiagen DNeasy Blood and Tissue extraction kit or an Omega Bio-tek EZNA Tissue DNA Kit. Partial sequences of the 12S, 16S, and barcode region of COI mitochondrial genes were amplified with the following primers respectively: 12SF (Mokady et al. 1994) and 12S1R (Shull et al. 2005), 16SF/16SR (Hultgren and Stachowicz 2008), and LCO1490/HCO2198 (Folmer et al. 1994). The nuclear loci histone-H3 (H3AF/H3AR, Colgan et al. 1998) and the small subunit 18S rRNA (A/L, C/Y, O/B of Medlin et al. 1988, Apakupakul et al. 1999, or B/D18s1R, D18s2FD18s2R, D18s3F-D18s3R, D18s4F-D18s4R and D18s5F-A of Bracken et al. 2009) were also sequenced from supporting majoid taxa. Annealing temperatures for PCRs were 58 °C, 54 °C, and 48 °C for 12S/18S, 16S/H3, and COI, respectively. Reagent volumes and concentrations followed manufacturer instructions; primer concentrations were 10 μM. Sequencing reactions were performed using 1 μL of purified PCR product in a 10 μL reaction containing 0.5 μL primer, 1.75 μL Big Dye buffer and 0.5 μL BigDye (Life Technologies). Reactions were purified using Millipore Sephadex plates (MAHVN–4550) according to the manufacturer's instructions and sequenced on the ABI 3730XL automated DNA sequencer. Sequences were assembled, trimmed of primers, and checked for quality using Geneious 9.1.8.

Molecular data analysis

Sequences generated for this study were combined with those from Windsor and Felder (2014, 2017), other sequences available from GenBank, and previously unpublished sequences generated by A Windsor in order to place the new taxa, particularly *Solinca aulix* gen. n. et sp. n, within the context of Majoidea. Locality information and GenBank accession numbers for taxa included in the molecular analyses are provided in Suppl. material 1: Table S1.

Multiple sequence alignment was performed using the MAFFT FFT-NS-I (Katoh et al. 2005) alignment algorithm for the individual molecular markers. The individual datasets were concatenated in SequenceMatrix (Vaidya et al. 2011) and the perl script PartitionFinder (Lanfear et al. 2017) was run to determine the appropriate model of evolution and partitioning scheme. Phylogenetic trees were constructed using maximum likelihood in RAxML 7.0.4 (Stamatakis 2006) and Bayesian inference (BI) in

MrBayes (v3.2.1) (Huelsenbeck and Ronquist 2001). In RAxML, we used the '-f ae' option with 1000 bootstrap replicates. Likelihood parameters followed the General Time Reversible (GTR) model with a gamma distribution on the partitioned dataset and RAxML estimated all free parameters. The resulting best tree was used to reflect phylogeny (Fig. 1). Bayesian inference was performed with 10,000,000 generations with a 25% burn-in and sampling every 1000 generations. A mixed model was applied to the partitioned dataset. A 50% majority-rule consensus tree was constructed from the post-burn-in trees. DNA extraction and sequencing for *Collodes anartius* sp. n., *Nibilia machala* sp. n. and *Solinca aulix* gen. n. et sp. n. was carried out at the Smithsonian Institution's Laboratories of Analytical Biology, and phylogenetic trees were generated on the Smithsonian Institution High Performance Computing Cluster (SI/HPC).

Results

All three mitochondrial loci (12S, 16S, COI) were successfully amplified and sequenced for the three new species. Nodes where maximum likelihood bootstrap support and Bayesian posterior probabilities greater than 50/0.5 are shown on the maximum likelihood phylogram (Fig. 1). *Nibilia machala* is supported (100/1) as sister to *N. antilocapra* and *Nibilia* is sister to *Herbstia condyliata* (Fabricius, 1787) with high support (93/1). However, their position within a clade comprised of Atlantic members of Pisinae sensu Ng et al. (2008) is unresolved. *Solinca aulix* is highly supported (100/1) as sister to *Scyra acutifrons* within a well-supported subclade containing *Pugettia* spp. and *Chorilia*. Both *Nibilia* and *Solinca* are nested within Epialtidae sensu Ng et al. (2008). *Collodes anartius* is represented here by five individuals that are highly supported (100/1) as sister to *C. robustus* (97/1). Interestingly, *C. anartius* is more closely allied to Gulf of Mexico/western Atlantic Ocean species than to *C. tenuirostris,* which it closely resembles.

Systematics

Superfamily Majoidea Samouelle, 1819
Family Inachoididae Dana, 1851

Collodes Stimpson, 1860

Collodes Stimpson, 1860: 193, pl. II, fig. 4. [Type species: *Collodes granosus* Stimpson, 1860, by original designation and monotypy].

Included species. *Collodes anartius* sp. n.; *Collodes armatus* Rathbun, 1898; *C. gibbosus* (Bell, 1835) (formerly in *Mycrorhynchus*); *C. granosus* Stimpson, 1860; *C. inermis* A Milne-Edwards, 1878; *C. leptocheles* Rathbun, 1894; *C. levis* Rathbun, 1901; *C. nudus* Stimpson, 1871; *C. obesus* A Milne-Edwards, 1878; *C. robsonae* Garth, 1958;

Figure 1. Molecular phylogenetic tree represented as maximum likelihood topology of three mitochondrial and two nuclear genes (12S, 16S, COI, 18S, H3) to place *Collodes anartius* sp. n., *Nibilia machala* sp. n. and *Solinca aulix* gen. n. et sp. n. within the context of Majoidea based on 32 genera. Node support values are shown with maximum likelihood bootstrap support above line and Bayesian posterior probabilities below line.

C. robustus Smith, 1883; *C. rostratus* A Milne-Edwards, 1878; *C. tenuirostris* Rathbun, 1893; *C. trispinosus* Stimpson, 1871 (= *Collodes depressus* A Milne-Edwards, 1878 junior subjective synonym); *C. tumidus* Rathbun, 1898; *C. tuerkayi* Santana & Tavares, 2017.

***Collodes anartius* sp. n.**
http://zoobank.org/DE0C558B-A35A-4E21-903F-35B83C026485
Figures 2A, C, E, F; 3A, C; 4A, C, E, 7A, B

Holotype. Peru, off Paita, Piura, Southeast Pacific Biological Oceanographic Project (SEPBOP), R/V Anton Bruun, cruise 16, stn 625–A, 04°57' / 05°01'S; 81°23'W, 02.vi.1966, Smithsonian Oceanographic Sorting Center coll., 118–133 m, male, cl 27 mm, cw 23.5 mm (USNM 1462817).

Paratypes. Peru, off Paita, Piura Southeast Pacific Biological Oceanographic Project (SEPBOP), R/V Anton Bruun, cruise 16, stn 625–A, 04°57' / 05°01'S; 81°23'W, 02.vi.1966, Smithsonian Oceanographic Sorting Center coll., 118–133 m, 49 males, 7 females (USNM 1462747). Idem, 1 male (MZUSP 38889) 1 female (MZUSP 38890). Southeast Pacific Biological Oceanographic Project (SEPBOP), R/V Anton Bruun, cruise 16, stn 626–B, 05°07' / 04°59'S; 81°27'W, 03.vi.1966, Smithsonian Oceanographic Sorting Center coll., 365–457 m, male, cl 28.47 mm, cw 24.0 mm, 1 female, cl 24.0 mm, cw 19.2 mm, illustrated (USNM 1462821). Idem, 16 males, 2 juvenile females, 2 females, 32 ovigerous females (USNM 1462818). Southeast Pacific Biological Oceanographic Project (SEPBOP), R/V Anton Bruun, cruise 6, stn 627–A, 05°01'/ 04°59'S; 81°25'W/ 81°25'W, 03.vi.1966, Smithsonian Oceanographic Sorting Center coll., 200–311 m, 4 males, 1 female (USNM 1462676).

Comparative material. *Collodes tenuirostris*. Mexico, Sonora, Puerto Lobos, R/V Albatross, stn 3018, 30°16'00"N; 133°05'00"W, 24.iii.1889, USFC coll., MJ Rathbun det., 66 m, male holotype, 1 male paratype (USNM 17333). Costa Rica, off Playa Flamingo, R/V Urraca, stn CR–23, 15.vii.2005, R Collin coll., 1 male, DNA only (ULLZ 8235). Gulf of Nicoya, vii.1979, 9°48.27'N; 85°08.43'W, 25 m, 2 ovigerous females (USNM 1462759). Panama, Gulf of Panama, R/V Shimada, stn 63, 08° 11'N; 79°36'W, 13.iv.1967, A Windsor det., 4 ovigerous female (USNM 1479280). Ecuador, Manabi, off Cape San Lorenzo, Southeast Pacific Biological Oceanographic Project (SEPBOP), R/V Anton Bruun, cruise 18B, stn 775, 01°05'S; 80°98'W, 12.ix.1966, Smithsonian Oceanographic Sorting Center coll., 185 m, 1 juvenile male (USNM 1155058). Peru, west of Paita, Piura, Southeast Pacific Biological Oceanographic Project (SEPBOP), R/V Anton Bruun, cruise 16, stn 624–E, 04°51' / 04°57'S; 81°20' / 81°23'W, 02.vi.1966, Smithsonian Oceanographic Sorting Center coll., 79–91 m, 4 males, 5 ovigerous female, 1 juvenile female (USNM 1462819). West of Paita, Piura, Southeast Pacific Biological Oceanographic Project (SEPBOP), R/V Anton Bruun, cruise 16, stn 625–A, 04°57' / 05°01'S; 81°23'W, 02.vi.1966, 118–133 m, 1 ovigerous female, DNA only (USNM 1479343).

Collodes gibbosus. Costa Rica, off Playa Flamingo, R/V Urraca, stn CR–18, 15.vii.2005, R Collin coll., 15.5 m, 1 male, DNA only (ULLZ 8229). Ecuador,

Salango Bay, Salango Island, R/V Velero III, Allan Hancock Pacific Expedition, stn 396–35, 18.i.1935, J Garth det., 22 m., neotype, female (USNM 100921).

Collodes granosus. Mexico, Baja California, San Lucas Bay, Cabo San Lucas, R/V Albatross, stn 5681, 23.iii.1911, MJ Rathbun det., 24 m, 1 ovigerous female (USNM 55766). Panama, Panama Bay, R/V Urraca, 24.ii.2007, DL Felder coll., 20–30 m, 1 male, DNA only (ULLZ 9760).

Collodes robsonae. Costa Rica, Gulf of Nicoya, 16.ii.1980, Dean & Howe coll., 70 m, 1 ovigerous female (USNM 1462812).

Collodes tumidus. Mexico, Baja California, Magdalena Bay, R/V Albatross, stn 2831, 24°32'00"N; 111°59'00"W, 02.v.1888, MJ Rathbun det., 22 m, holotype, male (USNM 21571).

Type-locality. Peru, west of Paita, Piura, 04°57'S to 05°07'S; 81°23'W to 81°27'W, 118–133 m.

Diagnosis. Carapace pyriform, granulose, particularly on cardiac, branchial and intestinal regions. Second antennal article ventrolateral surface with strong, unarmed longitudinal keel. Third maxillipeds granulated; ischium and carpus with dense granulation, propodus smooth. First pleonal segment with a short spine or distinctly strong tubercle with several small tubercles around. P2–P5 dactylus smooth ventrally; dactylus of P5 longer than propodus; carpus of P5 more than half of merus.

Description. Carapace pyriform, longer than wide; dorsal surface covered by tubercles of different sizes (more prominent in females), particularly on cardiac, branchial and intestinal regions; gastric and branchial regions covered with hooked setae. Gastric, branchial, cardiac, intestinal regions with small tubercles. Gastric, hepatic, branchial, cardiac, intestinal regions clearly delimited laterally by grooves. Metagastric region with mesial prominent tubercle; gastric region with few small tubercles; mesocardiac region with four tubercles in line longitudinally, distal tubercles more prominent. Groove between cardiac and intestinal region smooth or with a few small tubercles in males and females. Hepatic, branchial, intestinal regions densely covered with sub-equal tubercles. Metabranchial region slightly depressed. Thoracic pleurites V–VIII gymnopleura not fused to one another, usually densely covered with small hooked setae.

Rostrum simple, short, slightly curved upwards. Supraorbital spine absent; orbital margin unarmed dorsally. Postorbital spine longer than the ocular peduncle, directed laterally and upwards around eyes. Antennular fossae longitudinally ovate; anteroventral margin unarmed. Interantennular septum longer than epistomial spine, compressed laterally, forming ventrally-directed keel. Antenna (flagellum included) distinctly exceeding rostral length. First and second antennal articles fused to epistome. Second article protruding anterolaterally; ventrolateral surface with strong longitudinal keel, unarmed; ventrolateral margin dentate, teeth acute. Third antennal article massive; fourth longest, cylindrical; fifth article smaller.

Epistome markedly wider than long. Epistomial spine separated by small gap from interantennular septum. Mouthfield sub-rectangular. Pterygostomial region subtriangular, smooth near mouth frame, densely tuberculated laterally, tubercles sub-equal. Sub-hepatic region strongly swollen, delimited from pterygostome by distinct slope, densely covered with sub-equal tubercles, several long setae.

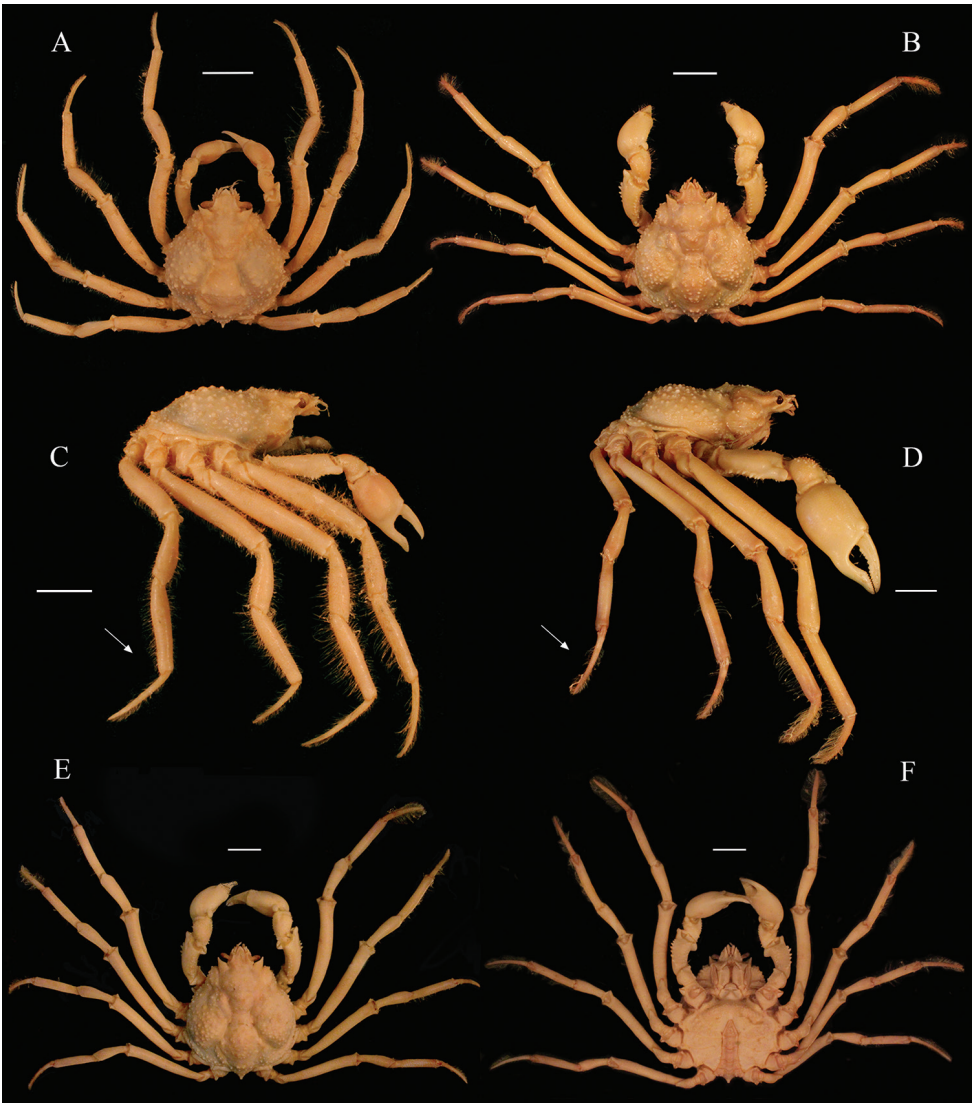

Figure 2. *Collodes anartius* sp. n., male paratype, cl 28.4 mm, cw 24.0 mm (USNM 142821) (**A, C**); male holotype, cl 27.0 mm, cw 23.5 mm (USNM 1462817) (**E, F**). *Collodes tenuirostris* Rathbun, 1893, male, cl 36.2 mm, cw 29.5 mm (USNM 1462819) (**B, D**). Habitus, dorsal view (**A, B, E**). Lateral view (**C, D**). Ventral view (**F**). Note the proportions of the dactylus and propodus of P5 in both species (white arrows) (**C, D**). Scale bars: 10 mm.

Third maxillipeds almost completely covering buccal frame, ischia leaving distinct gap. Exopod long, nearly reaching distal margin of merus; granulated; lateral margin with strong lobe in proximal third. Ischium distinctly longer than broad, dorsal face with longitudinal, smooth, deep groove; with granules; mesial margin slightly convex; crista dentata with small, rounded, irregularly sized teeth. Merus slightly longer than

half of ischium, granulated. Anterior margin deeply incised, anterolateral and anteromedial margins expanded, mesial margin with a row of setae. Palp cylindrical, slightly overreaching ischiomeral suture. Carpus granulated; propodus and dactylus smooth, fringed with row of long setae.

Thoracic sternites II–IV broadly triangular in males, with sparse hooked setae, small tubercles medially. Anterior half of sternites I–IV strongly sloping down laterally, forming prominent triangle medially; fourth sternite densely tuberculated, with smaller projection ventrally directed in males. Male sternites IV–VII covered with distinct, large tubercles, outside sterno-pleonal cavity; smooth in females.

Male and female chelipeds sub-cylindrical, homochelous, robust in males, slender in females. Dactylus (movable) and fixed finger approximately same length as palm in males and females, covered with sparse setae. Males with finger cutting edges with small teeth, sub-equal in distal half, leaving distinct proximal depressed gap in sub-proximal edge of dactylus. Distal two-thirds of finger cutting edges with sub-equal teeth in females. Male propodus conspicuously inflated, with sparse setae, small tubercles in dorsal margin, fewer tubercles in ventral margin. Propodus slender, smooth in females. Carpus setose, with several tubercles dorsally, unarmed in females. Merus with two rows of small tubercles in dorsal and mesoventral faces, row of strong tubercles in lateral face, with long setae. Ischium sparsely tuberculate, setose. P2–5 similar in shape, slender, cylindrical; P2 longest, P3–P5 progressively decreasing in length. Dactylus of P3–P5 longer than propodus, without tubercles, carpus more than half of merus. Dactylus, propodus, carpus, merus densely setose, covered with long setae interspersed with hooked setae.

Male pleonal somites I–V free, sixth fused to telson. Pleotelson sub-triangular, rounded distally. Female pleonal somites I–IV free, somites V, VI, telson fused; pleotelson markedly arched, transversally oval. Male and female first pleonal somite with short spine or strong tubercle with several tubercles surrounding. Male somite I densely tubercular; somite VI-telson with scattered tubercles in the anterior margin. Female somites II–IV tubercular laterally; somites V–VI, telson evenly, densely tubercular in mesolateral region.

Distribution. Northwest of Peru, from 04°57'S to 05°01'S; 81°23'W, 118 to 457 m.

Etymology. The specific epithet is derived from the Greek adjective *anartius* for "uneven", alluding to the rough similarity between the new species and *C. tenuirostris* and contours of the carapace.

Remarks. Although the phylogenetic analyses of seven of the 15 described species of *Collodes* pointed to *C. robustus*, a western Atlantic species, as the sister species of *C. anartius* they are very distinct morphologically, with characters that clearly differentiate both species. For instance, (i) dorsal surface covered by tubercles of different sizes (more prominent on females) in *C. anartius* (vs. carapace evenly covered by small, similar in size tubercles in males and females of *C. robustus*); (ii) sternites V–VII with few, distinct, large tubercles in *C. anartius* (vs. sternites IV–VII with numerous, small, evenly distributed tubercles in *C. robustus*).

Collodes anartius superficially resembles *C. tenuirostris* Rathbun, 1893, in the general morphology with respect to size and distribution of carapace tubercles, the postor-

Figure 3. *Collodes anartius* sp. n., male paratype, cl 28.4 mm, cw 24.0 mm (USNM 142821) (**A**); Female paratype, cl 24.0 mm, cw 19.2 mm (USNM 142821) (**C**). *Collodes tenuirostris* Rathbun, 1893, male, cl 36.2 mm, cw 29.5 mm (USNM 1462819) (**B**); Female, cl 25.25 mm, cw 20.51 mm (USNM 1462819) (**D**). Ventral view (**A–D**). Scale bars: 10 mm.

bital spines are also very similar in both species (Fig. 2A, B). Because they inhabit the same substrates, mud bottoms, and have the habit of completely camouflaging in the sediment, these species are difficult to separate. The bathymetric range was nevertheless different for both species in the Peruvian coast, wherein *C. anartius* can be found in deeper regions (118–457 m) than *C. tenuirostris* (25–133 m) (vide material examined).

Morphological characters that can distinguish *C. anartius* from *C. tenuirostris*, are: (i) third maxillipeds granulated; ischium and carpus with dense granulation, propodus smooth (in *C. anartius*) (vs. third maxilliped ischium and carpus sparsely granulate; propods granulate in *C. tenuirostris*) (Fig. 2A, B); (ii) first pleonal segment with a short spine or strong tubercle with several small tubercles around in *C. anartius* (vs. pleonal spine usually longer, with very few small tubercles around it in *C. tenuirostris*) (Fig. 2C, D); (iii) in males of *C. anartius* the fourth sternite has a small projection ventrally directed (vs. inflated projection in the fourth sternite in *C. tenuirostris*) (Figs 3A, B; 4A–D); (iv) all segments of female pleon of *C. anartius* are narrower, with fewer tubercles than in *C. tenuirostris* (Fig. 4E, F); (v) cutting edges of male cheliped fingers with small, sub-equal teeth in distal half and a distinct depressed gap distally in *C. anartius* (vs. well defined teeth in the cutting edges of fingers up to the distal gap in *C. tenuirostris*) (Fig. 2A, B); (vi) P2–P5 dactylus smooth ventrally in *C. anartius* (vs. P2–P5 dactylus with very small spines ventrally in *C. tenuirostris*, sometimes the spines

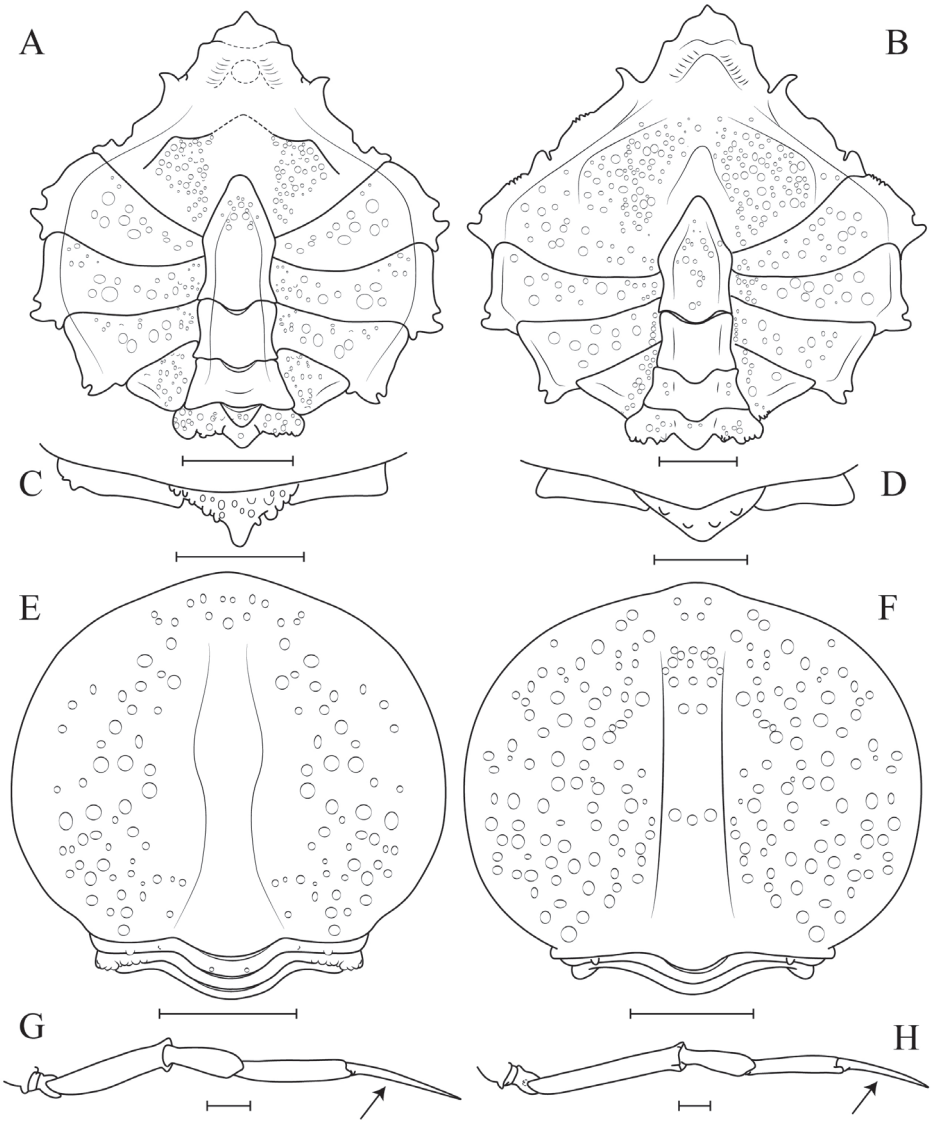

Figure 4. *Collodes anartius* sp. n., male paratype, cl 28.4, cw 24.0 (USNM 1462821) (**A, C, G**); Female paratype, cl 24.0 mm, cw 19.2 mm (USNM 1462821) (**E**). *Collodes tenuirostris* Rathbun, 1893, male, cl 36.2 mm, cw 29.5 mm (USNM 1462819) (**B, D, H**); Female, cl 25.2 mm, cw 20.5 mm (USNM 1462819) (**F**). Cephalothorax ventral view (**A, B, E, F**); Ventral view of the first pleonal somite (**C, D**); Lateral view of the pereiopod 5 (P5) (**G, H**). Note the proportions of the dactylus of P5: longer than the propodus in *Collodes anartius* sp. n. (black arrow) (**G, H**). Scale bar: 5 mm.

are worn) (Fig. 2C, D); (vii) dactylus of P5 longer than propodus (vs. P5 dactylus and propodus of same size or dactylus smaller than propodus in *C. tenuirostris*) (Figs 2C, D; 4G, H); (xi) carpus of P5 more than half of merus in *C. anartius* (vs. carpus of half or less of the size of merus in *C. tenuirostris*) (Figs 2C, D; 4G, H).

Family Epialtidae MacLeay, 1838
Subfamily Pisinae Dana, 1851

***Nibilia* A Milne-Edwards, 1878**

Nibilia A Milne-Edwards, 1878: 132, pl. 25. [Type taxon: *Nibilia erinacea* A Milne-Edwards, 1878 accepted as *Nibilia antilocapra* (Stimpson, 1871) by monotypy].

Included species. *Nibilia antilocapra* (Stimpson, 1871) (= *Pisa praelonga* Stimpson, 1871; = *Nibilia erinacea* A Milne-Edwards, 1878 subjective junior synonyms); *Nibilia machala* sp. n.

Emended diagnosis. Carapace densely covered with several long and short spines and acute tubercles. Rostrum bifurcated, proximally contiguous, becoming moderately divergent distally. Preorbital angles prolonged into long spines; postorbital margin cup-shaped, with small medial spine on anterior margin protecting eyes when retracted. Fissure between antennal basal article and postorbital margin closed. Basal article of antenna elongated with two strong spines in outer margin. Exopod of third maxilliped with small process in dorsal face extending into posterolateral margin of merus; ventral margin with strong spine in distal third; ischium dorsal face with longitudinal, smooth, deep "L" shaped groove. G1 with three well-developed lobes.

***Nibilia machala* sp. n.**
http://zoobank.org/D19B3071-E66E-4194-B2C4-B90859EE165F
Figure 5A, C, E

Holotype. Ecuador, off Machala, near Isla Santa Clara, Southeast Pacific Biological Oceanographic Project (SEPBOP), R/V Anton Bruun, Cruise 18B, stn 771, 03°15'S; 80°50'W, 10.ix.1966, Smithsonian Oceanographic Sorting Center coll., 77–80 m, juvenile female, cl 58.4 mm, cw 35.00 mm (USNM 1462701).

Comparative material. *Nibilia antilocapra.* United States of America, North Carolina, R/V Oregon II, stn 10695, 35°22'N; 74°57'W, 26.vii.1969, HB Roberts det., 104 m, 1 ovigerous female (USNM 1256400). Louisiana, Gulf of Mexico, R/V Pelican, stn NSF–RHODOLITH–28, 27°58.925'N; 91°39.831'W, 6.v.2018, 72 m, 1 juvenile (USNM 1479292). Florida, Tortugas, southeast from n° 2 red buoy, 17.vi.1932, MJ Rathbun det., 1 male (USNM 72957). Mexico, Gulf of Mexico, Suez and Campeche, R/V Oregon, stn 406, 22°14'N; 91°26'W, 16.viii.1951, FA Chace det., 1 female (USNM 92648). Gulf of Mexico, R/V Pelican, stn 10, 4.ii.1938, W Anderson; M Lindner coll., 1 female (USNM 1236185). Southwest Gulf of Mexico, R/V Pelican, stn NFS–11–034, 9.vi.2005, DL Felder coll., 94–93 m, 1 female, DNA only (ULLZ 7365). Nicaragua, R/V Oregon, stn 6426, 12°56'N; 82°21'W, 05.ii.1967, DJ Griffin det., 190 m, 1 female juvenile (USNM 1256401). Venezuela, R/V Oregon, stn 5641, 11°38'N; 69°27'W, 01.x.1965, DJ Griffin det., 55 m, 1 male

juvenile (USNM 1256402). Guyana, R/V Oregon II, stn 10513, 08°26'N; 58°11'W, 27.iv.1969, DJ Griffin & HB Roberts det., 183 m, 1 male (USNM 1256403). Brazil, Pernambuco, CEPEMAR, stn 54 L2, 150 m, 2 females (MOUFPE 15488). Bahia, Alfredo coll., 1 male (MZUSP 20258).

Type-locality. Ecuador, off Machala, near Isla Santa Clara, 03°15'S; 80°50'W, 77–80 m.

Diagnosis. Carapace pyriform, very spinulose, with one small spine on each side of the contiguous portion of the rostrum; one long, acute supraorbital spine; hepatic region with two long, distinct spines. Merus of P2 smooth.

Description. Carapace pyriform, longer than wide, with seven long lateral spines, eight spines in medial line; covered with sparsely distributed tufts of hooked setae, mainly in rostral, branchial regions. Carapace spines: base of rostrum with five spines, two between the orbits; two protogastric; six mesogastric; six metagastric; one urogastric; two long lateral, two smaller mesial hepatic. Branchial region with small sparse tubercles and short spines: eight protobranchial, with few interspaced tubercles; mesobranchial with six long lateral, four small mesial spines, few tubercles; three marginal metabranchial with acute tubercles interspaced; seven cardiac; two intestinal spines. Branchiostegal region with row of acute, strong spines along anterior-inferior half of molt line. Gastric, branchial, cardiac, intestinal regions delimited laterally by shallow grooves.

Rostrum long, bifurcated for distal 1/3 of entire length, divergent. Supraorbital spine long, acute; orbital margin with one small spine. Postorbital margin cup-shaped completely protecting eyes when retracted, with small medial spine on anterior margin. Basal article of antenna narrow, second article long with one long anterolateral spine aligned with supraorbital spine, one smaller posterolateral spine protecting eyestalk from below, one smaller spine below orbital fissure. Antenna almost exceeding rostral length (flagellum broken in holotype). Antennal article longest; third, fourth antennal articles thick, cylindrical; visible dorsally. Antennular fossae longitudinally ovate, longer than wider; posteroventral margin with one small projection. Interantennular septum long, compressed laterally, forming ventrally-directed keel.

Epistome narrower, more depressed than antennular fossae; posterior margin crenulate, antennal gland open in epistome with one tubercle at same level, another on mouthfield border. Endostome with two prominent, obliquely longitudinal endostomial ridges, completely closed.

Buccal field sub-rectangular, longer than wide, posterior edge narrower, with crenulated anterolateral angles with one strong acute spine on anterolateral margins. Pterygostomial region sub-triangular with four acute spines on lateral margin, 3–4 sub-equal tubercles; sub-hepatic region delimited from pterygostome by distinct slope.

Third maxillipeds completely covering buccal frame. Exopod long, nearly reaching distal margin of merus; dorsal face with one small process extending into posterolateral margin of merus; ventral margin with strong spine in distal third. Ischium distinctly longer than broad, dorsal face with longitudinal, smooth, deep "L" shaped groove; crista dentata with small, rounded, irregular sized teeth. Merus slightly longer than half of ischium, anteromesial border partially covering propodus; anterior margin deeply

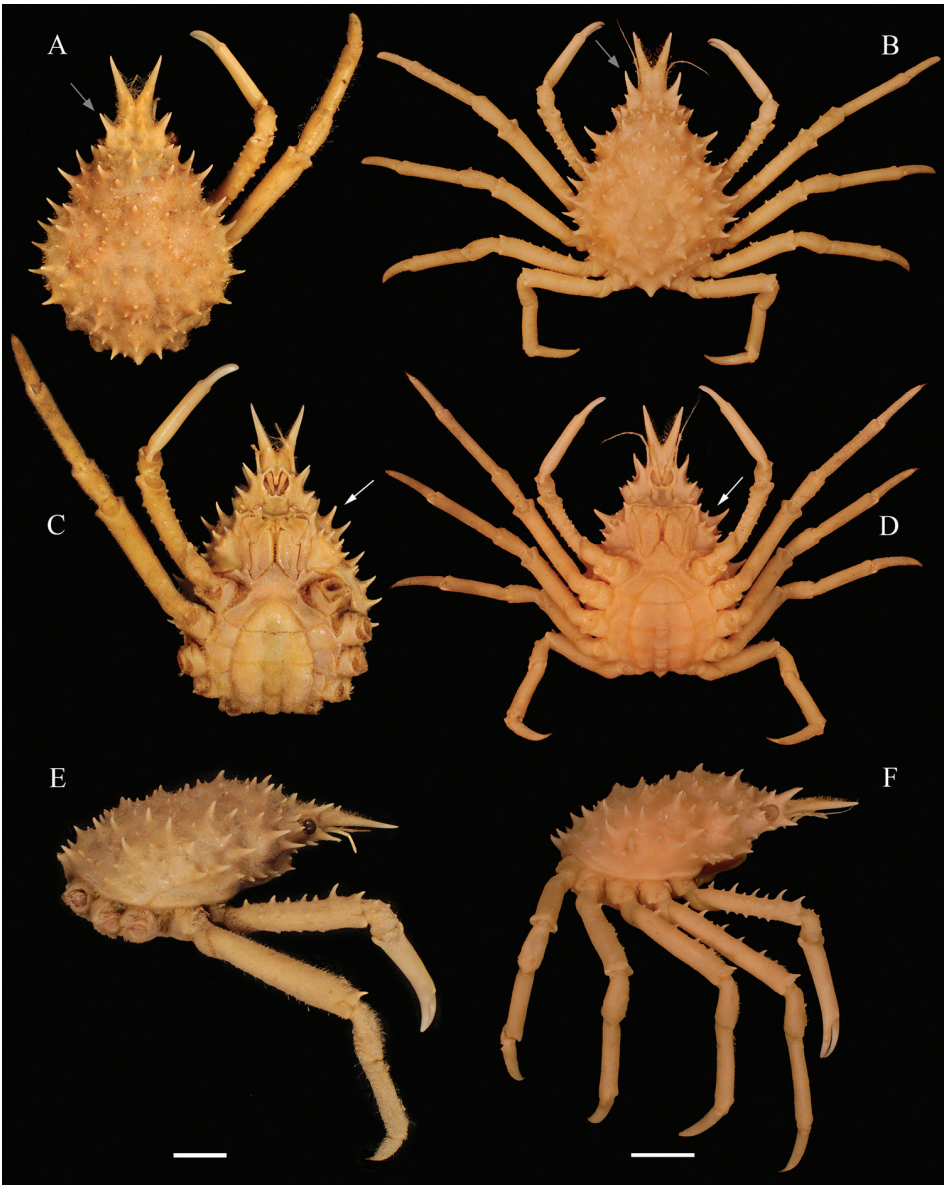

Figure 5. *Nibilia machala* sp. n., female holotype, cl 58.4 mm, cw 35 mm (USNM 1462701) (**A, C, E**). *Nibilia antilocapra* Stimpson (1871), female, cl 47.6 mm, cw 30.6 mm (USNM 1462686) (**B, D, F**). Habitus, dorsal view (**A, B**); Ventral view (**C, D**); Lateral view (**E, F**). Note the difference between the interorbital region spines (gray arrows) (**A, B**), and the hepatic spines (white arrows) (**C, D**). Scale bars: 10 mm.

incised, anterolateral margins slightly expanded. Palp cylindrical, slightly overreaching ischiomeral suture. Carpus, propodus, dactylus smooth; propodus, with long distomesial setae, dactylus fringed with row of long setae.

Juvenile female thoracic sternites I–IV fused, broadly triangular, smooth, dense, covered by closely adhered pubescence. Anterior half of fused sternites I–IV sloping

down in ventral view. Sterno-pleonal cavity completely closed by telson. Female sternites V–VII smooth; Margin of episternites IV–VII smooth.

Juvenile female pleonal somites I–VI, telson free, slightly raised medially forming low longitudinal ridge. One small spine in first somite; somites II–VI smooth. Telson triangular. Juvenile female holotype with a sealed pleon.

Juvenile female chelipeds subequal, long; ischium unarmed; merus armed with seven strong dorsal spines, row of six laterodistal tubercles, sparse tubercles present; carpus with sparse tubercles; propodus smooth; dactylus and fixed finger distinctly shorter than palm, slender, cutting edges with subequal teeth, tip incurving down. P2 slender, cylindrical, with a distinct spine in distal margin of merus, densely covered with small setae and sparse hooked setae. Only P2 preserved in the holotype.

Distribution. Only known from the type-locality in Ecuador, near Isla Santa Clara, 03°15'S; 80°50'W.

Etymology. The specific epithet *machala* is a noun in apposition referring to the coastal city of Machala, Ecuador.

Remarks. *Nibilia machala* superficially resembles *N. antilocapra* (Stimpson, 1871) in the highly spinulose appearance of the carapace, the long and semi-contiguous rostral spines, the distinct "L" shaped sulcus imprinted on the dorsal margin of the ischium of the third maxilliped, P2 with a distinct spine on the dorso-distal margin of merus, and similar shape of the female pleon (Fig. 5). *Nibilia machala*, however, differs from *N. antilocapra* by (i) the presence of one small spine on each side of the contiguous portion of the rostrum (vs. the contiguous portion of the rostrum unarmed in *N. antilocapra*) (Fig. 5A, B, black arrow); (ii) one long, acute supraorbital spine (vs. two acute spines, one long and one shorter in *N. antilocapra*) (Fig. 5A, B); (iii) hepatic region with two long, distinct spines (vs. one long, distinct spine in the hepatic region of *N. antilocapra*) (Fig. 5C, D, white arrow); (iv) P2 merus smooth (vs. P2 armed with two rows of six or seven spines in *N. antilocapra*) (Fig. 5E, F). *Pisa praelonga* Stimpson, 1871, is apparently a juvenile stage collected at the same locality of *N. antilocapra*, thus, considered a junior subjective synonym of *N. antilocapra* (Rathbun 1925; see also figures on Milne-Edwards and Bouvier 1923: pl 11, Figs 4–7). *Nibilia erinacea* A Milne-Edwards, 1878 is also considered a junior subjective synonym of *N. antilocapra*. The description and the figure presented by A Milne-Edwards (1878: 133, pl 25) fully agree with the description of *Pisa antilocapra* Stimpson, 1871. Both, *Pisa praelonga* and *Nibilia erinacea* where described from western Atlantic material.

Family Epialtidae MacLeay, 1838
Subfamily Pisinae Dana, 1851

Solinca gen. n.
http://zoobank.org/0DD6BA19-F0F6-401F-92C7-FE271F607D2A

Type species. *Solinca aulix* gen. n. et sp. n. by monotypy and original designation. Gender feminine.

Diagnosis. Carapace distinctly sub-circular in outline, dorsal surface prominently vaulted, particularly swollen at branchial regions. Urogastric region compressed by metabranchial lobes into a deep furrow. Four spines along dorsal midline of carapace: mesogastric, metagastric, cardiac, and intestinal. Branchiostegal region with two rows of small acute spines along molt line. Thoracic pleurites V–VII gymnopleura. Postorbital spine long, curved beyond eyes. Eyes not retractable. Endostomial ridge with two obliquely longitudinal, very curved prominences. Sterno-pleonal cavity longer than pleon plus telson, leaving gap between distal end of telson and its anterior margin. Gonopod reaching far beyond thoracic sternal suture IV/V, rather straight proximally and medially, distinctly curved inwards sub-distally, convergent anteriorly, apical plate curved down with three distinct lobes laterally.

Etymology. The genus name is an arbitrary noun formed by the combination of the Latin *Solis,* "sun" and alluding to the sub-circular carapace surrounded by spines, and *Inca* alluding to the Inca Empire. Gender: feminine.

Remarks. *Solinca* is phylogenetically allied to the epialtids *Scyra acutifrons*, *Pugettia nipponensis, Pugettia quadridens* and *Chorilia longipes* (Fig. 1). However, the only morphological character shared by these taxa is a distinct sulcus in each face of the chelipeds, albeit this character is less pronounced in *Solinca*. Considering overall morphological similarities, *Solinca* is closest to *C. longipes* in the following characters: (i) presence of several spines on the carapace in both *Solinca* and *C. longipes* (vs. carapace tuberculate or with strong spines in *S. acutifrons*, *P. nipponensis*, and *P. quadridens*); (ii) supraorbital spines acute in both *Solinca* and *C. longipes* (vs. short and truncated supraorbital spines in *S. acutifrons*, *P. nipponensis,* and *P. quadridens*.); (iii) rostral spines rounded (vs. rostral spines flatted in *S. acutifrons*, *P. nipponensis* and *P. quadridens*); (iv) long and very thin legs in *Solinca* and *C. longipes* (vs. short and robust legs in *S. acutifrons*, *P. nipponensis*, and *P. quadridens*); and (v) thoracic pleurites V–VII gymnopleura in *Solinca* and *C. longipes* (vs. gymnopleura condition not present in *S. acutifrons*, *P. nipponensis*, and *P. quadridens*). See remarks of the species for differences between *S. aulix* and *Chorilia longipes*.

Solinca aulix **sp. n.**

http://zoobank.org/4A973066-37F9-4705-BBA1-BA21C057832
Figures 6A–F, 7D–G

Holotype. Peru, off Paita, Piura, Southeast Pacific Biological Oceanographic Project (SEPBOP), R/V Anton Bruun, stn 627–A, 05°01' / 05°02'S; 81°25'/ 81°24'W, 03.vi.1966, Smithsonian Oceanographic Sorting Center coll., 200–311 m, male holotype, cl 37.3 mm, cw 28.2 mm (USNM 1462734).

Paratypes. Peru, off Paita, Piura, Southeast Pacific Biological Oceanographic Project (SEPBOP), R/V Anton Bruun, stn 627–A, 5°01' / 05°02'S; 81°25' / 81°24'W; 3.vi.1966, Smithsonian Oceanographic Sorting Center coll., 200–311 m, 1 female (MZUSP 38891), 1 male (MZUSP 38892). Idem, 1 female, cl 39.5, cw 29.8 mm,

1 male and 1 juvenile (USNM 1462685). Southeast Pacific Biological Oceanographic Project (SEPBOP), R/V Anton Bruun, cruise 16, stn 635-A, 06°45'S; 80°93'W, 5.ix.1966, Smithsonian Oceanographic Sorting Center coll., 160 m, 1 male, cl 40.31 mm, cw 32.05 mm (USNM 1462673).

Material examined. Ecuador, Gulf of Guayaquil, northwest of Tumbes, Southeast Pacific Biological Oceanographic Project (SEPBOP), R/V Anton Bruun, stn 768, 03°39'S; 80°41'W, 10.ix.1966, Smithsonian Oceanographic Sorting Center coll., 13 m, 1 juvenile female (USNM 1460378). Peru, off Paita, Piura, Southeast Pacific Biological Oceanographic Project (SEPBOP), R/V Anton Bruun, stn 627-A, 05°01' / 05°02'S; 81°25' / 81°24'W, 03.vi.1966, Smithsonian Oceanographic Sorting Center coll., 200–311 m, 6 males, 3 juveniles males, 5 females, 1 ovigerous females (USNM 1462735), off Isla Lobos de Tierra, Southeast Pacific Biological Oceanographic Project (SEPBOP), R/V Anton Bruun, stn 635A, 06°27' / 06°23'S; 80°56' / 80°55'W, 05.vi.1966, Smithsonian Oceanographic Sorting Center coll., 160 m, 4 males, 7 ovigerous female (USNM 1462736).

Comparative material. *Chorilia longipes* Dana, 1851. Canada, British Columbia, Queen Charlotte Islands, Port Hardy, United States Fish Commission, R/V Albatross, stn 2862, 50°49'N; 127°36'W, 1.ix.1888, 3 males, 5 females, 2 juveniles (USNM 15497). United States of America, Alaska, vicinity of Yes Bay, Behm Canal, east end Square Island, Spacious Bay S, 48W, 19 miles, 130–193 m, 8.vii.1903, 2 males, 2 females (USNM 31637). California, Farallon Island, R/V Velero, EPA Farallon Study Expedition, stn 1, R Carney coll. det., 17 specimens (USNM 1420706). California, NE of Santa Barbara Island, Channel Islands, United States Fish Commission, R/V Albatross, stn 4416, 591–819 m, 12.iv.1904, 13 specimens (USNM 46534).

Pugettia nipponensis Rathbun, 1932. Japan, Honshu Island, Doumiki-saki, R/V Albatross, stn 3771, 05.vi.1900, MJ Rathbun det., male holotype (USNM 48254).

Pugettia quadridens (De Haan, 1839). South Korea, Dolsan Island, Sea of Japan, 1 juvenile, DNA only (ULLZ 13538). Japan, Honshu Island, Suruga Bay, Omae Zaki, R/V Albatross, stn 3730, 16.v.1900, MJ Rathbun det., 1 male, 1 female (USNM 49925).

Scyramathia vesicularis Rathbun, 1907. Ecuador, South of Española, Galapagos Islands, 1°50'83"S; 89°58'33"W, R/V Albatross, stn 4642, 549 m, 7.xi.1904, MJ Rathbun det., male holotype (USNM 32860).

Scyra acutifrons Dana 1851. United States of America, Washington, Port Orchard, Puget Sound, vi.1889, OB Johnson coll., MJ Rathbun det., 8 males, 3 females (USNM 14966). Washington, Lopez Island, Rock Point, 48N; 122W, G Paulay coll., 22.vi.2007, DNA only (UF 11955).

Type-locality. Peru, off Paita, Piura, 05°01'S to 05°02'S; 81°25'W to 81°24'W, 200–311 m.

Diagnosis. Same as for the genus.

Description. Carapace distinctly sub-circular in outline, surface prominently inflated, particularly swollen at protogastric and branchial regions. Urogastric region compressed by metabranchial lobes into a deep furrow. Four spines - mesogastric, metagastric, cardiac, intestinal – along dorsal carapace midline. Dorsal carapace sparsely

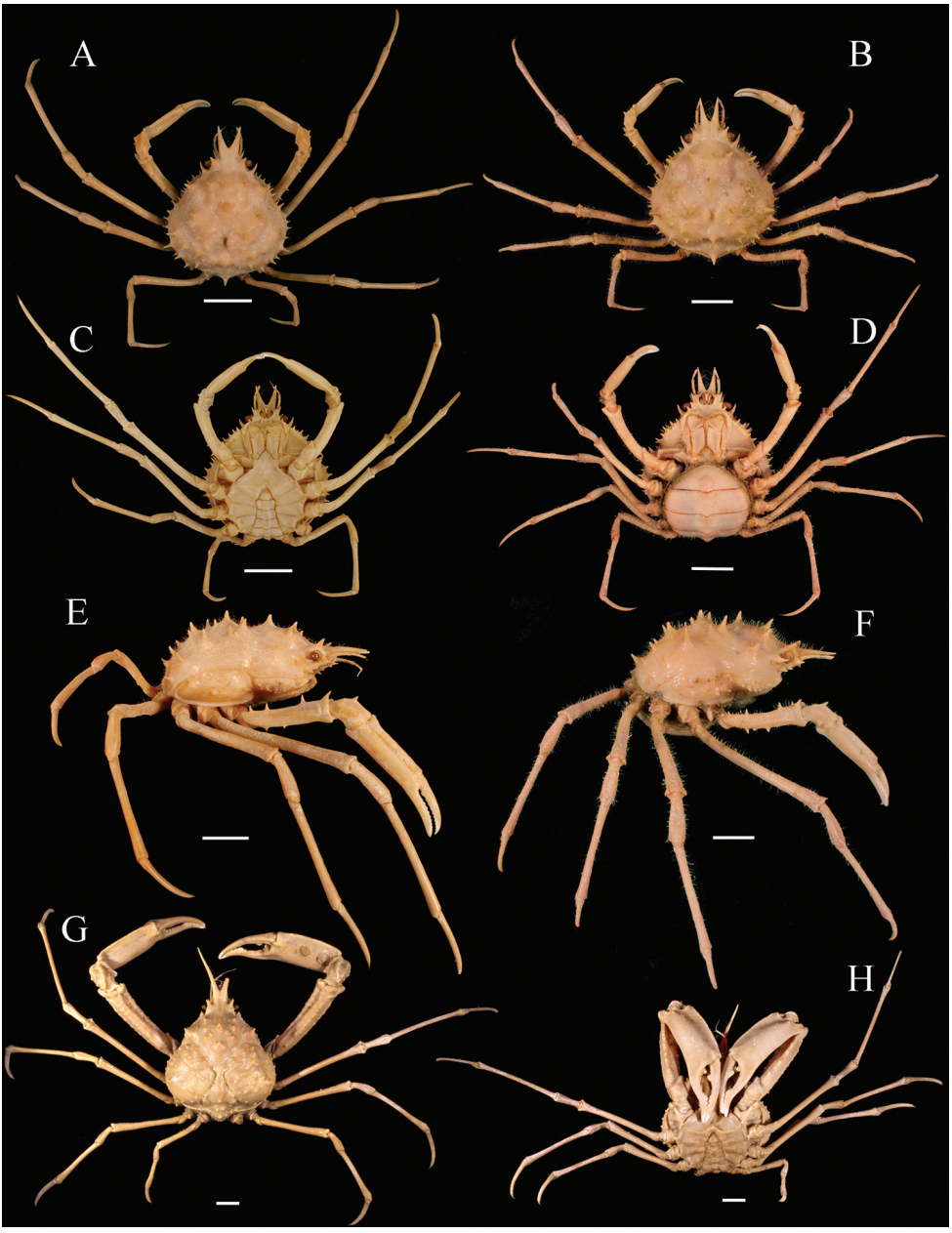

Figure 6. *Solinca aulix* gen. n. et sp. n. (**A–F**), male holotype, cl 37.30 mm, cw 28.2 mm, (USNM 1462734) (**A, C, E**); Female paratype, cl 39.5 mm, cw 29.8 mm (USNM 1462685) (**B, D, F**). *Chorilia longipes* Dana, 1851, male, cl 56.5 mm, cw 48.1 mm (USNM 46534) (**G, H**). Habitus, dorsal view (**A, B, G**); Ventral view (**C, D, H**); Lateral view (**E, F**). Scale bars: 10 mm.

covered with long simple and hooked setae. Gastric region with two lateral spines, one protogastric, one mesogastric. One hepatic, one small sub-hepatic spines. Branchial region with four protobranchial spines; mesobranchial with four long, five shorter

spines; two metabranchial, one lateral, one mesial spine above metabranchial lobe. Mesial border of branchial region with one distinct spine near the furrow, one cardiac and one intestinal spine. Branchiostegal region with two rows of spines, superior row with five strong, acute spines along most of posteroinferior half of molt line, at least five smaller spines in lower row. Gastric region delimited by shallow grooves; branchial, cardiac, intestinal regions delimited by well-marked grooves. Gastric, branchial regions with few tubercles or small spines. Pterygostomial region sub-triangular with five acute spines, few tubercles on lateral margin, smooth medially, inflated, visible in dorsal view. Thoracic pleurites V–VII gymnopleura.

Rostrum bifurcated, short, straight, more divergent in juveniles. Supraorbital spine acute, pointed forward. Postorbital spine long, curved beyond eyes. Eyes not retractable. Basal article of antenna narrow, second article long with two spines, one anterolateral, one posterolateral; one small sub-orbital spine in line with antennal gland. Antennae exceeding the rostral length, visible dorsally, flagellum short, thin; third antennal article longest; third and fourth antennal articles thick, cylindrical. Antennular fossae longitudinally ovate, longer than wide; interantennular septum long compressed laterally, forming ventrally-directed keel.

Epistome narrower than antennular fossae, anterior margin smooth, posterior margin crenulated; antennal gland open in epistome. Endostome with two obliquely prominent, longitudinal, very curved endostomial ridges. Buccal field sub-rectangular, longer than wide, narrower at posterior edge with smooth anterolateral angles.

Third maxillipeds covering buccal frame posteriorly, incompletely covering in anterior margin. Exopod long, nearly reaching distal margin of merus; ventral face with small process extending to posterolateral margin of merus. Ischium distinctly longer than broad, dorsal face smooth, deeply sculpted; crista dentata with very small, rounded teeth. Merus slightly longer than half of ischium, anteromesial border partially covering the propodus; anterior margin deeply incised, anterolateral margins slightly expanded, rounded. Palp cylindrical, slightly overreaching ischiomeral suture. Carpus, propodus and dactylus smooth; Propodus short, dactylus long and thin, with row of long setae on the distal margin. Male chelipeds equal, long, strong; merus, carpus and propodus sculpted by distinct sulcus in lateral and mesial faces; ischium smooth; merus armed with four dorsal spines, two smaller ventral spines; carpus with 3–4 blunt tubercles; propodus smooth; dactylus and fixed finger smooth, with same size as palm, cutting edges with sub-equal teeth in distal half, distinct proximal tooth in larger males; juvenile males and females fingers without gap.

P2–P5 long, slender, cylindrical, armed with distinct spine in distal margin of merus. P2 much longer than cheliped; P3–P5 progressively decreasing in length. Females with long, slender chelipeds. All legs covered with sparse, long simple setae.

Male thoracic sternite I-IV fused, broadly triangular, smooth; posterior half strongly sloping down in ventral view, forming a carina along lateral margin of telson. Sternopleonal cavity longer than telson, leaving gap between telson and anterior margin. Male sternites V–VII smooth; sternite VIII extending laterally beyond sterno-pleonal cavity, visible in ventral view. Margin of male episternites IV–VII smooth; female episternites IV–VII smooth, densely covered with small pubescence.

Figure 7. *Collodes anartius* sp. n., male paratype (USNM 142821) (**A–C**); First gonopod (G1), right side, sternal view (**A**), pleonal view (**B**); Second gonopod (G2), right side (**C**). *Solinca aulix* gen. n. et sp. n., paratype male (USNM 1462673) (**D–G**); First gonopod (G1), left side, pleonal view (**D, F**), sternal view (**E**); Second gonopod (G2), left side (**G**). Scale bars: 1 mm (**A, D**); 0.5 mm (**B, C, E–G**).

Male pleonal somites I–VI, telson free, smooth, slightly raised medially forming a low longitudinal ridge; first somite with distinct spine. Female pleonal somites I–IV, telson free; pleon markedly arched covering entire sterno-pleonal cavity; second somite

with a distinct tubercle, sometimes forming a spine. Telson sub-triangular, terminating in rounded apex in males; female telson transversely oval.

First gonopod longer than thoracic sternal suture IV-V, straight proximally and medially, distinctly curved inwards sub-distally, convergent anteriorly; apical plate curved down with three well-pronounced lobes. Mesial lobe small, densely spinulate, curving toward sternal margin; distal lobe bilobed, long, tip rounded upwards; lateral lobe shorter than distal lobe, curved upward. G2 slender, straight, about 1/4 of G1 total length.

Distribution. Ecuador, from Tumbes to Peru, Isla Lobos de Tierra at depths between 13 to 311 m.

Etymology. The specific epithet *aulix* is the feminine Latin noun for "furrow" or "sulcus", and alludes to the furrow in the intestinal region formed by the junction of the highly inflated branchial regions.

Remarks. *Solinca aulix* can be distinguished from *Chorilia longipes* by a unique set of characters, which include: (i) rostral spines of *Solinca aulix* shorter than *C. longipes* (Fig. 6A, B, G); (ii) postorbital spines long, curved beyond eyes in *Solinca* (vs. truncated postorbital process curved medially in *C. longipes*) (Fig. 6A, B, G); (iii) protogastric and branchial regions distinctly swollen in *Solinca aulix* (vs. protogastric and branchial regions weakly swollen in *C. longipes*) (Fig. 6A, B, G); (iv) urogastric region compressed by metabranchial regions forming a furrow in *Solinca aulix* (vs. urogastric region not compressed and with some tubercles in *C. longipes*) (Fig. 6A, B, G); (v) anterolateral border of the merus of the third maxilliped rounded in *Solinca aulix* (vs. anterolateral border of the merus of the third maxilliped pointed in *C. longipes*) (Fig. 6C, D, H); (vi) pterygostomial region inflated, visible in dorsal view in *Solinca aulix* (vs. pterygostomial region not inflated and not visible in dorsal view in *C. longipes*) (Fig. 6C, D, H); (vii) third and fourth antennal articles short and cylindrical in *Solinca aulix* (vs. third and fourth antennal articles long and flattened in *C. longipes*); and (viii) G1 slightly overreaching the thoracic sternal suture IV-V in *Solinca aulix* (Fig. 7D–G) (vs. G1 distinctly overreaching the thoracic sternal suture IV-V in *C. longipes*).

Acknowledgements

We are grateful to Rafael Lemaitre and Karen Reed (USNM) for facilitating access to materials and information from the USNM collections, and to Marcos Tavares (MZUSP) and Jesser Fidelis de Souza Filho (MOUFPE) for access to the comparative material. This work was supported by the Fundação de Amparo à Pesquisa do Estado de São Paulo (FAPESP) [2013/01201–0 and 2014/15549–0]. JC thanks FAPESP [2017/08969–1 BEPE]. We also thank Darryl Felder at the University of Louisiana at Lafayette for use of DNA sequences generated by AW under the USA National Science Foundation grant NSF/AToL EF–0531603 to DF. This work greatly benefited from the comments of PKL Ng (Lee Kong Chian Natural History Museum) and from Marcos Tavares (MZUSP).

References

Apakupakul K, Siddall ME, Burreson EM (1999) Higher level relationships of leeches (Annelida: Clitellata: Euhirudinea) based on morphology and gene sequences. Molecular Phylogenetics and Evolution 12(3): 350–359. https://doi.org/10.1006/mpev.1999.0639

Bracken HD, Toon A, Felder DL, Martin JW, Finley M, Rasmussen J, Palero F, Crandall KA (2009) The decapod tree of life: compiling the data and moving toward a consensus of decapod evolution. Arthropod Systematics & Phylogeny 67(1): 99–116. http://www.senckenberg.de/files/content/forschung/publikationen/arthropodsystematics/asp_67_1/asp_67_1_bracken_99–116.pdf

Bell T (1835) Some account of the Crustacea of the coasts of South America, with descriptions of new genera and species; founded principally on the collections obtained by Mr Cuming and Mr Miller. (Tribus 1, Oxyrhynchi). Proceedings of the Zoological Society of London 3: 169–173. https://biodiversitylibrary.org/page/12859433

Carmona–Suárez C, Poupin J (2016) Majoidea crabs from Guadeloupe Island, with a documented list of species for the Lesser Antilles (Crustacea, Decapoda, Brachyura, Majoidea). Zoosystema 38(3): 353–387. https://doi.org/10.5252/z2016n3a5

Child CA (1992) Pycnogonida of the southeast Pacific biological oceanographic project (SEPBOP). Smithsonian Contributions to Zoology, Washington DC 526: 1–52. https://doi.org/10.5479/si.00810282.526

Colgan DJ, Mclauchlan A, Wilson GDF, Livingston SP, Edgecombe GD, Macaranas J, Cassis G, Gray MR (1998) Histone 3 and U2 snRNA DNA sequences and arthropod molecular evolution. Australian Journal of Zoology 46: 419–437. https://doi.org/10.1071/ZO98048

Dana JD (1851) On the classification of the maioid Crustacea or Oxyrhyncha. American Journal of Science series 2, 11(33): 425–434. http://www.biodiversitylibrary.org/item/88952

Davie PJ, Guinot D, Ng PK (2015) Phylogeny of Brachyura. In: Castro P, Davie PJ, Guinot D, Schram FR, von VaupelKlein JC (Eds) Treatise on Zoology – Anatomy, Taxonomy, Biology. The Crustacea, Vol. 9 Part C-II. Brill, Leiden and Boston, 921–979. https://doi.org/10.1163/9789004190832_019

Folmer O, Black M, Hoeh R, Lutz R, Vrijenhoek R (1994) DNA primers for amplification of mitochondrial cytochrome c oxidase subunit I from diverse metazoan invertebrates. Molecular Marine Biology and Biotechnology 3(5): 294–299. https://www.mbari.org/wp-content/uploads/2016/01/Folmer_94MMBB.pdf

Garth JS, Haig J (1971) Decapod Crustacea (Anomura and Brachyura) of the Peru-Chile Trench. Anton Bruun Report 6: 3–20.

Hernández-Ávila I, Lira C, Bolaños J (2008) Primer hallazgo de *Nibilia antilocapra* (Stimpson, 1871) (Crustacea: Decapoda: Epialtidae) para Venezuela. Revista de biología marina y oceanografía 43(3): 687–689. https://doi.org/10.4067/S0718-19572008000300028

Huelsenbeck JP, Ronquist F (2001) MRBAYES: Bayesian inference of phylogenetic trees. Bioinformatics 17(8): 754–755. https://doi.org/10.1093/bioinformatics/17.8.754

Hultgren KM, Stachowicz JJ (2008) Molecular phylogeny of the brachyuran crab superfamily Majoidea indicates close congruence with trees based on larval morphology. Molecular Phylogenetics and Evolution 48(3): 986–996. https://doi.org/10.1016/j.ympev.2008.05.004

Katoh K, Kuma KI, Toh H, Miyata T (2005) MAFFT version 5: improvement in accuracy of multiple sequence alignment. Nucleic Acids Research 33(2): 511–518. https://doi.org/10.1093/nar/gki198

Lanfear R, Frandsen PB, Wright AM, Senfeld T, Calcott B (2017) PartitionFinder 2: New methods for selecting partitioned models of evolution for molecular and morphological phylogenetic analyses. Molecular Biology and Evolution 34(3): 772–773. https://doi.org/10.1093/molbev/msw260

Medlin L, Elwood HJ, Stickel S, Sogin ML (1988) The characterization of enzymatically amplified eukaryotic 16S-like rRNA-coding regions. Gene 71(2): 491–499. https://doi.org/10.1016/0378-1119(88)90066-2

Melo GAS (1996) Manual de identificação dos Brachyura (caranguejos e siris) do litoral brasileiro. Plêiade/FAPESP, São Paulo, 603 pp.

Milne-Edwards A (1878) Études sur les xiphosures et les crustacés de la région mexicaine. In: Mission scientifique au Mexique et dans l'Amérique centrale, ouvrage publié par ordre du Ministre de l'Instruction publique. Recherches zoologiques pour servir à l'histoire de la faune de l'Amérique central et du Mexique, publiées sous la direction de MH Milne Edwards, membre de l'Institut. Cinquième partie. 8 [unnumbered], Tome premier, Imprimerie Nationale, Paris, 368 pp. [63 pls] https://doi.org/10.5962/bhl.title.119116

Milne-Edwards A, Bouvier EL (1923) Reports on the results of dredging. Under the supervision of Alexander Agassiz, in the Gulf of Mexico (1877–78), in the Caribbean Sea (1878–79), and along the Atlantic coast of the United States (1880), by the US Coast Survey steamer "Blake." Lieut.-Com. CD Sigsbee, USN, and Commander JR Bartlett, USN, commanding. XLVII: Les Porcellanides et des Brachyures. Memoirs of the Museum of Comparative Zoology at Harvard College 47(4): 283–395. https://biodiversitylibrary.org/page/4368394

Mokady O, Rozenblatt S, Graur D, Loya Y (1994) Coral-host specificity of Red Sea *Lithophaga* bivalves: interspecific and intraspecific variation in 12S mitochondrial ribosomal RNA. Molecular Marine Biology Biotechnology 3: 158–164.

Ng PK, Guinot D, Davie PJ (2008) Systema Brachyurorum: Part I. An annotated checklist of extant brachyuran crabs of the world. The Raffles Bulletin of Zoology 17(1): 1–286.

Rathbun MJ (1893) Catalogue of the crabs of the family Maiidæ in the United States National Museum. Proceedings of the United States National Museum 16(927): 63–103. [pls I–VI] https://www.biodiversitylibrary.org/bibliography/7519

Rathbun, MJ (1894) Notes on the crabs of the family Inachidæ in the United States National Museum. Proceedings of the United States National Museum 17(984): 43–75. [pl I] https://doi.org/10.5479/si.00963801.17-984.43

Rathbun MJ (1898) The Brachyura of the biological expedition to the Florida Keys and the Bahamas in 1893. Bulletin from the Laboratories of Natural History, State University of Iowa 4(3): 250–294. [pls I–IX]

Rathbun MJ (1901) The Brachyura and Macrura of Porto Rico. Bulletin of the United States Fish Commission 20 [for 1900] (2): 1–127. [1–2 pls] https://www.biodiversitylibrary.org/bibliography/3971

Rathbun MJ (1925) The spider crabs of America. Bulletin of the United States National Museum 129: 1–613. https://doi.org/10.5479/si.03629236.129.i

Santana W, Tavares M (2017) A new western Atlantic species of *Collodes* Stimpson (Decapoda, Brachyura, Inachoididae). Crustaceana 90(7–10): 1145–1153. https://doi.org/10.1163/15685403-00003639

Shull HC, Pérez-Losada M, Blair D, Sewell K, Sinclair EA, Lawler S, Ponniah M, Crandall KA (2005) Phylogeny and biogeography of the freshwater crayfish *Euastacus* (Decapoda: Parastacidae) based on nuclear and mitochondrial DNA. Molecular Phylogenetics and Evolution 37(1): 249–263. https://doi.org/10.1016/j.ympev.2005.04.034

Stamatakis A (2006) RAxML-VI-HPC: maximum likelihood-based phylogenetic analyses with thousands of taxa and mixed models. Bioinformatics 22(21): 2688–2690. https://doi.org/10.1093/bioinformatics/btl446

Stimpson W (1860) Notes on North American Crustacea, in the museum of the Smithsonian Institution, No. II. Annals of the Lyceum of Natural History of New York 7(1): 176–246. https://doi.org/10.1111/j.1749-6632.1862.tb00153.x

Stimpson W (1871) Preliminary report on the Crustacea dredged in the Gulf Stream in the Straits of Florida by LF de Pourtales, Assista. U. S. Coast Survey. Part I. Brachyura. Bulletin of the Museum of Comparative Zoology at Harvard College 2: 109–160. https://www.biodiversitylibrary.org/bibliography/2803

Vaidya G, Lohman DJ, Meier R (2011) SequenceMatrix: concatenation software for the fast assembly of multi-gene datasets with character set and codon information. Cladistics 27(2): 171–180. https://doi.org/10.1111/j.1096-0031.2010.00329.x

Windsor AM, Felder DL (2014) Molecular phylogenetics and taxonomic reanalysis of the family Mithracidae Macleay (Decapoda: Brachyura: Majoidea). Invertebrate Systematics 28: 145–173. https://doi.org/10.1071/IS13011

Windsor AM, Felder DL (2017) Corrigendum to: Molecular phylogenetics and taxonomic reanalysis of the family Mithracidae MacLeay (Decapoda: Brachyura: Majoidea). Invertebrate Systematics 31(2): 232–232. https://doi.org/10.1071/IS13011_CO

Supplementary material 1

Taxa included in the molecular phylogenetic analyses to place the newly described taxa within the context of the superfamily Majoidea

Authors: Jessica Colavite, Amanda Windsor, William Santana

Data type: phylogenetic data

Copyright notice: This dataset is made available under the Open Database License (http://opendatacommons.org/licenses/odbl/1.0/). The Open Database License (ODbL) is a license agreement intended to allow users to freely share, modify, and use this Dataset while maintaining this same freedom for others, provided that the original source and author(s) are credited.

Link: https://doi.org/10.3897/zookeys.825.32271.suppl1

ZooKeys 825: 25–42 (2019)
doi: 10.3897/zookeys.825.31663
http://zookeys.pensoft.net

RESEARCH ARTICLE

A peer-reviewed open-access journal
ZooKeys
Launched to accelerate biodiversity research

Two new species and one new regional record of *Indonemoura* from Guangxi, China, with additions to larval characters (Plecoptera, Nemouridae)

Raorao Mo[1,3], Guoquan Wang[1], Ding Yang[2], Weihai Li[3], Dávid Murányi[4,5]

1 *Guangxi key laboratory of Agric-Environment and Agric-Products Safety and National Demonstration Center for Experimental Plant Science Education, Agricultural College, Guangxi University, Nanning, China* **2** *Department of Entomology, China Agricultural University, 2 Yuanmingyuan West Road, Beijing 100193, China* **3** *Department of Plant Protection, Henan Institute of Science and Technology, Xinxiang, Henan 453003, China* **4** *Plant Protection Institute, Centre for Agricultural Research, Hungarian Academy of Sciences, Herman Ottó út 15, Budapest H-1022, Hungary* **5** *Department of Zoology, Hungarian Natural History Museum, Baross u. 13, Budapest H-1088, Hungary*

Corresponding author: Guoquan Wang (wangguoquan0@163.com); Weihai Li (lwh7969@163.com)

Academic editor: *M. Gottardo* | Received 15 November 2018 | Accepted 19 January 2019 | Published 18 February 2019

http://zoobank.org/8FBE5928-026F-4C89-9CD4-56974183A207

Citation: Mo R, Wang G, Yang D, Li W, Murányi D (2019) Two new species and one new regional record of *Indonemoura* from Guangxi, China, with additions to larval characters (Plecoptera, Nemouridae). ZooKeys 825: 25–42. https://doi.org/10.3897/zookeys.825.31663

Abstract

Two new species of Nemouridae of the genus *Indonemoura* Baumann, 1975, *Indonemoura quadrata* **sp. n.** and *Indonemoura quadrispina* **sp. n.**, are described from Guangxi Zhuang Autonomous Region of southern China, on the basis of both sexes and larval stage. The affinities towards related species are discussed, together with generic characters of the larvae. *Indonemoura scalprata* (Li & Yang, 2007) is recorded from Guangxi for the first time, and its hitherto unknown female is described.

Keywords

China, *Indonemoura*, new record, new species, Plecoptera

Copyright *Raorao Mo et al.* This is an open access article distributed under the terms of the Creative Commons Attribution License (CC BY 4.0), which permits unrestricted use, distribution, and reproduction in any medium, provided the original author and source are credited.

Introduction

The genus *Indonemoura* Baumann, 1975, a member of the Amphinemurinae, currently contains 55 species worldwide, and is mainly distributed in the Oriental Region but with a few species also in the Eastern Palaearctic (Shimizu 1994; Sivec and Stark 2010; Yang et al. 2015; Fochetti and Ceci 2016; Li et al. 2017a, b; DeWalt et al. 2018). Presently 24 species are known from China (Wu 1935, 1938, Yang and Yang 1991; Zhu et al. 2002; Li et al. 2005, 2017a, b; Li and Yang 2005, 2006, 2007, 2008a, b, c; Wang et al. 2006; Wang and Du 2009, Yang et al. 2015), and three species: *I. furcoloba* Li & Yang, 2017 (in: Li et al. 2017b), *I. voluta* Li & Yang, 2008b, and *I. yangi* Li & Yang, 2006 are known from Guangxi (Li and Yang 2006, 2008b; Li et al. 2017b). In the present paper, two new species are described from Guangxi Zhuang Autonomous Region of southern China. Additionally, *I. scalprata* (Li & Yang, 2007) is newly recorded for Guangxi.

Materials and methods

Specimens were collected by hand or using an aerial net and are stored in 75% ethanol. The terminalia used for illustrations were cleared in 10% KOH. Types are deposited in the Department of Plant Protection, Henan Institute of Science and Technology (**HIST**) and the Collection of Smaller Insect Orders, Department of Zoology, Hungarian Natural History Museum, Budapest (**HNHM**), respectively, as indicated in the text. Illustrations were made with the aid of a Leica S8APO microscope, further colour illustrations were made with the aid of Imaging Source CCD attached to a Leica M420 microscope. The morphological terminology follows that of Baumann (1975).

Taxonomic part

***Indonemoura quadrata* sp. n.**
http://zoobank.org/2ACE6570-AA65-4336-A091-D89B13F4C6FA
Figs 1–4, 10a, b

Adult habitus (Fig. 1a, b). Medium sized species, forewing length in males 6.8–7.4 mm, females 7.9 mm. Head and mouthparts dark brown, antennae brown; compound eyes black. Thorax brown; pronotum darker with pale band along lateral margins; legs (Fig. 1b) mostly dark brown, distal half of hind femora with distinct yellow brown band; wings subhyaline with darker veins; Abdominal segments mostly brown except terminalia darker; hairs on abdomen mostly pale brown.

Male Terminalia (Figs 1c–e, 2a–e). Tergum IX (Fig. 2a) distinctly sclerotised, gradually constricted medially, bearing scattered, tiny black spines along mid-posterior margin; the median part of tergum IX weakly sclerotised and semicircular. Sternum IX

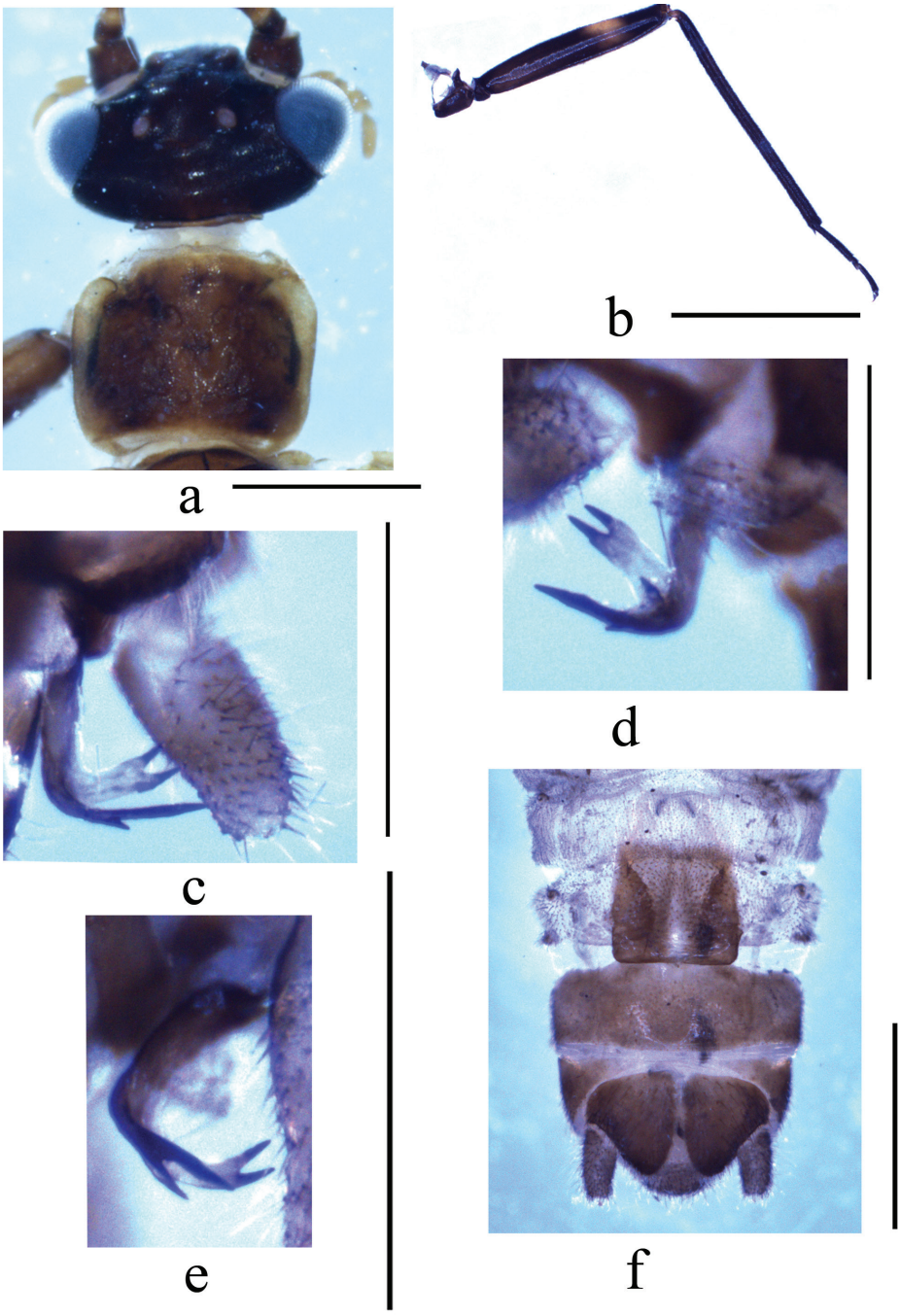

Figure 1. *Indonemoura quadrata* sp. n. (**a–e** male **f** female) **a** head and pronotum, dorsal view **b** hindleg, lateral view **c** left paraproct, spines of outer lobe, ventral view **d** right paraproct, spines of outer lobe, ventral view **e** right paraproct, spines of outer lobe, dorsolateral view **f** terminalia, ventral view. Scale bars: 0.5 mm.

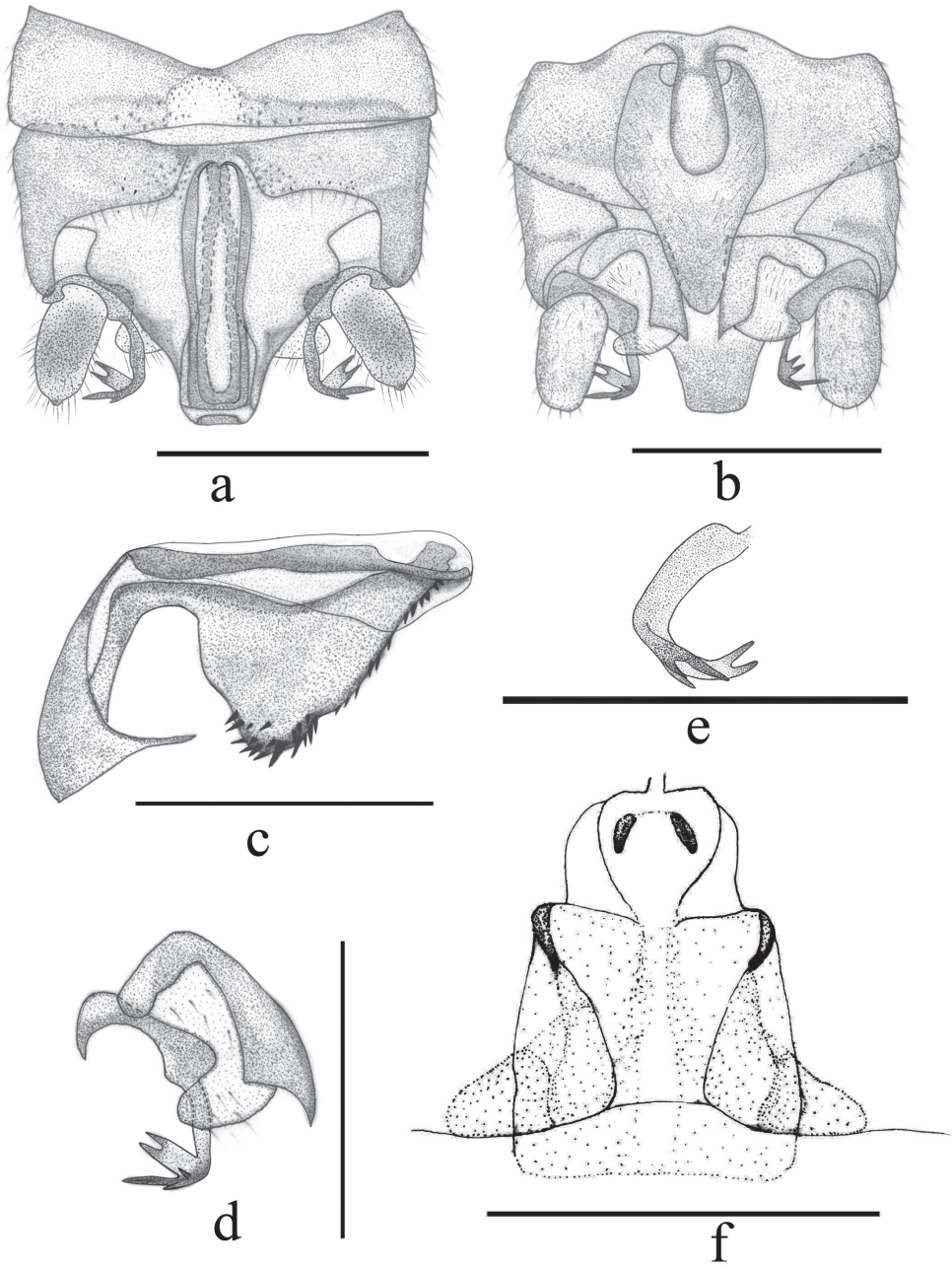

Figure 2. *Indonemoura quadrata* sp. n. (**a–e** male, **f** female) **a** terminalia, dorsal view **b** terminalia, ventral view **c** epiproct, lateral view **d** right paraproct, ventral view **e** right paraproct, spines of outer lobe, lateral view **f** inner genitalia, dorsal view. Scale bars: 0.5 mm.

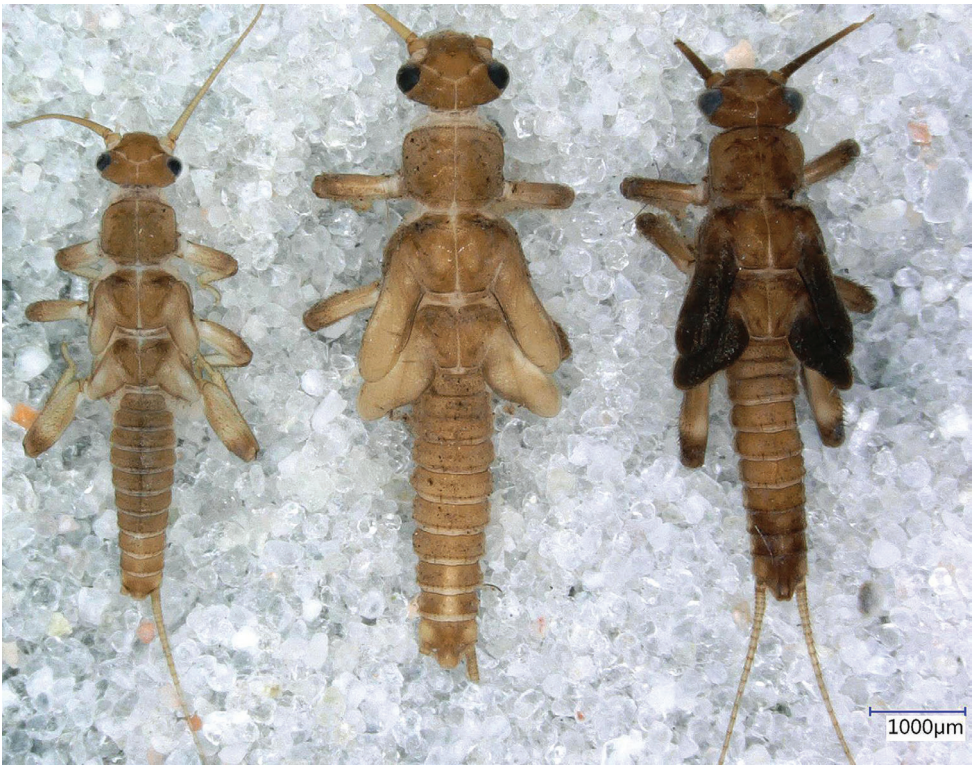

Figure 3. *Indonemoura quadrata* sp. n. penultimate, ultimate, and pharate male larvae (from left to right).

(Fig. 2b) with claviform vesicle, slightly constricted basally; hypoproct broad and subquadrate at basal half, then gradually tapering toward tip, and covered by dense hairs. Tergum X mostly sclerotised, with narrow longitudinal concavity beneath epiproct. Cercus slightly sclerotised, nearly cylindrical with distinct hairs and a black oval process at tip, length varies ca. 2–3× width. Epiproct (Fig. 2a, c) basal half nearly parallel-sided, apical half slightly enlarged in dorsal view, with distinct apical incision; ventral sclerite strongly sclerotised, broad at base and becoming narrower toward apex, expanded ventrally into a very large semicircular ridge with rows of black spines, and the middle of ventral sclerite with two incisions forming a small semicircular process. Paraproct (Figs 1c–e, 2a, b, d, e) divided into three lobes: inner lobe sclerotised and slender, adhering to median lobe and mostly hidden by hypoproct then hardly observed; inner portion of median lobe sclerotised forming a hook-like structure with sharp tip, and remainder membranous with dense hairs at the apex; outer lobe darkly sclerotised, much longer than median lobe with two subapical prongs; the outer flat prong pale brown and curved ventrad, bifurcate apically; the inner prong much slim, forked subapically with a shorter spine ca. 1/3 of other spine.

Female (Figs 1f, 2f). Sternum VII membranous, two dark inner sclerite belonging to inner genitalia easily detected by transparency. Sternum VIII with large quadrate sclerotised subgenital plate covering the entire length, posterior margin slightly concaved, slightly overlapping the anterior margin of sternum IX, paired paragenital plate is pale brown and triangular, located at the posterolateral corner of the subgenital plate, inner portion fused with subgenital plate, being dark brown and nearly semicircular which also can be seen by transparency. Sternum IX sclerotised anteriorly forming a produced arch shaped extension. Sternum X and paraproct typical. Inner genitalia mostly membranous, anterolateral margin of subgenital plate with a pair of curved thin sclerites; a large, beneath the spermathecal ductus with a pair of slender central sclerite.

Mature larva (Figs 3, 4): Body relatively slender, body length without antennae and cerci 5.5–7.5 mm. General colour brown, with contrasting pale pattern on terminal segments of abdomen, less distinct dark brown pattern on thorax and distinct bands on the femora. Terminal pattern consists of paired lateral and a posteromedial light patch on tergum X (Fig. 3 penultimate and ultimate larvae), and medial light patches on terga VIII–IX; dark bands on femora occupies distal fourth. Antennae, mouth parts and cerci pale, as well as ventral aspect of the body. Setation long but less distinct. Legs moderately long, width of hind femora more than 1/3 of their length. The pronotum is trapezoidal with rounded corners, wider than long, as wide as head. Cervical gills shorter than the length of cervical sclerite where the gill is attached. Wing pads twice as long as the corresponding segments. Abdomen relatively slender, integument light matt brown, first five abdominal segments terga and sterna entirely divided by pleura, next two partly divided by pleura. Posterior margin of sternum IX of the male larva shortly rounded, sternum VIII of female larva slightly incised; paraprocts blunt. Cerci long, with 30–32 cylindrical segments; length of the 15th segment is ca. two times of its width.

Setation of the larva (Fig. 4): Head, antennae and palpi with dense short setae. Pronotum covered with very short setae; marginal setae distinct and blunt, row continuous but setae in anteromedial and posteromedial half, corners have the longest setae that are as long as one 20th of pronotum width (Fig. 4a). Setae on meso- and metanotum short, as long as marginal setae on pronotum; wing pads with short, acute setae. Legs with dense setation, all tibia bears indistinct swimming hairs shorter than femur width (Fig. 4b). Longest acute setae of all outer femur margins are longer than fourth of the corresponding femur width, not arranged in line but restricted to apical half. Tarsi and claws typical. Tergal segments covered with short setae of different width; row of posterior margin with distinctly longer, acute paired setae reaching ca. third of segment length, but on posterior terga more, similar long setae occur; paired setae slightly raised in lateral view (Fig. 4c–e). Cercal segments with sparse and indistinct intercalary setation but apical setae dense and relatively long; cercomeres 14–16 with an apical whorl of 10–12 acute setae that are as long as 2/3 of segment length (Fig. 4f).

Type material. Holotype: 1 male (HIST), China: Guangxi Province, Wuming County, Damingshan National Natural Reserve, stream and seep beneath Golden Turtle Waterfall, 1150 m, 23°30.373'N, 108°26.141'E, 2015.III.21, leg. J Kontschán, JN Li, S Li, WH Li, D Murányi, GQ Wang. Paratypes: 2 males and 1 female (HIST), 1 male, 3

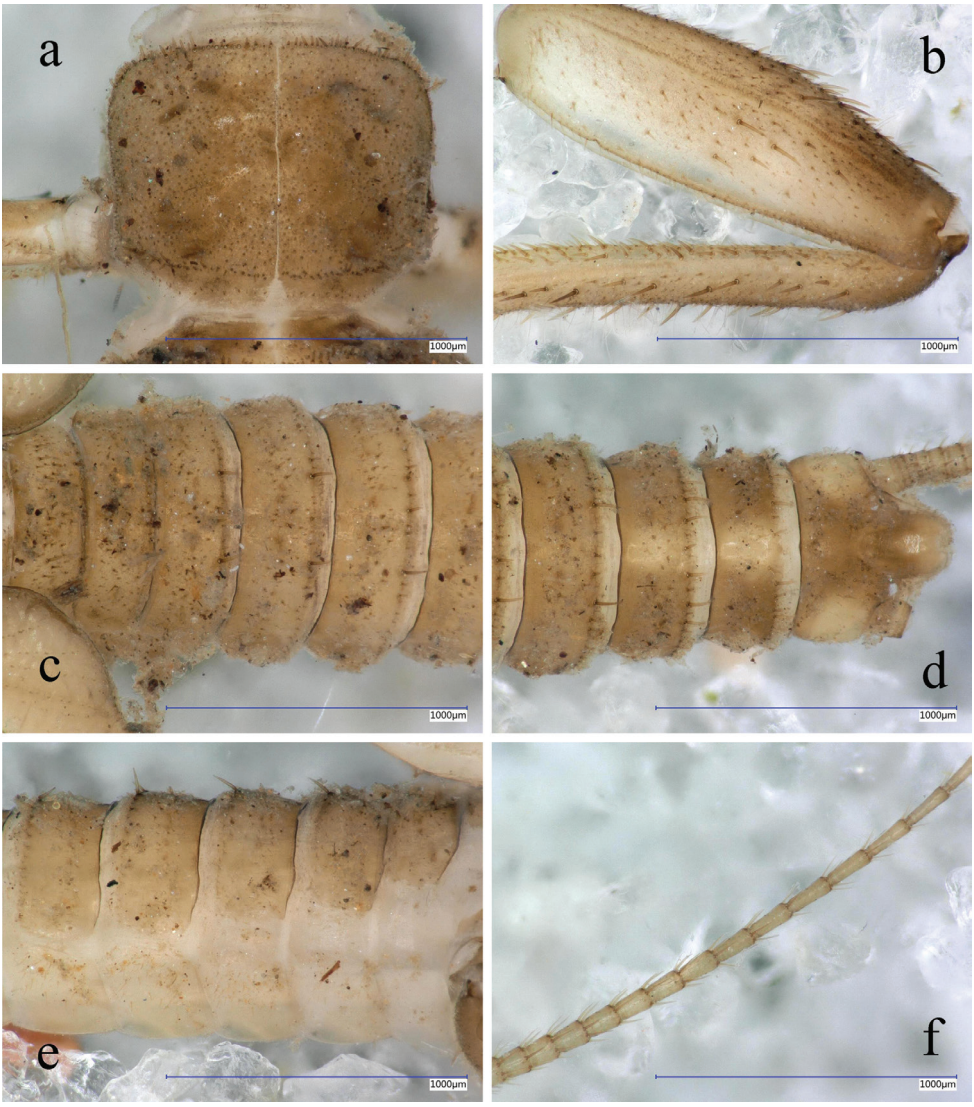

Figure 4. *Indonemoura quadrata* sp. n. matured larvae **a** pronotum, dorsal view **b** left hind leg, outer face **c** terga I–V , dorsal view **d** male terminalia, dorsal view **e** terga I–V , lateral view **f** cercomeres 10–22, dorsal view.

pharate male and 2 pharate female larvae, 18 penultimate and ultimate instar larvae, and 1 exuviae (HNHM), same data as holotype; Guangxi Province, Wuming County, Damingshan National Natural Reserve, inflow stream above Dragon Lake, 1225 m, 23°29.751'N, 108°26.242'E, 2015.III.22, leg. J Kontschán, JN Li, S Li, WH Li, D Murányi, GQ Wang: 2 males (one with its exuviae), 3 ultimate instar larvae, and 1 exuviae (HNHM).

Etymology. The specific name refers to the sternum VIII of female with quadrate subgenital plate.

Distribution. China (Guangxi).

Ecology. The species was found only on the plateau of the Daming Mountains, inhabiting the same two habitats where the recently described *Cryptoperla teana* Li & Murányi, 2018 was collected (Fig. 10a, b). These two species, as well as *Rhopalopsole triangulis* Li, Murányi & Yang, 2017 (in Li et al. 2017c) seem to be connected to the 'tea-coloured' waters of the Damingshan plateau. March is the beginning of its emergence period, since many penultimate and ultimate stage larvae were still in the hygropetric water layer, while only a few pharate and emerged adults were found.

Remarks. *Indonemoura quadrata* is a member of the *fujianensis* complex which is characterised by ventral sclerite of epiproct with a wide, semicircular structure in lateral view. There are nine species in the *fujianensis* complex (Sivec and Stark 2010); including seven recorded from China: *I. auriformis* Li & Yang, 2008a, *I. baishanzuensis* Li & Yang, 2006, *I. fujianensis* Li & Yang, 2005, *I. guangdongensis* Li & Yang, 2006, *I. hubeiensis* Yang & Yang, 1991, *I. macrolamellata* (Wu, 1935), and *I. yangi* Li & Yang, 2006; *I. clavata* Sivec & Stark, 2010 and *I. tricantha* Sivec & Stark, 2010 have been described from Vietnam. The members of the complex can also be distinguished from the basis of the outer lobe of paraproct, that is elongated, slender, and armed with spikes.

Indonemoura quadrata is most similar to *I. fujianensis* Li & Yang, 2005 from Fujian both in number of spines on the outer lobes of left and right paraprocts. However, the new species may be easily separated from *I. fujianensis*: ventral sclerite of epiproct with an apical semicircular projection in lateral view; outer lobe with two prongs at apex, and both bifurcate subapically; the outer prong is flat and the size of spines approximately equal; the inner prong's spines with different length; especially, outer lobe of right paraproct added a black spine at distal half which cannot be seen on the left paraproct. In *I. fujianensis*, apical spines of the outer lobe number three and two on the left and right paraprocts respectively (Li and Yang 2005: figs 2, 5). This species also easily confused with *I. auriformis* by the dorsal view of terminalia because of the same inner prong of the outer paraproct lobe, especially when the outer prong of the outer lobe is hardly observed sometimes due to its paler colour and more or less erect position (Li and Yang 2008a: figs 8, 11). Among the congeners where females are known, the female of *I. quadrata* is distinctive by its regular quadrate subgenital plate. Hitherto only two congeners, the Himalayan *I. adunca* (Harper, 1974) and *I. indica* (Kimmins, 1947) are known in the larval stage (Sivec 1981). On the basis of these two Himalayan species, the two species described herein and a further larva that we recently reported from Shaanxi as *Indonemoura* sp. (Li et al. 2018), there are no distinctive generic character to distinguish *Indonemoura* larvae from those of *Mesonemoura* Baumann, 1975. Both genus can be characterised by the presence of single, short cervical gills, posterior row of setae on terga having longer paired setae, and long setae on femora not arranged in line. The larva of *I. quadrata* can be distinguished from the few known congeners on the basis of characteristic pale and dark pattern on terga VIII–X. However, similar pattern was observed on the Shaanxi larvae, suggesting the pattern is not a specific character.

***Indonemoura quadrispina* sp. n.**
http://zoobank.org/1C0796EA-5B4D-4127-9EDF-969693F01BEE
Figs 5–8, 10c

Indonemoura sp. n.: Gamboa et al. 2019: S1 Table, using the sequence of the present specimens in phylogeny analysis.

Adult habitus (Fig. 5a). Medium sized species, forewing length in males 5.6–6.2 mm, females 6.5 mm. General colour brown. Head, mouth parts and legs dark brown; antennae brown; compound eyes dark. Thorax including pronotum dark brown; pronotum (Fig. 5a) nearly trapezoidal, corners bluntly round, lateral margins light brown, midlateral portion with dark rugosity. Wings brownish, subhyaline with dark veins. Abdominal segments brownish but terminalia darker with hairs light brown.

Male terminalia. Tergum IX (Fig. 6a) distinctly sclerotised anteriorly, with a large triangular mid-posterior incision. Sternum IX (Fig. 6b, c) with claviform vesicle; vesicle mostly membranous except anterior and lateral margins sclerotised, with an oval mid-anterior membrane, length greater than 4× width; hypoproct broad and nearly rectangular at basal half, then gradually tapering to a nipple-like tip. Tergum X distinctly sclerotised, with a deep median concavity present beneath epiproct, and a pair of upraised triangular process present mesolaterally. Cercus slightly sclerotised and nearly cylindrical, with many clothing hairs, length ca. 2.5× width. Epiproct (Figs 5b–d, 6a, c) recurved and long; dorsal sclerite nearly gourd-shaped and basal half roughly circular, slightly constricted medially, rectangular subapically, then distinctly tapering toward sharp tip; ventral sclerite strongly sclerotised, broad at base and becoming narrower toward apex, expanded ventrally into a straight ridge with rows of spines before fusing with dorsal sclerite; bearing a pair of dark thorn-like subapical structures. Paraproct (Figs 5b, e, f, 6a–d) divided into three lobes: inner lobe sclerotised, slender and rectangular basally, with an acute tip; median lobe mostly sclerotised and broad at base with a large triangular distal denticle at inner portion and a large, forked spine subapically, distinctly curved inward apically at outer margin; outer lobe strongly sclerotised, horn-shaped with a small projection near mid-point.

Female (Fig. 7). Sternum VII membranous, with two dark markings at its inner and median portion, as inner genitalia structures appear by transparency. Sternum VIII with wide, bicolored subgenital plate covering two third of length and slightly overhanging, its width is more than two thirds of segment's width; paired paragenital plate small and rounded, indistinct, attached to posterolateral sides of the subgenital plate. Lateral portions of the subgenital plate dark brown, medial area light and posteriorly narrowing; posterior margin laterally rounded and medially slightly concave. Sternum IX lightly sclerotised, anterior margin overlapped by the subgenital plate. Sternum X and paraproct typical. Inner genitalia mostly membranous, with two small lateral sclerites attached to the anterolateral edges of the subgenital plate, and a large, bulbous structure beneath spermathecal ductus, involving a pair of small central sclerite; genital opening narrow.

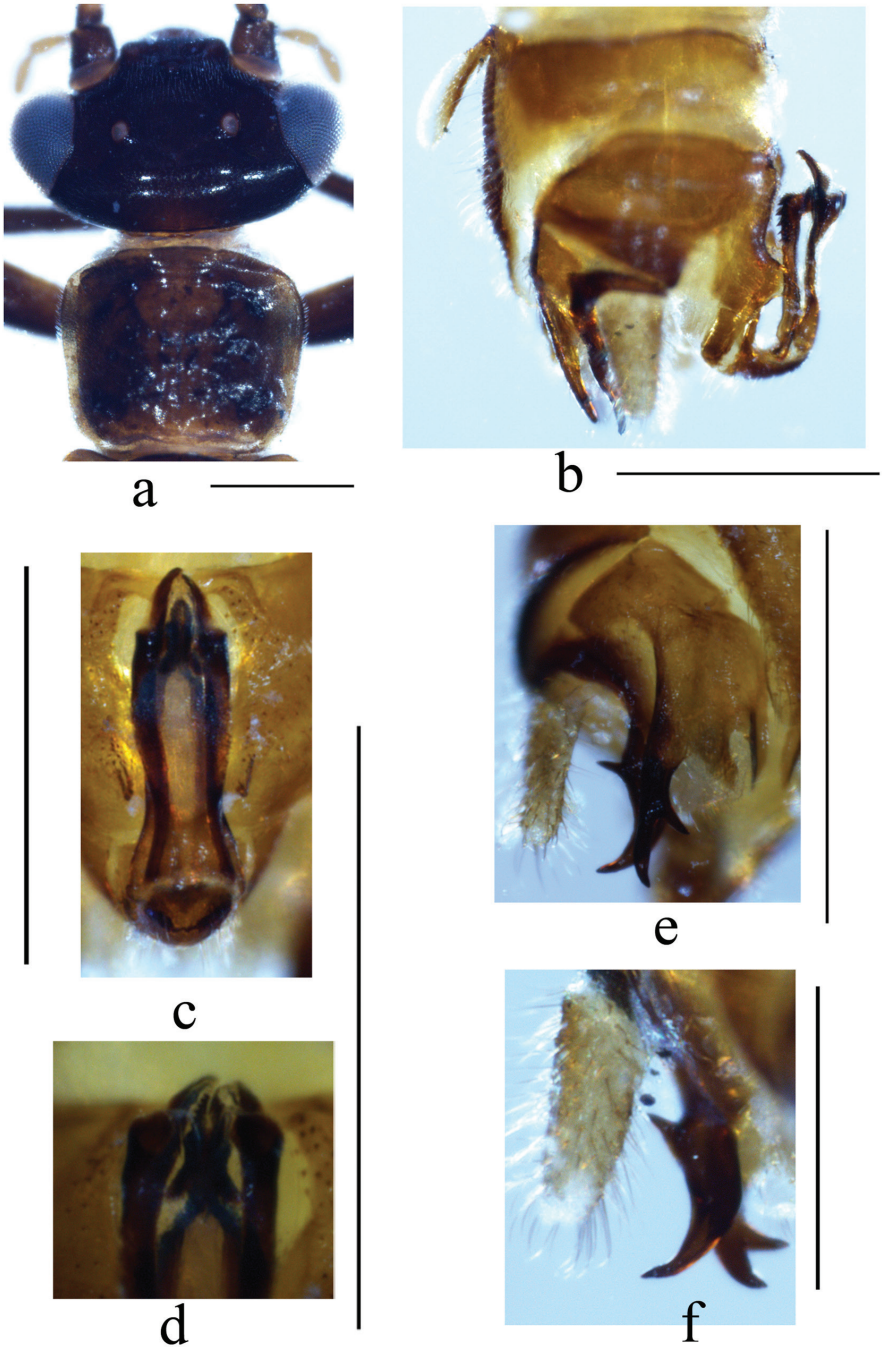

Figure 5. *Indonemoura quadrispina* sp. n. (male) **a** head and pronotum, dorsal view **b** terminalia, lateral view **c** epiproct, dorsal view **d** apex of epiproct, caudal view **e** right paraproct, ventral view **f** apex of mesal and outer left paraproct lobes, dorsal view. Scale bars: 0.5 mm.

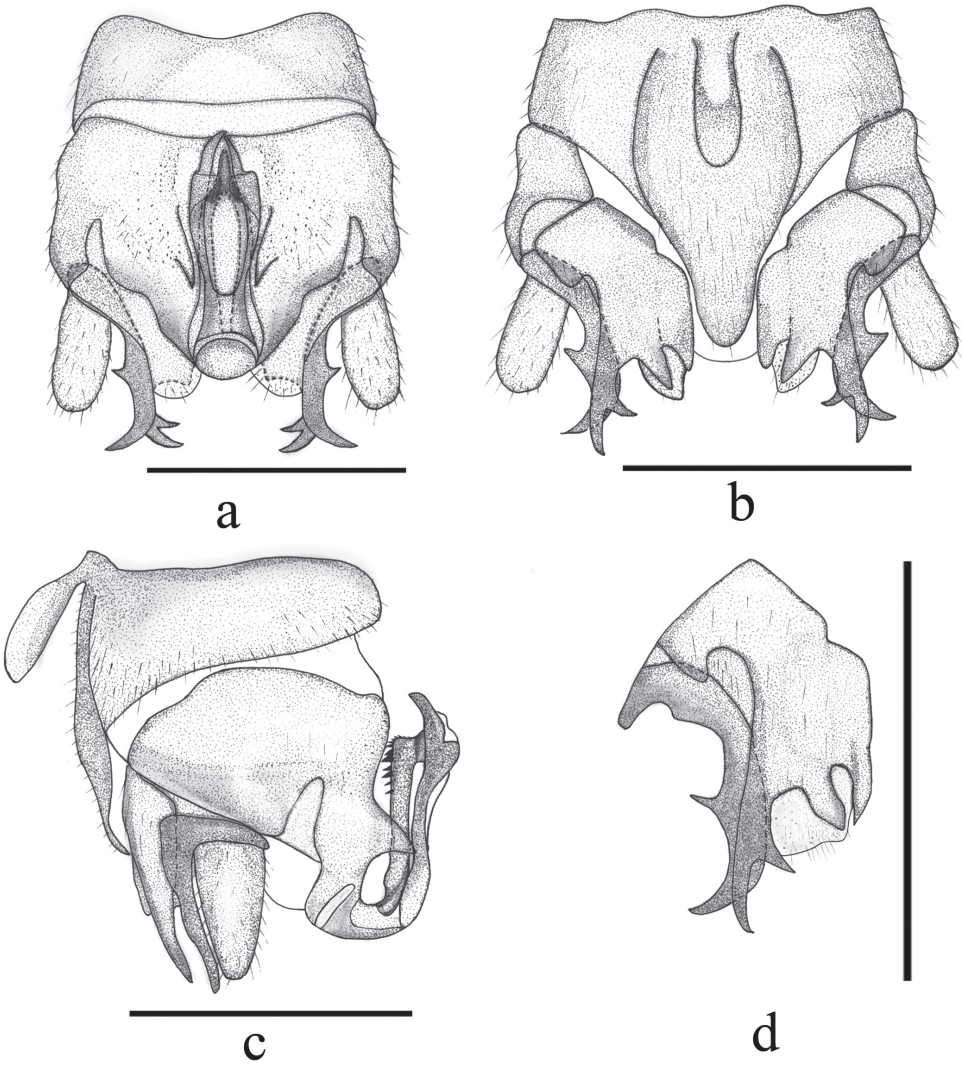

Figure 6. *Indonemoura quadrispina* sp. n. (male) **a** terminalia, dorsal view **b** terminalia, ventral view **c** terminalia, lateral view **d** right paraproct, ventral view. Scale bars: 0.5 mm.

Mature larva (Fig. 8): Body relatively slender, body length without antennae and cerci 4.8–5.2 mm. General colour brown, with indistinct dark brown pattern on thorax and slightly darker apical third on femora. Antennae, mouth parts and cerci pale, as well as ventral aspect of the body. Setation short and indistinct on the body but legs and cerci armed with longer setae. Legs moderately long, width of hind femora more than 1/3 of their length. The pronotum is trapezoidal with rounded corners, wider than long, as wide as head. Cervical gills shorter than the length of cervical sclerite where the gill is attached. Wing pads twice as long as the corresponding segments.

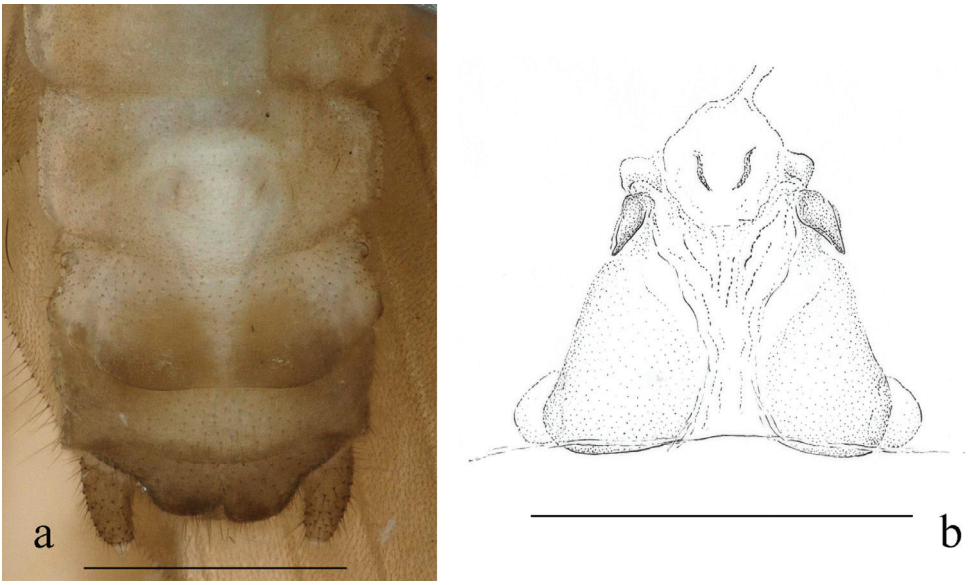

Figure 7. *Indonemoura quadrispina* sp. n. (female) **a** terminalia, ventral view **b** inner genitalia, dorsal view. Scale bars: 0.5 mm.

Abdomen slender, integument yellowish matt brown, first six abdominal segments completely, tergum VII partly divided by pleura. Posterior margin of sternum IX of the male larva sharply triangular in the middle, sternum VIII of female larva slightly incised; paraprocts slightly elongated but apex blunt. Cerci long, with 29–32 cylindrical segments; length of the 15th segment is ca. two times of its width.

Setation of the larva (Fig. 8): Head, antennae, and palpi with moderately dense, short setae. Pronotum covered with very short and scarce setae; marginal setae very short and blunt, of which bases are narrower than the rounded apices, row interrupted in anteromedial and posteromedial fifth, corners have the longest setae that are as long as one 35th of pronotum width (Fig. 8a). Setae on meso- and metanotum slightly longer than marginal setae on pronotum; wing pads with very short, blunt setae. Legs with scarce setation, all tibia bears indistinct, scarce swimming hairs as long as half of femur width (Fig. 8e, f). Longest acute setae on fore femora as long as half of femur width, while on hind femora only as one third of femur width; long setae not arranged in line, restricted to mediodorsal area. Tarsi and claws relatively long. Tergal segments covered with very short setae; row of posterior margin with slightly longer, blunt paired setae reaching ca. one seventh of segment length, but on posterior terga more, similar long setae occur (Fig. 8c, d). Cercal segments with sparse but relatively long intercalary setation, apical setae dense and relatively long; cercomeres 14–16 with an apical whorl of 9–11 acute setae that are longer than half of segment length (Fig. 8b).

Type material. Holotype: 1 male (HIST), China: Guangxi Zhuang Autonomous Region, Shangsi County, Shiwandashan National Natural Reserve, forest seep by the

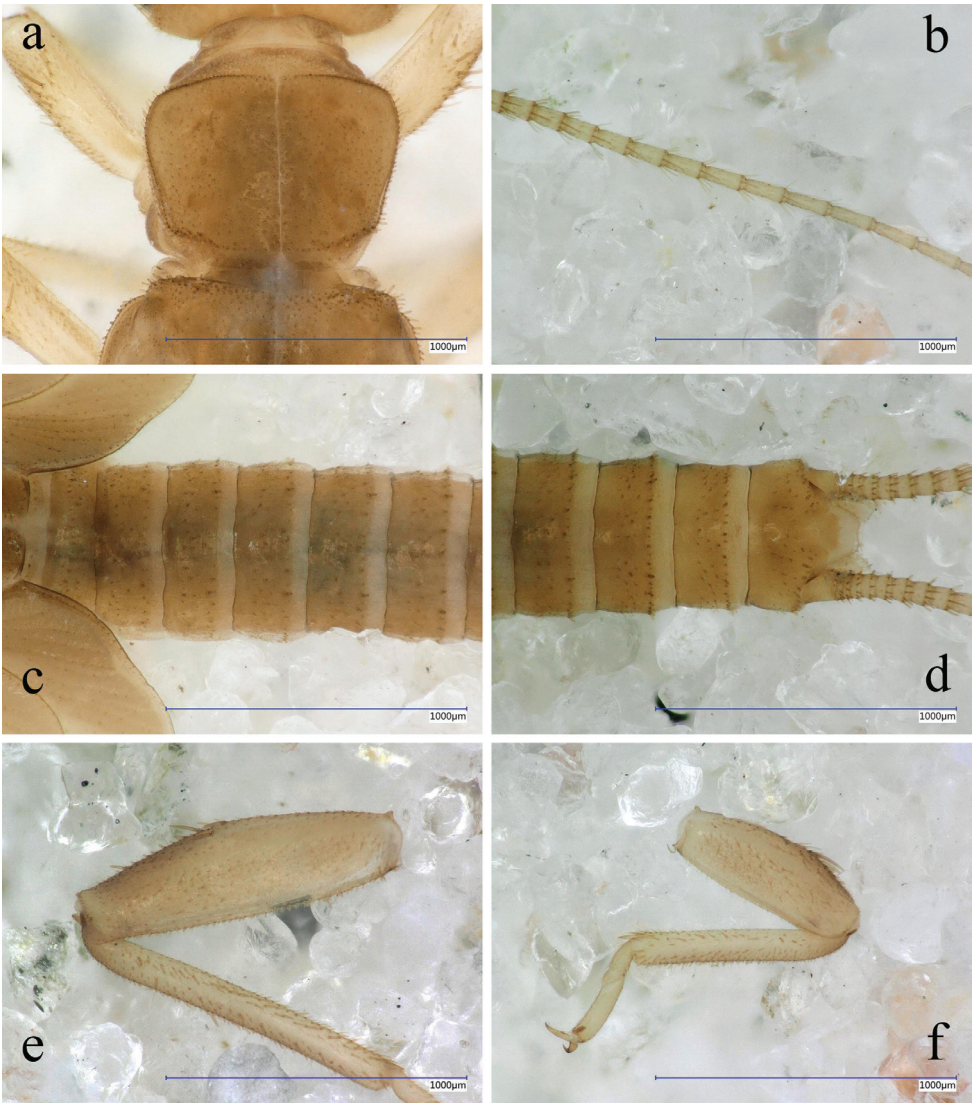

Figure 8. *Indonemoura quadrispina* sp. n. matured male larva **a** pronotum, dorsal view **b** cercomeres 10–21, dorsal view **c** terga I–VI , dorsal view **d** terminalia, dorsal view **e** right hind leg, outer face **f** right foreleg, outer face.

Pearl River, 265 m, 21°54.216'N, 107°54.240'E, 2015.III.27–29, leg. J Kontschán, JN Li, S Li, WH Li, D Murányi, GQ Wang. Paratypes: 2 males and 1 female, 2 pharate male larvae, 3 ultimate instar larvae (HNHM), same data as holotype.

Etymology. The specific name is a noun in apposition, referring to four apical spines on the median lobe and outer lobe of the paraproct.

Distribution. China (Guangxi).

Ecology. The species was found only in a small forest seep by the Pearl River in the Shiwandashan National Natural Reserve (Fig. 10c). The seep is having sandy or fine gravel substrate with plenty of organic materials like fallen leaves. Besides the new species, adults of *Rhopalopsole cestroidea* Li, Murányi & Gamboa, 2017 (in: Li et al. 2017c), *Amphinemura hainana* Li & Yang, 2008d and *A. hamiornata* Li & Yang, 2008c were also collected beaten from the riparian plants around the seep. However, only larvae of the new species were found in the water, and other adult stoneflies probably emerged from the Pearl River flowing only a few meters far from the seep. March seems to be the main season of its emergence, since more adults than larvae were found.

Remarks. The new species seems to be most similar to *I. curvicornia* Wang & Du, 2009 described from Zhejiang in the dorsal aspect of the long and narrow epiproct and similar outer lobe of paraprocts, especially the horn-shape of outer lobe with a small projection at apical half. However, the new species may be separated from *I. curvicornia* by its dorsal sclerite gourd-shaped in dorsal view and ventral sclerite of epiproct with straight ridge in lateral aspect; median lobe with a subtriangular denticle at apical inner portion and its outer portion is forked subapically. In *I. curvicornia*, the ventral sclerite of slim epiproct with narrow keel; median lobe membranous at inner portion and its outer portion slim and unforked apically (figs 15–19, 21 in Wang and Du 2009). Similar bifurcate median paraproctal lobes also occur in *I. trichotoma* Li & Yang, 2008b from Yunnan Province, but it is easily separated from that species by the forked outer paraproctal lobe and the spineless hypoproctal apex (comparing Figs 6–7 in Li and Yang 2008b and Figs 3b, e, f, 4a–d). The female of *I. quadrispina* is less distinctive, simple subgenital plate is similar to several congeners, e.g *I. clavata* Sivec & Stark, 2010 or the *I. scalprata* female described below. It can be distinguished from the latter on the basis of bicolored, wider, and less concave subgenital plate. The larva can be easily distinguished from known larvae of congeners on the basis of its very short tergal setation.

Indonemoura scalprata **(Li & Yang, 2007)**

Figs 9, 10d

Amphinemura scalprata: Li and Yang 2007: 61 (original description of the male from Guangdong).

Indonemoura scalprata: Yang et al. 2015: 284 (comb. n. and first record from Fujian).

Indonemoura scalprata: Gamboa et al. 2019: S1 Table, using the sequence of the present specimens in phylogeny analysis.

Description of the female (Fig. 9). Forewing length 6.5–7.2 mm; coloration similar to male. Sternum VII membranous, lacks pregenital plate. Sternum VIII with wide, entirely brown subgenital plate covering more than two third of length and slightly overhanging, its width is less than two thirds of segment's width; paired paragenital plate relatively large but indistinct, rounded triangular, weakly attached to lateral sides of the subgenital plate. Posterior margin of the subgenital plate laterally rounded and

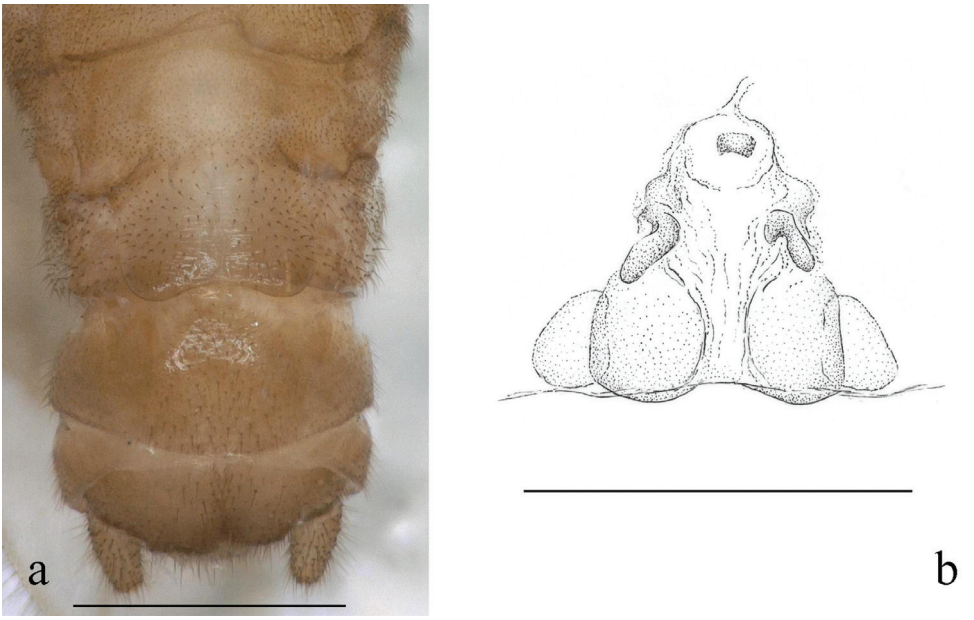

Figure 9. *Indonemoura scalprata* (Li & Yang, 2007) (female) **a** terminalia, ventral view **b** inner genitalia, dorsal view. Scale bars: 0.5 mm.

medially slightly concave. Sternum IX lightly sclerotised, anterior margin overlapped by the subgenital plate. Sternum X and paraproct typical. Inner genitalia mostly membranous, with two small lateral sclerites attached to the anterolateral edges of the subgenital plate, and a medium sized, bulbous structure beneath spermathecal ductus, involving a central sclerite ring; genital opening narrow.

Material examined. China: Guangxi Zhuang Autonomous Region, Wuming County, Liangjiang Town, Neichao, Neichao River above Neichao Ming Hotel, 220 m, 23°29.664'N, 108°21.622'E, 2015.III.24, leg. JN Li, S Li, WH Li, D Murányi: 1 male and 3 females (HNHM); the same locality, 230 m, 23°29.457'N, 108°21.600'E, 2017.VII.13, leg. RR Mo, Y Lai: 1 male (HIST); China: Guangxi, Laibin City, Jinxiu County, Dayaoshan National Nature Reserve, Yinshan Park, 1210 m, 24°16.133'N, 110°36.924'E, 2012.IV.8. Leg. WH Li: 1 male (HIST).

Distribution. China (Fujian, Guangdong, and Guangxi).

Ecology. In Guangxi, the species was found in a large, rocky stream by the foothills of the Damingshan (Fig. 10d). Other adult stoneflies collected at the locality are *Rhopalopsole sinensis* Yang & Yang, 1993 and a yet undescribed *Amphinemura* sp. Not any Euholognatha larvae were found, but several larvae and exuviae of Perlidae (*Agnetina* sp., *Neoperla* sp., *Togoperla* sp.). All the *I. scalprata* specimens were fully coloured, indicating that emergence period was past its peak.

Remarks. The female of *I. scalprata* is less distinctive, similar to the female of *I. quadrispina* as described above.

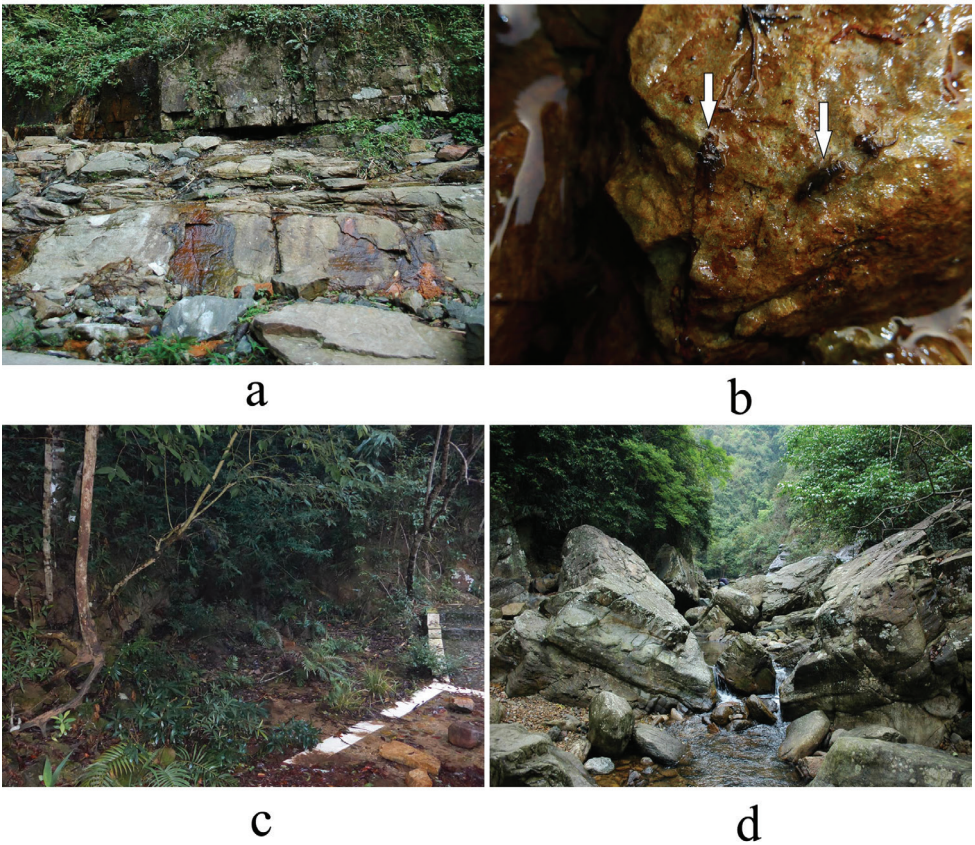

Figure 10. Habitats of *Indonemoura* from Guangxi **a** type locality of *I. quadrata* sp. n., Damingshan N.N.R. **b** exuviae (left arrow) and larva (right arrow) of *I. quadrata* sp. n. in the hygropetric water at the type locality **c** type locality of *I. quadrispina* sp. n., Shiwandashan NNR **d** habitat of *I. scalprata* (Li & Yang, 2007), Neichao.

Concluding remarks

Previous studies on the genus *Indonemoura* from Guangxi were explained by Li and Yang, who described *I. voluta* from Mountain Mao'ershan of Guilin (Li and Yang 2008b) and *I. yangi* from Mountain Jiuwandashan of Huanjiang (Li and Yang 2006). Recently, one new species *I. furcoloba* was added from Mountain Shengtang in Jinxiu by Li et al. (2017b). There was no record of this genus in previous works on the insect fauna of the Damingshan National Natural Reserve and Shiwandashan National Natural Reserve (Du and Sivec 2004). In this study, two additional new species are described and one new record for Guangxi is recorded from these two ranges. Therefore, there are up to six known *Indonemoura* species from Guangxi. The five species that were described from Guangxi are not yet known out of the region, while *I. scalprata* was originally described from the bordering Guangdong Province, and is also found in Fujian Province (Li and Yang 2007, Yang et al. 2015).

Acknowledgments

The research was partially supported by the National Natural Science Foundation of China (No. 31372251), the Aid program for Science and Technology Innovative Research Team in higher Educational Institutions of Henan Province (17IRTSTHN18), and the landmark Innovative Project of Institute of Science and Technology (No. 2015BZ04).

References

Baumann R-W (1975) Revision of the stonefly family Nemouridae (Plecoptera): A study of the world fauna at the generic level. Smithsonian Contributions to Zoology 211: 1–74. https://doi.org/10.5479/si.00810282.211

DeWalt R-E, Maehr M-D, Neu-Becker U, Stueber G (2018) Plecoptera Species File Online. Version 5.0/5.0. http://Plecoptera.Species.File.org [Accessed 20 Jul 2018]

Du Y-Z, Sivec I (2004) Plecoptera: Perlidae, Nemouridae, Leuctridae. In: Yang XK (Ed.) Insects from Mt. Shiwandashan area of Guangxi. China Forestry Publishing House, Beijing, 39–45.

Fochetti R, Ceci M (2016) *Indonemoura annamensis*–a new species of stonefly from Vietnam (Plecoptera: Nemouridae). Zootaxa 4121(1): 85–88. https://doi.org/10.11646/zootaxa.4121.1.8

Gamboa M, Murányi D, Kanmori S, Watanabe K (2019) Molecular phylogeny and diversification timing of the Nemouridae family (Insecta, Plecoptera) in the Japanese Archipelago. PloS ONE 14(1): e0210269. https://doi.org/10.1371/journal.pone.0210269

Harper P-P (1974) New *Protonemura* (s.l.) from Nepal (Plecoptera; Nemouridae). Psyche 81(3–4): 367–376. https://doi.org/10.1155/1974/57825

Kimmins D-E (1947) New species of Himalayan Plecoptera. The Annals and Magazine of Natural History 11(13): 721–740.

Li W-H, Murányi D (2018) A new species of *Cryptoperla* Needham, 1909 (Plecoptera: Peltoperlidae) from Guangxi of China, based on male, female, and larval stage. Zootaxa 4455(1): 177–188. https://doi.org/10.11646/zootaxa.4455.1.8

Li W-H, Yang D (2005) Two new species of *Indonemoura* (Plecoptera: Nemouridae) from Fujian, China. Zootaxa 1001: 59–63. https://doi.org/10.11646/zootaxa.1001.1.4

Li W-H, Yang D (2006) The genus *Indonemoura* Baumann, 1975 (Plecoptera: Nemouridae) from China. Zootaxa 1283: 47–61.

Li W-H, Yang D (2007) Review of the genus *Amphinemura* (Plecoptera: Nemouridae) from Guangdong, China. Zootaxa 1511: 55–64. https://doi.org/10.11646/zootaxa.1511.1.4

Li W-H, Yang D (2008a) Two new species and two new records of stonefly family Nemouridae from Henan (Plecoptera: Nemouroidea). In: Shen X, Lu C (Eds) The Fauna and Taxonomy of Insects in Henan 6. China Agricultural Science and Technology Press, Beijing, 11–16.

Li W-H, Yang D (2008b) Two new species of *Indonemoura* (Plecoptera: Nemouridae) from China, with redescription of *Indonemoura longiplatta* (Wu, 1949), comb. n. Aquatic Insects 30: 97–103. https://doi.org/10.1080/01650420701882988

Li W-H, Yang D (2008c) New species of Nemouridae (Plecoptera) from China. Aquatic Insects 30: 205–221. https://doi.org/10.1080/01650420802334038

Li W-H, Yang D (2008d) A new species of *Amphinemura* (Plecoptera: Nemouridae) from China. Zootaxa 1892: 65–68.

Li W-H, Wu L-M, Yang D (2017a) Two new species of *Indonemoura* (Plecoptera: Nemouridae) from Yunnan Province of southwestern China. Zootaxa 4231: 289–295. https://doi.org/10.11646/zootaxa.4231.2.11

Li W-H, Yang D, Sivec I (2005) Two new species of *Indonemoura* (Plecoptera: Nemouridae) from China. Zootaxa 893: 1–5. https://doi.org/10.11646/zootaxa.893.1.1

Li W-H, Zhang Q, Yang D, Yao G (2017b) A new Chinese species of *Indonemoura* (Plecoptera: Nemouridae) and a new subspecies of *I. nigrihamita* Li & Yang. Zootaxa 4311: 255–262. https://doi.org/10.11646/zootaxa.4311.2.6

Li W-H, Mo R-R, Dong W-B, Yang D, Murányi D (2018) Two new species of *Amphinemura* (Plecoptera: Nemouridae) from south Qinling Mountains of China based on male, female and larvae. ZooKeys 808: 1–21. https://doi.org/10.3897/zookeys.808.29433

Li W-H, Murányi D, Gamboa M, Yang D, Watanabe K (2017c) New species and records of Leuctridae (Plecoptera) from Guangxi, China, on the basis of morphological and molecular data, with emphasis on *Rhopalopsole*. Zootaxa 4243(1): 165–176. https://doi.org/10.11646/zootaxa.4243.1.8

Shimizu T (1994) *Indonemoura nohirae* (Okamoto, 1922), comb. nov. (Plecoptera, Nemouridae) newly recorded from Japan, with a redescription of *Amphinemura longispina* (Okamoto, 1922). Japanese Journal of Entomology 62: 619–627.

Sivec I (1981) Some notes about Nemouridae larvae (Plecoptera) from Nepal. Entomologica Basiliensia 6: 108–119.

Sivec I, Stark B-P (2010) Eleven new species of the genus *Indonemoura* Baumann (Plecoptera: Nemouridae) from Thailand and Vietnam. Illiesia 6(14): 210–226.

Wang Z-J, Du Y-Z (2009) Four new species of the genus *Indonemoura* (Plecoptera: Nemouridae) from China. Zootaxa 1976: 56–62.

Wang Z-J, Du Y-Z, Sivec I, Li Z-Z (2006) Records and descriptions of some Nemouridae species (Order: Plecoptera) from Leigong Mountain, Guizhou province, China. Illiesia 2: 50–56.

Wu C-F (1935) New species of stoneflies from East and South China. Bulletin of the Peking Society of Natural History 9: 227–243.

Wu C-F (1938) *Plecopterorum sinensium*: A monograph of stoneflies of China (Order Plecoptera). Yenching University, 225 pp.

Yang D, Yang C-K (1991) New species of Plecoptera from Hubei. Journal of Hubei University (Natural Science) 13: 369–372.

Yang D, Yang C-K (1993) New and little-known species of Plecoptera from Guizhou Province (III). Entomotaxonomia 15(4): 235–238.

Yang D, Li W-H, Zhu F (2015) Fauna Sinica, Insecta Vol. 58, Plecoptera: Nemouroidea. Science Press, Beijing, 518 pp.

Zhu F, Yang D, Yang C-K (2002) A new species of the genus *Indonemoura* Baumann (Plecoptera: Nemouridae) from Tibet. China Entomological Science 5: 317–320.

ZooKeys 825: 43–53 (2019)
doi: 10.3897/zookeys.825.29029
http://zookeys.pensoft.net

RESEARCH ARTICLE

A peer-reviewed open-access journal
ZooKeys
Launched to accelerate biodiversity research

New data of spiders (Arachnida, Araneae) of Cyprus. I. Dysderidae found in caves

Salih Gücel[1], Iris Charalambidou[2], Bayram Göçmen[3], Kadir Boğaç Kunt[4,5]

1 *Institute of Environmental Sciences and Herbarium, Near East University, Nicosia, Cyprus* **2** *Department of Life and Health Sciences, School of Sciences and Engineering, University of Nicosia, Cyprus* **3** *Department of Biology, Faculty of Science, Ege University, İzmir, Turkey* **4** *Department of Biology, Faculty of Science, Eskişehir Technical University, Eskişehir, Turkey* **5** *Zoological Collection of Cyprus Wildlife Research Institute, Taşkent, Kyrenia, Cyprus*

Corresponding author: *Salih Gücel* (sgucel@hotmail.com)

Academic editor: *Yuri Marusik* | Received 11 August 2018 | Accepted 14 January 2019 | Published 18 February 2019

http://zoobank.org/D9FC8D05-5A1F-4244-BBC5-A8074CA89B63

Citation: Gücel S, Charalambidou I, Göçmen B, Kunt KB (2019) New data of spiders (Arachnida, Araneae) of Cyprus. 1. Dysderidae found in caves. ZooKeys 825: 43–53. https://doi.org/10.3897/zookeys.825.29029

Abstract

This paper is the first in a series describing the previously unstudied cave spiders from Cyprus. Two new species, *Dysderocrates kibrisensis* **sp. n.** and *Harpactea kalavachiana* **sp. n.**, are described. Detailed morphological descriptions and diagnostic characteristics are presented. This is the first report of the genus *Dysderocrates* Deeleman-Reinhold & Deeleman, 1988 from Cyprus.

Keywords

Biospeleology, cavernicolous, island, Mediterranean, troglobiont

Introduction

The spider fauna of Cyprus, the third largest island of the Mediterranean, is poorly studied. One-hundred-fifteen species have been reported from the island (van Helsdingen 2018). The species diversity of the spider fauna on Cyprus, as compared to other Mediterranean islands, appears to be extremely low. For example, 555 species have been reported from Corsica, 523 from Sardinia, 421 from Sicily, 291 from Lesbos, 289 from Crete (van Helsdingen 2018), and approximately 315 species from Chios (Russell-Smith et al. 2011), an island in the Aegean that is a tenth the size of Cyprus. The distances of

Copyright *Salih Gücel et al.* This is an open access article distributed under the terms of the Creative Commons Attribution License (CC BY 4.0), which permits unrestricted use, distribution, and reproduction in any medium, provided the original author and source are credited.

these islands to source landmasses, as well as human influence, are crucial for explaining this difference; however, araneological studies in Cyprus are extremely few and limited.

To fill this gap, we have begun a survey of the spider fauna of the island. Here we present our findings from previously uninvestigated caves. We found two new species of the dysderid genera *Dysderocrates* and *Harpactea*, and describe them based on females. Males were not sampled because they are only present for a short time in populations and because of the relatively low densities of cave spider populations in general.

Materials and methods

Spider samples were collected from Beşparmak (Pentadactylos) and Saray (Palace) Caves (Fig. 1). Beşparmak Cave is approximately 500 m long and more than 200 m deep. The entrance is a small crack. After 5–6 m of crawling, there is a 3 m drop, and after this point, the cave is completely dark. The spider was found 50 m from the entrance in the second chamber. The temperature in this cave was approximately 17 °C. Saray Cave is a smaller cave, approximately 40 m long. The entrance is wide, and the cave is dark after 15 m, and after large boulders at 20 m, the cave is completely dark. The spider was found approximately 25 m from the entrance.

Figure 1. Collection localities.

Our specimens were preserved in 70% ethanol. Digital images of the copulatory organs were made with a Leica DFC295 digital camera attached to a Leica S8AP0 stereomicroscope. Between 5–15 photographs were taken at different focal planes and combined using Combine ZP (Hadley 2010). Terminology for the copulatory organs is adapted from Deeleman-Reinhold and Deeleman (1988), Deeleman-Reinhold (1993), and Chatzaki and Arnedo (2006). The number and disposition of spines follows the terminology of Özkütük et al. (2018). All measurements are given in mm.

The following abbreviations are used in the text and figures:

Carapace and abdomen:

AL	abdominal length;
CL	carapace length;
CWmax	maximum carapace width;
CWmin	minimum carapace width;
TL	total length.

Eyes:

AME	anterior median eyes;	AMEd	diameter of anterior median eyes;
PLE	posterior lateral eyes;	PLEd	diameter of posterior lateral eyes;
PME	posterior median eyes;	PMEd	diameter of posterior median eyes.

Chelicera:

ChF	length of cheliceral fang;
ChG	length of cheliceral groove;
ChL	total length of chelicera (lateral external view).

Legs:

Ta	tarsus;	Fe	femur;	pl	prolateral;
Mt	metatarsus,	Tr	trochanter;	rl	retrolateral;
Ti	tibia;	C	coxa;	v	ventral.
Pa	patella;	d	dorsal;		

Depository:

ETAM	Eskişehir Technical University, Arachnology Museum (Eskişehir, Turkey);
NMNU	Natural History Museum of Near East University (Nicosia, Cyprus);
ZMUT	Zoological Museum of the University of Turku (Turku, Finland).

Taxonomy

Family Dysderidae C.L. Koch, 1837

Genus *Dysderocrates* Deeleman-Reinhold & Deeleman, 1988

Type species. *Harpactocrates storkani* Kratochvíl, 1935, from Macedonia.

Dysderocrates kibrisensis sp. n.

http://zoobank.org/676DA5F8-6327-4035-964F-491568DD3444
Figures 2–6

Type. Holotype ♀ (NMNU); **CYPRUS**, Lefkoşa, Beşparmak Mountains, Beşparmak (Pentadactylos) Cave (35°17'22"N; 33°27'56"E), collected as a dead specimen inside the cave, ca 40 m from the cave entrance, 15.I.2018, leg. S. Gücel.

Comparative material. *Dysderocrates* cf. *regina* Deeleman-Reinhold, 1988: **TURKEY** 1♀ (ETAM), Konya, Beyşehir, Beyşehir Lake, Hacıakif Island (37°37'35.15"N; 31°28'55.66"E), 1183 m, 29.III.2011, leg. E.A. Yağmur (Fig. 7).

Dysderocrates tanatmisi Karakaş Kılıç & Özkütük, 2017: **TURKEY** 1♀ (ETAM), Antalya, Elmalı, Göltarla Village (36°34'38"N; 29°55'49"E), *Cedrus libani* forest, under stones, 1065 m, 24.XII.2015, leg. K.B. Kunt & E.A. Yağmur (Fig. 8).

Derivatio nominis. The specific name refers to the type locality "Kıbrıs", which is the Turkish name of Cyprus.

Diagnosis. *Dysderocrates kibrisensis* sp. n. can be differentiated from *D. silvestris* Deeleman-Reinhold, 1988 (spherical spermatheca) and *D. storkani* (pentagonal-shaped spermatheca) by the transverse spermatheca. The new species differs from *D. regina* by its longer spermatheca and triangular dorsal arch (*Da*, Fig. 7) and from *D. marani* (Kratochvíl, 1937) by its anchor-shaped spermatheca and the dorsal arch longer than spermatheca. The spermatheca of *D. kibrisensis* sp. n. is similar to those of *D. tanatmisi* but differs by the angular shape of the anterior part of the dorsal arch versus the semicircular shape of the same in *D. tanatmisi* (cf. Figs 5, 8).

Measurements of holotype. TL 17.00; AL 9.00; CL 8.00; CWmax 6.00; CWmin 4.80; AMEd 0.29; PLEd 0.21; PMEd 0.20; ChF 2.00; ChG 1.20; ChL 3.70. Leg measurements as shown in Table 1.

Description of holotype. Female. Carapace red, smooth. Cephalic region much narrower and darker than thoracic region (Fig. 2).

Eyes well developed (Figs 2, 3). Chelicerae blackish red. Labium and gnathocoxae blackish. Sternum reddish. Anterior part of sternum darker than posterior. Legs reddish orange. Coxae and trochanters of legs I–II darker than legs III–IV. Spines clumped prolaterally on leg I, uniformly distributed along a line on leg II (Fig. 4). Leg spination as shown in Table 2.

Table 1. Leg measurements of *Dysderocrates kibrisensis* sp. n.

Leg	C+Tr	Fe	Pa	Ti	Mt	Ta	Total
I	4.50	9.50	5.50	8.20	8.00	1.25	36.95
II	4.00	8.40	5.00	7.00	7.50	1.20	33.10
III	3.00	6.50	3.50	5.00	6.50	1.20	25.70
IV	3.50	8.50	3.50	6.70	8.30	1.25	31.75

Table 2. Leg spination of *Dysderocrates kibrisensis* sp. n.

♀	Fe	Ti	Mt
I	5, 5pl	0	0
II	1, 1, 2, 5pl	0	0
III	0–3d	2–3pl 2rl 1, 1 2v	4pl 3rl 1, 1, 2v
IV	8–10d	3pl 4rl 1, 1, 2v	5pl 7rl 1, 1, 2v

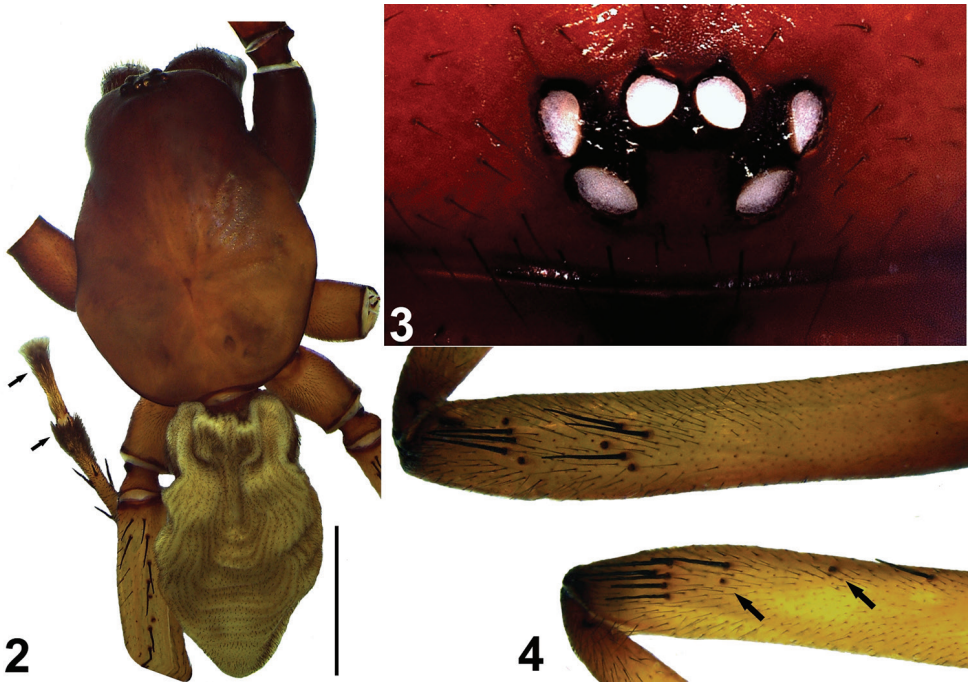

Figures 2–4. *Dysderocrates kibrisensis* sp. n. **2** Habitus of holotype female (arrows indicate tarsal and metatarsal scopulae) **3** Eyes **4** Femoral spination of anterior legs, left Leg I (above) right Leg II (below), prolateral view. Scale bar: 4 mm.

Tarsi and metatarsi III–IV with scopulae. Scopulae in the first quarter of the metatarsi very dense (Fig. 2). Abdomen greyish-cream, covered with short, adpressed, dark setae arranged longitudinally (Fig. 2).

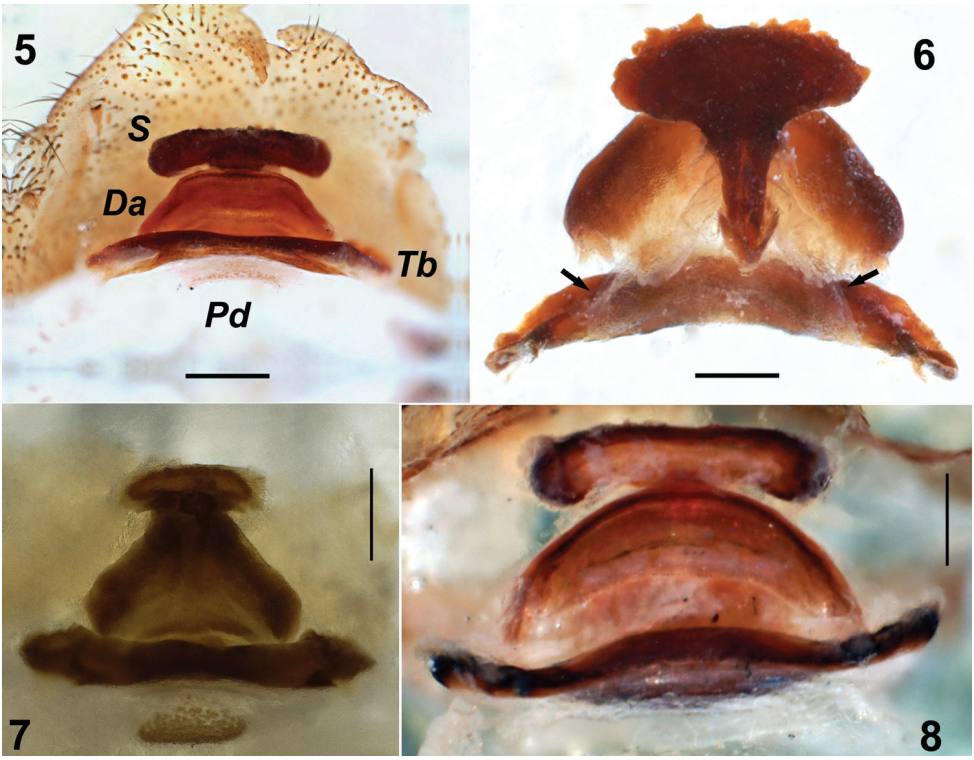

Figures 5–8. *Dysderocrates kibrisensis* sp. n. Vulva **5** dorsal view, arrow indicates triangular membranous structure **6** ventral view *Dysderocrates* cf. *regina* Vulva **7** ventral view *Dysderocrates tanatmisi* Vulva **8** ventral view. Abbreviations: ***Da*** Dorsal arch ***Pd*** Posterior diverticulum ***S*** Spermatheca ***Tb*** Transverse bar. Scale bars: 0.125 mm (**5–8**), 0.1 mm (**6**).

Vulva. Anterior spermatheca (*S*) and transverse bar (*Tb*) strongly sclerotized, dorsal arch (*Da*) relatively less sclerotized. Posterior diverticulum scarcely visible. Spermatheca flat with a button-shaped structure posteromedially. Anterior margin of spermatheca not smooth. Dorsal arch mushroom-cap-shaped. Dorsal arch (*Da*) and transverse bar (*Tb*) support triangular membranous structure. Transverse bar (*Tb*) arched (Figs 5, 6).

Male unknown.

Distribution. Known from the type locality only.

Comments. Seven species of *Dysderocrates* are known, and the entire genus is restricted to the Mediterranean Basin. We placed this species in *Dysderocrates* because it fits the diagnosis: large body size, three strong teeth on the cheliceral groove, and many spines on the anterior femora. *Dysderocrates kibrisensis* sp. n. is the first and only species of the genus reported from Cyprus.

Genus *Harpactea* Bristowe, 1939

Type species. *Aranea hombergi* Scopoli, 1763.

***Harpactea kalavachiana* sp. n.**
http://zoobank.org/45D4FDDE-3953-425D-97F8-F701CACF0957
Figures 9–11, 13, 14

Type. Holotype ♀ (NMNU); **CYPRUS** Lefkoşa, Kalavaç Village, Saray (Palace) Cave (35°16'56"N; 33°32'09"E), hand collecting, 521 m, 14.VII.2017, leg. K.B. Kunt.

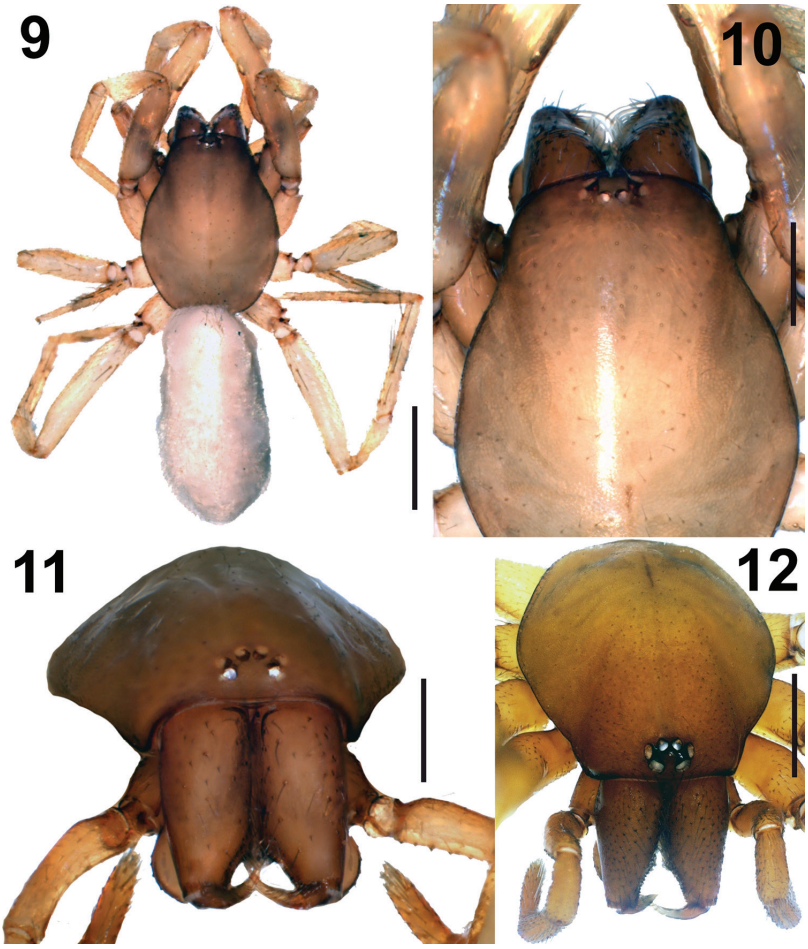

Figures 9–12. *Harpactea kalavachiana* sp. n. **9** Habitus of holotype female **10** Carapace, dorsal view **11** Carapace, anterior view **12** Anterior view of *H. alanyana*, female.

Comparative material. *Harpactea alanyana* Özkütük, Elverici, Marusik & Kunt, 2015: **TURKEY** 1♀ (ETAM) Antalya, Alanya, Taşatan Plateau (36°38'37.35"N; 32°4'42.09"E), 24.IV.2011, leg. R.S. Özkütük (Figs 12, 15).

Harpactea parthica Brignoli, 1980: **IRAN** 1♀ (ZMUT), Mazandaran, 16.IX.1971, leg. P.T. Lehtinen & K. Kavén (Fig. 16).

Derivatio nominis. The specific name refers to the type locality.

Diagnosis. The general appearance of the broad posterior diverticulum, short transverse bar, and basal transverse part of the the anterior spermathecae of *H. kalavachiana* sp. n. are similar to those of *H. alanyana* (Turkey) (Fig. 15), *H. parthica* (Iran) (Fig. 16), and *H. digiovannii* Gasparo, 2014 (Cyclades, Greece). However, the distal expansion of the spermathecae in *H. kalavachiana* is 4−5 times broader than the aforementioned species. *Harpactea kalavachiana* sp. n. differs from *H. gunselorum* Gücel, Fuller, Göçmen & Kunt, 2018 from Cyprus by the enlarged distal expansion of the spermatheca which is more than twice as wide as that of *H. gunselorum*, and from *H. cecconi* (Kulczyński, 1908) by its body length, which is larger (female of *H. cecconi*: 5.15 mm).

Measurements of holotype. TL 3.00; AL 1.70; CL 1.30; CWmax 1.00; CWmin 0.48; AMEd 0.03; PLEd 0.02; PMEd 0.02; ChF 0.31; ChG 0.15; ChL 0.78. Leg measurements as shown in Table 3.

Description of holotype. Female. Carapace light brown. Cephalic region narrower and lighter compared to the thoracic region. Carapace with short blackish setae, fovea distinct. Eyes reduced (Figs 10−12).

Chelicerae and cheliceral fangs light brown. Chelicerae with scattered setae of varying lengths on the anterior surface (Figs 9−11). Labium, gnathocoxae, and sternum milky brown. Sternum with more hairs on the edges compared to the middle. Legs greyish. Coxae, trochanters, and especially the femora of legs I and II are darker than others (Fig. 9). Leg spination shown in Table 4.

Legs III and IV with weakly developed scopulae on distal parts of tarsi and metatarsi. Abdomen cylindirical, grey-brownish (Fig. 9). Abdomen covered with short, greyish setae, anterior setae longer than the ventral and dorsal ones. Margins of the tracheal spiracles are slightly sclerotized.

Table 3. Leg measurements of *Harpactea kalavachiana* sp. n.

Leg	C+Tr	Fe	Pa	Ti	Mt	Ta	Total
I	0.60	1.00	0.64	1.40	0.56	0.24	4.20
II	0.60	0.92	0.50	0.75	0.66	0.24	3.67
III	0.38	0.80	0.33	0.50	0.50	0.30	2.81
IV	0.50	1.10	0.45	0.88	1.00	0.30	4.23

Table 4. Leg spination of *Harpactea kalavachiana* sp. n.

♀	C	Fe	Pa	Ti	Mt
I	0	2pl	0	0	0
II	0	1, 1pl	0	0	0
III	1d	1, 1pl 1, 1d 1, 1rl	1rl	2, 2pl 2, 2rl 1, 1, 2v	1pl 1, 1rl 1, 1, 2v
IV	1d	2–3d	0	4pl 1, 1, 1rl 5v	1, 1, 1pl 1, 1, 1rl 4v

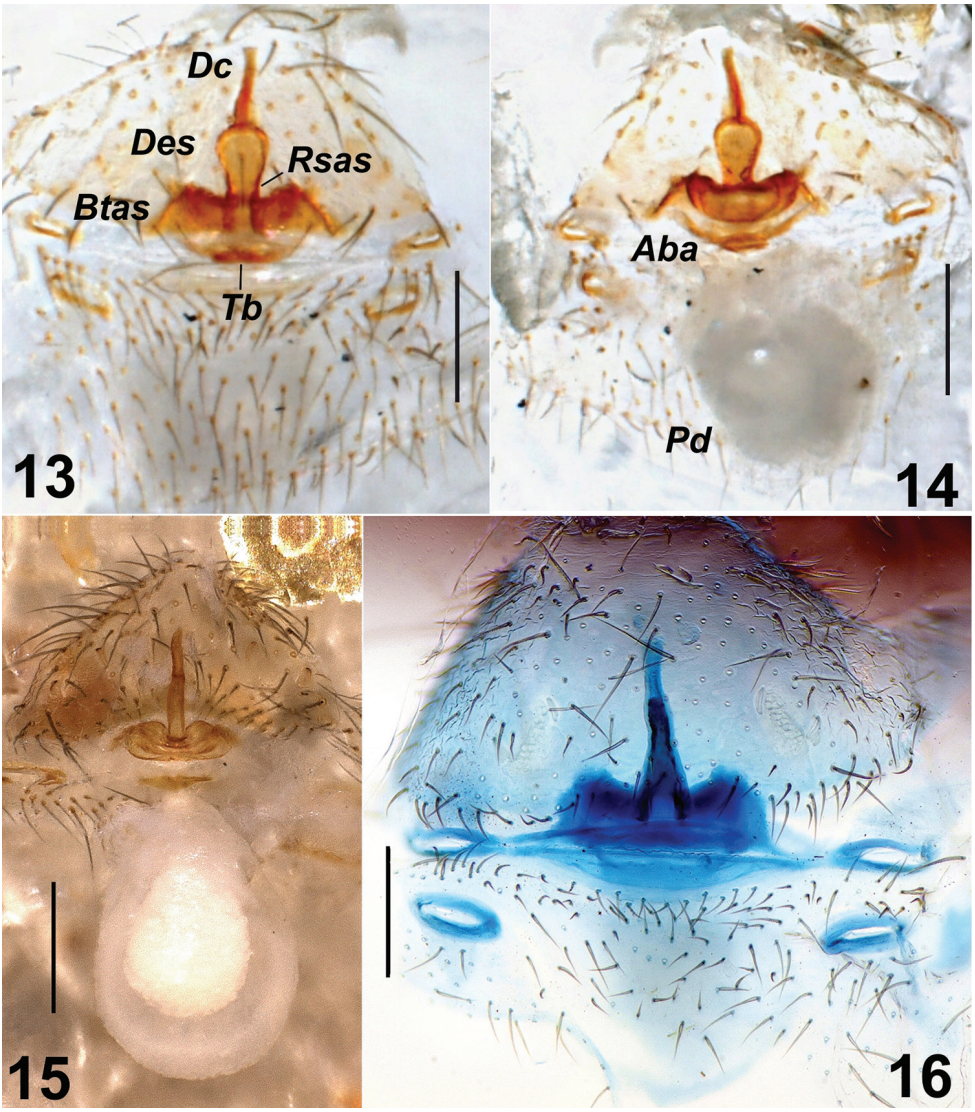

Figures 13–16. *Harpactea kalavachiana* sp. n. Vulva **13** ventral view **14** dorsal view *H. alanyana* Vulva **15** dorsal view *H. parthica* Vulva **16** ventral view. Abbreviations: ***Aba*** Anterior basal arc ***Btas*** Basal transverse part of the anterior spermatheca ***Dc*** Distal crest ***Des*** Distal expansion of the spermatheca ***Pd*** Posterior diverticulum ***Rsas*** Rod shaped part of the anterior spermatecha ***Tb*** Transverse bar. Scale bar: 0.2 mm.

Vulva. Anterior part of vulva sclerotized. Distal crest (*Dc*) spinose. Distal crest (*Dc*) and the length of the rod-shaped part of the anterior spermatheca (*Rsas*) subequal in length. The width of the distal expansion of the spermatheca (*Des*) about twice longer than rod-shaped part of the anterior spermatheca (*Rsas*). Transverse bar (*Tb*) short and straight. Posterior diverticulum (*Pd*) well developed (Figs 13, 14).

Male unknown.

Distribution. Known from the type locality only.

Comments. *Harpactea* is the second largest genus of the Dysderidae with 181 named species. Most *Harpactea* species have six well-developed eyes, although several cave-dwelling species exhibit different levels of eye reduction. *Harpactea sanctidomini* Gasparo, 1997 (Tremiti Islands, Italy) has only four eyes, with the PME entirely reduced. *Harpactea persephone* Gasparo, 2011 (Kournas Cave, Chania Prefecture, Crete, Greece), *H. karaschkhan* Kunt et al., 2016 (Yalandünya Cave, Gazipaşa, Antalya, Turkey), *H. stalitoides* Ribera, 1993 (Iberian Peninsula), and *H. strinatii* Brignoli, 1979 (Diros Caves, Peloponnese, Greece) are eyeless.

The eyes of *H. kalavachiana* sp. n. are reduced, and the AME are distant from each other, much more than average (Fig. 11). Epigean species of *Harpactea* are usually reddish, however, *H. kalavachiana* is paler compared to the other epigean species of *Harpactea* (Fig. 12).

Harpactea kalavachiana sp. n. can be considered part of the *rubicunda* (D) species group according to the grouping by Deeleman-Reinhold (1993) due to the large, membranous posterior diverticulum and the spination of the coxae and patellae.

Results and discussion

The results of our study increase the number of dysderid species on Cyprus from seven to nine, which increases the entire spider fauna to 117. Because the distributions of the two new species are limited to their type localities and because most cave species have small distributions, it is very likely that they are endemic to Cyprus.

Our arachnological sampling on the island continues. Future additional samples, including males of these two new species, will help determine their generic position more precisely.

Acknowledgements

This study was produced with the financial support of the European Union as part of the “Caves of Kyrenia Mountains Project: Research, Conservation, and Education through "Cypriot Civil Society in Action V Program” (contract number: 2015/371-989) and co-funded by the US Embassy in Nicosia. This research was led by Mağara Meraklıları Derneği (Cave Enthusiasts NGO) in Cyprus and the Union of International Speleology (UIS) in Slovenia. Its contents are the sole responsibility of the authors and do not necessarily reflect the views of the European Union. We are deeply indebted to Ferhat Altunsoy (Eskişehir, Turkey) and Mert Elverici (Ankara, Turkey) who photographed the holotypes of the new species. We also thank Yuri Marusik (Magadan, Russia) who kindly provided a photograph of the vulva of *Harpactea parthica* from Iran. We thank the anonymous reviewers for their careful reading of our manuscript and their many insightful comments and suggestions. The English of the final text was kindly checked by Sarah Crews (San Francisco, USA).

References

Chatzaki M, Arnedo MA (2006) Taxonomic revision of the epigean representatives of the spider subfamily Harpacteinae (Araneae: Dysderidae) on the island of Crete. Zootaxa 1169: 1–32. http://dx.doi.org/10.11646/zootaxa.1169.1.1

Deeleman-Reinhold CL (1993) The genus *Rhode* and the harpacteine genera *Stalagtia*, *Folkia*, *Minotauria*, and *Kaemis* (Araneae, Dysderidae) of Yugoslavia and Crete, with remarks on the genus *Harpactea*. Revue Arachnologique 10(6): 105–135.

Deeleman-Reinhold CL, Deeleman PR (1988) Revision des Dysderinae (Araneae, Dysderidae), les espèces mediterranéennes occidentales exceptées. Tijdschrift voor Entomologie 131: 141–269.

Gücel S, Fuller ÖÖ, Göçmen B, Kunt KB (2018) *Harpactea gunselorum* sp. n., a new spider species from northern Cyprus (Araneae: Dysderidae). Serket 16(2): 80–86.

Hadley A (2010) CombineZP Image Stacking Software.

Karakaş Kılıç G, Özkütük RS (2017) *Dysderocrates tanatmisi* sp. n., a new spider species from Turkey (Araneae, Dysderidae). Turkish Journal of Zoology 41(6): 1072–1075. https://doi.org/10.3906/zoo-1612-22

Koch, CL (1837) Übersicht des Arachnidensystems. Heft 1. C.H. Zeh, Nürnberg, 1–39. https://doi.org/10.5962/bhl.title.39561

Özkütük RS, Yağmur EA, Kunt KB, Karakaş Kılıç G, Elverici M (2018) Redescription of two species of *Harpactea* Bristowe, 1939 (Araneae, Dysderidae) known from Turkey. Anadolu University Journal of Science and Technology C 7(1): 20–30. https://doi.org/10.18036/aubtdc.335037

Russell-Smith A, Allison R, Askins M, Blumsom W, Snazell R., Spilling, C (2011) A provisional checklist and gazetteer of the spiders of Chios, Greece (Arachnida: Araneae). Bulletin British Arachnological Society 15(5): 133–167. https://doi.org/10.13156/arac.2010.15.5.133

van Helsdingen PJ (2018) Araneae. Fauna Europaea Database European spiders and their distribution. Distribution. Version 2018.1. [Accessed on: 2019-01-20]

ZooKeys 825: 55–69 (2019)
doi: 10.3897/zookeys.825.31542
http://zookeys.pensoft.net

RESEARCH ARTICLE

A peer-reviewed open-access journal
ZooKeys
Launched to accelerate biodiversity research

Review of the genus *Vekunta* Distant from China, with descriptions of two new species (Hemiptera, Fulgoromorpha, Derbidae)

Yong-Jin Sui[1,2,3], Xiang-Sheng Chen[1,2,3]

1 *Institute of Entomology, Guizhou University, Guiyang, Guizhou, 550025, China* **2** *Special Key Laboratory for Development and Utilization of Insect Resources of Guizhou, Guizhou University, Guiyang, Guizhou, 550025, China* **3** *Guizhou Key Laboratory for Plant Pest Management of Mountainous Region, Guizhou University, Guiyang, Guizhou, 550025, China*

Corresponding author: *Xiang-Sheng Chen* (chenxs3218@163.com)

Academic editor: *Mike Wilson* | Received 11 November 2018 | Accepted 23 January 2019 | Published 19 February 2019

http://zoobank.org/E2016844-A2FF-4BC8-8E62-01F041E5CF14

Citation: Sui Y-J, Chen X-S (2019) Review of the genus *Vekunta* Distant from China, with descriptions of two new species (Hemiptera, Fulgoromorpha, Derbidae). ZooKeys 825: 55–69. https://doi.org/10.3897/zookeys.825.31542

Abstract

The derbid genus *Vekunta* Distant, 1906 is reviewed. Two new species, *V. bambusana* **sp. n.** and *V. pentaprocessusa* **sp. n.**, are described and illustrated from the southwest of China to give the genus twenty-nine species in China. A checklist and a key to species of the genus from China are also provided.

Keywords

Cenchreini, distribution, Fulgoroidea, planthoppers, taxonomy

Introduction

The planthopper family Derbidae (Hemiptera, Fulgoromorpha) was established by Spinola in 1839, containing three subfamilies in twenty tribes (Bourgoin 2018). Approximately eight tribes, 38 genera, and 154 species of Derbidae are known in China.

Copyright *Yong-Jin Sui, Xiang-Sheng Chen*. This is an open access article distributed under the terms of the Creative Commons Attribution License (CC BY 4.0), which permits unrestricted use, distribution, and reproduction in any medium, provided the original author and source are credited.

Almost all members of the family in China are distributed in the Oriental region, especially in southern China.

The planthopper genus *Vekunta* was established by Distant (1906b) with two species from Sri Lanka and with *Temesa tenella* Melichar, 1903 as its type species. This genus belongs to the tribe Cenchreini of subfamily Derbinae (Hemiptera: Derbidae). The tribe Cenchreini was established by Muir in 1913, containing 23 genera and 185 species to date, is a larger tribe of Derbidae (Bourgoin 2018). Characteristics of the tribe Cenchreini are the forewing with clavus closed rarely open; clavus at least half as long as whole forewing; MP and CuA usually with less than eight branches at margin; Pcu on clavus (forewing) with sensory pits; hindwing more than half as long as forewing; frons narrow, usually not strongly compressed (Fennah 1952, Emeljanov 1996). The genus *Vekunta* is the largest one of Cenchreini (Hemiptera: Derbidae); 43 species have hitherto been recorded in this genus (Bourgoin 2018), including 27 species from China (Matsumura 1914, 1940; Muir 1914; Fennah 1956; Yang and Wu 1993; Liang and Wu 2001), seven from Indonesia (Walker 1857; Bierman 1910; Muir 1913, 1915, 1923, 1926; Liang 2000), two from Philippines (Melichar 1914; Muir 1917), two from India (Muir 1922; Liang and Wu 2001), two from Korea (Rahman et al. 2012), one from Japan (Matsumura 1914), one from Vietnam (Fennah 1978), one from Papua New Guinea (Walker 1870; Liang 2000), and one from the Seychelles (Löcker et al. 2009).

Herein, two new species, *Vekunta bambusana* sp. n. and *V. pentaprocessusa* sp. n., are described and illustrated from Guizhou and Yunnan provinces, China. A checklist and a key to species of the genus from China are also provided.

Materials and methods

The morphological terminology follows Bourgoin (1987) and Yang and Wu (1993). The morphological terminology of female genitalia follows Bourgoin (1993). Body length was measured from apex of vertex to tip of forewing. The standard terminology of venation follows Bourgoin et al. (2015). The term "anal style" used here follows Rahman et al. (2012). Dried specimens were used for the description and illustration. External morphology was observed under a stereoscopic microscope and characters were measured with an ocular micrometer. Color pictures for adult habitus were obtained by the Nikon SMZ25 system. The genital segments of the examined specimens were macerated in 10% NaOH and drawn from preparations in glycerin jelly using a Leica MZ 12.5 stereomicroscope. Illustrations were scanned with a Canon CanoScan LiDE 220 and imported into Adobe Photoshop CS5 for labeling and plate composition. The dissected genitalia were preserved in glycerin in small plastic tubes pinned together with the specimens.

The type specimens are deposited in the Institute of Entomology, Guizhou University, Guiyang, Guizhou Province, China (**GUGC**).

Taxonomy

Genus *Vekunta* Distant, 1906

Figs 1–34

Temesa Melichar, 1903: 40; preoccupied by *Temesa* (Mollusca) Adams, 1855.
Vekunta Distant, 1906a: 8; 1906b: 287; Yang and Wu 1993: 97; Liang and Wu 2001: 511–512; Löcker et al. 2009: 15; Rahman et al. 2012: 24.

Type species. *Temesa tenella* Melichar, 1903 by original designation.

Diagnosis. Combination of the following characters: head (Figs 2, 4, 7, 22) in profile distinctly angulate. Vertex (Figs 1, 3, 5, 20) quadrate, at base wider than at apex, slightly projecting in front of eyes, covered with sensory pits, divided from frons by transverse carina. Frons (Figs 6, 21) without median carina, elongate to quadrate. Postclypeus with three carinae. Antennae (Figs 5–7, 20–22) short, second antennomere oval, subantennal process (Figs 6, 7, 21, 22) small or absent. Ocelli (Figs 7, 22) present. Forewing (Figs 8, 23) with short subcostal cell, Sc+R fused with MP for a short distance, forking nearly basal one-fifth, MP with two sectors, CuA two branched, forking nearly basal one-third, costal margin and vein Pcu covered with tubercles, Pcu+A1 reaching forewing margin near middle. Hindwing (Figs 9, 24) shorter than forewing, MP two branched, forking apically, CuA three branched, forking near middle, CuP and Pcu single, A1 two branched. Spinal formula of hind leg 7–6–6.

Checklist of species of *Vekunta* Distant, 1906 from China

V. albipennis Matsumura, 1914; China (Taiwan)
V. asymmetrica Liang & Wu, 2001; China (Xizang)
V. atripennis Matsumura, 1940; China (Taiwan)
V. bambusana sp. n.; China (Guizhou)
V. botelensis Matsumura, 1940; China (Taiwan)
V. commendata Yang & Wu, 1993; China (Taiwan)
V. diluta Yang & Wu, 1993; China (Taiwan)
V. extima Yang & Wu, 1993; China (Taiwan)
V. fera Yang & Wu, 1993; China (Taiwan)
V. gracilenta Yang & Wu, 1993; China (Taiwan)
V. intermedia Yang & Wu, 1993; China (Taiwan)
V. kotoshonis Matsumura, 1940; China (Taiwan)
V. lyricen Fennah, 1956; China (Taiwan)
V. maculata Matsumura, 1914; China (Taiwan)
V. makii Muir, 1914; China (Taiwan)
V. malloti Matsumura, 1914; China (Taiwan), Japan (Honshu, Kyushu, Shikoku)
V. memoranda Yang & Wu, 1993; China (Taiwan)

V. nigra Yang & Wu, 1993; China (Taiwan)
V. nigrolineata Muir, 1914; China (Taiwan)
V. nivea Fennah, 1956; China (Zhejiang)
V. nutabunda Yang & Wu, 1993; China (Taiwan)
V. obaerata Yang & Wu, 1993; China (Taiwan)
V. obliqua Yang & Wu, 1993; China (Taiwan)
V. parca Yang & Wu, 1993; China (Taiwan)
V. pentaprocessusa sp. n.; China (Yunnan)
V. shirakii Matsumura, 1914; China (Taiwan)
V. stigmata Matsumura, 1914; China (Taiwan)
V. triprotrusa Wu & Liang, 2001; China (Yunnan)
V. umbripennis Muir, 1914; China (Taiwan)

Key to species of the genus *Vekunta* Distant from China (based on Rahman et al. 2012)

1 Thorax with propleura with a large dark spot ..... ***V. albipennis***
– Thorax with propleura not as above..... **2**
2 Forewing along costal and anal margins with brown to dark brown stripe..... **3**
– Forewing along costal and anal margins without brown to dark brown stripe.... **6**
3 Female sternite VII with protrusion asymmetrical (Yang and Wu 1993: fig. 62E) ..... ***V. diluta***
– Female sternite VII with protrusion symmetrical (Figs 17, 32)..... **4**
4 Female sternite VII with protrusion length longer than width at base (Yang and Wu 1993: fig. 64D) ..... ***V. nigrolineata***
– Female sternite VII with protrusion length shorter than width at base (Figs 17, 32)..... **5**
5 Male with gonostyli bilaterally symmetrical (Fig. 10); left side of aedeagus with a laminal process near middle, apex of aedeagus valviform, reaching to middle of periandrium (Figs 13–14) ..... ***V. bambusana* sp. n.**
– Male with gonostyli asymmetrical, right gonostylus larger than left one (Fig. 25); aedeagus with five spinous processes at apex, the largest process produced reaching to basal of periandrium (Figs 28–29)..... ***V. pentaprocessusa* sp. n.**
6 Forewing yellowish white..... **7**
– Forewing pale brown, dark or with dark markings **16**
7 Pygofer of male with dorsocaudal processes asymmetrical **8**
– Pygofer of male with dorsocaudal processes symmetrical..... **9**
8 Aedeagus of male not reaching to middle of periandrium (Yang and Wu 1993: fig. 55H)..... ***V. nutabunda***
– Aedeagus of male reaching to middle of periandrium (Yang and Wu 1993: fig. 60H–I) ..... ***V. commendata***
9 Aedeagus of male with process(es) at base..... **10**
– Aedeagus of male without process at base (Yang and Wu 1993: fig. 52G) ... ***V. extima***

10 Periandrium with 4–5 processes in male **11**
– Periandrium with 2 processes in male **13**
11 Periandrium with 5 processes in male (Yang and Wu 1993: fig. 50G–H) .... ***V. maculata***
– Periandrium with 4 processes in male **12**
12 Periandrium of male with one pair of slender processes at base (Yang and Wu 1993: fig. 51H); anal tube almost straight apically (Yang and Wu 1993: fig. 51E) ..... ***V. makii***
– Periandrium of male with one spinous process at base (Fennah 1956: fig. 12D); anal tube abruptly turned downward then cephalad apically (Fennah 1956: fig. 12E) ..... ***V. nivea***
13 Male with apical part of anal tube strongly curved in lateral profile **14**
– Male with apical part of anal tube slightly curved in lateral profile **15**
14 Periandrium of male with 2 short processes near middle, one directed caudally, another one directed dorsally (Yang and Wu 1993: fig. 56H) ..... ***V. gracilenta***
– Periandrium of male with 2 long processes near middle, all directed caudally (Yang and Wu 1993: fig. 59H) ..... ***V. obliqua***
15 Male with apical margin of anal tube broadly rounded; periandrium with short process at left base reaching less than middle (Yang and Wu 1993: fig. 57G) ..... ***V. intermedia***
– Male with apical margin of anal tube truncate obliquely; periandrium with long process at left base reaching over than middle (Yang and Wu 1993: fig. 58G) ..... ***V. obaerata***
16 Aedeagus of male, in right lateral view, with a small process near base and another lobe-like process in the middle (Yang and Wu 1993: fig. 53H) ..... ***V. parca***
– Aedeagus of male not as above **17**
17 Forewing with scattered dark markings **18**
– Forewing uniformly dark except stigma **22**
18 Mesothorax pale yellow **19**
– Mesothorax fuscous or brown **20**
19 Pygofer of male with symmetrical dorsocaudal processes; periandrium with one pair of stout processes at base (Yang and Wu 1993: fig. 45F) ..... ***V. lyricen***
– Pygofer of male with asymmetrical dorsocaudal processes; periandrium without process at base (Yang and Wu 1993: fig. 46G) ..... ***V. kotoshonis***
20 Frons between the lateral carinae reddish yellow ..... ***V. botelensis***
– Frons between the lateral carinae brownish **21**
21 Forewing veins very dark, paler toward apex ..... ***V. atripennis***
– Forewing veins sordid yellow ..... ***V. shirakii***
22 Hindwing black **23**
– Hindwing not black **26**
23 Antennae yellow ..... ***V. triprotrusa***
– Antennae brown **24**
24 Male with dorsocaudal processes of pygofer triangularly produced (Yang and Wu 1993: fig. 63B) ..... ***V. malloti***
– Male with dorsocaudal processes of pygofer not triangularly produced **25**

25 Aedeagus of male with 2 hooked processes at basoventral portion (Yang and Wu 1993: fig. 47G); male with dorsocaudal processes of pygofer not produced (Yang and Wu 1993: fig. 47E) ..... ***V. stigmata***
– Aedeagus of male without hooked process at basoventral portion (Yang and Wu 1993: fig. 48G); male with dorsocaudal process of pygofer broadly rounded (Yang and Wu 1993: fig. 48E) ..... ***V. memoranda***
26 Hindwing white **27**
– Hindwing gray **28**
27 Periandrium of male with a process at base (Yang and Wu 1993: fig. 61I); apex of anal tube curved (Yang and Wu 1993: fig. 61E) ..... ***V. fera***
– Periandrium of male without process at base (Wu and Liang 2001: fig. 19); apex of anal tube straight (Wu and Liang 2001: fig.16) ..... ***V. asymmetrica***
28 Pygofer of male with dorsocaudal processes asymmetrical; periandrium without process at base (Yang and Wu 1993: fig. 49G) ..... ***V. umbripennis***
– Pygofer of male with dorsocaudal processes symmetrical; periandrium with one pair of hooked processes at base ventrally and two long processes laterally, one process at base and another in the middle (Yang and Wu 1993: fig. 54H) ..... ***V. nigra***

***Vekunta bambusana* sp. n.**
http://zoobank.org/12B8BE91-60B4-46C7-A7AB-3EF08D50F70A
Figs 1, 2, 5–19

Type material. ***Holotype*** ♂, CHINA: **Guizhou**, Wangmo, Dayi (25°22'N, 106°06'E), 21 August 2012, Z-M Chang. ***Paratypes***, **Guizhou:** 1♂, Wangmo, Dayi, 23 August 2012, Z-M Chang; 2♂♂, Wangmo, Dayi, 13 August 2014, Z-M Chang; 3♂♂4♀♀, Wangmo, Dayi, 13–14 August 2014, Y Liu; 2♂♂, Suiyang, Wangcao (28°07'N, 107°16'E), 29 July 2014, H-Y Sun; 1♂, Suiyang, Wangcao, 29 July 2014, Y-J Wang.

Measurements. Body length (including forewing): male 5.99–6.37 mm (n = 10), female 6.98–7.03 mm (n = 4); forewing length: male 5.02–5.45 mm (n = 10), female 5.96–6.02 mm (n = 4).

Description. *Coloration.* General color yellow. Head (Figs 1, 2, 5–7) yellow. Vertex (Figs 1, 5) yellow, lateral and apical carinae yellow to brownish yellow. Frons and clypeus yellow (Fig. 6). Rostrum (Fig. 7) yellow with apex fuscous. Gena (Fig. 7) yellow. Eyes (Figs 1, 2, 5–7) black, ocelli yellow. Antennae (Figs 5–7) yellow. Pronotum, mesonotum and tegula yellow (Fig. 5). Forewing (Figs 1, 2) yellowish white except costal and clavus margins from base to near apex brown to dark brown, veins yellowish white. Hindwing subhyaline, yellowish white, veins white. Thorax with ventral areas yellow, mesopleura (Figs 2, 7) with an oval black spot. Legs brownish yellow. Genital segment yellow.

Head and thorax. Head (Figs 1, 5) including eyes distinctly narrower than pronotum (1:1.65). Vertex (Figs 1, 5) at base wider than length in middle line (1:0.62), apex narrower than base (1:1.31), straightly projecting before eyes, median carina ab-

Figures 1–4. Male habitus (dorsal and lateral view). **1–2** *Vekunta bambusana* sp. n. **3–4** *Vekunta pentaprocessusa* sp. n. Scale bar: 0.5 mm.

sent, lateral margin distinctly carinate, posterior margin slightly concave. Frons (Fig. 6) moderately narrow, near frontoclypeal suture widest, disc concave, separated on both sides, subparallel, lateral margin distinctly carinate, median carina absent. Postclypeus (Fig. 6) with median and lateral carinae; anteclypeus with weak median carina, lateral carinae absent. Apical segment of rostrum longer than wide. Antennae (Figs 5–7) short, second antennomere oval, flagellum originated from apical point. Subantennal processes (Figs 6, 7) small. Eyes (Figs 5–7) semicircular; ocelli present, adjacent to eyes. Median length of pronotum short, anterior margin between eyes convex, posterior margin deeply concave, median carina distinct. Mesonotum (Fig. 5) as long as broad, convex, in lateral view raised above vertex, with median and lateral carinae weak, posterior end triangularly depressed. Forewing (Fig. 8) narrow, 3.5 times as long as the widest point, clavus closed, claval veins with a prominent ridge of tubercles, base of costal margin curved inward, costal margin also granulated. Hindwing (Fig. 9) shorter than forewing. Hind tibia without lateral spine.

Male genitalia. Anal tube (Fig. 10) in profile broad at basal half, abruptly narrowed medially, apex evenly turned downward, directed ventrally, anal style sets at basal two-fifths; in dorsal view (Fig. 11), length in middle line approximately three times as long as wide at middle, symmetrical, apical margin evenly incised medially. Pygofer (Fig. 10) in lateral view narrowed, dorsocaudal processes (Fig. 12) of pygofer asymmetrical, right dorsocaudal process distinctly longer than left one. Gonostyli (Fig. 10) bilaterally symmetrical, large, elongate and slightly reaching over apex of anal tube in lateral view, dorsal margin serrate at apex, curved dorsally, inner side of laterodorsal

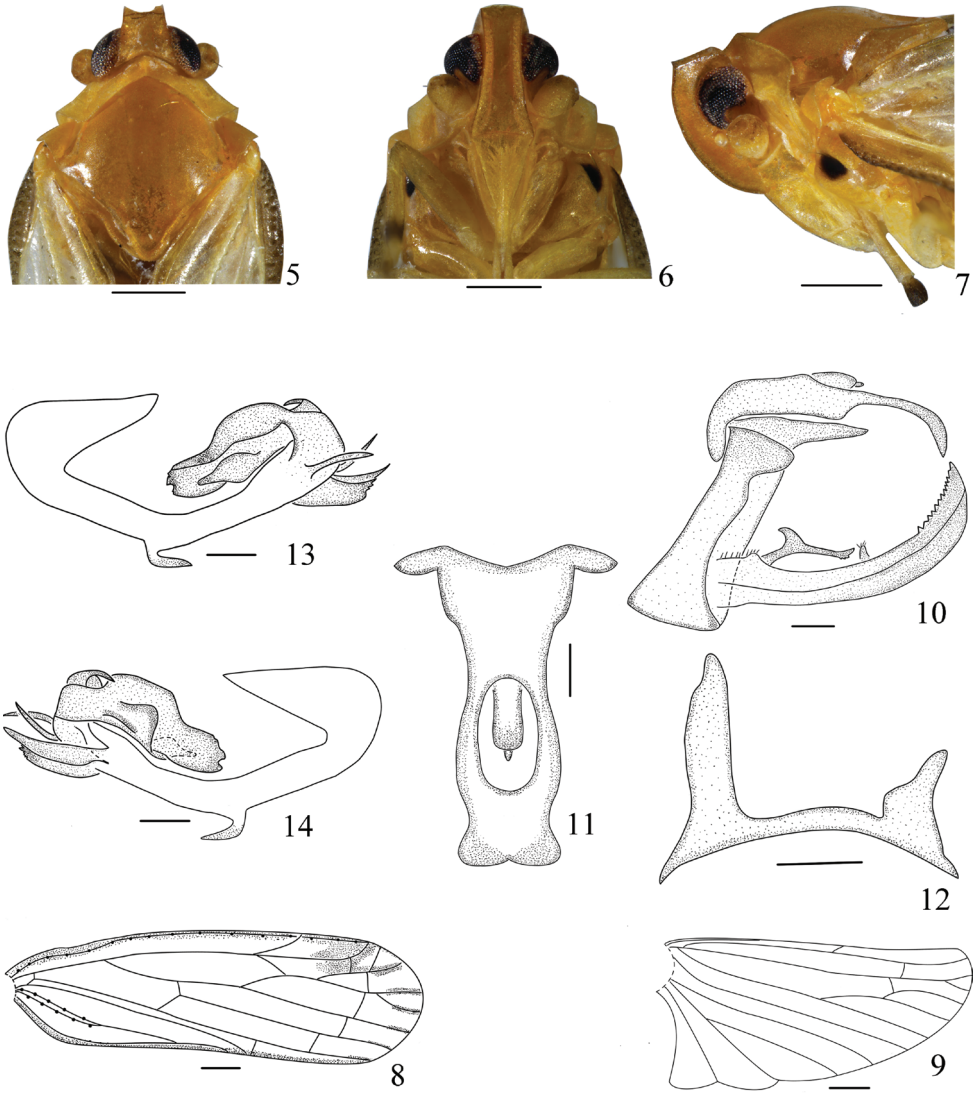

Figures 5–14. *Vekunta bambusana* sp. n., male. **5** Head and thorax, dorsal view **6** face **7** head and thorax, left lateral view **8** forewing **9** hindwing **10** genitalia, left lateral view **11** anal tube, dorsal view **12** dorsocaudal processes of pygofer, dorsal view **13** phallus, left lateral view **14** phallus, right lateral view. Scale bars: 0.5 mm (**5–7**); 0.2 mm (**8–14**).

margin with a bifurcate process at base and a finger-shaped process medially. Phallus (Figs 13, 14) asymmetrical, periandrium curved, with a hooked process near middle ventrally directed caudally, apex with two spinous processes, below them with two sheet processes, all visible in both left and right lateral view. Aedeagus at base with a process curved dorsally, pointed ventrally, left side of aedeagus with a laminal process near middle, apex of aedeagus valviform, reaching to middle of periandrium.

Female genitalia. Anal tube (Figs 15, 16) symmetrical and ring-shaped in dorsal view; apex of anal tube slightly exceeding apex of anal style. Abdominal sternite VII (Fig. 17) in ventral view symmetrical, posterior margin protruded medially, with protrusion length shorter than width at base, lateral margin widened toward the middle and then narrowed gradually toward apex, apical margin rounded. Gonapophysis VIII (Figs 17, 18) with nine teeth at ventral margin. Gonapophysis IX (Fig. 19) with two lobes incompletely symmetrical, lateral margin with dense setae, each lobe with a membrane sheet dorsally, blunt apically. Gonoplac (Figs 15, 17) in lateral view nearly rectangular, with a small angulate process at apex dorsally, lateral margin with spiniform setae.

Remarks. This species is similar to *V. pentaprocessusa* sp. n., but distinguished from the latter by: gonostyli (Fig. 10) symmetrical (gonostyli asymmetrical, with right gonostylus distinctly larger than left one in *V. pentaprocessusa* sp. n.); anal tube (Fig. 11) of male symmetrical in dorsal view (asymmetrical in dorsal view in *V. pentaprocessusa* sp. n.); right dorsocaudal process (Fig. 12) of pygofer in dorsal view distinctly longer than left one in male (left dorsocaudal process in dorsal view slightly longer than right one in *V. pentaprocessusa* sp. n.); periandrium (Figs 13, 14) with a hooked process near middle ventrally (periandrium with a hooked process near base ventrally in *V. pentaprocessusa* sp. n.); aedeagus (Figs 13, 14) valviform at apex, reaching to middle of periandrium (aedeagus with five spinous processes at apex, the largest process reaching to base of periandrium in *V. pentaprocessusa* sp. n.).

Etymology. The species name is derived from the host plant scientific name, Bambusoideae.

Host plant. Bamboo.

Distribution. China (Guizhou).

***Vekunta pentaprocessusa* sp. n.**
http://zoobank.org/21579E13-C4AB-440D-966E-D8CE49FFB568
Figs 3, 4, 20–34

Type material. ***Holotype***: ♂, CHINA, **Yunnan:** Mt Gaoligong National Natural Reserve (25°17'N, 98°48'E), light trap, 15 August 2013, Y- J Wang. ***Paratypes***, **Yunnan:** 5♂♂1♀, same date as holotype; 3♂♂, Mt Gaoligong National Natural Reserve, light trap, 13 June 2011, J-K Long; 6♂♂2♀♀, Mt Gaoligong National Natural Reserve, light trap, 13–16 August 2013, W-C Yang, H-Y Sun, Y-J Wang; 1♂, Mt Gaoligong National Natural Reserve, light trap, 12 August 2018, L-J Yang.

Measurements. Body length (including forewing): male 6.17–6.48 mm (n = 16), female 6.96–6.99 mm (n = 3); forewing length: male 5.36–5.40 mm (n = 16), female 6.04–6.11 mm (n = 3).

Description. *Coloration.* General color yellow. Head (Figs 3, 4, 20–22) yellow. Vertex (Figs 3, 20) with lateral and apical carinae yellow. Frons (Fig. 21) with lateral margins yellow. Clypeus (Fig. 21), gena (Fig. 22), and antennae (Figs 20–22) yellow. Rostrum yellow with apex fuscous. Eyes (Figs 3, 4, 20–22) black, ocelli yellow. Prono-

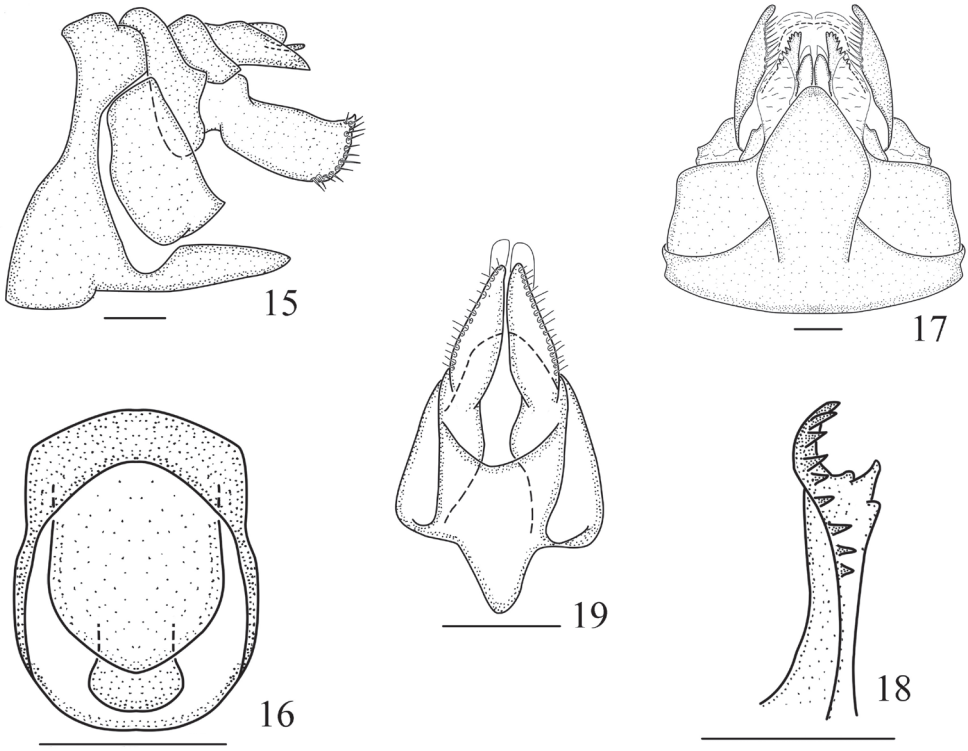

Figures 15–19. *Vekunta bambusana* sp. n., female. **15** Genitalia, lateral view **16** anal tube, dorsal view **17** genitalia, ventral view **18** gonapophysis VIII, right lateral view **19** gonapophysis IX, ventral view. Scale bar: 0.2 mm.

tum, mesonotum and tegula yellow (Figs 3, 20). Forewing (Figs 3, 4) white except with costal and clavus margins from base to near apex brown to dark brown, veins white. Hindwing subhyaline, white, veins white. Thorax with ventral areas yellow, mesopleura (Figs 4, 22) with an oval black spot. Legs pale yellow. Genital segment yellow.

Head and thorax. Head (Figs 3, 20) including eyes distinctly narrower than pronotum (1:1.63). Vertex (Figs 3, 20) at base wider than length in middle line (1:0.62), apex narrower than base (1:1.45), straightly projecting before eyes, median carina absent, lateral margin distinctly carinate, posterior margin slightly concave. Frons (Fig. 21) moderately narrow, near frontoclypeal suture widest, disc concave, lateral margins broadly concave inward, distinctly carinate, median carina absent. Postclypeus (Fig. 21) with median and lateral carinae, anteclypeus with weak median carina, lateral carinae absent. Apical segment of rostrum longer than wide. Antennae (Figs 20, 22) short, second antennomere oval, flagellum originated from apical point. Subantennal processes (Figs 21, 22) small. Eyes (Figs 21, 22) semicircular; ocelli present, adjacent to eyes. Median length of pronotum short, anterior margin between eyes convex, posterior margin deeply concave, median carina distinct. Mesonotum (Fig. 20) as long as broad, slightly convex, in lateral view raised above vertex, with median carina distinct

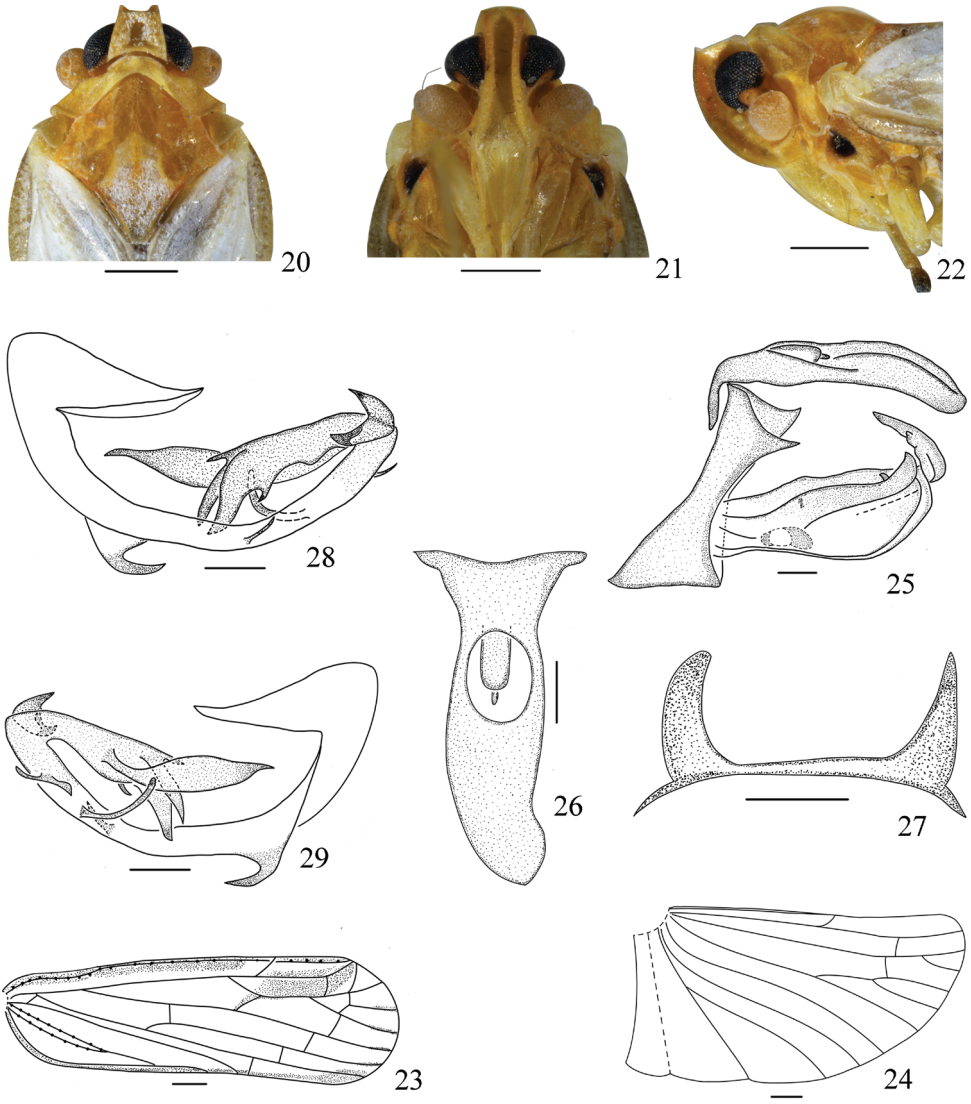

Figures 20–29. *Vekunta pentaprocessusa* sp. n., male. **20** Head and thorax, dorsal view **21** face **22** head and thorax, left lateral view **23** forewing **24** hindwing **25** male genitalia, left lateral view **26** anal tube of male, dorsal view **27** dorsocaudal processes of pygofer, dorsal view **28** phallus, left lateral view **29** phallus, right lateral view. Scale bars: 0.5 mm (**20–22**); 0.2 mm (**23–29**).

and lateral carina weak, posterior end triangularly depressed. Forewing (Fig.23) narrow, 3.3 times as long as the widest point, clavus closed, claval veins with a prominent ridge of tubercles, base of costal margin curved inward, costal margin also granulated. Hindwing (Fig. 24) shorter than forewing. Hind tibia without lateral spine.

Male genitalia. Anal tube (Fig. 25) in lateral view, obliquely, slender at basal half, apical margin rounded, anal styles sets at basal one-fifth; in dorsal view (Fig. 26),

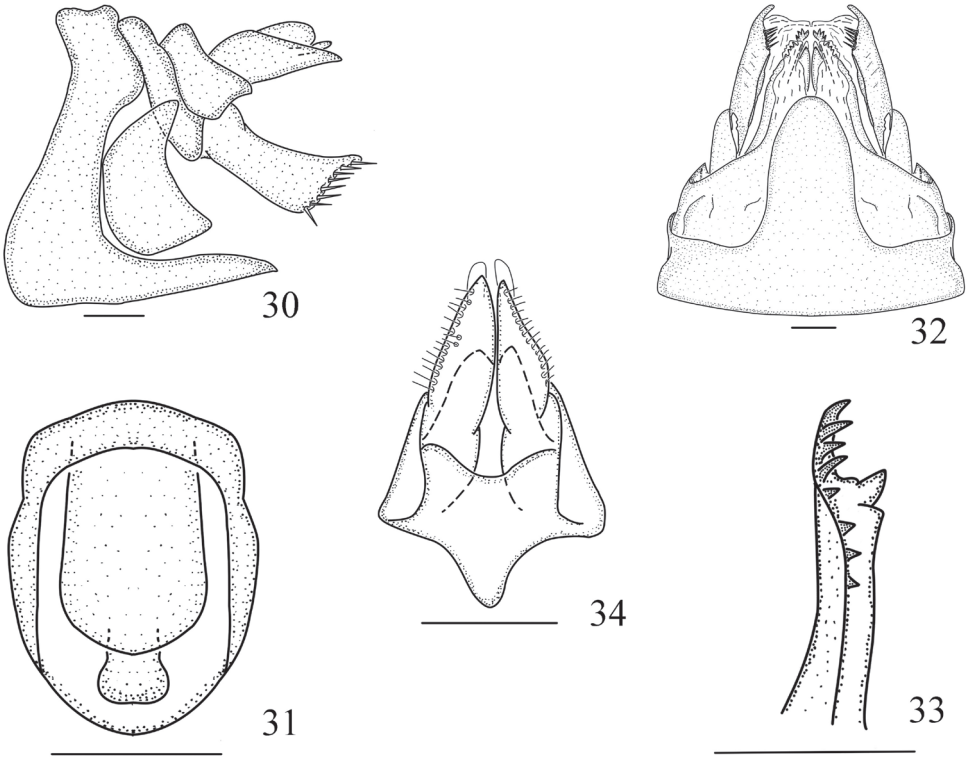

Figures 30–34. *Vekunta pentaprocessusa* sp. n., female. **30** Genitalia, lateral view **31** anal segment, dorsal view **32** genitalia, ventral view **33** gonapophysis VIII, right lateral view **34** gonapophysis IX, ventral view. Scale bar: 0.2 mm.

length in middle line approximately three times as long as wide at middle, asymmetrical, apex rounded. Pygofer (Fig. 25) in lateral view distinctly narrowed medially, processes (Fig. 27) of pygofer asymmetrical, left dorsocaudal process slightly longer than right one. Gonostyli (Fig. 25) bilaterally asymmetrical, right gonostylus larger than left one, large, elongate and slightly reaching less than apex of anal tube in lateral view, inner side with saccate process at basal two-thirds near ventral margin, left gonostylus with a small process rising from apical one-fifth of dorsal margin. Phallus asymmetrical, periandrium curved, with a hooked process near base ventrally directed caudally, in left lateral view (Fig. 28), with a slender process near middle, directed dorsocaudally, and two stout processes at apex, in right lateral view (Fig. 29), with a plate near apex, and a long process at apical two-thirds, slightly curved, directed dorsally, apical margin serrate. Aedeagus with five spinous processes at apex, the largest process produced reaching to base of periandrium, acute at apex.

Female genitalia. Anal tube (Figs 30, 31) symmetrical and ring-shaped in dorsal view; apex of anal tube slightly exceeding apex of anal style. Abdominal sternite VII (Fig. 32) in ventral view symmetrical, posterior margin protruded medially, with protrusion length shorter than width at base, apical margin rounded. Gonapophysis VIII

(Figs 32, 33) with eight teeth at ventral margin. Gonapophysis IX (Fig. 34) with two lobes incompletely symmetrical, lateral margin with dense setae, each lobe with a membrane sheet dorsally, blunt apically. Gonoplac (Figs 30, 32) in lateral view nearly rectangular, with a small angulate process at apex dorsally, lateral margin with spiniform setae.

Remarks. This species is similar to *V. fuscolineata* Rahman et al., 2012, but distinguished from the latter by the slightly dark yellow mesonotum (Fig. 20) (mesonotum distinctly dark brown on each side, golden yellow in middle in *V. fuscolineata*); periandrium (Figs 28, 29) with a hooked process near base ventrally, directed caudally (periandrium without process ventrobasally in *V. fuscolineata*); anal tube of male (Fig. 26) asymmetrical in dorsal view (symmetrical in dorsal view in *V. fuscolineata*); gonostyli (Fig. 25) asymmetrical, with right gonostylus distinctly larger than left one in lateral view (symmetrical in lateral view in *V. fuscolineata*).

Etymology. The new species name is derived from the Latin words *penta-* (five) and *processus* (process), referring to the apex of aedeagus with five processes in male.

Host plant. Unknown.

Distribution. China (Yunnan).

Discussion

The genus *Vekunta* is a diverse genus in the subtropical and tropical regions of Australasian, Oriental, and Palaearctic regions (Löcker et al. 2009, Rahman et al. 2012). To date, there are 43 species recorded in the world (Bourgoin 2018). Approximately 27 species of genus *Vekunta* are known in China, distributed in Zhejiang (one species), Yunnan (one species), Tibet (one species), and Taiwan (twenty-four species). Almost all members of the genus in China are distributed in the Oriental region, hence especially in southern China.

Due to the original literature not recording host plants of this genus, many host plants are unknown. In our study, we find that *V. bambusana* sp. n. lives on bamboo in Guizhou, and some species of *Vekunta* we collected on weeds in some humid environments, for example, *V. triprotrusa* Wu & Liang, 2001. The new species *V. pentaprocessusa* sp. n. was collected by light trap. Thus, we speculate that this group prefers warm and moist environments and some species of the genus *Vekunta* have phototaxis. The natural environment of China is diverse, such as Yunnan Province (southern China), one of China's richest regions in terms of biodiversity; however, only one species of genus *Vekunta* has been recorded in this region, so we believe there should be more species of this genus waiting to be discovered in this region and other parts of China.

Acknowledgements

The authors are grateful to the specimen collectors for their hard work in the field collections. This work was supported by the National Natural Science Foundation

of China (No. 31472033), the Program of Excellent Innovation Talents, Guizhou Province (No. 20154021), the Program of Science and Technology Innovation Talents Team, Guizhou Province (No. 20144001), the International Cooperation Base for Insect Evolutionary Biology and Pest Control (No. 20165802), and the Program of Science and Technology Program in Guizhou Province (LH [2017] 7267).

References

Bierman CJH (1910) Homopteren aus Niederlandisch Ost-Indien. II herausgegeben von D Mac-Gillivray und KW Dammerman. Notes from the Leyden Museum 33: 1–68.

Bourgoin T (1987) A new interpretation of the homologies of the Hemiptera male genitalia, illustrated by the Tettigometridae (Hemiptera, Fulgoromorpha). Proceedings 6th Auchenorrhyncha Meeting, Turin, Italy, 7–11 September 1987, 113–120.

Bourgoin T (1993) Female genitalia in Hemiptera Fulgoromorpha, morphological and phylogenetic data. Annales de la Société Entomologique France 29(3): 225–244.

Bourgoin T (2018) FLOW (Fulgoromorpha Lists on The Web): a world knowledge base dedicated to Fulgoromorpha. Version 8. http://hemiptera-databases.org/flow/ [updated 11 December 2018]

Bourgoin T, Wang RR, Asche M, Hoch H, Soulier-Perkins A, Stroinski A, Yap S, Szwedo J (2015) From micropterism to hyperpterism: recognition strategy and standardized homology-driven terminology of the fore wing venation patterns in planthoppers (Hemiptera: Fulgoromorpha). Zoomorphology 134(1): 63–77. https://doi.org/10.1007/s00435-014-0243-6

Distant WL (1906a) Preoccupied generic names in the Homopterous family Fulgoridae. The Entomologist, An illustrated Journal of Entomology, London 39: 8.

Distant WL (1906b) The Fauna of British India, including Ceylon and Burma. Rhynchota 3 (Heteroptera-Homoptera). Taylor & Francis, London, 503 pp.

Emeljanov AF (1996) On the system and phylogeny of the family Derbiade (Homoptera, Cicadina). Entomological Review 75(2): 70–100.

Fennah RG (1952) On the generic classification of Derbidae (Fulgoroidea), with descriptions of new Neotropical species. Transactions of the Royal Entomological Society London 103: 109–170. https://doi.org/10.1111/j.1365-2311.1952.tb01063.x

Fennah RG (1956) Fulgoroidea from Southern China. Proceedings of the California Academy of Sciences (Series 4) 28(13): 441–527.

Fennah RG (1978) Fulgoroidea from Vietnam. Annales zoologici 34(9): 207–209.

Liang AP (2000) Taxonomic notes on Oriental and Eastern Palaearctic Fulgoroidea (Hemiptera). Journal of the Kansas Entomological Society 73(4): 235–237.

Löcker H, Löcker B, Holzinger WE (2009) Revision of the Derbidae of Seychelles Islands (Insecta: Hemiptera: Fulgoromorpha). Zootaxa 2221: 1–26.

Matsumura S (1914) Beitrag zur kenntnis der Fulgoriden Japans. Annales Musei Nationalis Hungarici 12: 261–305.

Matsumura S (1940) Homopterous Insects Collected at Kotosho (Botel Tabago), Formosa, by Mr Tadao Kano. Insecta Matsumurana 15: 34–51.

Melichar L (1903) Homopteren Fauna von Ceylon. Verlag von Felix L Dames, Berlin, 248 pp.
Melichar L (1914) Neue Fulgoriden von den Phlippinen: I Theil. Philippine Journal of Science 9: 269–283.
Muir F (1913) On some new species of leafhoppers. Part II. Derbidae. Bulletin of the Hawaiian Sugar Planters' Association. Division of Entomology 12: 28–92.
Muir F (1914) On some Derbidae from Formosa and Japan. Proceedings of the Hawaiian Entomological Society 3: 42–52. https://doi.org/10.5962/bhl.part.24593
Muir F (1915) New and little-known Derbidae. Proceedings of the Hawaiian Entomological Society 3: 116–136. https://doi.org/10.5962/bhl.part.24595
Muir F (1917) The Derbidae of the Philippine Islands. Philippine Journal of Science 12: 49–105.
Muir F (1922) On some Indian Derbidae. Records of the Indian Museum 24: 335–342.
Rahman MA, Kwon YJ, Suh SJ (2012) Two new species of the genus *Vekunta* Distant (Hemiptera: Fulgoromorpha: Derbidae) from Korea. Zootaxa 3313: 23–33.
Walker F (1857) Catalogue of the homopterous insects collected at Sarawak, Borneo, by Mr AR Wallace, with descriptions of new species. Journal and proceedings of the Linnaean Society 1: 141–175. https://doi.org/10.1111/j.1096-3642.1857.tb00966.x
Walker F (1870) Catalogue of the homopterous insects collected in the Indian Archipelago by Mr. A.R. Wallace, with descriptions of new species. Journal of the Linnaean Society, Zoology 10: 82–193. https://doi.org/10.1111/j.1096-3642.1868.tb00660.x
Wu HX, Liang AP (2001) Descriptions of three new species of *Vekunta* Distant (Homoptera: Derbidae). Acta Zootaxonomica Sinica 26(4): 511–517.
Yang CT, Wu RH (1993) Derbidae of Taiwan (Homoptera: Fulgoroidea). Cheng Chung Shu Chü, T'ai-pei, 230 pp.

ZooKeys 825: 71–103 (2019)
doi: 10.3897/zookeys.825.30455
http://zookeys.pensoft.net

RESEARCH ARTICLE

A peer-reviewed open-access journal
ZooKeys
Launched to accelerate biodiversity research

Successional and seasonal changes of leaf beetles and their indicator value in a fragmented low thorn forest of northeastern Mexico (Coleoptera, Chrysomelidae)

Uriel Jeshua Sánchez-Reyes[1], Santiago Niño-Maldonado[2], Shawn M. Clark[3], Ludivina Barrientos-Lozano[1], Pedro Almaguer-Sierra[1]

1 *Tecnológico Nacional de México-Instituto Tecnológico de Ciudad Victoria. Boulevard Emilio Portes Gil No.1301, C.P. 87010, Ciudad Victoria, Tamaulipas, Mexico* **2** *Universidad Autónoma de Tamaulipas, Facultad de Ingeniería y Ciencias, Centro Universitario Victoria, C.P. 87149, Ciudad Victoria, Tamaulipas, Mexico* **3** *Brigham Young University, Monte L. Bean Life Science Museum, Provo, Utah 84602, USA*

Corresponding author: *Ludivina Barrientos-Lozano* (ludivinab@yahoo.com)

Academic editor: *Astrid Eben* | Received 9 October 2018 | Accepted 14 January 2019 | Published 27 February 2019

http://zoobank.org/3D6F8F20-2A31-48A7-9373-52AF291B23D4

Citation: Sánchez-Reyes UJ, Niño-Maldonado S, Clark SM, Barrientos-Lozano L, Almaguer-Sierra P (2019) Successional and seasonal changes of leaf beetles and their indicator value in a fragmented low thorn forest of northeastern Mexico (Coleoptera, Chrysomelidae). ZooKeys 825: 71–103. https://doi.org/10.3897/zookeys.825.30455

Abstract

Leaf beetles (Chrysomelidae: Coleoptera) constitute a highly diverse family of phytophagous insects with high ecological relevance, due to their host plant specificity and their close association to vegetation variables. Therefore, secondary succession and seasonal changes after loss of vegetal cover will have a significant influence on their community patterns. Accordingly, responses of leaf beetles to such environmental heterogeneity make them a suitable taxon for monitoring disturbance, which is more important for endangered habitats such as the low thorn forests (LTF) in northeastern Mexico. We conducted a study in a LTF fragment in order to assess the effects of secondary succession and seasonality on leaf beetle communities, as well as to quantify the importance of Chrysomelidae as an indicator taxon. Landsat scenes were used for delimiting a successional gradient, in which four succession categories were selected: four years, 17 years, and 31 years since loss of vegetal cover, and conserved areas. Eight plots of 100 m^2 were randomly delimited in each category; plots were sampled monthly, using an entomological sweep net, from May 2016 to April 2017. In total, 384 samples were collected by the end of study, from which 6978 specimens, six subfamilies, 57 genera, and 85 species were obtained. Species richness was higher in early succession areas. Abundance declined significantly from early successional to conserved areas, but the conserved areas had the higher diversity. Furthermore, differences in abundance were significant between rainy and dry seasons

Copyright *U.J. Sánchez-Reyes et al.* This is an open access article distributed under the terms of the Creative Commons Attribution License (CC BY 4.0), which permits unrestricted use, distribution, and reproduction in any medium, provided the original author and source are credited.

in areas of four, 17, and 31 years of succession, but not in conserved areas; also, all categories had a similar abundance during the dry season. Intermediate (17 and 31 years) and conserved areas differed in the season of higher diversity. Regarding inventory completeness, it was close to or above 70 % for all comparisons, although it was very low for the 17-year category during the rainy season. Faunistic similarity was higher between intermediate categories. A total of 24 species had a significant indicator value. Effects of succession time and seasonality on leaf beetle communities are here quantified for first time in LTF forests. Influences of environmental heterogeneity and intermediate disturbance are discussed as main drivers of the results obtained. Several leaf beetle species are proposed that could be useful for monitoring succession time and secondary LTF vegetation in northeastern Mexico. However, studies must be replicated at other regions, in order to obtain a better characterization of disturbance influence on leaf beetles.

Keywords

Chronosequence, community patterns, disturbance, seasonality, secondary succession, phytophagous beetles

Introduction

Chrysomelidae is the third most diverse family of Coleoptera in the world, with more than 36,000 described species (excluding Bruchinae) (Bouchard et al. 2009). However, recent estimates suggest that this number may be higher, ranging between 55,000 to 60,000 species (Jolivet 2015). This variety resulted from a diversification after the origin of their host plants, as well as from repeated radiations from preexisting diverse plant resources (Gómez-Zurita et al. 2007). Therefore, leaf beetles are almost entirely phytophagous, and their success in ecosystems is determined by their ability to occupy many different feeding niches (Jolivet 1988), and by their host specificity to almost all groups of plants (Riley et al. 2002). Most adults feed on living parts of plants, such as leaves, young stems, flowers, pollen, or fruits (White 1968, Wilcox 1972, Flowers 1996, Riley et al. 2002, Staines 2002, Jolivet and Verma 2008). The larvae are found on the surface of leaves or as leaf miners; others feed on roots, plant litter or submerged parts of plants (White 1968, Riley et al. 2002, Staines 2002, Jolivet and Verma 2008). Some larvae are myrmecophilous and feed on eggs and wastes of ants in their nests (Chamorro-Lacayo 2014). Therefore, leaf beetles are a key group in ecosystems as primary consumers, competing directly with other herbivores (González-Megías and Gómez 2003), and as important components in trophic webs (Basset and Samuelson 1996).

As phytophagous insects, the structure and composition of chrysomelid communities are determined largely by vegetation variables. These include, for example, the type and height of each forest stratum (floristic structure), percentage of vegetation or tree cover, diversity of plants, abundance of young foliage, and specific characteristics of the host plant (Bach 1981, Morrow et al. 1989, Řehounek 2002, Charles and Basset 2005, Baselga and Jiménez-Valverde 2007, Şen and Gök 2009, 2014). In addition, because of their food specificity, leaf beetles are also significantly impacted by modifications in various ecological gradients (Sánchez-Reyes et al. 2015, Sandoval-Becerra et al. 2017), which abiotic factors influence the ability to acquire available resources (Sandoval-Becerra et al. 2018). Therefore, any disturbance as a result of the loss of vegetation cover and land use change will have a direct effect on these insects (Wąsowska 2004).

After disturbance, secondary succession involves subsequent modifications of the vegetation following removal of vegetal cover, and it occurs through different routes, mechanisms, and processes (Pulsford et al. 2016). In turn, these modifications lead to further abiotic and microclimatic changes, which are related to seasonality (Lebrija-Trejos et al. 2011). Despite their importance, the consequences of fragmentation, disturbance, and secondary succession on chrysomelid communities have been quantified only in a few studies (Brown and Hyman 1986, Bach 1990), mainly in temperate wet forests (Linzmeier et al. 2006, Marinoni and Ganho 2006, Linzmeier and Ribeiro-Costa 2009, 2011) and tropical savannas (Pimenta and De-Marco 2015). In addition, in temperate oak forests of northeastern Mexico, the amount of time since last disturbance influences diversity, abundance and spatial distribution of Chrysomelidae (Sandoval-Becerra et al. 2018), as well as their microclimatic niche parameters (Sandoval-Becerra et al. 2017). On the other hand, few works have assessed consistently the effect of seasonality on successional changes of insect communities (Janzen 1976, Linzmeier and Ribeiro-Costa 2009), and some robust studies conducted during several years in areas with different level of conservation in South America, have shown a strong relation between leaf beetles and seasonal changes (Linzmeier and Ribeiro-Costa 2012, 2013). Thus, in order to standardize conservation strategies, it is necessary to evaluate whether the response patterns of leaf beetles to disturbance, secondary succession, and seasonality occur homogeneously in different habitats and ecosystems.

The extent of low thorn forest (LTF) vegetation in northeastern Mexico has been drastically reduced in the last 40 years (Sánchez-Reyes et al. 2017). This ecosystem harbors a high species richness of plants, with a large number of endemics (Rzedowski 2006), and, due to its geographical position, it shares characteristics (presence of deciduous or semi-deciduous species, climate regime) with other important subtropical communities, like the submontane scrub and Tamaulipan thorn scrub (García-Morales et al. 2014). Such floristic complexity presumably leads to a high species richness and diversity of leaf beetles, although this has not been evaluated since the faunistic studies of this family in Mexico are focused in other plant communities (Andrews and Gilbert 2005, Niño-Maldonado et al. 2005, Martínez-Sánchez et al. 2009, Furth 2013, Ordóñez-Reséndiz et al. 2015). In addition, a significant proportion of the current LTF cover in northeastern Mexico is composed of patches of conserved vegetation, together with large areas of secondary vegetation with varying lengths of succession time (Sánchez-Reyes et al. 2017). However, the influences of these disturbances and the time of secondary succession on the faunistic and ecological patterns of Chrysomelidae have never been quantified to date in this ecosystem.

The importance of evaluating changes in leaf beetle communities during secondary succession arises from their potential as indicator taxa. Chrysomelidae is cited as a useful family for monitoring local biodiversity (Farrell and Erwin 1988, Kalaichelvan and Verma 2005, Baselga and Novoa 2007, Aslan and Ayvaz 2009) and quality of the environment (Linzmeier et al. 2006), as well as assessing changes in natural areas (Staines and Staines 2001, Flowers and Hanson 2003). Since leaf beetles are sensitive to environmental modifications in the microhabitat (Sandoval-Becerra et al. 2017), the

changes in their community parameters and the presence of certain species could be useful to evaluate ecosystem integrity. However, only a few studies have quantitatively analyzed the indicator value of leaf beetles in the face of habitat changes after disturbance (Pimenta and De-Marco 2015, Sandoval-Becerra 2018). Therefore, the objectives of this study were to: 1) compose a faunistic list of Chrysomelidae in a low thorn forest fragment, 2) compare the species richness, abundance, and diversity in areas with different times of succession, 3) evaluate the seasonal effect in the successional stages, and 4) quantify the indicator value of chrysomelid species to secondary succession.

Methods

Study area

The study was conducted in a LTF fragment, located in the municipality of Victoria in the state of Tamaulipas, northeastern Mexico. In order to rule out the influence of topography on successional community patterns, a specific polygon of approximately 400 hectares was delimited on a plain area with little slope, at a homogeneous elevation between 320 and 350 m a.s.l. (23°51.75'N, 99°14'W and 23°51'N, 99°13.25'W). In addition, the area was located on the eastern foothills of the Sierra Madre Oriental, adjacent to the rural localities of Ejido (Ej.) Rancho Nuevo and Ej. Santa Ana (Figure 1).

Climate is classified as warm subhumid with summer rains, with an average annual temperature between 18 °C and 24.3 °C, and a total annual rainfall of 717.3 to 1058.8 mm (Almaguer-Sierra 2005). The highest volume of precipitation occurs between May and October, although occasional rains of less intensity may occur in other months. Due to this climatic regime, LTF vegetation in northeastern Mexico, particularly in the state of Tamaulipas, can be characterized as deciduous (INEGI 2013) or semideciduous (Treviño-Carreón and Valiente-Banuet 2005). However, there are long drought periods without rain for several months; so, the vegetation could also be classified as a dry forest (Challenger and Soberón 2008), although not with as strongly marked seasonality as that observed in communities of the Mexican Pacific (Ceballos et al. 2010, Trejo 2010). Among the dominant plant species are *Celtis pallida* Torr., *Casimiroa greggi* (S. Watson) F. Chiang, *Ebenopsis ebano* (Berland.) Barneby & JW Grimes, *Havardia pallens* (Benth.) Britton & Rose, *Randia obcordata* S Watson, *Cordia boissieri* A DC, and *Croton cortesianus* Kunth. In addition, the LTF in the study area is mixed with communities of submontane scrub and Tamaulipan thorn scrub (Treviño-Carreón and Valiente-Banuet 2005, INEGI 2013, García-Morales et al. 2014). In this way, it constitutes a complex plant community of high diversity, with a notable number of endemic plants (García-Morales et al. 2014).

To the southwest, the study area approaches the Natural Protected Area Altas Cumbres (NPAAC, Figure 1), which constitutes a focal point for biodiversity in northeastern Mexico (Morrone and Márquez 2008, Secretaría de Gobierno 2015). However, the distribution of LTF in the areas surrounding the NPAAC, including the studied fragment, has been reduced significantly from 1973 to 2015 due to land use-cover

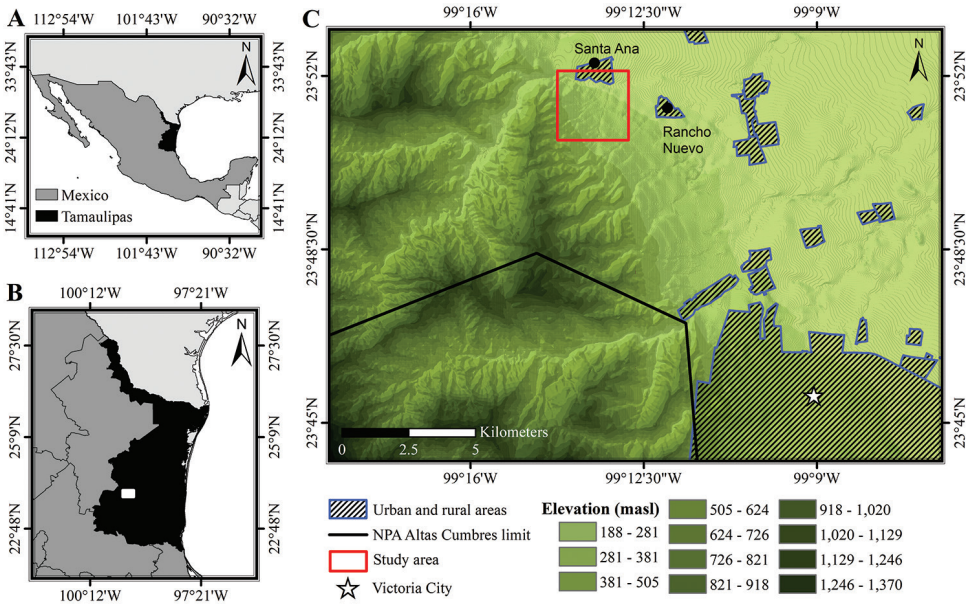

Figure 1. Location of the low thorn forest fragment in northeastern Mexico. **A** Tamaulipas, Mexico **B** location of the fragment within the State **C** detailed location of the LTF fragment in the foothills of the Sierra Madre Oriental, north of the Natural Protected Area Altas Cumbres.

change as a result of frequent fires and conversion to agriculture areas (Sánchez-Reyes et al. 2017), and is currently endangered (Secretaría de Gobierno 2015). Therefore, the study area constitutes a fragment of LTF composed of patches with differing degrees of conservation and times of secondary succession (Sánchez-Reyes et al. 2017).

Successional gradient delimitation

In the study of secondary succession, it is not always possible to measure the process of modification in a vegetal community over time, usually several years, in the same plot or site (Foster and Tilman 2000, Myster and Malahy 2008). An alternative to evaluate these changes is the use of chronosequences, where the study of succession takes place in space instead of time (Walker et al. 2010). Through this approach, it is assumed, among other factors, that selected sites have the same recovery history and that all succession stages have been developed under similar conditions (Denslow and Guzman 2000, Walker et al. 2010). However, these conditions are rarely considered when succession analysis is performed with chronosequences (Johnson and Miyanishi 2008). The use of geographic information systems and satellite images is an effective strategy to assess these assumptions when quantifying the recovery time on vegetation (Vieira et al. 2003, Arroyo-Mora et al. 2005); so, it can be a useful tool for establishing succession time and delimiting valid chronosequences (Sánchez-Reyes et al. 2017).

Table 1. Land use and cover categories in the study area.

Land cover/land use	Description	Reclassification
Conserved low thorn forest	Primary, conserved vegetation of low deciduous or semi-deciduous thorn forest.	Vegetation
Secondary vegetation of low thorn forest	Secondary arboreal vegetation of low thorn forest; predominance of arboreal species characteristic of submontane scrub and Tamaulipan thorn scrub.	Vegetation
Modified areas	Disturbance areas. Dense or low crop vegetation, active or abandoned agricultural areas, low secondary herbaceous vegetation, grassland cover at ground level.	Disturbance
Bare soil areas	Disturbance areas. Sparse or absent vegetation, dry rivers, rocks, bare soil, rural areas or buildings (human settlements).	Disturbance

Table 2. Transitional and persistence processes used to delimit succession categories in the study area. 1 = presence of vegetation (conserved and secondary low thorn forest); 0 = presence of disturbance (modified and bare soil areas).

Category / time of succession	Description	Landsat image					Field validation
		1973	1986	2000	2005	2013	2016, 2017
Conserved areas	Areas with vegetation in 1973 that remained unchanged until 2017	1	1	1	1	1	1
44 years	Areas with disturbance in 1973, but with vegetation in 1986, which persisted until 2017	0	1	1	1	1	1
31 years	Areas with disturbance in 1986, but with vegetation in 2000, which persisted until 2017	–	0	1	1	1	1
17 years	Areas with disturbance in 2000, but with vegetation in 2005, which persisted until 2017	–	–	0	1	1	1
12 years	Areas with disturbance in 2005, but with vegetation in 2017	–	–	–	0	1	1
4 years	Areas with disturbance in 2013, but with vegetation in 2017	–	–	–	–	0	1
Persistence of disturbance	Areas with disturbance in 1973, and remaining unchanged until 2017	0	0	0	0	0	0

We followed the chronosequence approach in this study. Delimitation of succession time of the LTF in the study area was carried out through the analysis of Landsat satellite images of the years 1973, 1986, 2000, 2005 and 2013 (Gutman et al. 2013), employing previously established methodology to calculate the approximate time of succession and define valid chronosequences (Sánchez-Reyes et al. 2017). Briefly, through this method, each of the five images was classified into four types of land use and cover (Table 1), using an unsupervised segmentation, together with the manual selection of training fields and the maximum likelihood algorithm. Afterwards, the four land use and cover categories were unified by means of an image reclassification into only two categories: vegetation and disturbance (Table 1). Finally, the reclassified images were subjected to a cross-tabulation analysis to delimit the time of succession, based on the date since the last disturbance and the transition or persistence of vegetation (LTF) from 1973 to 2013 (Table 2). Complementarily, the current presence of vegetation or disturbance was validated directly in the field during 2016–2017, as well as with recent Google Earth images. In this way, the final succession time in each area was delimited by the changes from 1973 to 2017 (Table 2). Procedures were conducted in the software IDRISI Selva 17.0.

Leaf beetles sampling

Sampling sites were selected according to the extent, location, and accessibility of the successional patches in the study area. Only four categories were selected for this study: 1) areas with four years of succession, 2) areas with 17 years of succession, 3) areas with 31 years of succession, and 4) conserved areas (Figure 2). In each of the four categories, a sample size of eight plots of 10 × 10 m was established; sample size was delimited through the analysis of preliminary data with the Clench model (Jiménez-Valverde and Hortal 2003). Sampling plots were located randomly using a previously established procedure (Sánchez-Reyes et al. 2016) using geographic information systems and specialized software (ArcView GIS, IDRISI Selva 17.0). With this method, it was possible to assess the geographical location of each plot before field sampling, in order to minimize the edge effect, as well as the closeness between plots, which guarantees the feasibility of sampling and the independence of the samples.

Leaf beetles were sampled using an entomological sweep net (60 centimeters long and 40 centimeters in diameter). Each sample consisted of 200 sweeps on all the shrub and herbaceous vegetation in each plot, from soil level up to a maximum height of 2 m, between 10:00 and 14:00 hrs. All contents of the net after 200 sweeps were deposited

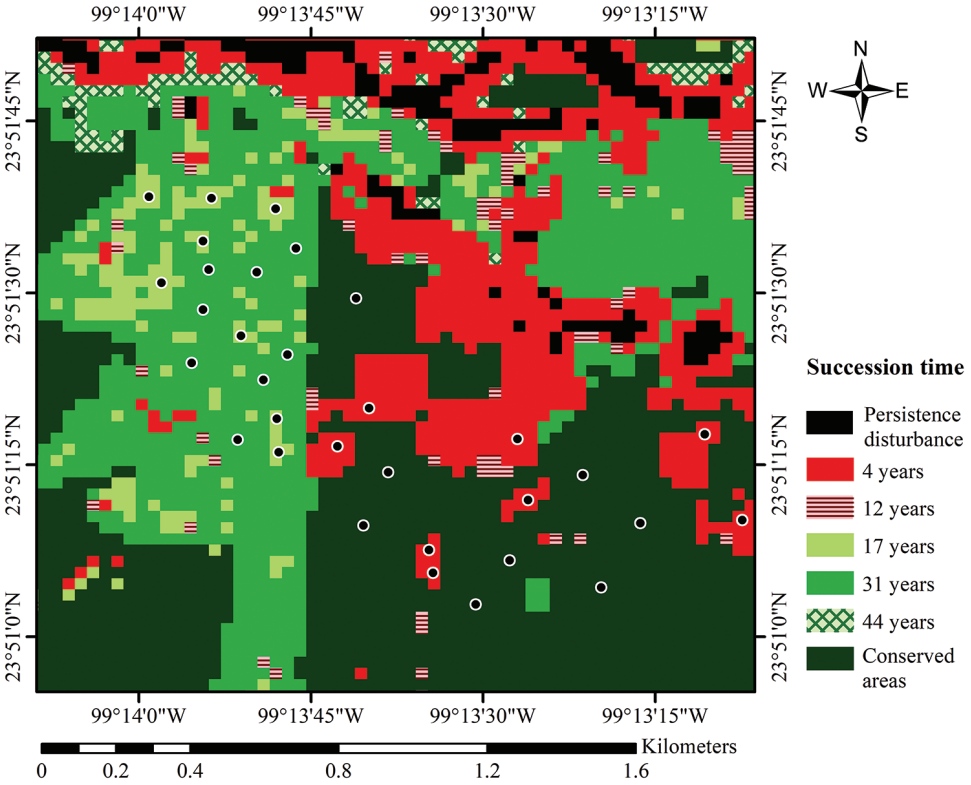

Figure 2. Successional gradient of low thorn forest in northeastern Mexico, and location of the sampling plots.

in a plastic bag, adding 70 % ethyl alcohol, as well as a label with the corresponding data. Each plot of each successional category was sampled once a month, from May 2016 to April 2017, for a total of 384 samples (8 plots x 4 categories x 12 months).

The processing of samples and preparation of specimens were conducted in the laboratory according to previously established methods (Sánchez-Reyes et al. 2014). Taxonomic identification was made using specialized literature (Wilcox 1965, Wilcox 1972, Scherer 1983, White 1993, Flowers 1996, Riley et al. 2002, Staines 2002) and by comparison with specimens in the collection of the Facultad de Ingeniería y Ciencias, Universidad Autónoma de Tamaulipas (FIC-UAT), and identified taxa were organized following the arrangement proposed by Riley et al. (2003) and Bouchard et al. (2011). Specimens that could not be identified to species level were differentiated as morphospecies, based on characteristics of internal genitalia. In this way, the term "species" in this study includes both specimens determined at a specific level and morphospecies. Specimens were deposited in collections of the Instituto Tecnológico de Ciudad Victoria (ITCV) and the FIC-UAT, as well as in the personal collection of the first author (IC-UJSR).

Data analysis

The observed species richness was measured as the total number of species in the LTF fragment, as well as at each successional category. Significant differences in the number of species among categories were determined by the diversity permutation test implemented in PAST 3.07 (Hammer et al. 2001). Estimated species richness was calculated for the entire study area and for each category, using the Chao 1, Chao 2, Jackknife 1, Jackknife 2, ACE and ICE nonparametric indices. Inclusion of these indices is recommended in biodiversity studies to evaluate the estimated range of species in the faunistic inventory (Hortal et al. 2006); calculations were made in EstimateS 8.2 (Colwell 2013), using 100 randomizations without replacement. We also calculated the estimated species richness through the Clench model, as well as the slope value, in order to determine the quality of inventories, where values close to or less than 0.1 are considered characteristic of reliable inventories (Jiménez-Valverde and Hortal 2003). The Clench model was performed in STATISTICA 8.0 (StatSoft Inc. 2007), following the parameters indicated by Jiménez-Valverde and Hortal (2003). Completeness of the total inventory and of each category was obtained as the proportion of observed richness with respect only to the estimated value of the Chao 1 index, since it takes into account the abundance of species and acts as a lower bound for species richness (Chao and Chiu 2016), and was expressed as percentage.

Overall differences in abundance of leaf beetle communities in the successional gradient were calculated with the Kruskal-Wallis test, after discarding a normal distribution. In addition, significant differences in abundance between categories were obtained through pairwise comparisons, using the Mann-Whitney test. Diversity was considered as a proportional value between species richness and abundance values,

and was quantified by Simpson's dominance index and the Shannon entropy index (Magurran 2004); these were calculated for the entire study area and for each successional category. Pairwise comparisons of diversity values between categories were carried out using the diversity permutation test. Changes in species composition between successional categories were evaluated by comparing faunistic similarity, using the Bray-Curtis index (Magurran 2004). All analyzes were performed in PAST 3.07.

Seasonal effect was measured separately, by comparing observed and estimated species richness, abundance, and diversity in each category during the rainy (May to October 2016) and dry seasons (November 2016 to April 2017); differences in abiotic conditions between both seasons were confirmed in a previous study (Sánchez-Reyes et al. in press). The aforementioned indices and statistical tests were used for such comparisons: nonparametric estimation of species richness, Kruskal-Wallis and Mann-Whitney tests for differences in abundance, diversity permutation tests for observed species richness, and Simpson and Shannon indices, which were conducted in PAST 3.07. An agglomerative Cluster analysis was performed in order to include the seasonal effect in faunistic composition, with the objective of grouping categories and seasons according to their similarity in species composition. For this, a dissimilarity matrix based on Bray-Curtis distance and Ward's amalgamation algorithm was used. Cluster analysis was performed in STATISTICA 8.0.

The indicator value of chrysomelid species was quantified by the Indicator Value Index, or IndVal (Dufrêne and Legendre 1997). The index is based on the degree of specificity (exclusivity of the species to a particular site based on its abundance) and the degree of fidelity (frequency of occurrence within the same habitat) (Tejeda-Cruz et al. 2008), expressed in a percentage value. The analysis was carried out using the *labsdv* package in platform R version 3.2.2, using 1000 random permutations to define the significance level. Indicator species with an index equal to or greater than 70 % were categorized as "characteristic" species, while species with a value less than 70 % but equal to or greater than 30 % were considered "detector" species.

Results

Successional variation of leaf beetle communities

In total, 6978 specimens of leaf beetles were collected distributed in six subfamilies, 57 genera, and 85 species (Appendix 1). The greatest abundance and species richness were observed in the subfamily Galerucinae (6416 specimens and 40 species respectively). Total values of estimated richness in the low thorn forest fragment suggested a reliable inventory (slope = 0.029), with a total completeness of 82.52 %. The dominance was 0.284, while the Shannon index was 2.009 (Table 3).

The analysis of successional categories revealed that the species richness was significantly higher in the areas of four years of succession. The conserved areas also demonstrated a high number of species, although the value was similar to that observed

Table 3. Succession parameters of leaf beetle communities in a low thorn forest in northeastern Mexico.

Ecological parameter	Low thorn forest total	Succession time			
		4 years	17 years	31 years	Conserved areas
Observed richness*	85	58 a	36 b	31 b	45 ab
Chao 1	103	70.07	66.23	33.57	52.55
Chao 2	97.86	72.07	53.81	34.96	56.95
Jackknife 1	103.95	73.83	47.88	38.92	57.86
Jackknife 2	108.96	80.78	55.75	39	63.81
ICE	101.34	71.4	44.43	37.63	58.64
ACE	99.91	68.05	44.52	34.9	52.43
Clench model	95.53	68.40	46.32	40.27	55.16
Slope	0.029	0.103	0.087	0.075	0.093
Completeness (%)	82.52	82.77	54.35	92.34	85.63
Abundance*	6978	2725 a	1753 a	1674 ab	826 b
Dominance (Simpson index)*	0.2841	0.2174 a	0.6543 b	0.781 c	0.1469 d
Diversity (Shannon index)*	2.009	2.084 a	0.9797 b	0.6796 c	2.521 d

*Different letters between columns are significantly different from each other.

Table 4. Faunistic similarity of Chrysomelidae between successional categories of a low thorn forest in northeastern Mexico. Upper diagonal, values of the Bray-Curtis index. Lower diagonal, values expressed in percentage.

	4 years	17 years	31 years	Conserved areas
4 years	1	0.3135	0.2629	0.2225
17 years	31.35 %	1	0.9456	0.2300
31 years	26.29 %	94.56 %	1	0.2265
Conserved areas	22.25 %	23 %	22.65 %	1

in the intermediate categories (17 and 31 years of succession). In all categories, the inventories were reliable according to the Clench slope values, and the observed species richness values were close to the estimated values; areas of 4 and 31 years of succession, as well as conserved areas, had a completeness value above 70 %. However, a low value of completeness (54.35 %) was obtained only in the areas of 17 years of succession (Table 3). The abundance decreased significantly with the increase in time of succession ($H = 12.56$, $p = 0.005$). Thus, early succession sites had the highest number of specimens when compared to the conserved areas. The values of diversity were significantly different among all the categories ($p < 0.05$). Highest dominance and lowest diversity were obtained in the intermediate succession areas (17 and 31 years); in contrast, the conserved areas recorded the highest diversity value (Table 3).

With respect to the Bray-Curtis index, a very high similarity was observed in the faunistic composition between the intermediate (17 and 31 years) successional areas (94.56 %). Remaining comparisons were below 50 % similarity (Table 4).

Effect of seasonality on the successional changes of Chrysomelidae

Seasonal effect was absent in the observed species richness, since there were no significant differences ($p > 0.05$) between the rainy and dry seasons in any of the four categories (Figure 3). The estimated richness analysis revealed that both inventory reliability and completeness were higher in the dry season than in the rainy season, in all categories (Table 5). On the other hand, in all cases the completeness was higher than 70 %; however, in the 17-year category, the estimated richness reached very high proportions during the rainy season, with a total completeness of 35.54 % (Table 5).

Differences in abundance between the rainy and dry season were significant in each category ($p < 0.05$), except for the conserved areas where the number of specimens was similar in both seasons ($p = 0.0904$). In addition, during the rainy season, the abundances observed in the areas of 4, 17, and 31 years were similar, but significantly different from the conserved areas; contrarily, during the dry season there were no differences in abundance between categories (Figure 3). Regarding diversity, the seasonal effect was not observed in the areas of 4 years of succession, since there were no differences in either the Simpson or Shannon indices between seasons. In the case of the intermediate areas (17 and 31 years of succession), lower dominance and higher diversity occurred during the dry season. Conversely, the minimum dominance and maximum diversity values in the study area were obtained in the conserved areas during the rainy season (Figure 3).

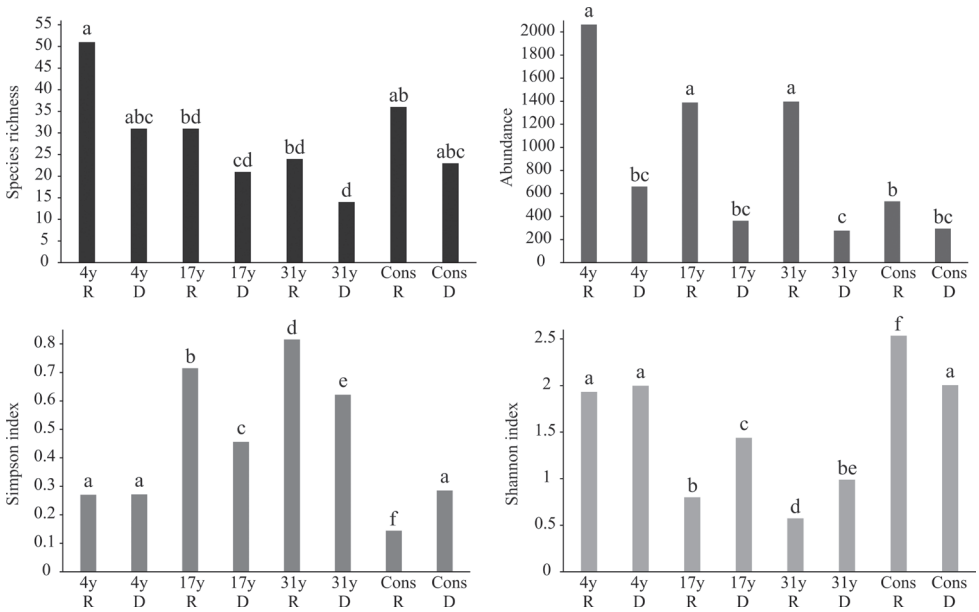

Figure 3. Seasonal variation of community parameters of Chrysomelidae in a successional gradient of low thorn forest in northeastern Mexico. Different letters between bars indicate significant differences.

Table 5. Influence of seasonality on the estimated species richness and inventory completeness of successional categories in a low thorn forest in northeastern Mexico.

	4 years		17 years		31 years		Conserved	
Estimator index	**Rainy**	**Dry**	**Rainy**	**Dry**	**Rainy**	**Dry**	**Rainy**	**Dry**
Chao 1	70.59	31.64	87.21	21.07	27.12	14.1	42.39	23.9
Chao 2	71.21	31.37	66.37	21.05	32	14.06	52.32	23.63
Jack 1	67.65	33.94	47.65	21.98	30.85	14.98	45.79	25.94
Jack 2	77.37	25.56	60.19	13.56	34.75	8.43	52.56	22.25
ICE	68.37	32.09	66.59	21.36	29.21	14.4	44.56	24.6
ACE	63.47	32.35	57.91	21.36	27.45	14.47	42.27	24.82
Clench model	63.12	38.40	47.94	27.51	30.67	18.80	43.22	28.69
Slope	0.222	0.121	0.233	0.096	0.111	0.071	0.136	0.091
Completeness (%)	72.24	97.97	35.54	99.66	88.49	99.29	84.92	96.23

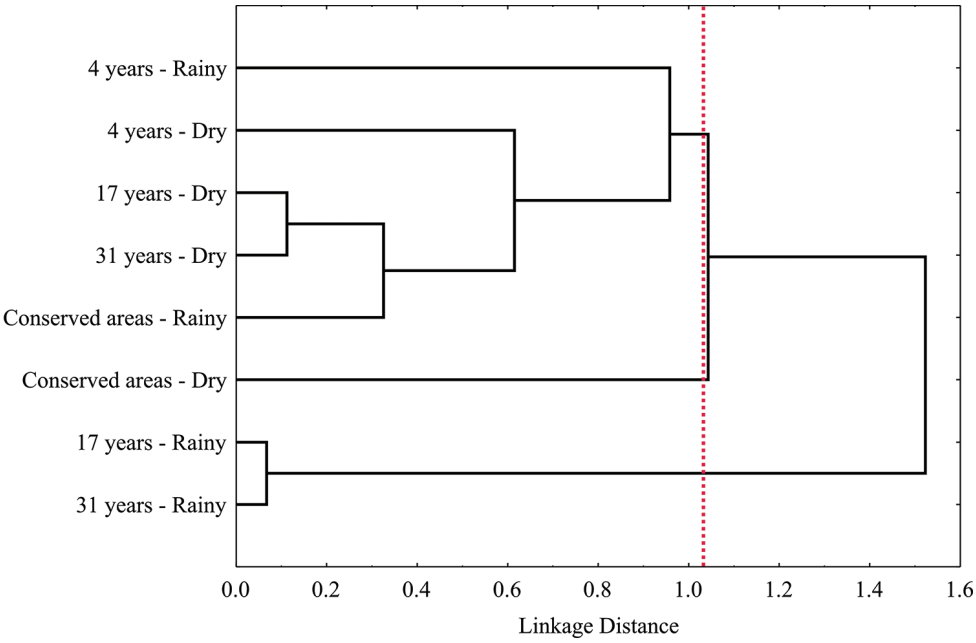

Figure 4. Cluster analysis of leaf beetle composition between succession and seasonal categories (rainy and dry) in a low thorn forest in northeastern Mexico. The dotted line indicates the delimitation of the groups.

The analysis of similarity in species composition between successional categories, considering the seasonal effect, suggested the presence of three faunistic groups. The first group consisted of the areas of 17 and 31 years of succession during the rainy season. Conserved areas during the dry season represented another group. The category of four years of succession, intermediate areas during the dry season, and conserved areas in the rainy season formed a third group with higher heterogeneity (Figure 4).

Indicator value of leaf beetles in the successional gradient

Of the 85 total species found in the LTF, only 24 had a significant indicator value ($p < 0.05$, Table 6, Figures 5, 6). The highest proportion involved detector species, with an IndVal between 30 and 70 % (17 species). The remaining seven were characteristic species, with values higher than 70 % (Table 6). Four species were considered as characteristic of areas with four years of succession, of which *Brachycoryna pumila* Guérin-Méneville, 1844 and *Chaetocnema* sp. 1 had the highest indicator values; the other six species were detectors of this category. *Cyclotrypema furcata* (Olivier, 1808) and *Heterispa vinula* (Erichson, 1847) were detector species of areas with 17 years of succession, while *Centralaphthona diversa* (Baly, 1877), *Dysphenges* sp. 1 and *Sumitrosis inaequalis* (Weber, 1801) were detectors of 31 years of succession. In the conserved areas, six species were detectors; only *Acrocyum dorsalis* Jacoby, 1885, *Margaridisa* sp. 1 and *Parchicola* sp. 1 were characteristic indicators, the latter being the one with the highest specificity.

Table 6. Leaf beetle species with a significant indicator value in a successional gradient of low thorn forest in northeastern Mexico. Indicator values in succession categories are expressed in percentage. Key: C = characteristic; D = Detector, *p* = probability.

Species	Succession time				*p*	Indicator category
	4 years	17 years	31 years	Conserved areas		
Acallepitrix sp. 1	0.00	7.89	0.66	47.37	0.0048	D
Acrocyum dorsalis	0.00	0.00	0.00	75.00	0.0003	C
Alagoasa jacobiana	4.46	2.38	5.36	56.25	0.0017	D
Asphaera sp. 1	34.09	1.14	0.00	0.00	0.0433	D
Babia tetraspilota texana	53.85	7.21	11.54	0.48	0.0021	D
Brachycoryna pumila	88.73	2.82	0.00	0.00	0.0001	C
Centralaphthona diversa	11.08	40.83	42.74	5.35	0.0241	D
Chaetocnema sp. 1	93.47	5.55	0.00	0.02	0.0001	C
Colaspis townsendi	53.35	0.30	0.00	3.05	0.0072	D
Cryptocephalus trizonatus	37.50	0.00	0.00	0.00	0.0492	D
Cyclotrypema furcata	30.65	55.91	0.81	0.00	0.0047	D
Dysphenges sp. 1	21.88	14.51	42.19	0.45	0.0282	D
Epitrix sp. 1	90.87	0.15	0.02	5.24	0.0001	C
Epitrix sp. 2	19.44	4.86	0.52	63.89	0.0001	D
Epitrix sp. 3	75.38	0.34	0.10	3.89	0.0003	C
Epitrix sp. 4	7.34	0.27	0.00	58.70	0.0036	D
Epitrix sp. 5	1.97	7.89	0.00	39.47	0.0327	D
Helocassis clavata	5.07	2.70	0.68	61.49	0.0014	D
Heterispa vinula	7.50	45.21	18.33	0.97	0.0351	D
Margaridisa sp. 1	12.74	0.12	1.14	72.96	0.0002	C
Parchicola sp. 1	1.32	0.00	0.00	78.29	0.0001	C
Parchicola sp. 2	37.50	0.00	0.00	0.00	0.0483	D
Plagiodera thymaloides	42.86	0.45	19.64	0.00	0.0257	D
Sumitrosis inaequalis	0.83	5.00	36.67	0.00	0.0353	D

Figure 5. Chrysomelidae species with significant indicator value of successional time in a low thorn forest fragment in northeastern Mexico. **A** *Acallepitrix* sp. 1 **B** *Epitrix* sp. 5 **C** *Acrocyum dorsalis* Jacoby, 1885 **D** *Alagoasa jacobiana* (Horn, 1889) **E** *Asphaera* sp. 1 **F** *Babia tetraspilota texana* Schaeffer, 1933 **G** *Brachycoryna pumila* Guérin-Méneville, 1844 **H** *Centralaphthona diversa* (Baly, 1877) **I** *Chaetocnema* sp. 1 **J** *Colaspis townsendi* Bowditch, 1921 **K** *Cryptocephalus trizonatus* Suffrian, 1858 **L** *Cyclotrypema furcata* (Olivier, 1808). Scale bar: 1 mm.

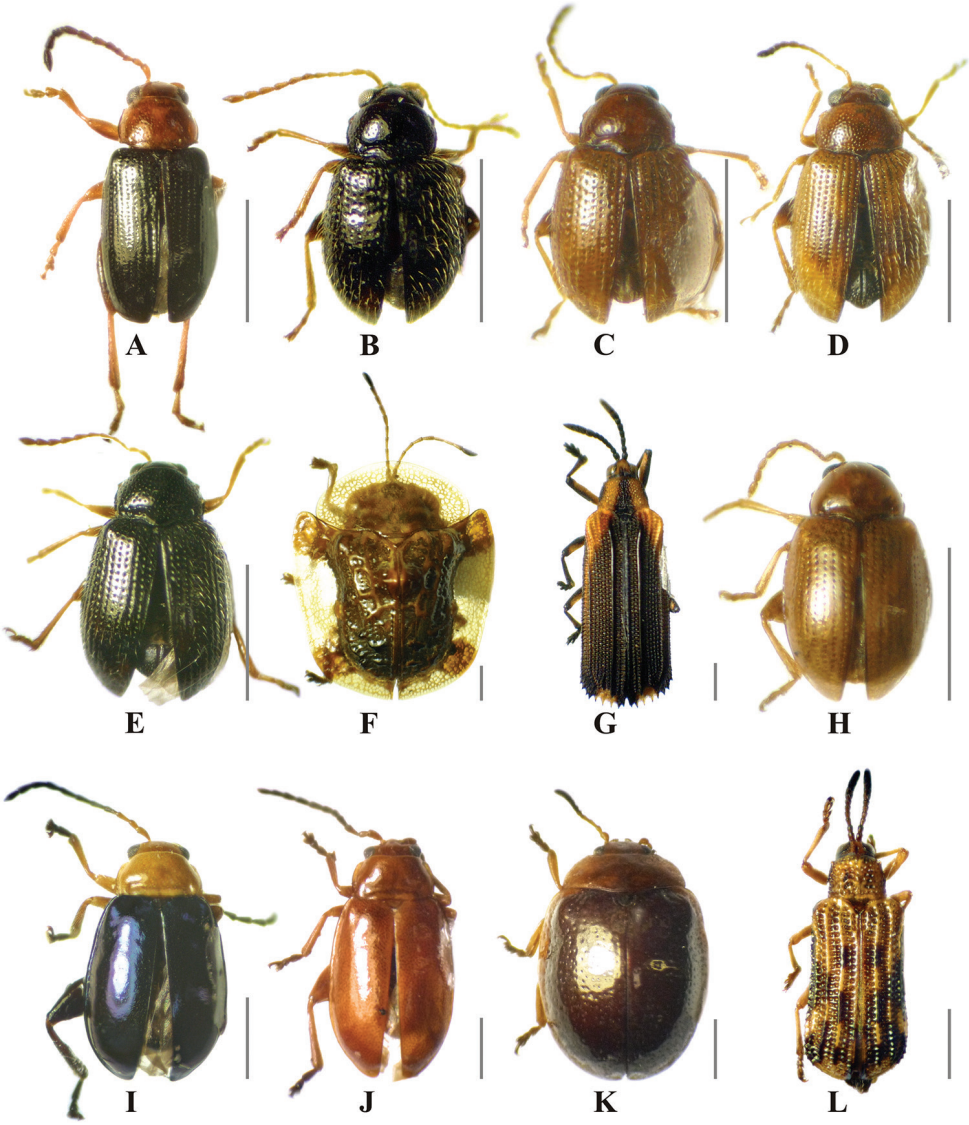

Figure 6. Chrysomelidae species with significant indicator value of successional time in a low thorn forest fragment in northeastern Mexico. **A** *Dysphenges* sp. 1 **B** *Epitrix* sp. 1 **C** *Epitrix* sp. 2 **D** *Epitrix* sp. 3 **E** *Epitrix* sp. 4 **F** *Helocassis clavata* (Fabricius, 1798) **G** *Heterispa vinula* (Erichson, 1847) **H** *Margaridisa* sp. 1 **I** *Parchicola* sp. 1 **J** *Parchicola* sp. 2 **K** *Plagiodera thymaloides* Stål, 1860 **L** *Sumitrosis inaequalis* (Weber, 1801). Scale bar: 1 mm.

Discussion

The present study constitutes the first faunistic contribution of Chrysomelidae in the low thorn forest vegetation. The observed species richness and completeness values suggest that the fauna of leaf beetles in the LTF is close or superior to other types of low tropical forest (Sánchez-Reyes et al. 2014, Lucio-García 2018). In general terms, the values represent 34 % of the observed chrysomelid richness in Tamaulipas (Niño-Maldonado et al. 2014), as well as 3.19 % of the country-wide values (Niño-Maldonado and Sánchez-Reyes 2017). In addition, the abundance values were higher than for other studies carried out in the region, including those conducted in larger geographical areas also during an annual period (Niño-Maldonado et al. 2005, Sánchez-Reyes et al. 2014, 2016). One of the factors that can give rise to such results is the complexity of the plant structure in the study area, which consists of tropical vegetation elements in conjunction with species from semi-arid or subtropical areas, such as Tamaulipan thorn scrub or submontane scrub (Treviño-Carreón and Valiente-Banuet 2005, García-Morales et al. 2014). This floristic complexity was mirrored in the presence of an equally complex chrysomelid fauna. In addition, the proximity to the NPA Altas Cumbres (Secretaría de Gobierno 2015) and the adjacent location of one of the panbiogeographic nodes of Mexico (Morrone and Márquez 2008) should undoubtedly be related to the species composition observed.

However, the environmental heterogeneity in the LTF, resulting from disturbance and secondary succession, is perhaps the most important factor leading to the observed patterns. Previous studies had been carried out mainly in natural protected areas, where ecosystems have a high degree of conservation and low occurrence of fragmentation (Niño-Maldonado et al. 2005, Sánchez-Reyes et al. 2014, 2016). Contrastingly, LTF in northeastern Mexico, particularly in the eastern boundaries of the NPA Altas Cumbres, constitutes a highly heterogeneous habitat, which has been subject to strong fragmentation and presently is composed of patches with different succession times (Sánchez-Reyes et al. 2017). Environmental heterogeneity is one determining factor in the structure of communities, and, although it can be variable, its increase is positively related to the species richness (Tamme et al. 2010, Stein et al. 2014, Yang et al. 2015). Such an effect has been observed in other studies of Chrysomelidae; for example, in temperate forests of northeastern Mexico, a high diversity is associated with a heterogeneous mosaic of vegetation with different times since last disturbance (Sandoval-Becerra et al. 2018). In that sense, the influence of heterogeneity was made evident in this study through the detailed comparisons of species richness, abundance, and diversity between areas with different times of succession.

Responses of communities to disturbance are diverse (Winter et al. 2015). Overall, in the LTF the greatest number of species occurred in the category of 4 years of succession. Early successional areas (those without dense tree cover or with open canopy) can promote diversity due to their high structural and spatial complexity (Swanson et al. 2011). On the other hand, the estimators were very close to the observed richness for each successional category, indicating that faunistic inventory was nearly complete,

and thus that the calculated parameters are reliable. Several studies in disturbance-succession gradients found that the greatest number of insects occurred in advanced stages of recovery, or in mature, conserved areas (Barberena-Arias and Aide 2003, Jeffries et al. 2006, Villa-Galaviz et al. 2012, Perry et al. 2016). However, this depends on the ecological characteristics of the taxa analyzed, since disturbance can contribute to the increase in diversity (Steffan-Dewenter and Tscharntke 2001, Stephen and Sánchez 2014, Winter et al. 2015, Yuan et al. 2016, O'Brien et al. 2017). In the case of leaf beetles, it has been observed that species richness augments in modified areas (Heusi-Silveira et al. 2012), as was observed in this study. This is because, in recently disturbed or early succession areas, the density of herbaceous and shrub plants is usually higher. This favors the presence of a greater number of phytophagous insects in these areas, given their close association with successional changes of vegetation (Fernandes et al. 2010, O'Brien et al. 2017). In addition, in the area of this study, the early succession stages of LTF are also dominated by species from other plant communities, such as submontane scrub or Tamaulipan thorn scrub (Canizales-Velázquez et al. 2009). Therefore, early succession areas constitute habitats of a complex floristic structure, which triggers a higher environmental heterogeneity and thus explains the high number of chrysomelid species. With respect to abundance, the obtained results agree with trends observed in other studies, since the number of specimens decreased linearly from early succession to the most conserved areas (Heusi-Silveira et al. 2012, O'Brien et al. 2017). Similarly, this is attributed to a higher density of herbaceous and shrub plants in recently disturbed areas (Guariguata and Ostertag 2001, Pickett et al. 2008, Swanson et al. 2011). Besides, this decline in abundance was related to a drop in dominance values in conserved areas, in a way that this category registered the highest diversity, that is, the highest effective number of species considering an equitable community (Jost 2006). Over the course of succession, increase in stability of communities occurs, while fluctuations in availability of resources for species decrease (Anderson 2007). This homogeneity in environmental conditions allows for an even distribution in the relationship between species richness and abundance, thus increasing diversity (Magurran 2004).

Seasonality had a very important influence on the successional patterns. However, differences in species richness were non-existent between seasons. Thus, the number of leaf beetle species was similar throughout the year in each successional category. On the other hand, the number of specimens was significantly higher during the rainy season in all successional categories (4, 17, and 31 years); contrarily, no differences were observed in conserved areas. This is attributed to the vegetation characteristics in successional areas. An open structure of the canopy allows for a greater light input, which during the rainy season favors a high density of annual herbaceous and shrub species (Guariguata and Ostertag 2001, Pickett et al. 2008, Swanson et al. 2011), which constitute a very abundant food resource, but only during one season. Over the course of succession, dominance of shrubs and other perennial herbaceous plants increases (Swanson et al. 2011); indeed, the understory in conserved areas of LTF is dominated mostly by perennial or semiperennial species (Treviño-Carreón and Valiente-Banuet 2005, García-Morales et al. 2014), and these satisfy nourishing requirements of leaf

beetles even during the dry season. Such an effect of transition from annual to perennials plants during succession has also been observed in other groups of insects (Steffan-Dewenter and Tscharntke 2001).

With respect to diversity, the intermediate categories (17 and 31 years of succession) showed significantly higher values in the dry season, while in the conserved areas they were higher during the rainy season. Intermediate areas of LTF are spatially and floristically heterogeneous; thus, the existence of annual species from other scrub communities must be responsible for the drastic reduction of understory vegetation in the dry season; consequently, this causes the decrease in abundance, reducing dominance and increasing diversity. Oppositely, the environmental conditions during the rainy season in conserved areas seem to be supporting a greater availability of resources, in such a way that leaf beetle species are uniformly dispersed; this can be attributed to the higher specialization of species in mature or conserved areas (Pellissier 2015). In contrast, the absence of differences in seasonal diversity at early succession areas can be attributed to generalist species, which are dominant in highly heterogeneous areas (Büchi and Vuilleumier 2014). Consequently, dominance and diversity remain constant throughout the year, regardless of available resources in each season, since generalists feed on multiple plant species and tolerate a wide range of microclimatic conditions (Sandoval-Becerra et al. 2018). An example of such species is *Brachycoryna pumila*, because its abundance was higher in areas of four years of succession in both seasons, thus suggesting a wide abiotic tolerance; also, *B. pumila* is associated with several species of plants in different genera, such as *Abutilon*, *Malvastrum*, or *Sida*, among others (Staines 1986). However, biological and ecological information is lacking for most of the leaf beetle species in the region; therefore, future assessments on niche requirements of leaf beetles need to be conducted.

In addition to the consequences to abundance and diversity, disturbance and successional changes also influence species composition (Perry et al. 2016). For example, it has been observed that dry season results in greater faunistic similarity between different sites, despite having different degrees of conservation (Janzen 1976). Such an influence was evident in this work, since, according to the Cluster analysis, the areas of 4, 17, and 31 years had the same species composition during the dry season. Besides, the conserved areas had a totally different composition with respect to the other successional stages, which agrees with patterns observed in several other insect taxa (Barberena-Arias and Aide 2003, Perry et al. 2016). In this regard, early succession areas and high heterogeneity due to disturbance may indeed increase the number of species, as was discussed above; however, the similarity of faunistic composition between such areas and conserved sites is very low. Thus, it is necessary to point out the importance of the conserved areas for Chrysomelidae distribution in the low thorn forest vegetation, as their communities are unique to these types of habitats when compared with disturbed areas.

An important theory that aims to explain the relationship between disturbance and diversity is the intermediate disturbance hypothesis (IDH, Connell 1978, Willig and Presley 2018). It postulates that with the increase of the disturbance an imbalance is created in the environmental conditions, and that this reduces the probability of exclusion among coexisting species (Connell 1978, Huston 2014). Thus, intermediate areas

represent a convergence of both ends of the gradient, promoting greater heterogeneity in conditions that allows an increase in the resource availability, as well as in the richness and diversity of species (Shea et al. 2004, Bongers et al. 2009, Roxburgh et al. 2004, Winter et al. 2015). Also, intermediate areas may increase herbivory patterns (Chapin et al. 2011). The influence of IDH has been proven previously with Chrysomelidae in other types of vegetation (Linzmeier et al. 2006, Linzmeier and Ribeiro-Costa 2009, Sandoval-Becerra et al. 2018). Observed results in the LTF were contrary, since as explained above, the intermediate areas of 17 and 31 years of succession had very low values of richness and diversity. However, richness estimators can determine the validity of the IDH in the study area, because the category of 17 years of succession could reach above 87 species during the rainy season, while the completeness was higher in the other categories and seasons. Such an estimated value was close to the total observed richness for the entire LTF fragment, confirming that areas of 17 years are a heterogeneous environment with characteristics of both early and late successional stages, creating niches for numerous species (Sandoval-Becerra et al. 2018). It is possible that the randomized design of the study caused that location of most of the intermediate sampling plots fell in areas with low density of herbaceous and shrub vegetation, while only a few plots had contrasting conditions. Such differences would be enhanced due to a higher environmental heterogeneity in the rainy season. In addition, the convergence of species from early and late succession areas was supported by the higher faunistic similarity observed between the categories of 17 and 31 years of succession, even when including a seasonal effect. Therefore, it is fairly possible that community patterns of Chrysomelidae in the LTF are consistent with IDH, although future studies with a higher number of samples are necessary to corroborate this presumption.

Overall, the seasonal effect on leaf beetle communities has been previously assessed in natural gradients (Bouzan et al. 2015, Sánchez-Reyes et al. 2014, 2016). However, the interaction between seasonality and secondary succession, as investigated here, has been poorly quantified (Janzen 1976, Linzmeier and Ribeiro-Costa 2009). Analysis of these patterns is important to determine the magnitude of changes in insect communities after disturbance, so that conservation strategies can be applied successfully. Besides, the understanding of seasonal influence on successional trajectories is critical not only for leaf beetles, but also for other biological groups, since incoming environmental modifications due to climate change surely will affect the mechanisms in which communities response to disturbance, and will therefore affect their resilience aptitude. Hence, more studies are sorely needed in order to clarify these associations, since the responses to succession and disturbance are influenced by microenvironmental changes, and these responses differ depending on the species (Sandoval-Becerra et al. 2017).

Regarding the indicator potential of Chrysomelidae, other studies have suggested that the higher proportion and abundance of leaf beetles are characteristics of early succession or recently disturbed areas (Pimenta and De-Marco 2015), which was corroborated in this study. However, it is evident that the observed community patterns (such as abundance) are driven by the specific response of each species, since leaf beetles can tolerate different microclimatic and microhabitat conditions after disturbance (Sand-

oval-Becerra et al. 2017). Therefore, these characteristics may allow species within this family to be used as indicators. The potential of leaf beetles for environmental monitoring has been suggested by other authors (Nummelin and Borowiec 1992, Flowers and Hanson 2003, Linzmeier et al. 2006). Similarly, the usefulness of chrysomelid diversity as an indicator of plant species richness has been recognized (Kalaichelvan and Verma 2005, Baselga and Novoa 2007). However, only a few exceptional studies have presented quantifiable indicator values (Pimenta and De-Marco 2015).

The indicator value index (IndVal) allows for statistical evaluation of the degree of association between species and their environment (Dufrêne and Legendre 1997, De-Cáceres et al. 2012). Species with a significant IndVal can be separated into characteristic and detector species, according to their specificity towards a particular habitat condition. The characteristic indicator species are those with high specificity and fidelity to a given habitat, and therefore a high percentage of indicator value (Dufrêne and Legendre 1997, McGeoch et al. 2002, Tejeda-Cruz et al. 2008). These may be important from an ecological perspective, but not very useful for disturbance quantification, since their presence is exclusive of certain habitats and thus the destruction or modification of such areas would drive local extinction (Hodkinson and Jackson 2005). In contrast, indicator species with moderate levels of specificity (i.e., detector species) have differing degrees of preference for the various ecological states (Dufrêne and Legendre 1997, McGeoch et al. 2002, Tejeda-Cruz et al. 2008). Such detector species are ideal for monitoring, because their wide niche breadth and their changes in abundance during disturbance ensure that they can be dispersed along a disturbance gradient (McGeoch et al. 2002, Hodkinson and Jackson 2005). Accordingly, we consider that indicator species in this study, such as *Centralaphthona diversa*, *Cyclotrypema furcata* and *Heterispa vinula*, are potentially suitable as indicators of succession time and for environmental monitoring in other areas with similar vegetation; in addition, species like *Acrocyum dorsalis* could be useful to detect conserved areas of LTF (Figure 7). These species are easily identifiable (even in the field), are abundant (so their proportion in different degrees of disturbance can be statistically quantified), and are widely distributed in the region (Niño-Maldonado et al. 2014, Sánchez-Reyes et al. 2016). Therefore, they fulfill the expected characteristics for a good indicator taxon (Carignan and Villard 2002, Ribera and Foster 1997). Besides, their response as significant indicator species is consistent with other ecological gradients, such as microclimate or elevation (Sánchez-Reyes et al. 2016, 2017). However, their presence as an indicator in this study does not guarantee that their response to succession time will be homogeneous in other areas; such responses must be consistent and repeatable in different sites and time scales in order to consider a species as a reliable indicator (McGeoch et al. 2002, Hodkinson and Jackson 2005). Currently, we suggest the inclusion and use of these (and maybe the other species that were found) for the monitoring of secondary vegetation and quantification of succession time in LTF in northeastern Mexico. Further evidence of their usefulness as indicator species will contribute to the implementation of new and better conservation strategies, and to an efficient delimitation of natural protected areas which take into account the importance of secondary vegetation for species distribution.

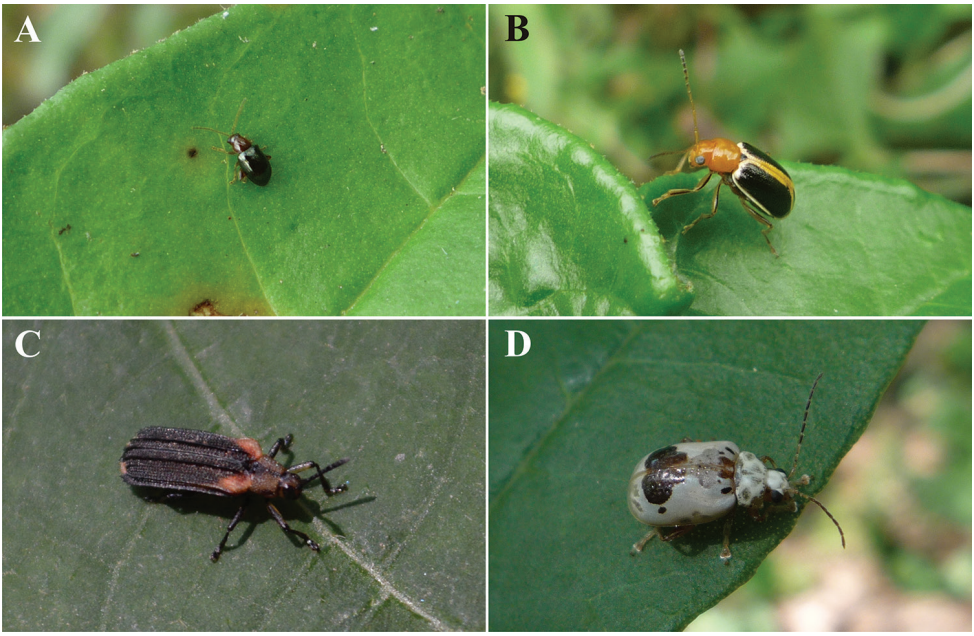

Figure 7. Suggested species of Chrysomelidae for evaluating successional time and environmental monitoring of low thorn forest in northeastern Mexico. **A** *Centralaphthona diversa* (Baly, 1877) **B** *Cyclotrypema furcata* (Olivier, 1808) **C** *Heterispa vinula* (Erichson, 1847) **D** *Acrocyum dorsalis* Jacoby, 1885.

Conclusions

The study of effects of disturbance and secondary succession on species and communities is a key issue in ecology and conservation. In that sense, faunistic patterns of leaf beetles and their association to secondary succession are evaluated for first time in low thorn forest vegetation in northeastern Mexico. A highly fragmented landscape in early and intermediate successional stages, as well as the convergence of other vegetation communities, could be related to the high number of species found, due to a complex environmental heterogeneity. Overall, observed changes in communities were similar to those observed in other studies with leaf beetles in disturbance gradients. However, the inclusion of a seasonal effect results in some differences, depending on the evaluated parameter. Seasonal changes trigger differences in abundance, diversity, and species composition, but not in species richness, in each category and between categories. Major influence of seasonality occurred at intermediate successional categories, which could be due to the influence of intermediate disturbance hypothesis. Therefore, we point out the importance of evidence here obtained, since the influence of seasonal changes on successional trajectories is important for every biological taxon. Thus, accelerating climate change would exert modifications in the way communities are structured during secondary succession after disturbance, which is of major importance for species and ecosystem restoration. On the other hand, we propose that the use of

several species of leaf beetles for monitoring secondary vegetation and quantifying the succession time of low thorn forest is feasible, at least in northeastern Mexico. However, further studies are necessary to assess the potential of these and other species of leaf beetles to be indicators.

Acknowledgments

Authors are indebted to Fatima Magdalena Sandoval-Becerra, Ricardo Vizcaya, and José Norberto Lucio-García, who assisted during leaf beetle sampling. Edmar Meléndez-Jaramillo provided advice in a preliminary characterization of plant species in the study area. Pablo Ruiz and responsible authorities from Ej. Santa Ana and Ej. Rancho Nuevo granted permissions for accessing sampling areas. Diana Angélica Sánchez-Reyes assisted in taking pictures of *H. vinula* in field. The first author acknowledges facilities provided by Tecnológico Nacional de México-Instituto Tecnológico de Cd. Victoria. In addition, financial support for this study was granted by the Consejo Nacional de Ciencia y Tecnología (CONACYT) to the first author (Doctoral scholarship No. 401277).

References

Almaguer-Sierra P (2005) Fisiografía del Estado de Tamaulipas. In: Barrientos-Lozano L, Correa-Sandoval A, Horta-Vega JV, García-Jiménez J (Eds) Biodiversidad Tamaulipeca Vol 1. Dirección General de Educación Superior Tecnológica, Instituto Tecnológico de Cd. Victoria, Victoria, Tamaulipas, 2–20.

Anderson KJ (2007) Temporal patterns in rates of community change during succession. The American Naturalist 169: 780–793. https://doi.org/10.1086/516653

Andrews FG, Gilbert AJ (2005) A preliminary annotated checklist and evaluation of the diversity of the Chrysomelidae (Coleoptera) of the Baja California peninsula, Mexico. Insecta Mundi 19: 89–116.

Arroyo-Mora JP, Sánchez-Azofeifa GA, Kalacska MER, Rivard B (2005) Secondary forest detection in a Neotropical dry forest landscape using Landsat 7 ETM+ and IKONOS imagery. Biotropica 37: 497–507. https://doi.org/10.1111/j.1744-7429.2005.00068.x

Aslan EG, Ayvaz Y (2009) Diversity of Alticinae (Coleoptera, Chrysomelidae) in Kasnak Oak Forest Nature Reserve, Isparta, Turkey. Turkish Journal of Zoology 33: 251–262. https://doi.org/10.3906/zoo-0806-2

Bach CE (1981) Host plant growth form and diversity: effects on abundance and feeding preference of a specialist herbivore, *Acalymma vittata* (Coleoptera: Chrysomelidae). Oecologia 50: 370–375. https://doi.org/10.1007/BF00344978

Bach CE (1990) Plant successional stage and insect herbivory: flea beetles on sand-dune willow. Ecology 71: 598–609. https://doi.org/10.2307/1940313

Barberena-Arias MF, Aide TM (2003) Species diversity and trophic composition of litter insects during plant secondary succession. Caribbean Journal of Science 39: 161–169.

Baselga A, Jiménez-Valverde A (2007) Environmental and geographical determinants of beta diversity of leaf beetles (Coleoptera: Chrysomelidae) in the Iberian Peninsula. Ecological Entomology 32: 312–318. https://doi.org/10.1111/j.1365-2311.2007.00880.x

Baselga A, Novoa F (2007) Diversity of Chrysomelidae (Coleoptera) at a mountain range in the limit of the Eurosiberian region, northwest Spain: species richness and beta diversity. Entomologica Fennica 18: 65–73.

Basset Y, Samuelson GA (1996) Ecological characteristics of an arboreal community of Chrysomelidae in Papua New Guinea. In: Jolivet PHA, Cox ML (Eds) Chrysomelidae Biology Volume 2: Ecological Studies. SPB Academic Publishing, Amsterdam, 243–262.

Bongers F, Poorter L, Hawthorne WD, Sheil D (2009) The intermediate disturbance hypothesis applies to tropical forests, but disturbance contributes little to tree diversity. Ecology Letters 12: 798–805. https://doi.org/10.1111/j.1461-0248.2009.01329.x

Bouchard P, Bousquet Y, Davies AE, Alonso-Zarazaga MA, Lawrence JF, Lyal CHC, Newton AF, Reid CAM, Schmitt M, Ślipiński A, Smith ABT (2011) Family-group names in Coleoptera (Insecta). ZooKeys 88: 1–972. https://doi.org/10.3897/zookeys.88.807

Bouchard P, Grebennikov VV, Smith ABT, Douglas H (2009) Biodiversity of Coleoptera. In: Foottit RG, Adler PH (Eds) Insect Biodiversity: Science and Society. Blackwell Publishing, Oxford, 265–301. https://doi.org/10.1002/9781444308211.ch11

Bouzan A, Flinte V, Macedo MV, Monteiro RF (2015) Elevation and temporal distributions of Chrysomelidae in southeast Brazil with emphasis on the Galerucinae. ZooKeys 547: 103–117. https://doi.org/10.3897/zookeys.547.9723

Brown VK, Hyman PS (1986) Successional communities of plants and phytophagous Coleoptera. Journal of Ecology 74: 963–975. https://doi.org/10.2307/2260227

Büchi L, Vuilleumier S (2014) Coexistence of specialist and generalist species is shaped by dispersal and environmental factors. The American Naturalist 183: 612–624. https://doi.org/10.1086/675756

Canizales-Velázquez PA, Alanís-Rodríguez E, Aranda-Ramos R, Mata-Balderas JM, Jiménez-Pérez J, Alanís-Flores G, Uvalle-Sauceda JI, Ruiz-Bautista MG (2009) Caracterización estructural del matorral submontano de la Sierra Madre Oriental, Nuevo León, México. Revista Chapingo Serie Ciencias Forestales y del Ambiente 15: 115–120.

Carignan V, Villard M-A (2002) Selecting indicator species to monitor ecological integrity: a review. Environmental Monitoring and Assessment 78: 45–61. https://doi.org/10.1023/A:1016136723584

Ceballos G, Martínez L, García A, Espinoza E, Creel JB, Dirzo R (2010) Diversidad, amenazas y áreas prioritarias para la conservación de las selvas secas del Pacífico de México. Fondo de Cultura Económica, Comisión Nacional para el Conocimiento y Uso de la Biodiversidad, México, D.F., 594 pp.

Challenger A, Soberón J (2008) Los ecosistemas terrestres. In: CONABIO (Ed.) Capital natural de México, vol I: Conocimiento actual de la biodiversidad. Comisión Nacional para el Conocimiento y Uso de la Biodiversidad, México, 87–108.

Chapin FS, Matson PA, Vitousek PM (2011) Principles of Terrestrial Ecosystem Ecology, Second Edition. Springer Science+Business Media, New York, 529 pp. https://doi.org/10.1007/978-1-4419-9504-9

Chamorro-Lacayo ML (2014) 2.7.5 Chrysomelidae: Cryptocephalinae Gyllenhal 1813. In: Leschen RAB, Beutel RG (Eds) Handbook of Zoology. Arthropoda: Insecta: Coleoptera Volume 3: Morphology and Systematics (Phytophaga). De Gruyter, USA, 81–87.

Chao A, Chiu C-H (2016) Nonparametric estimation and comparison of species richness. John Wiley & Sons Ltd, Chichester, 1–11. https://doi.org/10.1002/9780470015902.a0026329

Charles E, Basset Y (2005) Vertical stratification of leaf-beetle assemblages (Coleoptera: Chrysomelidae) in two forest types in Panama. Journal of Tropical Ecology 21: 329–336. https://doi.org/10.1017/S0266467405002300

Colwell RK (2013) EstimateS: Statistical estimation of species richness and shared species from samples. Version 9. User's Guide and application. http://purl.oclc.org/estimates

Connell JH (1978) Diversity in tropical rain forests and coral reefs. Science 199: 1302–1310. https://doi.org/10.1126/science.199.4335.1302

De-Cáceres M, Legendre P, Wiser SK, Brotons L (2012) Using species combinations in indicator value analyses. Methods in Ecology and Evolution 3: 973–982. https://doi.org/10.1111/j.2041-210X.2012.00246.x

Denslow JS, Guzman GS (2000) Variation in stand structure, light and seedling abundance across a tropical moist forest chronosequence, Panama. Journal of Vegetation Science 11: 201–212. https://doi.org/10.2307/3236800

Dufrêne M, Legendre P (1997) Species assemblages and indicator species: the need for a flexible asymmetrical approach. Ecological Monographs 67: 345–366. https://doi.org/10.1890/0012-9615(1997)067[0345:saaist]2.0.co;2

Farrell BD, Erwin TL (1988) Leaf-beetle community structure in an amazonian rainforest canopy. In: Jolivet P, Petitpierre E, Hsiao TH (Eds) Biology of Chrysomelidae. Kluwer Academic Publishers, Dordrecht, 73–90. https://doi.org/10.1007/978-94-009-3105-3_5

Fernandes GW, Almada ED, Carneiro MAA (2010) Gall-inducing insect species richness as indicators of forest age and health. Environmental Entomology 39: 1134–1140. https://doi.org/10.1603/EN09199

Flowers RW (1996) La subfamilia Eumolpinae (Coleoptera: Chrysomelidae) en América Central. Publicación Especial de la Revista de Biología Tropical 2: 1–60.

Flowers RW, Hanson PE (2003) Leaf beetle (Coleoptera: Chrysomelidae) diversity in eight Costa Rican habitats. In: Furth DG (Ed.) Special topics in leaf beetle biology Proceedings of the 5th International Symposium on the Chrysomelidae, Iguassu Falls (Brazil), August 2000. Pensoft Publishers, Sofia-Moscow, 25–51.

Foster BL, Tilman D (2000) Dynamic and static views of succession: testing the descriptive power of the chronosequence approach. Plant Ecology 146: 1–10. https://doi.org/10.1023/A:1009895103017

Furth DG (2013) Diversity of Alticinae in Oaxaca, Mexico: A preliminary study (Coleoptera, Chrysomelidae). ZooKeys 332: 1–32. https://doi.org/10.3897/zookeys.332.4790

García-Morales LJ, Estrada-Castillón AE, García-Jiménez J, Villarreal-Quintanilla JA, Cantú-Ayala C, Jurado-Ybarra E, Vargas-Vázquez VA (2014) Florística y vegetación del Área Natural Protegida Altas Cumbres, Tamaulipas, México. In: Correa-Sandoval A, Horta-Vega JV, García-Jiménez J, Barrientos-Lozano L (Eds) Biodiversidad tamaulipeca Volumen 2,

Número 1. Tecnológico Nacional de México, Instituto Tecnológico de Ciudad Victoria, Tamaulipas, 15–73.

Gómez-Zurita J, Hunt T, Kopliku F, Vogler AP (2007) Recalibrated tree of leaf beetles (Chrysomelidae) indicates independent diversification of angiosperms and their insect herbivores. PLoS ONE 2: e360. https://doi.org/10.1371/journal.pone.0000360

González-Megías A, Gómez JM (2003) Consequences of removing a keystone herbivore for the abundance and diversity of arthropods associated with a cruciferous shrub. Ecological Entomology 28: 299–308. https://doi.org/10.1046/j.1365-2311.2003.00510.x

Guariguata MR, Ostertag R (2001) Neotropical secondary forest succession: changes in structural and functional characteristics. Forest Ecology and Management 148: 185–206. https://doi.org/10.1016/S0378-1127(00)00535-1

Gutman G, Huang C, Chander G, Noojipady P, Masek JG (2013) Assessment of the NASA–USGS Global Land Survey (GLS) datasets. Remote Sensing of Environment 134: 249–265. https://doi.org/10.1016/j.rse.2013.02.026

Hammer Ø, Harper DAT, Ryan PD (2001) PAST: Paleontological statistics software package for education and data analysis. Palaeontologia Electronica 4(1): 1–9.

Heusi-Silveira M, Lopes BC, Ide S, Castellani TT, Hernández MIM (2012) Beetle (Insecta, Coleoptera) assemblage in a Southern Brazilian restinga: effects of anthropogenic disturbance and vegetation complexity. Studies on Neotropical Fauna and Environment 47: 203–214. https://doi.org/10.1080/01650521.2012.740258

Hodkinson ID, Jackson JK (2005) Terrestrial and aquatic invertebrates as bioindicators for environmental monitoring, with particular reference to mountain ecosystems. Environmental Management 35: 649–666. https://doi.org/10.1007/s00267-004-0211-x

Hortal J, Borges PAV, Gaspar C (2006) Evaluating the performance of species richness estimators: sensitivity to sample grain size. Journal of Animal Ecology 75: 274–287. https://doi.org/10.1111/j.1365-2656.2006.01048.x

Huston MA (2014) Disturbance, productivity, and species diversity: empiricism vs. logic in ecological theory. Ecology 95: 2382–2396. https://doi.org/10.1890/13-1397.1

INEGI (2013) Conjunto de datos vectoriales de uso del suelo y vegetación escala 1:250,000, Serie V (Capa Unión). Aguascalientes, México: Instituto Nacional de Estadística y Geografía.

Janzen DH (1976) Sweep samples of tropical deciduous forest foliage-inhabiting insects: seasonal changes and inter-field differences in adult bugs and beetles. Revista de Biología Tropical 24: 149–161.

Jeffries JM, Marquis RJ, Forkner RE (2006) Forest age influences oak insect herbivore community structure, richness, and density. Ecological Applications 16: 901–912. https://doi.org/10.1890/1051-0761(2006)016[0901:FAIOIH]2.0.CO;2

Jiménez-Valverde A, Hortal J (2003) Las curvas de acumulación de especies y la necesidad de evaluar la calidad de los inventarios biológicos. Revista Ibérica de Aracnología 8: 151–161.

Johnson EA, Miyanishi K (2008) Testing the assumptions of chronosequences in succession. Ecology Letters 11: 419–431. https://doi.org/10.1111/j.1461-0248.2008.01173.x

Jolivet P (1988) Food habits and food selection of Chrysomelidae: bionomic and evolutionary perspectives. In: Jolivet P, Petitpierre E, Hsiao TH (Eds) Biology of Chrysomelidae. Kluwer Academic Publishers, Dordrecht, 1–24. https://doi.org/10.1007/978-94-009-3105-3_1

Jolivet P (2015) Together with 30 years of Symposia on Chrysomelidae! Memories and personal reflections on what we know more about leaf beetles. Zookeys 547: 35–61. https://doi.org/10.3897/zookeys.547.7181

Jolivet P, Verma KK (2008) Eumolpinae – a widely distributed and much diversified subfamily of leaf beetles (Coleoptera, Chrysomelidae). Terrestrial Arthropod Reviews 1: 3–37. https://doi.org/10.1163/187498308X345424

Jost L (2006) Entropy and diversity. Oikos 113: 363–375. https://doi.org/10.1111/j.2006.0030-1299.14714.x

Kalaichelvan T, Verma KK (2005) Checklist of leaf beetles (Coleoptera: Chrysomelidae) of Bhilai-Durg. Zoos' Print Journal 20: 1838–1842. https://doi.org/10.11609/JoTT.ZPJ.1114.1838-42

Lebrija-Trejos E, Pérez-García EA, Meave JA, Poorter L, Bongers F (2011) Environmental changes during secondary succession in a tropical dry forest in Mexico. Journal of Tropical Ecology 27: 477–489. https://doi.org/10.1017/S0266467411000253

Linzmeier AM, Ribeiro-Costa CS (2009) Spatio-temporal dynamics of Alticini (Coleoptera, Chrysomelidae) in a fragment of araucaria forest in the state of Parana, Brazil. Revista Brasileira de Entomologia 53: 294–299. https://doi.org/10.1590/S0085-56262009000200013

Linzmeier AM, Ribeiro-Costa CS (2011) Body size of Chrysomelidae (Coleoptera, Insecta) in areas with different levels of conservation in south Brazil. ZooKeys 157: 1–14. https://doi.org/10.3897/zookeys.157.1083

Linzmeier AM, Ribeiro-Costa CS (2012) Spatial–temporal composition of Chrysomelidae (Insecta: Coleoptera) communities in southern Brazil. Journal of Natural History 46(31–32): 1921–1938. https://doi.org/10.1080/00222933.2012.707237

Linzmeier AM, Ribeiro-Costa CS (2013) Seasonal pattern of Chrysomelidae (Coleoptera) in the state of Paraná, southern Brazil. Biota Neotropica 13(1): 1–10. https://doi.org/10.1590/S1676-06032013000100018

Linzmeier AM, Ribeiro-Costa CS, Marinoni RC (2006) Fauna de Alticini (Newman) (Coleoptera, Chrysomelidae, Galerucinae) em diferentes estágios sucessionais na Floresta com Araucária do Paraná, Brasil: diversidade e estimativa de riqueza de espécies. Revista Brasileira de Entomologia 50: 101–109. https://doi.org/10.1590/S0085-56262006000100015

Lucio-García JN (2018) Efecto de la estacionalidad y el microclima sobre Chrysomelidae (Coleoptera) en un bosque tropical subcaducifolio de Victoria, Tamaulipas. Bachelor thesis, Tamaulipas, México: Universidad Autónoma de Tamaulipas.

Magurran AE (2004) Measuring biological diversity. Blackwell Science Ltd., Oxford, 256 pp.

Marinoni RC, Ganho NG (2006) A diversidade diferencial beta de Coleoptera (Insecta) em uma paisagem antropizada. Revista Brasileira de Entomologia 50: 64–71. https://doi.org/10.1590/S0085-56262006000100009

Martínez-Sánchez I, Niño-Maldonado S, Barrientos-Lozano L, Horta-Vega JV (2009) Dinámica poblacional de Chrysomelidae (Coleoptera) en un gradiente altitudinal en tres municipios del estado de Hidalgo, México. TecnoINTELECTO 6: 2–4.

McGeoch MA, Rensburg BJV, Botes A (2002) The verification and application of bioindicators: a case study of dung beetles in a savanna ecosystem. Journal of Applied Ecology 39: 661–672. https://doi.org/10.1046/j.1365-2664.2002.00743.x

Morrone JJ, Márquez J (2008) Biodiversity of Mexican terrestrial arthropods (Arachnida and Hexapoda): a biogeographical puzzle. Acta Zoológica Mexicana (ns)24: 15–41. https://doi.org/10.21829/azm.2008.241613

Morrow PA, Tonkyn DW, Goldburg RJ (1989) Patch colonization by *Trirhabda canadensis* (Coleoptera: Chrysomelidae): effects of plant species composition and wind. Oecologia 81: 43–50. https://doi.org/10.1007/BF00377008

Myster RW, Malahy MP (2008) Is there a middle way between permanent plots and chronosequences? Canadian Journal of Forest Research 38: 3133–3138. https://doi.org/10.1139/X08-148

Niño-Maldonado S, Riley EG, Furth DG, Jones RW (2005) Coleoptera: Chrysomelidae. In: Sánchez-Ramos G, Reyes-Castillo P, Dirzo R (Eds) Historia Natural de la Reserva de la Biósfera El Cielo, Tamaulipas, México. Universidad Autónoma de Tamaulipas, Victoria, 417–425.

Niño-Maldonado S, Romero-Nápoles J, Sánchez-Reyes UJ, Jones RW, De-León-González EI (2014) Inventario preliminar de Chrysomelidae (Coleoptera) de Tamaulipas, México. In: Correa-Sandoval A, Horta-Vega JV, García-Jiménez J, Barrientos-Lozano L (Eds) Biodiversidad Tamaulipeca Volumen 2, Número 2. Tecnológico Nacional de México, Instituto Tecnológico de Cd. Victoria, Tamaulipas, 121–132.

Niño-Maldonado S, Sánchez-Reyes UJ (2017) Taxonomía de insectos. Orden Coleoptera. Familia Chrysomelidae. In: Cibrián-Tovar D (Ed.) Fundamentos de entomología forestal. Red de salud forestal. Redes temáticas de la Comisión Nacional de Ciencia y Tecnología (CONACYT), México, 282–288.

Nummelin M, Borowiec L (1992) Cassidinae beetles of the Kibale Forest, western Uganda; comparison between virgin and managed forests. African Journal of Ecology 30: 10–17. https://doi.org/10.1111/j.1365-2028.1992.tb00474.x

O'Brien MJ, Brezzi M, Schuldt A, Zhang J-Y, Ma K, Schmid B, Niklaus PA (2017) Tree diversity drives diversity of arthropod herbivores, but successional stage mediates detritivores. Ecology and Evolution 7: 8753–8760. https://doi.org/10.1002/ece3.3411

Ordóñez-Reséndiz MM, Serrano-Resendiz V, Hernández-Sosa L (2015) Riqueza de la familia Chrysomelidae (Coleoptera) en comunidades vegetales de las Sierras de Taxco-Huautla. Entomología Mexicana 2: 601–607.

Pellissier L (2015) Stability and the competition-dispersal trade-off as drivers of speciation and biodiversity gradients. Frontiers in Ecology and Evolution 3: 1–10. https://doi.org/10.3389/fevo.2015.00052

Perry J, Lojka B, Ruiz LQ, Damme PV, Houška J, Cusimamani EF (2016) How natural forest conversion affects insect biodiversity in the Peruvian Amazon: can agroforestry help? Forests 7: 1–13. https://doi.org/10.3390/f70400822

Pickett STA, Cadenasso ML, Meiners SJ (2008) Ever since Clements: from succession to vegetation dynamics and understanding to intervention. Applied Vegetation Science 12: 9–21. https://doi.org/10.1111/j.1654-109X.2009.01019.x

Pimenta M, De-Marco P (2015) Leaf beetle (Chrysomelidae: Coleoptera) assemblages in a mosaic of natural and altered areas in the Brazilian Cerrado. Neotropical Entomology 44: 242–255. https://doi.org/10.1007/s13744-015-0280-y

Pulsford SA, Lindenmayer DB, Driscoll DA (2016) A succession of theories: purging redundancy from disturbance theory. Biological Reviews 91: 148–167. https://doi.org/10.1111/brv.12163

Řehounek J (2002) Comparative study of the leaf beetles (Coleoptera: Chrysomelidae) in chosen localities in the district of Nymburk. Acta Universitatis Palackianae Olomucensis Facultas Rerum Naturalium Biologica 39–40: 123–130.

Ribera I, Foster G (1997) El uso de artrópodos como indicadores biológicos. Boletín de la Sociedad Entomológica Aragonesa 20: 265–276.

Riley EG, Clark SM, Flowers RW, Gilbert AJ (2002) 124 Chrysomelidae Latreille 1802. In: Arnett RH, Thomas MC, Skelley PE, Frank JH (Eds) Volume 2, American Beetles. Polyphaga: Scarabaeoidea through Curculionoidea. CRC Press LLC, USA, 617–691.

Riley EG, Clark SM, Seeno TN (2003) Catalog of the Leaf Beetles of America North of Mexico. Coleopterists Society, special publication no. 1, 290 pp.

Roxburgh SH, Shea K, Wilson JB (2004) The intermediate disturbance hypothesis: patch dynamics and mechanisms of species coexistence. Ecology 85: 359–371. https://doi.org/10.1890/03-0266

Rzedowski J (2006) Vegetación de México. 1ra. Edición digital. Comisión Nacional para el Conocimiento y Uso de la Biodiversidad, México, 504 pp.

Sánchez-Reyes UJ, Niño-Maldonado S, Barrientos-Lozano L, Clark SM, Jones RW (2016) Faunistic patterns of leaf beetles (Coleoptera, Chrysomelidae) within elevational and temporal gradients in Sierra de San Carlos, Mexico. ZooKeys 611: 11–56. https://doi.org/10.3897/zookeys.611.9608

Sánchez-Reyes UJ, Niño-Maldonado S, Barrientos-Lozano L, Jones RW, Sandoval-Becerra FM (2015) Análisis del nicho ecológico de Cryptocephalinae (Coleoptera: Chrysomelidae) en la Sierra de San Carlos, Tamaulipas, México. Entomología Mexicana 2: 526–532.

Sánchez-Reyes UJ, Niño-Maldonado S, Barrientos-Lozano L, Treviño-Carreón J (2017) Assessment of land use-cover changes and successional stages of vegetation in the Natural Protected Area Altas Cumbres, Northeastern Mexico, using Landsat satellite imagery. Remote Sensing 9: 1–33. https://doi.org/10.3390/rs9070712

Sánchez-Reyes UJ, Niño-Maldonado S, Barrientos-Lozano L, Treviño-Carreón J, Almaguer-Sierra P (in press) Seasonal microclimatic variation in a succession gradient of low thorn forest in Northeastern Mexico. Revista de Biología Tropical.

Sánchez-Reyes UJ, Niño-Maldonado S, Jones RW (2014) Diversity and altitudinal distribution of Chrysomelidae (Coleoptera) in Peregrina Canyon, Tamaulipas, Mexico. ZooKeys 417: 103–132. https://doi.org/10.3897/zookeys.417.7551

Sandoval-Becerra FM (2018) Ensamble de Chrysomelidae (Coleoptera) en un mosaico de disturbio dentro del Área Natural Protegida Altas Cumbres, Victoria, Tamaulipas. MSc thesis, Tamaulipas, México: Tecnológico Nacional de México, Instituto Tecnológico de Ciudad Victoria.

Sandoval-Becerra FM, Niño-Maldonado S, Sánchez-Reyes UJ, Horta-Vega JV, Venegas-Barrera CS, Martínez-Sánchez I (2017) Respuesta de la comunidad de Chrysomelidae (Coleoptera) a la variación microclimática en un fragmento de bosque de encino del noreste de México. Entomología Mexicana 4: 420–426.

Sandoval-Becerra FM, Sánchez-Reyes UJ, Clark SM, Venegas-Barrera CS, Horta-Vega JV, Niño-Maldonado S (2018) Influence of habitat heterogeneity on structure and composition of a Chrysomelidae (Coleoptera) assemblage in a temperate forest in northeast Mexico. Southwestern Entomologist 43: 115–130. https://doi.org/10.3958/059.043.0129

Scherer G (1983) Diagnostic key for the Neotropical Alticinae genera. Entomologische Arbeiten aus dem Museum G Frey 31–32: 2–89.

Secretaría de Gobierno (2015) Decreto Gubernamental mediante el cual se aprueba el Programa de Manejo del Área Natural Protegida "Altas Cumbres", localizada en los municipios de Jaumave y Victoria, Tamaulipas. Órgano del Gobierno Constitucional del Estado Libre y Soberano de Tamaulipas, Periódico Oficial del Estado de Tamaulipas, Tomo CXL, Secretaría General de Gobierno, Ciudad Victoria, Tamaulipas.

Şen I, Gök A (2009) Leaf beetle communities (Coleoptera: Chrysomelidae) of two mixed forest ecosystems dominated by pine-oak-hawthorn in Isparta province, Turkey. Annales Zoologici Fennici 46: 217–232. https://doi.org/10.5735/086.046.0306

Şen İ, Gök A (2014) Leaf beetle (Coleoptera: Chrysomelidae) communities of Kovada Lake and Kızıldağ national parks (Isparta, Turkey): assessing the effects of habitat types. Entomological Research 44: 176–190. https://doi.org/10.1111/1748-5967.12064

Shea K, Roxburgh SH, Rauschert ESJ (2004) Moving from pattern to process: coexistence mechanisms under intermediate disturbance regimes. Ecology Letters 7: 491–508. https://doi.org/10.1111/j.1461-0248.2004.00600.x

Staines CL (1986) A revision of the genus *Brachycoryna* (Coleoptera: Chrysomelidae: Hispinae). Insecta Mundi 1(4): 231–241.

Staines CL (2002) The New World tribes and genera of hispines (Coleoptera: Chrysomelidae: Cassidinae). Proceedings of the Entomological Society of Washington 104(3): 721–784.

Staines CL, Staines SL (2001) The leaf beetles (Insecta: Coleoptera: Chrysomelidae): potential indicator species assemblages for natural area monitoring. In: Therres GD (Ed.) Proceedings of conservation of biological diversity: a key to restoration of the Chesapeake Bay ecosystem and beyond. Maryland Department of Natural Resources, Maryland, 233–244.

StatSoft (2007) STATISTICA, version 8.0. http://www.statsoft.com

Steffan-Dewenter I, Tscharntke T (2001) Succession of bee communities on fallows. Ecography 24: 83–93. https://doi.org/10.1034/j.1600-0587.2001.240110.x

Stein A, Gerstner K, Kreft H (2014) Environmental heterogeneity as a universal driver of species richness across taxa, biomes and spatial scales. Ecology Letters 17: 866–880. https://doi.org/10.1111/ele.12277

Stephen C, Sánchez R (2014) Species richness and relative species abundance of Nymphalidae (Lepidoptera) in three forests with different perturbations in the north-central Caribbean of Costa Rica. Revista de Biología Tropical 62: 919–928. https://doi.org/10.15517/rbt.v62i3.14057

Swanson ME, Franklin JF, Beschta RL, Crisafulli CM, DellaSala DA, Hutto RL, Lindenmayer DB, Swanson FJ (2011) The forgotten stage of forest succession: early-successional ecosystems on forest sites. Frontiers in Ecology and the Environment 9: 117–125. https://doi.org/10.1890/090157

Tamme R, Hiiesalu I, Laanisto L, Szava-Kovats R, Pärtel M (2010) Environmental heterogeneity, species diversity and co-existence at different spatial scales. Journal of Vegetation Science 21: 796–801. https://doi.org/10.1111/j.1654-1103.2010.01185.x

Tejeda-Cruz C, Mehltreter K, Sosa VJ (2008) Indicadores ecológicos multi-taxonómicos. In: Manson RH, Hernández-Ortiz V, Gallina S, Mehltreter K (Eds) Agroecosistemas cafetaleros de Veracruz: biodiversidad, manejo y conservación. Instituto Nacional de Ecología A. C., México, 271–278.

Trejo I (2010) Las selvas secas del Pacífico mexicano. In: Ceballos G, Martínez L, García A, Espinoza E, Creel JB, Dirzo R (Eds) Diversidad, amenazas y áreas prioritarias para la conservación de las selvas secas del Pacífico de México. Fondo de Cultura Económica, Comisión Nacional para el Conocimiento y Uso de la Biodiversidad, D.F., México, 41–51.

Treviño-Carreón J, Valiente-Banuet A (2005) La vegetación de Tamaulipas y sus principales asociaciones vegetales. In: Barrientos-Lozano L, Correa-Sandoval A, Horta-Vega JV, García-Jiménez J (Eds) Biodiversidad tamaulipeca Vol 1. Dirección General de Educación Superior Tecnológica, Instituto Tecnológico de Ciudad Victoria, Ciudad Victoria, Tamaulipas, México, 22–46.

Vieira ICG, Almeida ASd, Davidson EA, Stone TA, Carvalho CJRd, Guerrero JB (2003) Classifying successional forests using Landsat spectral properties and ecological characteristics in eastern Amazonia. Remote Sensing of Environment 87: 470–481. https://doi.org/10.1016/j.rse.2002.09.002

Villa-Galaviz E, Boege K, Del-Val E (2012) Resilience in plant-herbivore networks during secondary succession. PLoS ONE 7: e53009. https://doi.org/10.1371/journal.pone.0053009

Walker LR, Wardle DA, Bardgett RD, Clarkson BD (2010) The use of chronosequences in studies of ecological succession and soil development. Journal of Ecology 98: 725–736. https://doi.org/10.1111/j.1365-2745.2010.01664.x

Wąsowska M (2004) Impact of humidity and mowing on chrysomelid communities (Coleoptera, Chrysomelidae) in meadows of the Wierzbanówka valley (Pogórze Wielickie hills, Southern Poland). Biologia Bratislava 59: 601–611.

White RE (1968) A review of the genus *Cryptocephalus* in America north of Mexico (Chrysomelidae: Coleoptera). United States National Museum Bulletin 290: 1–124. https://doi.org/10.5479/si.03629236.290.1

White RE (1993) A revision of the subfamily Criocerinae (Chrysomelidae) of North America north of Mexico. Technical Bulletin 1805. United States Department of Agriculture, Agricultural Research Service, Washington, DC, 158 pp.

Wilcox JA (1965) A synopsis of the North American Galerucinae (Coleoptera: Chrysomelidae). New York State Museum and Science Service Bulletin 400: 1–226.

Wilcox JA (1972) A review of the North American Chrysomelinae leaf beetles (Coleoptera: Chrysomelidae). Bulletin 421. University of the State of New York, State Education Department, State Museum and Science Service, 37 pp.

Willig MR, Presley SJ (2018) Biodiversity and disturbance. In: DellaSala DA, Goldstein MI (Eds) The Encyclopedia of the Anthropocene, vol 3. Elsevier, Oxford, 45–51. https://doi.org/10.1016/B978-0-12-809665-9.09813-X

Winter M-B, Ammer C, Baier R, Donato DC, Seibold S, Müller J (2015) Multi-taxon alpha diversity following bark beetle disturbance: Evaluating multi-decade persistence of a diverse early-seral phase. Forest Ecology and Management 338: 32–45. https://doi.org/10.1016/j.foreco.2014.11.019

Yang Z, Liu X, Zhou M, Ai D, Wang G, Wang Y, Chu C, Lundholm JT (2015) The effect of environmental heterogeneity on species richness depends on community position along the environmental gradient. Scientific Reports 5: 1–7. https://doi.org/10.1038/srep15723

Yuan ZY, Jiao F, Li YH, Kallenbach RL (2016) Anthropogenic disturbances are key to maintaining the biodiversity of grasslands. Scientific Reports 6: 1–8. https://doi.org/10.1038/srep22132

Appendix I

Table 7. Taxonomic checklist of Chrysomelidae per season in each category of succession time, in a fragment of low thorn forest in northeastern Mexico. Key: 4y = 4 years of succession, 17y = 17 years of succession, 31y = 31 years of succession, CA = Conserved areas.

Species	Rainy season				Dry season			
	4y	17y	31y	CA	4y	17y	31y	CA
CRIOCERINAE Latreille, 1807								
Tribe Lemini Heinze, 1962								
Lema sp. 1								1
Lema sp. 2							1	
Oulema sp. 1 *	1							
Neolema sp. 1	1							
CASSIDINAE Gyllenhal, 1813								
Tribe Chalepini Weise, 1910								
Baliosus sp. 1	2		4	3		2		
Brachycoryna pumila Guérin-Méneville, 1844	33				30	8		
Chalepus amabilis Baly 1885								3
Chalepus bellulus (Chapuis, 1877)	3							
Chalepus digressus Baly 1885				2				
Heterispa vinula (Erichson, 1847)	21	50	23	7	15	43	21	
Pentispa distincta (Baly 1885)								2
Sumitrosis inaequalis (Weber, 1801)	1	1	4			2	7	
Tribe Ischyrosonychini Chapuis, 1875								
Physonota alutacea Boheman, 1854		6	3			4		
Tribe Cassidini Gyllenhal, 1813								
Agroiconota vilis (Boheman, 1855)					1			
Charidotella bifossulata (Boheman, 1855)								1
Charidotella sexpunctata (Fabricius, 1781)	2			2			3	3
Charidotis auroguttata Boheman, 1855				4				
Helocassis clavata (Fabricius, 1798)	3	1		17	2	3	2	9
CHRYSOMELINAE Latreille, 1802								
Tribe Chrysomelini Latreille, 1802								
Subtribe Doryphorina Motschulsky, 1860								
Calligrapha ancoralis Stål, 1860	10	1						
Calligrapha piceicollis Stål, 1859	1				2			
Deuterocampta atromaculata Stål, 1859)		1	3	2			2	
Subtribe Chrysomelina Latreille, 1802								
Plagiodera semivittata Stål, 1860		1					3	
Plagiodera thymaloides Stål, 1860	8	1	8		8		3	
GALERUCINAE Latreille, 1802								
Tribe Galerucini Latreille, 1802								
Group Coelomerites Chapuis, 1875								
Coraia subcyanescens (Schaeffer, 1906)		3	1	1				
Derospidea ornata (Schaeffer, 1905)			2					
Miraces aeneipennis Jacoby, 1888								1
Tribe Luperini Chapuis, 1875								
Subtribe Diabroticina Chapuis, 1875								
Group Diabroticites Chapuis, 1875								
Diabrotica litterata Sahlberg 1823	8			4	2			
Group Cerotomites Chapuis, 1875								
Cyclotrypema furcata (Olivier, 1808)	31	32	3		7	20		
Tribe Alticini Newman, 1835								
Acallepitrix sp. 1		4	1	8		2		4

Species	Rainy season				Dry season			
	4y	17y	31y	CA	4y	17y	31y	CA
Acallepitrix sp. 2				5				
Acrocyum dorsalis Jacoby, 1885				11				4
Alagoasa bipunctata (Chevrolat, 1834)		4	4	9				2
Alagoasa jacobiana (Horn, 1889)	5		6	17		4		10
Alagoasa sp. 1						1		
Alagoasa sp. 2	2							
Asphaera sp. 1	7	1			3			
Centralaphthona diversa (Baly, 1877)	280	1172	1261	167	103	240	217	18
Chaetocnema sp. 1	976	61			41	8		2
Chaetocnema sp. 2	1				3			2
Dibolia sp. 1				1				
Disonycha glabrata (Fabricius, 1781)	4	1		1				
Disonycha sp. 2					16			
Disonycha stenosticha Schaeffer, 1931			2	1				
Dysphenges sp. 1	14	13	25	2			2	
Epitrix sp. 1	287	1	1	44	320	3		12
Epitrix sp. 2	16	3	3	25		4		21
Epitrix sp. 3	183	7		27	41		2	
Epitrix sp. 4	5	1		16	4			20
Epitrix sp. 5	1	2		4	2	2		8
Heikertingerella sp. 1				3				
Longitarsus sp. 1	32	10	10	40	7	4		8
Macrohaltica jamaicensis (Fabricius, 1792)	1							
Margaridisa sp. 1	46		21	80	8	3	8	152
Margaridisa sp. 2								4
Monomacra bumeliae (Schaeffer, 1905)	4	3		3		2		
Omophoita cyanipennis (Fabricius, 1798)					3			
Parchicola sp. 1				11	2			6
Parchicola sp. 2	6							
Parchicola sp. 3				1				
Syphrea sp. 1	2			1				
Syphrea sp. 2								2
Syphrea sp. 3	3							
Systena sp. 1					1			
EUMOLPINAE Hope, 1840								
Tribe Eumolpini Hope, 1840								
Group Iphimeites Chapuis, 1874								
Brachypnoea sp. 1	4							
Colaspis melancholica Jacoby, 1881				3				
Colaspis sp. 1	1							
Colaspis townsendi Bowditch, 1921	20	1		5	15			
Zenocolaspis inconstans (Lefèvre, 1878)	3		2	2	3			
Tribe Typophorini Chapuis, 1874								
Group Typophorites Chapuis, 1874								
Paria sp. 1			1	1				
CRYPTOCEPHALINAE Gyllenhal, 1813								
Tribe Cryptocephalini Gyllenhal, 1813								
Subtribe Pachybrachina Chapuis, 1874								
Pachybrachis sp. 1	5	1			2	4		
Pachybrachis sp. 2	1				4			
Pachybrachis sp. 3	3	1					4	
Pachybrachis sp. 4	3	2			4		2	
Pachybrachis sp. 5	1							
Pachybrachis sp. 6	1							

Species	Rainy season				Dry season			
	4y	17y	31y	CA	4y	17y	31y	CA
Subtribe Cryptocephalina Gyllenhal, 1813								
Cryptocephalus guttulatus Olivier,1808	1							
Cryptocephalus trizonatus Suffrian, 1858	3				4			
Diachus sp. 1			2					
Tribe Clytrini Lacordaire, 1848								
Subtribe Clytrina Lacordaire, 1848								
Anomoea rufifrons mutabilis (Lacordaire, 1848)	1	1						
Smaragdina agilis (Lacordaire, 1848)					2			
Subtribe Ischiopachina Chapuis, 1874								
Ischiopachys bicolor proteus Lacordaire, 1848	5		1					
Subtribe Babiina Chapuis, 1874								
Babia tetraspilota texana Schaeffer, 1933	10	3	6	1	4	2		
Subtribe Megalostomina Chapuis, 1874								
Proctophana sp. 1					1			
Tribe Fulcidacini Jakobson, 1924								
Chlamisus sp. 1	1							
Diplacaspis prosternalis (Schaeffer, 1906)	2	1				2		

ZooKeys 825: 105–122 (2019)
doi: 10.3897/zookeys.825.32434
http://zookeys.pensoft.net

RESEARCH ARTICLE

A peer-reviewed open-access journal
ZooKeys
Launched to accelerate biodiversity research

A recent record of *Romanogobio antipai* (Actinopterygii, Cyprinidae, Gobioninae) from the Danube River in Bulgaria

Nina G. Bogutskaya[1], Tihomir Stefanov[2], Alexander M. Naseka[1], Oleg A. Diripasko[3]

1 *Naturhistorisches Museum Wien, Burgring 7, Vienna 1010, Austria* **2** *National Museum of Natural History, 1 Tsar Osvoboditel Blvd, 1000 Sofia, Bulgaria* **3** *Institute of Fisheries and Marine Ecology, 8 Konsulska St, Berdyansk, 71118, Ukraine*

Corresponding author: *Nina G. Bogutskaya* (nina.bogutskaya@nhm-wien.ac.at)

Academic editor: *S. Kullander* | Received 14 December 2018 | Accepted 23 January 2019 | Published 27 February 2019

http://zoobank.org/73D054EE-A662-43B1-AC5D-1A7176839372

Citation: Bogutskaya NG, Stefanov T, Naseka AM, Diripasko OA (2019) A recent record of *Romanogobio antipai* (Actinopterygii, Cyprinidae, Gobioninae) from the Danube River in Bulgaria. ZooKeys 825: 105–122. https://doi.org/10.3897/zookeys.825.32434

Abstract

The Danube delta gudgeon, *Romanogobio antipai*, has been considered to be extinct because there were no reliable recent observations. The latest record confirmed by a voucher specimen dating from 1992. We report here on a specimen of *R. antipai* collected in 2016 in the Bulgarian sector of the Danube main stream using a bottom drift net at a depth of 8 m. The species determination is supported by morphological examination including discriminant and cluster analyses in comparison with three syntypes and five non-type specimens of *R. antipai,* samples of the *R. kesslerii* species complex and *R. vladykovi*. *Romanogobio antipai* most clearly differs from both *R. kesslerii* and *R. vladykovi* by proportional measurements (caudal peduncle depth, head width, eye horizontal diameter, and interorbital width), from *R. kesslerii* also by the number of scales above and below the lateral line (6 and 4, respectively, (vs. commonly 5 and 3), and from *R. vladykovi*, also by 8½ branched dorsal-fin rays (vs. 7½) and the vertebral caudal region longer than the abdominal vertebral region (abdominal+caudal vertebrae 19+21 or 20+21, vs. commonly 20+20 or variants with a caudal region shorter than the abdominal one). The possibility that *R. antipai* represents a deep-water cophenotype of either *R. kesslerii* or *R. vladykovi*, cannot be excluded. The new record demonstrates that *R. antipai* is still extant in the lower Danube but may be restricted to greater depths in the main channel and the deltaic branches.

Copyright *Nina G. Bogutskaya et al.* This is an open access article distributed under the terms of the Creative Commons Attribution License (CC BY 4.0), which permits unrestricted use, distribution, and reproduction in any medium, provided the original author and source are credited.

Keywords
Danube delta gudgeon, morphology, meristics, distribution, conservation status

Introduction

Romanogobio Bănărescu, 1961 is a genus of bottom-dwelling, rheophilic gudgeons with a wide distribution in temperate Eurasia. Six species were reported from the Danube basin (Kottelat and Freyhof 2007, Friedrich et al. 2018). Among them, *Romanogobio antipai* was described, as *Gobio kessleri antipai*, by Bănărescu (1953: 300, 318) based on a series of syntypes from the Danube delta at Sulina (12 specimens collected by Grigore Antipa before 1909) and the lower reaches of the Danubian tributary Argeş (one specimen collected by Băcescu). In the same paper, representing a study of morphometric features within the "*Gobio kessleri*" group of populations distributed in Romania, Bănărescu also recognized a new form, *Gobio kessleri kessleri* natio *banaticus* (the name is not available from this publication, but available as *Gobio kessleri banaticus* from Bănărescu 1960: 121) and compared both new forms with the nominotypical subspecies. As the correct original spelling of the specific name is *kesslerii* (Kottelat 1997), we use it hereafter.

Bănărescu (1953) distinguished *Romanogobio antipai* from *R. kesslerii* and *R. k. banaticus* on average values of the postorbital distance (10.5% of body length vs 8.5–10%), barbel length (10.5–13% of body length vs 8–11.5%), eye diameter (5.5% of body length vs 5.6–6.4% *R.* excluding *kesslerii* (Dybowsky, 1862) from Bulgaria with 4.8–5.6%, and 75.2% of interorbital distance vs 81.9–98.5%), snout length (9.4% of body length vs 9.4–11.7%), and maximum body depth (18.4% of body length vs 1.8–17.7% excluding *R. kesslerii* from the Dniester with an average of 18.5%). Consequently, no clear differences between the three taxa were presented, and later Bănărescu (1960, 1961) reported the occurrence of specimens morphologically intermediate between *R. antipai* and *R. kesslerii* in the Danube tributaries Ialomiţa, Argeş (Dâmboviţa) and Siret (Bizau and Milcov Rivers), recognized as such also by Bănărescu and Nalbant (1973). Bănărescu (1961, 1999: 151) repeated the most typical features of *R. antipai* from the Danube delta (smaller eye and deeper body), adding smaller body length in adults ("apparently not exceeding 6 cm"), commonly 4 scales (vs commonly 3) between the lateral line and the pelvic-fin origin, caudal-peduncle width at the anal-fin origin commonly about equal to caudal-peduncle depth (vs larger in *kesslerii*), and short lateral blotches (vs commonly elongated in *banaticus*). The distribution range was widened (Bănărescu 1961: 344) to include the lower reaches of the Siret River and its tributaries, the Milcov, Putna, and Birlad Rivers, and the lowest reaches of the Argeş and Ialomiţa Rivers. Similar data were later published in the book on the fishes of Romania (Bănărescu 1964: 454–455, fig. 195).

Bănărescu (1992, 1994a, 1999: 150, fig. 21) again restricted the range of *R. antipai* to the lowest reaches of the Danube, mentioning that before 1959, it was distributed upstream to the Argeş River mouth (some 430 river kilometres). He emphasized that it

markedly differed from other members of the *R. kesslerii* complex by its morphological features, which were related to dwelling in deep water of the main stream of the river.

Bănărescu (1992, 1994a, 1999) treated the Danube delta gudgeon as a subspecies (*Gobio kesslerii antipai*) but mentioned that it deserved the rank of species. Kottelat and Freyhof (2007) considered it as a valid species and Friedrich et al. (2018) found no arguments to reject this status.

The sample of *Romanogobio antipai* from the Danube delta at Sulina, described by Bănărescu based on G. Antipa's collections (before 1909) was not the only one from the Danube delta. Smirnov (1971) provided meristic and morphometric data on a sample of 24 specimens collected by him in April 1961 in the Ukrainian part of the delta (Chilia Arm) near Izmail and identified it as *R. kesslerii*. This sample was later included in the book on Ukrainian fishes by Movchan and Smirnov (1981: 344, tab. 181). Bănărescu (1999: 158) suggested that Smirnov's (1971) specimens from Izmail belonged to *R. antipai* because they had a deeper body and a smaller eye.

The most recent published record of *R. antipai* from the lower section of the Danube may be that of Marinov (1978) who reported *Gobio kesslerii* from the main course of the Danube in Bulgaria. The true *R. kesslerii* only occurs in middle reaches of tributaries and has not been recorded from the deep main stream of the Danube (e.g., Chichkoff 1937, Mihailova 1970, Dikov et al. 1994).

The absence of recent records of *R. antipai* lead some authors to the conclusion that the species might be extinct (Bănărescu 1994b, Kottelat 1997). Its conservation status was later evaluated as extinct (Kottelat and Freyhof 2007, Freyhof and Kottelat 2008) because it was supposed that all known ichthyological surveys conducted since the 1960s to 2003 in suitable habitats in the Danube delta had failed to find it; however, this statement is not entirely correct as there is a specimen in Natural History Museum 'Grigore Antipa' collected in 1992 (described below).

In 2016, TS collected a gudgeon specimen in the Bulgarian sector of the Danube main stream using a bottom drift net at a depth of 8 m, near the village of Vetren (river kilometer 395). This specimen (Figs 1–2) was preliminarily identified by AN as *Romanogobio antipai* because of its small eye and 8½ branched dorsal-fin rays distinguishing it from both *R. kesslerii* and *R. vladykovi* (Fang, 1943). The present note is devoted to a comparative description of the specimen to test this hypothesis.

Material and methods

Methods for counting fin rays and scales, and for measurements, follow Kottelat and Freyhof (2007) except that head length, postorbital length, and interorbital width include the skin fold. In the examined samples, standard length is used for some relative measurements. Body length, which is the length to the posterior margin of the posterior-most scale on the base of the caudal fin (called standard length II by Holčík et al. (1989: fig. 12), is also measured and the data are compared for diagnostic charac-

Figure 1. Lateral view of *Romanogobio antipai* NMNHS specimen 68.7 mm SL, Danube at Vetren (**a**) MGAB/BN760 specimen 64.9 mm SL, lower Argeş R. (**b**) ANSP syntype 47.8 mm SL, Sulina (**c**) and *R. kesslerii* NMNHS, 65.7 mm SL, Tsibritsa River (**d**).

ters taken from the literature. All measurements were made point-to-point with a dial caliper and recorded to the nearest 0.1 mm. Vertebral counts taken from radiographs follow the scheme by Naseka (1996). To avoid probable discrepancy in lateral-line count, we provide not only the number of lateral-line scales to the posterior margin of the hypurals but also numbers of total lateral scales and total lateral-line scales. Statistical analyses were done using Microsoft Excel, Statistica 6.0 (Statistic for Windows. Statsoft; Discriminant Functional Analysis, DFA), and SPSS Statistics V23.0 (IBM SPSS; Cluster Analysis, CA).

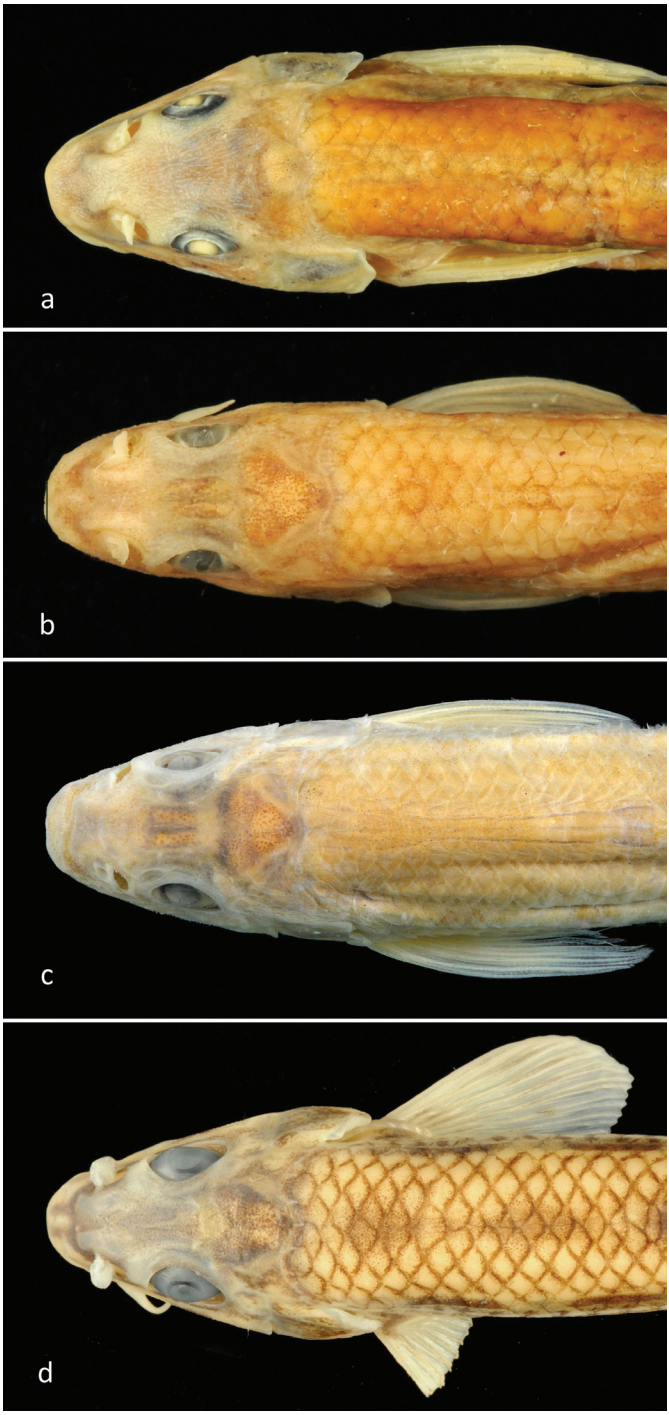

Figure 2. Dorsal view of the head of *Romanogobio antipai*, NMNHS specimen 68.7 mm SL, Danube at Vetren (**a**) MGAB/BN759, SL 47.7 mm, Sulina (**b**) ANSP syntype 47.8 mm SL, Sulina (**c**) and *R. kesslerii* NMNHS, 65.7 mm SL, Tsibritsa River (**d**).

Abbreviations

ANSP, Academy of Natural Sciences, Philadelphia, USA; NB, Bănărescu Nalbant Ichthyology Collection (now in Muzeul de Istorie Naturala 'Grigore Antipa'); ICBB, Institutui of Stiinte Biologice, Bucharest, Romania; IUCN, International Union for Conservation of Nature; MGAB, Muzeul de Istorie Naturala 'Grigore Antipa', Bucharest, Romania; NMNHS, National Museum of Natural History, Sofia, Bulgaria; NMW, Naturhistorisches Museum Wien, Vienna, Austria. BL, body length; HL, lateral head length; rkm, river kilometer; SD, standard deviation; SL, standard length.

Material examined

We specifically selected for comparison mostly those specimens of *R. kesslerii* that were donated and/or identified by Petru Bănărescu and followed his original descrimination of the forms within the *R. kesslerii* species complex. Specimens of *Romanogobio vladykovi* were selected from localities geographically close to Bulgaria and of a comparable length range.

NMNHS [no number], SL 68.7 mm, Bulgaria: Danube near Vetren, 395 rkm, 44.142637N, 27.029662E, 8 July 2016, coll. T. Stefanov.

Romanogobio antipai. All from Romania. Type material: MGAB 49908 (as *Gobio kessleri antipai*), 1, SL 46.2 mm, labelled as holotype, Romania: [Danube at] Sulina, before 1909, leg. G. Antipa; MGAB (ISBB 0519), 1, SL 50.8 mm, labelled as paratype, same data as MGAB 49908; ANSP 98961 (as *Gobio kessleri antipai*), 1, SL ca. 47.8 mm, labelled as paralectotype (misspelled as lectoparatype), same data as MGAB 49908, don. P. Bănărescu as paratype; non-type: MGAB (ISBB 0714, BN760, as *Gobio kessleri antipai*), 3, SL 64.9, 28.6 and 26.2 mm, Romania: lower Argeş River at Oltenița, 26 July 1961, coll. and det. P. Bănărescu; MGAB (BN759, as *Gobio kessleri antipai*), 1, SL 47.7 mm, Romania: Sulina Branch, "27–28th miles", Danube delta, Oct. 1992; MGAB (ISBB 3567, BN758, as *Gobio kessleri antipai*), 1, SL 30.1 mm, Romania: Saint Gheorghe Branch, Danube delta, no date, coll. V. Leonte. ANSP 98961 was examined on photos (lateral, dorsal, and ventral aspects) and an X-radiograph.

Romanogobio banaticus (but see Friedrich et al. 2018: 346 on *R. carpathorossicus* (Vladykov, 1931) as senior synonym of this species). NMW 65539, 30, SL 31.1–7.9 mm, Romania: Timiş at Urseni, Timişoara, 6 Sept. 1962, don. and det. P. Bănărescu as *Gobio kesslerii banaticus*.

Romanogobio kesslerii s.l.. NMW65532, 12, SL 33.3–57.9 mm, Romania: Tur at Turulung, northeast of Satu-Mare, 5 Sept. 1963, don. and det. P. Bănărescu, as intermediate between *Gobio kesslerii kesslerii* and *Gobio kesslerii banaticus*; NMW 65538, 9, SL 39.4–74.7 mm; Romania: Milcov at Focsani, Moldau, 14 Sept. 1963, don.

and det. P. Bănărescu as *Gobio kessleri antipai* with a comment: "not very typical", as *Gobio kessleri kessleri* in Bănărescu (1999: 146); NMNHS [no number], 10, SL 55.1–66.5 mm; Bulgaria: Tsibritsa River [right tributary to Danube, NW Bulgaria] near Yakimovo, 43.62245N, 23.33022E, 18 July 2012, coll. T. Stefanov.

Romanogobio kesslerii kesslerii. NMW 60250, 6, SL 50.1–61.2 mm; Romania: Areş River at mouth of Mureş, Transsylvania, 2 Oct.1949, don. and det. P. Bănărescu (in *Gobio*); NMW 65535, 4, SL 50.6–61.5 mm; Romania: Bereteu at Roşiori-Bihor, north of Oradea, 4 Sept. 1963, don. and det. P. Bănărescu (in *Gobio*); NMW 90883, 2, SL 85.3–91.2 mm; Ukraine: Smotrich River at Kamenetz Podol'ski [Dniester drainage], 7 May 1921, det. P. Bănărescu, 1991 (in *Gobio*).

Romanogobio vladykovi. NMW 53356, 2, SL 76.7–81.4 mm; Serbia: Nisch [Niš, Great Morava-Danube], Dec. 1894; NMW65537, 20, SL 46.4–81.4 mm; Romania: Timiš River at Peciu Nou [Danube drainage], 28 Aug. 1863; NMW 60234, 2, SL 73.2–77.2 mm; Romania: Bega R. [Danube drainage], Banat, Sept. 1943.

Results

General appearence of the NMNHS presumed *R. antipai* specimen from the Danube at Vetren is shown in Figs 1–2 together with a syntype and a non-type *R. antipai* specimen in comparison to *R. kesslerii* and *R. vladykovi*. Counts, descriptive states of the pectoral-fin length, and measurements are presented in Tables 1, 2. Examined character states in this specimen coincide considerably with those in the three type specimens of *R. antipai* and five non-type specimens, and demonstrate its differences from the samples of both the *R. kesslerii* species complex and *R. vladykovi*. As the standard length averages 96.8% of the BL (calculated in the *Romanogobio* material examined in this study), the difference between relative measurements (in % SL and in % BL) is slight and the morphometric character states that have been considered as diagnostic for *R. antipai* vs. *R. kesslerii* are confirmed. They include maximum body depth, 19–25% SL (17–25.5% of BL; in parentheses, data from Bănărescu (1953, 1961, 1999) and Movchan and Smirnov (1981) are summarized); caudal peduncle depth, 8–9% SL (7–9% of BL) and 35–38.5% of caudal peduncle length; eye diameter, 5–6% SL (5–6% of BL), 20–23% HL (18–24% HL), and 59–68.5% of interorbital width (61–81% of interorbital width). The NMNHS specimen has 6 and 4 scales, respectively, above (to the dorsal-fin origin) and below (to the pelvic-fin origin) the lateral line similar to the three type specimens of *R. antipai* and the topotypical specimen from Sulina thus confirming the opinion (Kottelat and Freyhof 2007, Friedrich et al. 2018) that this character is one of the most dependable diagnostic characters for the species. All other counts are identical or very close in the NMNHS specimen and *R. antipai* examined in this study (Table 1). None of the *R. antipai* specimens had 7½ branched dorsal-fin rays thus confirming its main difference from *R. vladykovi* characterized by 7½ branched dorsal-fin rays (Naseka et al. 1999; Naseka 2001).

Table 1. Meristic data for examined specimens of *Romanogobio antipai* and *R. kesslerii* species complex.

	Dorsal-fin branched rays			Anal-fin branched rays		Pectoral fin relative to pelvic-fin origin				Scales between lateral line and dorsal-fin origin		Scales between lateral line and pelvic-fin origin		
	7½	8½	9½	6½	7½	not reaching	almost reaching	reaching	behind	5	6	2	3	4
R. antipai MGAB 49908 syntype		1		1		1					1			1
R. antipai MGAB/ISBB 0519 syntype		1		1		1					1			1
R. antipai ANSP 98961 syntype		1		1		1					1			1
Non-type MGAB *R. antipai,* n=5		5		1		4	1				5			5
Presumed *R. antipai* NMNHS specimen		1		1			1				1			1
R. k. kesslerii. NMW 60250, 65535. Danube drainage, n=10		10		10		7	1	2		10			10	
R. k. kesslerii. NMW 908803, Dniester drainage, n=2		2		2		2				2			2	
R. banaticus. NMW 65539, Danube drainage, n=30		27	3	30		26	3	1		29	1		30	
R. kesslerii s.l. NMW 65532, NW Romania, n=12		12		12		6	1	5		12		1	11	
R. kesslerii s.l. NMW 65538, NE Romania, n=9		8	1	6	3		5	3	1	9			9	
R. kesslerii s.l. NMNHS, NW Bulgaria, n=10		10		10	10	6	2	1	1	10			10	
R. vladykovi NMW 53356, 60234, 65537, Danube drainage, n=24	24			24		24				10	14		15	9

Table 1. Continued.

	Predorsal abdominal vertebrae		Abdominal vertebrae				Pre-anal caudal vertebrae			Caudal vertebrae			Total vertebrae				
	10	11	18	19	20	21	2	3	4	19	20	21	38	39	40	41	42
R. antipai ANSP 98961 syntype	1			1				1			1			1			
Non-type MGAB *R. antipai,* n=5	2	3		4	1			3	2			5			4	1	
Presumed *R. antipai* NMNHS, n=1		1			1			1				1				1	
R. k. kesslerii NMW 60250, 65535. Danube drainage, n=10	2	8		1	8	1	7	3		3	5	2		2	7	1	
R. k. kesslerii NMW 908803, Dniester drainage, n=2		2			2			2			2				2		
R. banaticus. NMW 65539, Danube drainage, n=30	9	21		26	4		4	21	5	2	19	8	1	18	10	2	
R. kesslerii s.l. NMW 65532, NW Romania, n=12	1	11		7	5		5	7		1	7	4		4	8		
R. kesslerii s.l. NMW 65538, NE Romania, n=9	1	8		3	6		4	5		1	5	3		1	8		
R. kesslerii s.l. NMNHS, NW Bulgaria, n=10	10		2	8			2	8		2	8		4	6			
R. vladykovi Danube drainage, Romania and Ukraine, n=46 (from Naseka 2001).	9	37		4	38	4	12	46	8	4	29	12		3	31	11	1
R. vladykovi NMW 53356, 60234, 65537, Danube drainage, Romania and Serbia, n=24	3	21			19	5	12	12		5	15	4		2	16	6	

Table 1. Continued.

	Total lateral-series scales						Total lateral-line scales					Lateral-line scales to posterior hypural margin					
	39	**40**	**41**	**42**	**43**	**44**	**39**	**40**	**41**	**42**	**43**	**37**	**38**	**39**	**40**	**41**	**42**
R. antipai MGAB 49908 syntype				1					1					1			
R. antipai MGAB/ISBB 0519 syntype					1					1					1		
R. antipai ANSP 98961 syntype			1						1					1			
Non-type MGAB *R. antipai,* n=5			1		3	1			2	3	1		1	2	1		1
Presumed *R. antipai* NMNHS, n=1						1					1						1
R. k. kesslerii NMW 60250, 65535. Danube drainage, n=10			3	4	3			1	2	5	2		2	2	5	1	
R. k. kesslerii NMW 908803, Dniester drainage, n=2			1	1					1	1				1	1		
R. banaticus NMW 65539, Danube drainage, n=30			8	9	3			1	8	9	2		4	6	9	1	
R. kesslerii s.l. NMW 65532, NW Romania, n=12		2	4	6				4	3	5		2	2	6	2		
R. kesslerii s.l. NMW 65538, NE Romania, n=9			7	2				3	4	2			3	4	2		
R. kesslerii s.l. NMNHS, NW Bulgaria, n=10		6	3	1			2	5	2	1			6	4			
R. vladykovi NMW 53356, 60234, 65537, Danube drainage, Romania and Serbia, n=24	1	7	5	10	1		1	8	6	8	1	1	9	8	6		

Table 2. Measurements and counts for examined specimens of *R. antipai*, *R. kesslerii* and *R. vladykovi*. Gap between ranges or ranges only slightly overlapping: * between *R. antipai* and *R. kesslerii*, ** between *R. antipai* and both *R. kesslerii* and *R. vladykovi*, *** between *R. antipai* and *R. vladykovi*; **** no statistical difference; remaining characters display statistically significant differences (Kruskal-Wallis test, p<0.01) but ranges overlapping.

Characters		*R. antipai* n=6				*R. kesslerii* n=26				*R. vladykovi* n=22			
	R. antipai **NMNHS**	**min**	**max**	**Mean**	**SD**	**min**	**max**	**Mean**	**SD**	**min**	**max**	**Mean**	**SD**
SL, mm	68.67	46.20	68.67	54.44	9.743	45.11	74.69	59.53	5.776	46.39	81.42	60.21	10.310
Body depth at dorsal-fin origin (% SL)*	25.43	18.56	25.43	20.37	2.671	15.59	18.63	16.88	0.834	17.50	23.00	19.20	1.277
Depth of caudal peduncle (% SL)*	9.20	8.13	9.20	8.49	0.388	6.33	7.67	7.04	0.358	8.30	10.15	9.06	0.416
Depth of caudal peduncle (% length of caudal peduncle)**	38.47	34.80	38.47	36.72	1.416	24.90	33.44	30.23	2.599	39.32	49.69	44.12	3.117
Predorsal length (% SL)	46.56	44.43	46.56	45.57	0.832	43.41	49.32	46.73	1.415	46.29	49.40	47.57	0.949
Postdorsal length (% SL)	41.90	37.29	41.90	39.89	1.945	39.56	47.49	43.91	1.884	39.48	43.83	41.56	1.432
Prepelvic length (% SL)	48.89	47.76	50.60	48.79	0.989	44.79	49.78	47.45	1.218	48.41	52.79	50.65	1.423
Preanal length (% SL)	70.21	69.60	72.20	70.74	0.875	67.12	73.01	69.91	1.653	69.90	76.28	73.23	1.181
Pectoral – pelvic-fin origin length (% SL)	23.92	22.95	24.60	23.88	0.650	21.15	25.42	23.51	0.865	23.29	27.32	25.58	1.423
Pelvic – anal-fin origin length (% SL)	23.13	21.70	23.13	22.17	0.535	18.66	24.84	21.55	1.374	20.12	24.59	22.86	1.080
Caudal peduncle length (% SL)	23.93	22.61	24.00	23.15	0.632	20.21	29.11	23.80	2.502	18.68	22.98	20.63	1.440
Pectoral-fin length (% SL)	23.18	22.05	23.18	22.55	0.440	19.69	24.00	22.20	1.320	18.49	22.89	20.75	1.162
Pelvic-fin length (% SL)	19.67	17.52	19.67	18.54	0.732	16.13	19.10	17.94	0.743	14.22	18.69	16.35	1.266
Head length (% SL)****	25.99	24.80	25.99	25.34	0.499	23.35	27.20	25.75	0.986	24.05	27.60	26.21	0.794
Head length (% body depth)	102.23	102.23	132.63	121.08	10.537	127.58	186.49	153.40	11.409	111.64	156.60	137.16	11.096
Head depth at nape (% SL)*	17.21	14.90	17.21	16.10	0.791	13.06	15.84	14.38	0.734	14.60	16.57	15.79	0.531
Head depth at nape (% HL)	66.22	59.30	68.70	64.48	3.209	52.81	59.43	55.82	1.971	57.09	64.32	60.27	1.975
Barbel length (% HL)	34.29	34.29	47.90	41.41	5.128	26.90	50.00	39.45	5.569	25.42	40.21	31.97	4.092
Maximum head width (% SL)**	15.42	14.61	16.20	15.38	0.653	13.13	15.19	13.83	0.547	12.90	15.77	14.70	0.767
Maximum head width (% HL)	59.33	58.20	64.00	61.25	2.719	50.03	56.98	53.64	2.192	49.83	59.08	55.98	2.024
Snout length (% SL)****	11.33	8.40	11.33	9.75	0.997	8.94	11.98	10.57	0.625	9.07	11.74	10.16	0.696
Snout length (% HL)	43.59	36.00	43.60	39.40	2.654	37.86	46.38	41.04	2.337	35.93	42.79	38.75	1.903
Eye horizontal diameter (% SL)**	5.24	5.20	5.94	5.49	0.285	5.78	8.15	6.63	0.642	6.36	8.28	7.48	0.463

Characters	*R. antipai* n=6					*R. kesslerii* n=26				*R. vladykovi* n=22			
	R. antipai **NMNHS**	**min**	**max**	**Mean**	**SD**	**min**	**max**	**Mean**	**SD**	**min**	**max**	**Mean**	**SD**
Eye horizontal diameter (% HL)***	20.17	20.17	23.97	22.06	1.301	22.72	29.97	26.25	1.809	24.69	32.29	28.54	1.874
Eye horizontal diameter (% interorbital width)**	58.73	58.73	67.50	63.35	4.101	75.25	130.37	103.18	14.774	86.33	121.43	103.22	7.479
Postorbital distance (% HL)****	44.15	43.20	48.76	45.89	2.111	37.27	48.97	42.38	2.756	37.93	45.81	41.91	2.408
Interorbital width (% SL)*	8.93	8.15	8.93	8.56	0.375	5.23	8.33	6.56	0.811	6.74	7.96	7.26	0.368
Interorbital width (% HL)**	34.34	32.48	35.78	34.25	1.316	19.46	31.26	25.45	2.970	25.12	30.25	27.70	1.384
Number of predorsal vertebrae****	11	10.00	11.00	10.67	0.516	10.00	11.00	10.50	0.510	10.00	11.00	10.82	0.395
Number of abdominal vertebrae***	19	19.00	19.00	19.00	0.000	18.00	21.00	19.42	0.703	20.00	21.00	20.18	0.395
Number of caudal vertebrae	21	20.00	21.00	20.83	0.408	19.00	21.00	20.00	0.632	19.00	21.00	19.91	0.610
Number of preanal caudal vertebrae	4	3.00	4.00	3.50	0.548	2.00	3.00	2.58	0.504	2.00	3.00	2.45	0.510
Total vertebrae****	40	39.00	40.00	39.83	0.408	38.00	41.00	39.42	0.809	39.00	41.00	40.09	0.610
Difference between abdominal and caudal numbers***	-2	-2.00	-1.00	-1.83	0.408	-2.00	2.00	-0.58	1.065	-1.00	2.00	0.27	0.827
Dorsal-fin branched rays (without ½)***	8	8.00	8.00	8.00	0.000	8.00	8.00	8.00	0.000	7.00	7.00	7.00	0.000
Scales in lateral row	44	41.00	44.00	42.67	1.033	40.00	42.00	41.08	0.744	39.00	43.00	41.14	1.037
Lateral-line scales (total)***	43	41.00	43.00	42.00	0.894	39.00	42.00	40.73	1.002	39.00	43.00	41.00	1.024
Lateral-line scales (to posterior margin of hypurals)***	42	39.00	42.00	40.33	1.366	38.00	40.00	38.88	0.766	37.00	40.00	38.77	0.869
Scales above lateral line*	6	6.00	6.00	6.00	0.000	4.00	5.00	4.96	0.196	5.00	6.00	5.59	0.503
Scales below lateral line*	4	4.00	4.00	4.00	0.000	3.00	3.00	3.00	0.000	3.00	4.00	3.32	0.477

Note on syntypes of *R. antipai*

As already clarified (Kottelat 1997), the species group name *antipai* is based on 13 syntypes (Bănărescu 1953: 300) without any catalogue numbers. Soon after, Bănărescu (1961: 344) designated a holotype ("Mus. Gr. Antipa Bukarest, Col. Ichth. Nr. 4) but this action is not valid (Art. 74.5 of the International Code of Zoological Nomenclature; International Commission on Zoological Nomenclature 1999). The referred article of the Code says that a subsequent use of the term "holotype" does not constitute a valid lectotype designation *unless* (italics ours) the author, when wrongly using that term, explicitly indicated that he or she was selecting from the type series that particular specimen to serve as the name-bearing type. We do not know a publication by Petru Bănărescu where he used the term holotype for that specimen *explicitly* indicating its name-bearing role. However, it cannot be excluded that a valid lectotype designation has been already undertaken by someone because the ANSP syntype is labelled as a paralectotype.

Comparisons

The three examined samples of *Romanogobio kesslerii* s.l. demonstrate a statistically significant difference in ten morphometric and five meristic characters (Table 3) but the ranges of character values overlap considerably and the number of specimens is small. We combined all specimens in a single sample in order to estimate general ranges of character values without a special analysis of variation within the *R. kesslerii* complex.

As can be seen from Table 2, examined specimens of *R. antipai* including the NMNHS specimen from the Danube at Vetren, most clearly (with a gap or ranges only slightly overlapping) differ from both *R. kesslerii* and *R. vladykovi* by the caudal peduncle depth (35–38.5% caudal peduncle length vs 25–33 and 39–50, respectively), a wider head (58–64% HL vs 50–59), a smaller eye (5–6% SL and 59–67.5% interorbital width vs 6–8 and 75–130), and a wider interorbital space (32.5–36% HL vs 19.5–31; 8–9% SL vs 5–8) with shallow orbital notches (Fig. 2a–c). *Romanogobio antipai* can be further distinguished from *R. kesslerii,* besides the number of scales above and below the lateral line (6 and 4, respectively, in all examined *R. antipai* vs commonly 5 and 3 in *R. kesslerii* s.l.), by a deeper body (19–25% SL vs 16–19), a deeper caudal peduncle (8–9% SL vs 6–8), and a deeper head (59–69% HL vs 53–59).

Besides morphometric characters mentioned above, all examined specimens of *R. antipai* including the NMNHS specimen can be clearly distinguished from *R. vladykovi* by the number of branched dorsal-fin rays, 8½, in contrast to 7½ found in all specimens of *R. vladykovi* examined in this study. Naseka (2001: 111) mentioned that 8½ rays can be rarely found in *R. vladykovi*; a revision of his primary data (radiographs) revealed a single specimen with 8½ branched dorsal-fin rays out of 46 examined. *Romanogobio antipai* further differs from *R. vladykovi* by the vertebral structure (Table 1, 2) having abdominal+caudal counts 19+21 or 20+21, which means that the caudal region is longer than the abdominal region vs. commonly (in 52 out of 70 specimens) 20+20 or 21+21 or variants with a caudal region shorter than the abdominal one.

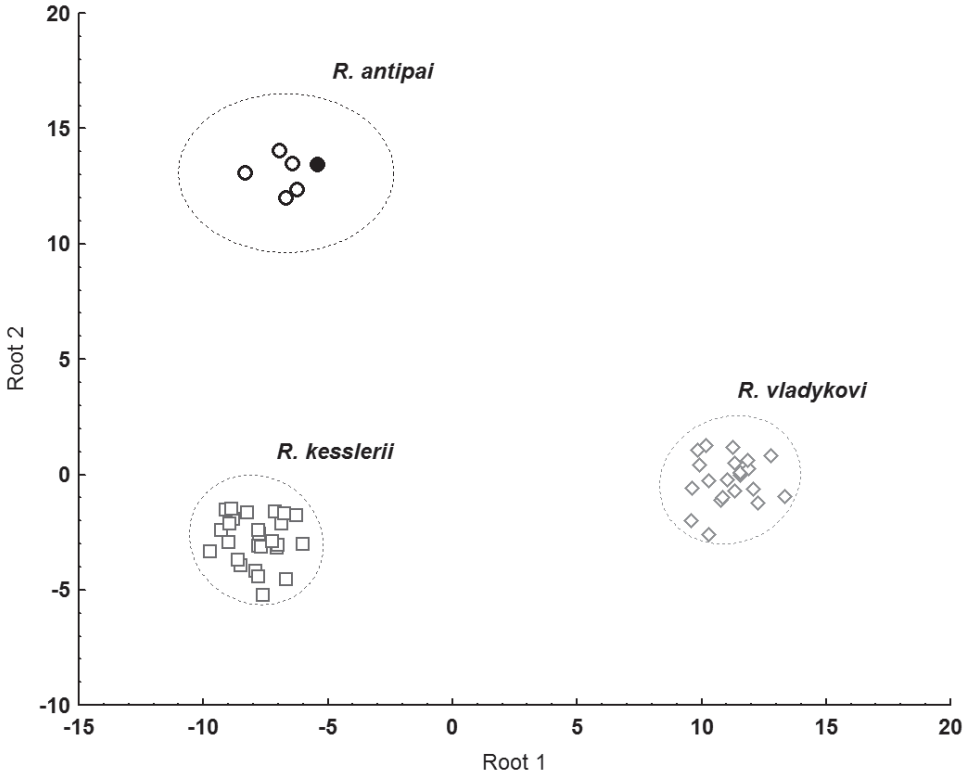

Figure 3. DFA (Euclidean distance, complete linkage clustering algorithm), distribution of discriminant scores along two canonical discriminant functions established to discriminate between three groups of samples (*R. antipai*, *R. kesslerii* and *R. vladykovi*). Solid circle corresponds to NMNHS specimen identified as *Romanogobio antipai.*

A DFA (Fig. 3) showed differentiation of the three groups of samples identified as *R. antipai, R. kesslerii* and *R. vladykovi* (the number of unbranched dorsal-fin rays was excluded from the analysis as demonstrating zero variability within the groups) and the groups were 100% classified as predicted (Table 4). A CA (Fig. 4) supported the grouping.

To conclude, the analysis confirmed previously reported discriminating character states (number of branched dorsal-fin rays, relative size of the eye and the interorbital space, relative depth of the caudal peduncle) and introduces a new character (vertebral counts) for discriminating *Romanogobio antipai* from *R. kesslerii* and *R. vladykovi*. However, relative taxonomic status of these three species still waits for a phylogenetic analysis based on molecular data. It cannot be excluded that *R. antipai* is a deep-water ecophenotype of either *R. kesslerii* or *R. vladykovi*. The new record demonstrates that *R. antipai* is still extant in the lower Danube but at present can only be found at a greater depth in the main channel and the deltaic branches. Currently classified as Extinct using IUCN criteria, the conservation status of *Romanogobio antipai* needs revision, in light of the new record from 2016.

Table 3. Measurements and counts for examined specimens of *Romanogobio kesslerii* species complex. * refers to characters demonstrating statistically significant differences (Kruskal-Wallis test, p<0.01).

Characters	*R. kesslerii* Danube n=10				*R. kesslerii* Romania n=6				*R. kesslerii* Bulgaria n=10			
	min	max	Mean	SD	min	max	Mean	SD	min	max	Mean	SD
SL, mm	50.10	63.42	59.06	3.952	45.11	74.69	57.37	10.157	55.06	66.51	61.31	3.584
Body depth at dorsal-fin origin (% SL)	15.59	17.93	16.81	0.916	16.54	18.30	17.39	0.649	15.73	18.63	16.65	0.787
Depth of caudal peduncle (% SL)*	7.08	7.67	7.37	0.195	6.79	7.34	7.04	0.211	6.33	7.08	6.70	0.214
Depth of caudal peduncle (% length of caudal peduncle)	24.90	33.24	28.84	3.215	28.24	32.85	31.17	1.629	27.17	33.44	31.05	1.865
Predorsal length (% SL)	46.10	48.81	47.39	0.874	44.23	46.70	45.90	0.934	43.41	49.32	46.56	1.826
Postdorsal length (% SL)*	44.25	47.49	45.58	1.260	41.26	44.25	43.27	1.133	39.56	44.64	42.63	1.537
Prepelvic length (% SL)	46.33	49.78	47.84	1.324	46.27	48.69	47.32	0.976	44.79	49.33	47.15	1.250
Preanal length (% SL)	67.12	73.01	70.44	2.227	68.81	71.04	69.90	0.842	67.14	71.01	69.39	1.274
Pectoral – pelvic-fin origin length (% SL)	22.95	23.89	23.27	0.335	23.18	25.18	23.92	0.705	21.15	25.42	23.51	1.230
Pelvic – anal-fin origin length (% SL)	18.66	22.29	21.06	1.307	20.72	22.16	21.34	0.467	18.91	24.84	22.16	1.644
Caudal peduncle length (% SL)*	24.49	29.11	26.35	1.642	21.15	24.14	23.18	1.139	20.21	23.70	21.62	1.099
Pectoral-fin length (% SL)*	22.82	24.00	23.24	0.362	20.43	23.99	22.47	1.167	19.69	23.09	21.01	1.063
Pelvic-fin length (% SL)	17.69	19.10	18.36	0.451	17.19	18.71	18.09	0.508	16.13	18.74	17.44	0.832
Head length (% SL)	25.54	27.20	26.40	0.458	23.35	26.66	25.47	1.181	24.25	26.86	25.28	0.977
Head length (% body depth)	144.23	186.49	158.35	12.847	127.58	159.58	147.35	11.663	139.47	170.77	152.09	8.209
Head depth at nape (% SL)*	13.97	15.84	14.91	0.697	13.83	14.97	14.49	0.410	13.06	14.56	13.79	0.454
Head depth at nape (% HL)	53.04	59.43	56.36	2.349	54.72	59.23	57.01	1.428	52.81	56.20	54.56	1.058
Barbel length (% HL)	32.95	47.64	39.49	5.449	37.63	50.00	43.50	4.540	26.90	43.61	36.99	5.233
Maximum head width (% SL)	13.18	14.30	13.61	0.404	13.13	15.19	14.08	0.657	13.21	14.73	13.91	0.571
Maximum head width (% HL)*	50.03	52.57	51.25	0.976	53.24	56.98	55.35	1.504	53.15	56.43	55.01	0.861
Snout length (% SL)*	10.37	11.20	10.69	0.264	8.94	10.41	9.85	0.534	10.21	11.98	10.89	0.616
Snout length (% HL)*	39.37	42.13	40.40	0.869	37.86	39.61	38.66	0.687	38.32	46.38	43.12	2.260
Eye horizontal diameter (% SL)	6.20	8.15	7.03	0.772	5.78	7.26	6.47	0.570	5.92	6.77	6.31	0.244
Eye horizontal diameter (% HL)	25.14	29.97	27.47	1.896	25.31	27.57	26.29	0.802	22.72	27.36	25.00	1.321
Eye horizontal diameter (% interorbital width)	78.47	130.37	103.10	18.289	75.25	112.80	93.59	14.198	97.90	122.36	109.01	7.799

Characters	*R. kesslerii* Danube n=10				*R. kesslerii* Romania n=6				*R. kesslerii* Bulgaria n=10			
	min	**max**	**Mean**	**SD**	**min**	**max**	**Mean**	**SD**	**min**	**max**	**Mean**	**SD**
Postorbital distance (% HL)	39.71	48.97	43.11	3.323	42.00	45.47	43.86	1.350	37.27	43.56	40.75	2.001
Interorbital width (% SL)*	6.04	7.90	7.00	0.635	6.39	8.33	7.06	0.709	5.23	6.24	5.81	0.367
Interorbital width (% HL)*	22.93	30.92	26.52	2.674	25.06	31.26	27.71	2.241	19.46	25.43	23.03	1.827
Number of predorsal vertebrae*	10	11	10.80	0.422	10	11	10.83	0.408	10	10	10.00	0.000
Number of abdominal vertebrae*	19	21	20.00	0.471	19	20	19.50	0.548	18	19	18.80	0.422
Number of caudal vertebrae	19	21	19.90	0.738	20	21	20.50	0.548	19	20	19.80	0.422
Number of preanal caudal vertebrae	2	3	2.30	0.483	2	3	2.67	0.516	2	3	2.80	0.422
Total vertebrae*	39	41	39.90	0.568	40	40	40.00	0.000	38	39	38.60	0.516
Difference between abdominal and caudal numbers	-2	2	0.10	1.101	-2	0	-1.00	1.095	-2	0	-1.00	0.667
Dorsal-fin branched rays (without ½)	8	8	8.00	0.000	8	8	8.00	0.000	8	8	8.00	0.000
Scales in lateral row*	41	42	41.50	0.527	41	42	41.33	0.516	40	42	40.50	0.707
Lateral-line scales (total)	40	42	41.10	0.994	40	42	41.00	0.894	39	42	40.20	0.919
Lateral-line scales (to posterior margin of hypurals)*	39	40	39.50	0.527	38	40	38.67	0.816	38	39	38.40	0.516
Scales above lateral line	4	5	4.90	0.316	5.0	5	5.00	5.0	5	5	5.00	0.000
Scales below lateral line	3	3	3.00	0.000	3.0	3	3.00	3.0	3	3	3.00	0.000

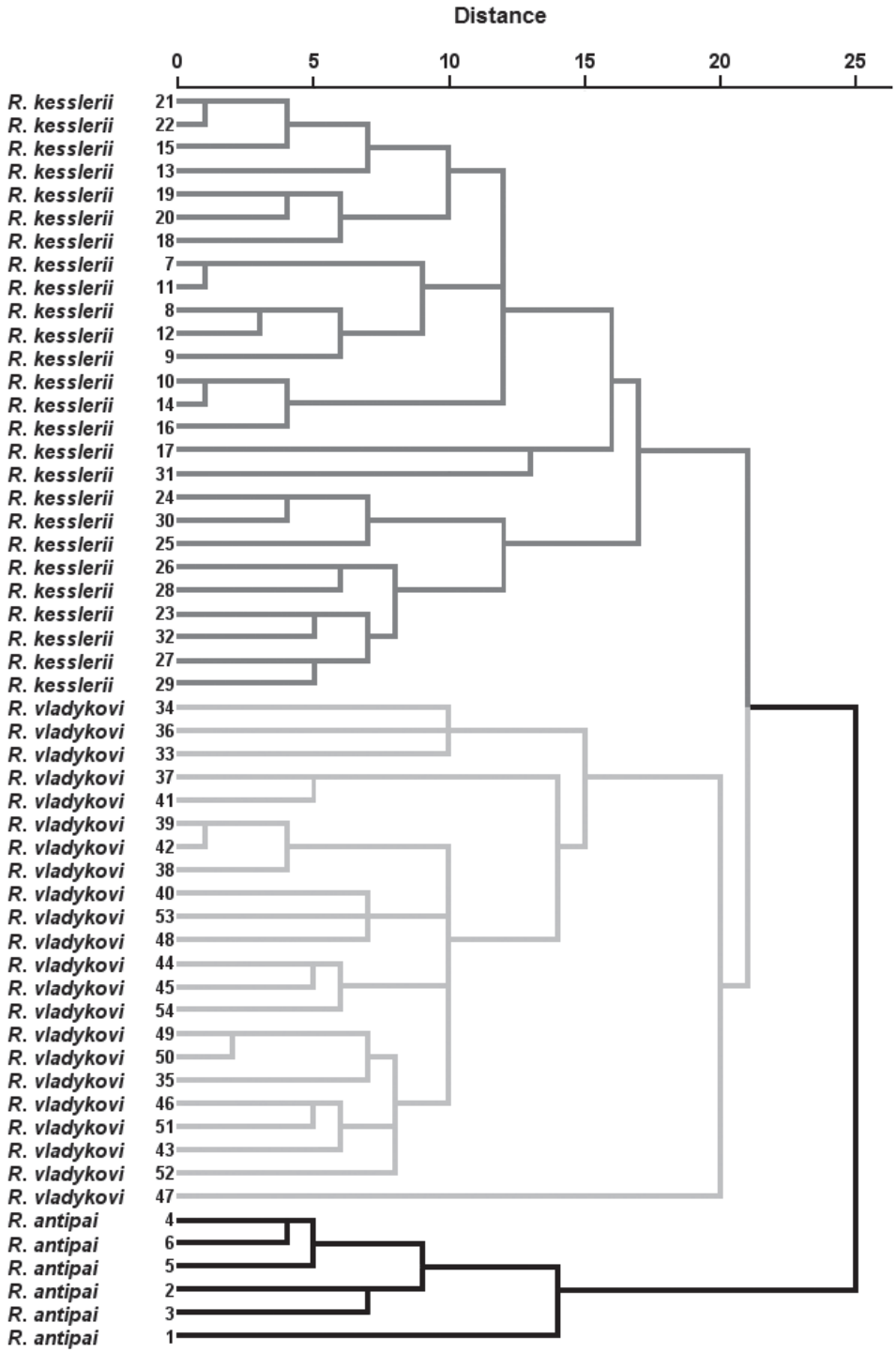

Figure 4. CA (SPSS, k-means) for three groups of samples (*R. antipai*, *R. kesslerii* and *R. vladykovi*). No 1 refers to NMNHS specimen identified as *Romanogobio antipai.*

Table 4. Results of DFA classification for three groups of samples (*R. antipai*, *R. kesslerii* and *R. vladykovi*).

Group	Classification matrix (*Romanogobio* 3 species)			
	Rows: Observed classifications			
	Columns: Predicted classifications			
	Percent correct	*R. antipai*	*R. kesslerii*	*R. vladykovii*
R. antipai	100.0	6	0	0
R. kesslerii	100.0	0	26	0
R. vladykovii	100.0	0	0	22
Total	100.0	6	26	22

Acknowledgements

NGB was supported by Lise Meitner Programme of National Science Foundation of Austria (M 2183-B25). Our sincere thanks go to Ernst Mikschi and all other members of the NMW Fish Collection, and Melanya Stan and Alexandru Iftime (MGAB), for their valuable help in studying the collections under their care; Mark Sabaj Pérez and Kyle Luckenbill (ANSP) for sending photos and a radiograph of a *R. antipai* syntype; and to Alice Schumacher (NMW) for making photos of NMW specimens.

References

Bănărescu P (1953) Variatia geografica, filogenia si ecologia Cyprinidului *Gobio kessleri*. Studii si cercetari stiintifice. Academia Republicii Populare Romine 4(1–2): 297–337.

Bănărescu P (1960) Einige Fragen zur Herkunft und Verbreitung der Süßwasserfischfauna der europäisch-mediterranen Unterregion. Archiv für Hydrobiologie 57(1/2): 16–134.

Bănărescu P (1961) Weitere systematische Studien über die Gattung *Gobio* (Pisces, Cyprinidae), insbesondere im Donaubecken. Věstnik Československé společnosti zoologické 25(4): 318–346.

Bănărescu P (1964) Fauna Republicii Populare Romîne. Volumul XIII. Pisces – Osteichthyes (pesti ganoizi si osisi). Editura Academiei Republicii Populare Romîne, Bucureşti, 962 pp.

Bănărescu P (1992) A critical updated checklist of Gobioninae (Pisces, Cyprinidae). Travaux du Muséum d'Histoire Naturelle Grigore Antipa 32: 303–330.

Bănărescu P (1994a) On the presumed origin of *Gobio albipinnatus* Lukasch in the upper Danube by sympatric speciation. Senckenbergiana biologica 73(1–2): 49–55.

Bănărescu P (1994b) The present-day conservation status of the fresh water fish fauna of Romania. Ocrotirea Naturii şi a Mediului Înconjurător 38(1): 5–20.

Bănărescu P (1999) *Gobio kessleri*. In: Bănărescu P (Ed.) The freshwater fishes of Europe. Vol 5/I, Cyprinidae 2/I. AULA-Verlag, Wiebelsheim, 135–162.

Bănărescu P, Nalbant T (1973) Pisces, Teleostei. Cyprinidae (Gobioninae). Das Tierreich 93: 1–304.

Chichkoff G (1937) Sur les goujons habitant les eaux douces de la Bulgarie. Annulaire de l'Université de Sofia, Faculte de Sciences 33(3): 227–289. [In Bulgarian]

Dikov T, Jankov S, Jocev S (1994) Fish stocks in rivers of Bulgaria. Polskie Archiwum Hydrobiologii 41(3): 377–391.

Dybowski B (1862) Versuch einer Monographie der Cyprinoiden Livlands, nebst einer synoptischen Aufzählung der europäischen Arten dieser Familie. Archiv für die Naturkunde Liv-, Ehst- und Kurlands. Zweiter Serie. Biologische Naturkunde. Vol. 3. Heinrich Laakmann, Dorpat, 133–362. https://doi.org/10.5962/bhl.title.14430

Fang P-W (1943) Sur certains types peu connus de cyprinidés des collections du muséum de Paris (III). Bulletin du Muséum National d'Histoire Naturelle (Série 2) 15(6): 399–405.

Freyhof J, Kottelat M (2008) *Romanogobio antipai*. The IUCN Red List of Threatened Species 2008: e.T135636A4167651. https://doi.org/10.2305/IUCN.UK.2008.RLTS.T135636A4167651.en [Downloaded on 22 August 2018]

Friedrich T, Wiesner C, Zangl L, Daill D, Freyhof J, Koblmüller S (2018) *Romanogobio skywalkeri*, a new gudgeon (Teleostei: Gobionidae) from the upper Mur River, Austria. Zootaxa 4403(2): 336–350. https://doi.org/10.11646/zootaxa.4403.2.6

Holčík J, Bănărescu P, Evans D (1989) General introduction to fishes. In: Holčík J (Ed.) The freshwater fishes of Europe. Vol 1/II, General introduction to fishes. Acipenseriformes. AULA-Verlag, Wiesbaden, 18–147.

ICZN (1999) International Code of Zoological Nomenclature (4th edn). International Trust of Zoological Nomenclture, London, 306 pp.

Kottelat M (1997) European freshwater fishes. Biologia (Bratislava) 52(suppl. 5): 1–271.

Kottelat M, Freyhof J (2007) Handbook of European Freshwater Fishes. Kottelat, Cornol and Freyhof, Berlin, 646 pp.

Marinov B (1978) Die Fischfauna im bulgarischen Donauabschnitt und ihre Bedeutung für die Wirtschaft. In: Russev B, Naidenow W (Eds) Limnologie des bulgarischen Donauabschnitts. Bulgarische Akademie der Wissenschaften, Sofia, 201–228. [In Bulgarian]

Mihailova L (1970) Die Fische im Westlichen Balkangebirge. Bulletin de l'Institut de Zoologie et Musee 31: 19–43. [In Bulgarian]

Movchan YV, Smirnov AI (1981) Fauna Ukrainy. Tom. 8, Ryby. Vypusk 2. Koropovi. Chastina 1 [Fishes of Ukraine. Vol. 8, 2, cyprinids. Part 1], Naukova Dumka, Kyiv, 424 pp. [In Ukrainian]

Naseka AM (1996) Comparative study on the vertebral column in the Gobioninae (Pisces, Cyprinidae) with special reference to its systematics. Publicaciones Especiales, Instituto Español de Oceanografía 21: 149–167.

Naseka AM (2001) Contribution to the knowledge of infraspecific structure of whitefin gudgeon, *Romanogobio albipinnatus* (Lukasch, 1933) (Cyprinidae: Gobioninae), with a description of a new subspecies, *R. albipinnatus tanaiticus*, from the Don drainage. Proceedings of the Zoological Institute, Russian Academy of Sciences 287: 99–119.

Naseka AM, Bogutskaya NG, Bănărescu P (1999) *Gobio albipinnatus.* In: Bănărescu P (Ed.) The freshwater fishes of Europe. Vol. 5/1. Cyprinidae 2/1. AULA-Verlag, Wiebelsheim, 37–68.

Smirnov AI (1971) K izucheniyyu peskarey (*Gobio* Cuvier) Ukraini [Studies of gudgeons (*Gobio* Cuvier) of Ukraine]. Vestnik zoologii 6: 55–61. [In Russian]

Vladykov VD (1931) Poissons de la Russie sous-carpathique (Tchécoslovaquie). Mémoires de la Société Zoologique de France 29(4): 217–374.

ZooKeys 825: 123–144 (2019)
doi: 10.3897/zookeys.825.32443
http://zookeys.pensoft.net

RESEARCH ARTICLE

A peer-reviewed open-access journal
ZooKeys
Launched to accelerate biodiversity research

Review and integrative taxonomy of the genus *Prosopistoma* Latreille, 1833 (Ephemeroptera, Prosopistomatidae) in Thailand, with description of a new species

Boonsatien Boonsoong[1], Michel Sartori[2,3]

1 *Animal Systematics and Ecology Speciality Research Unit (ASESRU), Department of Zoology, Faculty of Science, Kasetsart University, Bangkok 10900, Thailand* **2** *Museum of Zoology, Palais de Rumine, Place Riponne 6, CH-1005 Lausanne, Switzerland* **3** *Department of Ecology and Evolution, Lausanne University, CH-1015 Lausanne, Switzerland*

Corresponding author: *Boonsatien Boonsoong* (fscibtb@ku.ac.th)

Academic editor: *B. Price* | Received 14 December 2018 | Accepted 24 January 2019 | Published 27 February 2019

http://zoobank.org/4F785350-7E19-4BED-92B0-5271E3165879

Citation: Boonsoong B, Sartori M (2019) Review and integrative taxonomy of the genus *Prosopistoma* Latreille, 1833 (Ephemeroptera, Prosopistomatidae) in Thailand, with description of a new species. ZooKeys 825: 123–144. https://doi.org/10.3897/zookeys.825.32443

Abstract

Three species of the genus *Prosopistoma* Latreille, 1833 (Prosopistomatidae) are currently reported from Thailand. A new species, *Prosopistoma carinatum* **sp. n.**, is described here based on specimens from western and southern Thailand. The new species can be easily distinguished from the other members of *Prosopistoma* by the following combination of characteristics: (i) the presence of two ridged longitudinal lines on each side of its carapace, (ii) antenna 7-segmented, (iii) a strongly convex carapace and (iv) nine pectinate setae on the ventral margin of the fore tibiae. A comparison between the key characteristics of *P. carinatum* **sp. n.** and the known Thai species is provided. Results of analysis of the mitochondrial cytochrome oxidase I (COI) gene (658 bp) of three species, as well as the distribution of the Thai species, are also discussed.

Keywords

Prosopistoma carinatum, *Prosopistoma annamense*, *Prosopistoma sinense*, COI, mayfly

Copyright *Boonsatien Boonsoong, Michel Sartori.* This is an open access article distributed under the terms of the Creative Commons Attribution License (CC BY 4.0), which permits unrestricted use, distribution, and reproduction in any medium, provided the original author and source are credited.

Introduction

Prosopistomatidae (Ephemeroptera) is a monogeneric family, represented by the genus *Prosopistoma*, which was originally established by Latreille (1833). Of the 27 species described to date, 16 species have been described from the Oriental region (Lieftinck 1932, Peters 1967, Soldán and Braasch 1984, Tong and Dudgeon 2000, Sartori and Gattolliat 2003, Zhou and Zheng 2004, Barber-James et al. 2008, Barber-James 2009, Shi and Tong 2013; Balachandran et al. 2016, Roopa et al. 2017). An updated key to the known species of this realm was provided by Shi and Tong (2013).

In Thailand, only the larvae of *Prosopistoma annamense* Soldán & Braasch, 1984, *P. sinense* Tong & Dudgeon, 2000, and *P. wouterae* Lieftinck, 1932 are known (Parnrong et al. 2002, Tungpairojwong and Boonsoong 2011). In the present study, we describe a new species of *Prosopistoma* based on specimens from western and southern Thailand. In addition, a distribution map of the genus in Thailand and mitochondrial COI sequence data are provided.

Materials and methods

The prosopistomatid mayfly larvae were collected from streams and rivers in northern, north-eastern, eastern, central, western, and southern Thailand from 2013 to 2018. Measurements (given in mm) and photographs were taken using a Visionary LK System (Dun, Incorporated, USA). All drawings were made with the aid of a camera lucida attached to a compound microscope. For Scanning electron microscopy (SEM), specimens (head, carapace, sternal plate, foreleg) were dried in a Critical Point Drier (CPD7501) and coated with gold (10 nm, Sputter Coater SC7620). SEM photographs were observed by a FEI Quanta 450 SEM. Final plates were prepared with Adobe Photoshop CC 2017. The material is deposited in the collection of the Zoological Museum at Kasetsart University in Bangkok, Thailand (**ZMKU**) and at the Museum of Zoology in Lausanne, Switzerland (**MZL**). The distribution map was generated via the Simple Mapper website (http://www.simplemappr.net) using GPS coordinates.

The collected specimens were fixed in absolute ethanol and preserved under refrigeration for description and DNA extraction. Details of the specimens from the three species used for the DNA experiment are shown in Table 1. Total DNA extraction was performed using a genomic DNA purification kit (NucleoSpin, Macherey-Nagel, Germany) following the manufacturer's protocol. A fragment of the mitochondrial gene cytochrome oxidase I (COI) gene was amplified (658 bp) using the primers LCO1490 (5'-GGT CAA ATC ATA AAG ATA TTG G-3') and HCO2198 (5'-TAA ACT TCA GGG TGA CCA AAA AAT CA-3'), designed by Folmer et al. (1994). Polymerase chain reaction (PCR) conditions were as follows: a 50 µl final reaction volume containing 25 µl of PCR Master mix solution, 1 µl (10 µm) of each primer, 2 µl of total DNA and 21 µl of nuclease free sterile water. PCR was performed as follows: 5 minutes at 94 °C, then 30 seconds at 94 °C, 30 seconds at 48 °C, and 60 seconds at 72 °C (40 cycles), and a final elongation step at 72°C for 10 minutes (Gattolliat et al. 2015). Pu-

Table 1. List of the sequenced specimens.

Species	Code	Collection locality	Collector	Date	GenBank accession number
P. annamense	PA-01-KN	Kanchanaburi	B. Boonsoong	15 Oct 2015	MK285321
	PA-12-RT	Ratchaburi	B. Boonsoong	13 Feb 2016	MK285322
	PA-13-LE	Loei	B. Boonsoong	19 Mar 2016	MK285323
	PA-17-NN	Nakhon Nayok	B. Boonsoong	25 Feb 2017	MK285324
	PA-18-CT	Chantaburi	B. Boonsoong	5 Jul 2018	MK285325
P. carinatum sp. n.	PC-01-KN	Kanchanaburi	B. Boonsoong	26 Apr 2014	MK285326
	PC-02-KN	Kanchanaburi	B. Boonsoong	26 Apr 2014	MK285327
P. sinense	PS-01-KN	Kanchanaburi	B. Boonsoong	20 Feb 2016	MK285328
	PS-02-KN	Kanchanaburi	B. Boonsoong	20 Feb 2016	MK285329
	PS-03-CM	Chaing Mai	B. Boonsoong	11 Mar 2017	MK285330

rification and sequencing were conducted by Macrogen, Inc. (South Korea). Sequence alignment and editing were performed using ClustalW. The best-fit evolution model obtained was T92 (Tamura 3-parameter) + G. Phylogenetic trees based on maximum likelihood (ML) were performed with MEGA 7 using the likelihood-ratchet method with 1,000 bootstrap replicates. Pairwise (uncorrected-p) sequence distances were also calculated using MEGA 7 (Kumar et al. 2016). Nucleotide sequences obtained in this study have been deposited in the GenBank database (MK285321-MK285330).

Abbreviations

C central; **N** northern; **W** western.
m meter; **NE** north-eastern;

Taxonomy

Family Prosopistomatidae Lameere, 1917
Genus *Prosopistoma* Latreille, 1833

***Prosopistoma annamense* Soldán & Braasch, 1984**
Figures 1A, 1B, 2A, 2B, 2C, 2D, 3A, 3B, 3C, 12A, 12B, 12C, 14

Prosopistoma annamense Soldán & Braasch, 1984: 370–376, figs. 2, 4, 6, 8, 13, 14. (orig.); Barber-James, 2009: 153–154, Table 2 (morph. matrix); Tungpairojwong & Boonsoong, 2011: 67–68; Shi & Tong, 2013: 95 (key).

Material examined. THAILAND; 1 larva, Chanthaburi province, Klong Kla Seu Yai, Khao Kitchakut, 12°52'35.94"N, 102°05'48.3"E, 40 m, 7.II.2013, 2 larvae, same place, 6.VII.2018, B Boonsoong leg. (ZMKU); 1 larva, Nakhon Nayok prov-

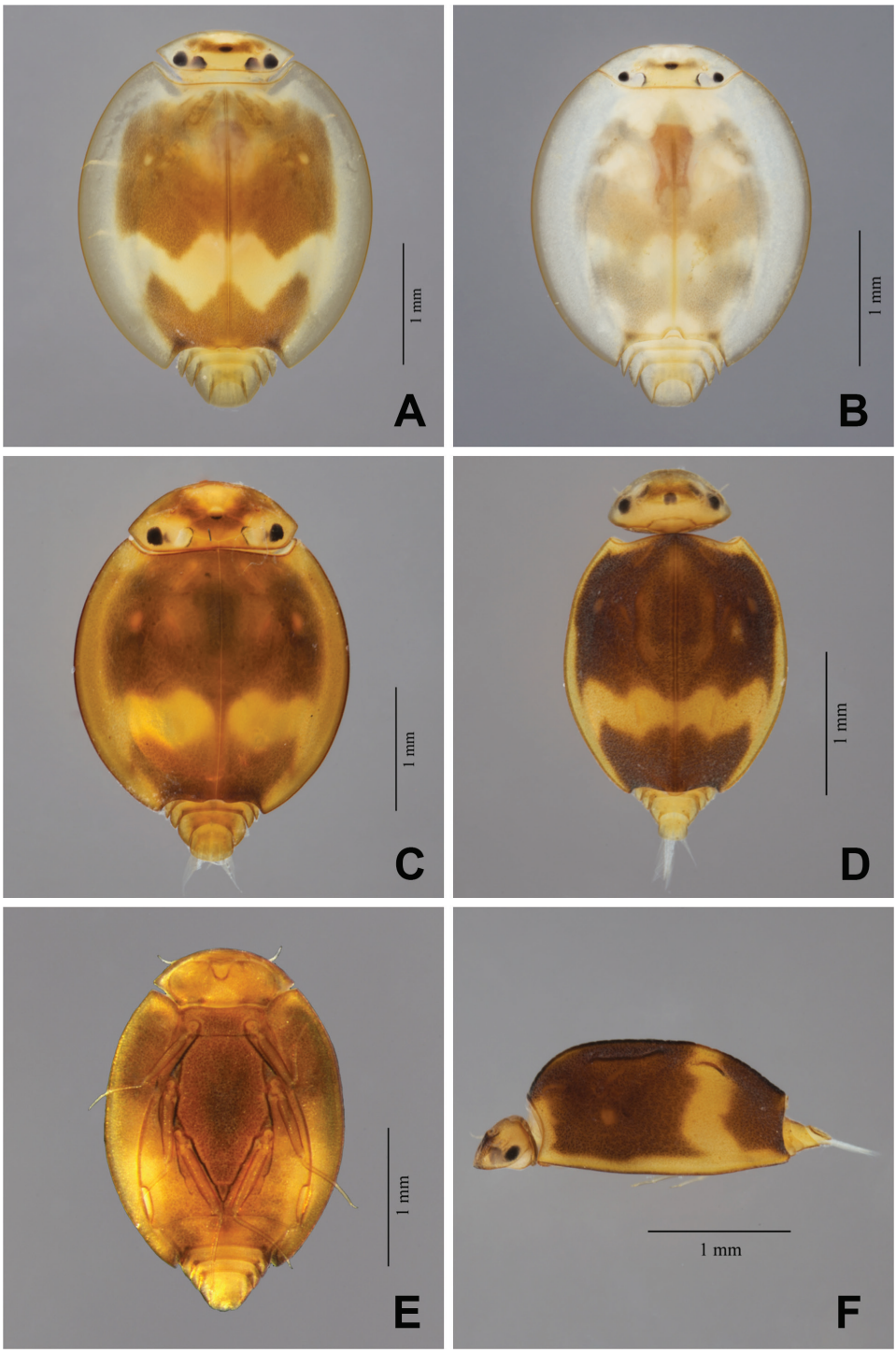

Figure 1. *Prosopistoma* spp. whole larvae: **A–B** *P. annamense*, specimens from stream (**A**) and river (**B**); **C** *P. sinense* **D–F** *P. carinatum* sp. n. **D** dorsal view **E** ventral view **F** lateral view.

Table 2. Uncorrected pairwise genetic distances (COI) between selected prosopistomatid and baetiscid species, using the Kimura 2-parameter.

	B. laurentina	*P. annamense*	*P. carinatum* sp. n.	*P. sinense*
B. laurentina	–	–	–	–
P. annamense	0.32	–	–	–
P. carinatum sp. n.	0.23	0.31	–	–
P. sinense	0.34	0.33	0.35	–

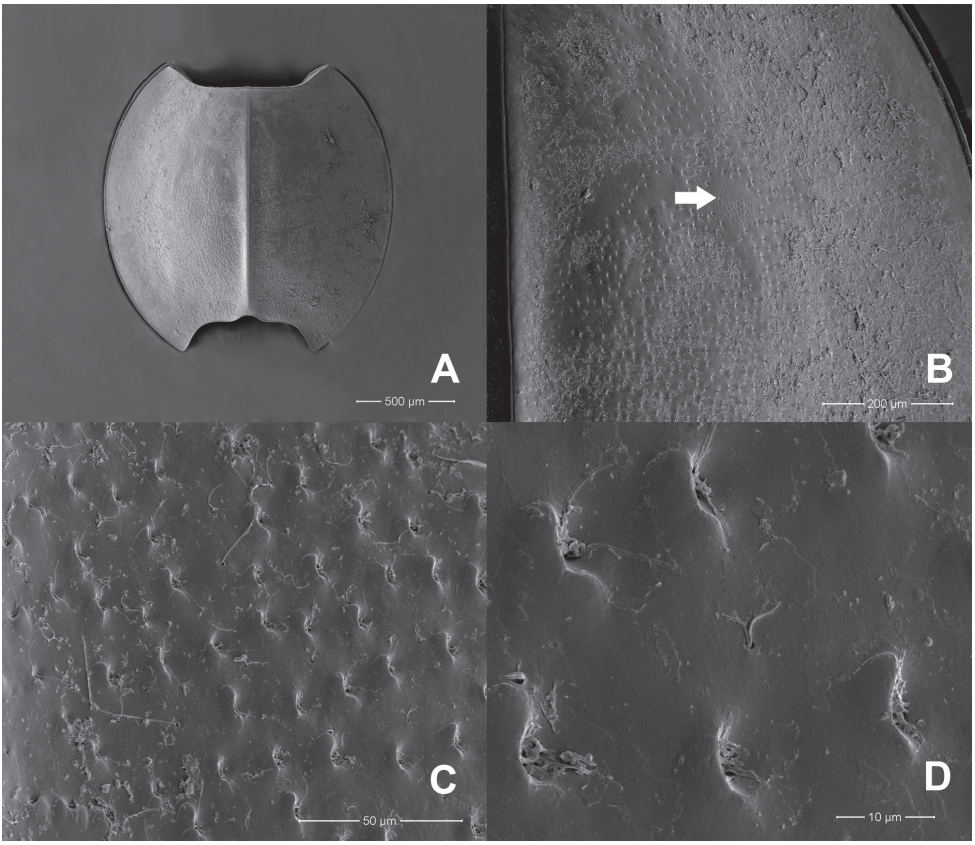

Figure 2. *Prosopistoma annamense*: **A** SEMs of notal shield, dorsal view **B** pale-coloured areas on carapace (arrow) **C** scale-like structures **D** closer view showing details of scale-like structures.

ince, Wang Ta Krai, 14°19'35.9"N, 101°18'05.9"E, 65 m, 24.III.2013, B Boonsoong leg. (ZMKU); 5 larvae, Kanchanaburi province, Thong Pha Phum, Phu Iyara Resort, 14°37'34.4"N, 98°34'17.0"E, 207 m, 6.IV.2013, B Boonsoong leg. (ZMKU), 1 larva same data (MZL, GBIFCH00657966); 1 larva, Ban Pra Chum Mai, 14°35'01.4"N, 98°34'54.3"E, 233 m, 26.IV.2014, B Boonsoong leg. (ZMKU); 5 larvae, Kanchanaburi province, Pung Wan Resort, 14°12'20"N, 98°03'36"E, 28 m, 14.X.2015, B Boon-

soong leg. (ZMKU), 1 larva same data (MZL, GBIFCH00657965); 3 larvae, Loei province, Ban Non Pattana, 17°06'24"N, 101°28'44"E, 530 m, 1.II.2016, B Boonsoong leg. (ZMKU); 3 larvae, Ratchaburi province, Kang Som Maew, Suan Phueng, 13°24'27.6"N, 99°16'51.3"E, 206 m, 13.II.2016, B Boonsoong leg. (ZMKU); 6 larvae, Loei province, Ban Non Pattana, 17°06'24"N, 101°28'44"E, 530 m, 19.III.2016, B Boonsoong leg. (ZMKU); 2 larvae, Nakhon Nayok province, Wang Ta Krai, 14°20'9.42"N, 101°18'22.5"E, 67 m, 25.II.2017, B Boonsoong leg. (ZMKU); 2 larvae, Chanthaburi province, Klong Sa Tor Bon, 12°43'12.42"N, 102°23'19.26"E, 115 m, 5.VII.2018, B Boonsoong leg. (ZMKU).

Diagnosis. The larvae of *P. annamense* can be distinguished from those of other Oriental congeners by (i) apex of the inner margin of the fore tibiae, with 4–6 serrated pectinate spines (Fig. 3B), (ii) three long, finely serrated bristles at the base of the inner incisor, on both right and left mandible, (iii) segment III of the maxillary palp slightly shorter than 1/3 the length of segment II and (iv) posterolateral spines at segments VII and VII parallel to or bent outwards from the body axis (Fig. 1A, B).

Distribution. Loei province (NE), Nakhon Nayok province (C), Chanthaburi province (E), Kanchanaburi province (W), Ratchaburi province (W).

Remarks. The larvae of *P. annamense* were originally described by Soldán and Braasch (1984) and collected from Vietnam (Thuan Hai province). They are widely distributed in southern and central Vietnam. Tungpairojwong and Boonsoong (2011) reported this species in middle and moderately disturbed streams in Loei province (NE), Chaiyaphum province (NE) and Kanchanaburi province (W). In this study, we found this species in several provinces, and it seems to have a wide distribution in Thailand. Surprisingly, we found larvae on the banks of the Khwae Noi River (Kanchanaburi province) (Fig. 12C). This is the first report of *Prosopistoma* larvae in large rivers in Thailand, and the larvae collected from large rivers are paler than those larvae from streams (Fig. 1B).

Prosopistoma sinense Tong & Dudgeon, 2000

Figures 1C, 4A, 4B, 4C, 4D, 5A, 5B, 5C, 12D, 14

Prosopistoma sinense Tong & Dudgeon, 2000: 122–128, figs. 1–14. (orig.); Barber-James, 2009: 153–154, Table 2 (morph. matrix); Tungpairojwong & Boonsoong, 2011: 68; Shi & Tong, 2013: 95 (key).

Material examined. THAILAND; 2 larvae, Kanchanaburi province, Thong Pha Phum, Pussaduklang Ranger Station, 14°33'13"N, 98°34'17"E, 317 m, 20.II.2016, B Boonsoong leg. (ZMKU); 2 larvae, Kanchanaburi province, Thong Pha Phum, Pak Kok stream, 14°39'32.1"N, 98°31'59.2"E, 161 m, 20.II.2016, B Boonsoong leg. (ZMKU), 1 larva same data (MZL, GBIFCH00657969); 4 larvae, Chiang Mai province, Chiang Dao, Mae Na, 19°19'13.08"N, 98°53'25.98"E, 742 m, 11.III.2017, B Boonsoong leg. (ZMKU).

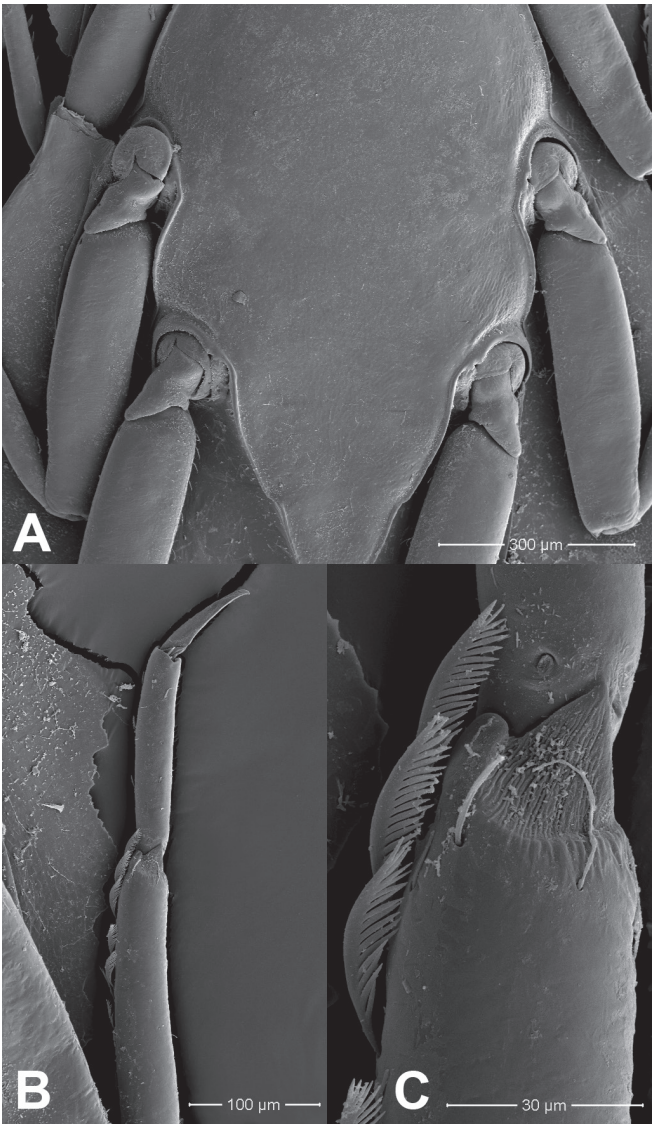

Figure 3. *Prosopistoma annamense*: **A** SEMs of sternal plate **B** ventral margin of fore tibia **C** pectinate setae.

Diagnosis. The larvae of *Prosopisoma sinense* can be distinguished from those of other congeners by (i) antennae with 4–5 segments, (ii) antenna segment III much longer than the combined length of segments IV–V (iii) and apex of the ventral margin of the fore-tibia with 6–8 serrated spines (Fig. 4B) (Shi and Tong 2013).

Distribution. Kanchanaburi province (W), Chiang Mai province (N).

Remarks. The larvae of *P. sinense* were originally described by Tong and Dudgeon (2000) and collected from China (Guangdong, Hongkong). In Thailand, Tungpairojwong and Boonsoong (2011) reported this species from a slightly disturbed stream

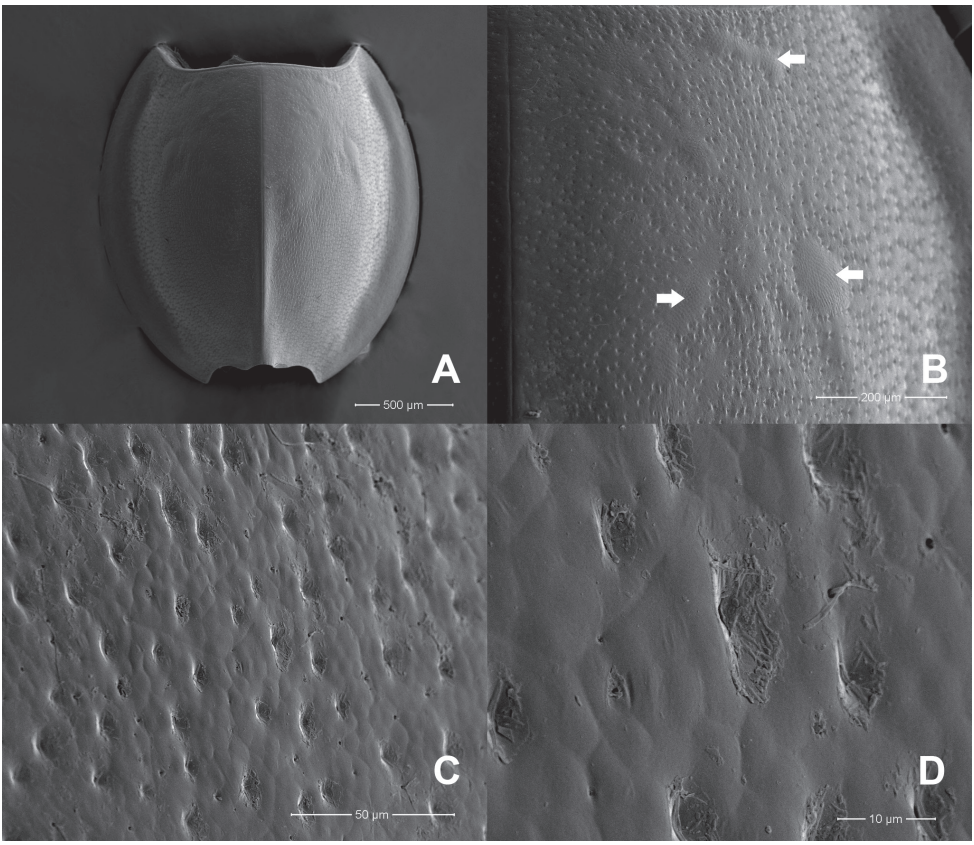

Figure 4. *Prosopistoma sinense*: **A** SEMs of notal shield, dorsal view **B** pale-coloured areas on carapace (arrow) **C** scale-like structures **D** closer view showing details of scale-like structures.

in Kanchanaburi province. In this study, we found the larvae in the same habitat (Fig. 12D) and streams as previous studies. In addition, we found this species at a slightly disturbed stream in Chiang Dao, Chiang Mai province (N).

Prosopistoma wouterae Lieftinck, 1932

Figure 14

Prosopistoma wouterae Lieftinck, 1932: 44–55, pls 1–2. (orig.); Lafon, 1952: 433 (table); Peters, 1967: 211–213, figs 2, 8, 10, 16, 26 (redescription); Soldán & Braasch, 1984; 374–375 (key); Barber-James, 2009: 153–154, Table 2 (morph. matrix); Shi & Tong, 2013: 95 (key).

Material examined. None.

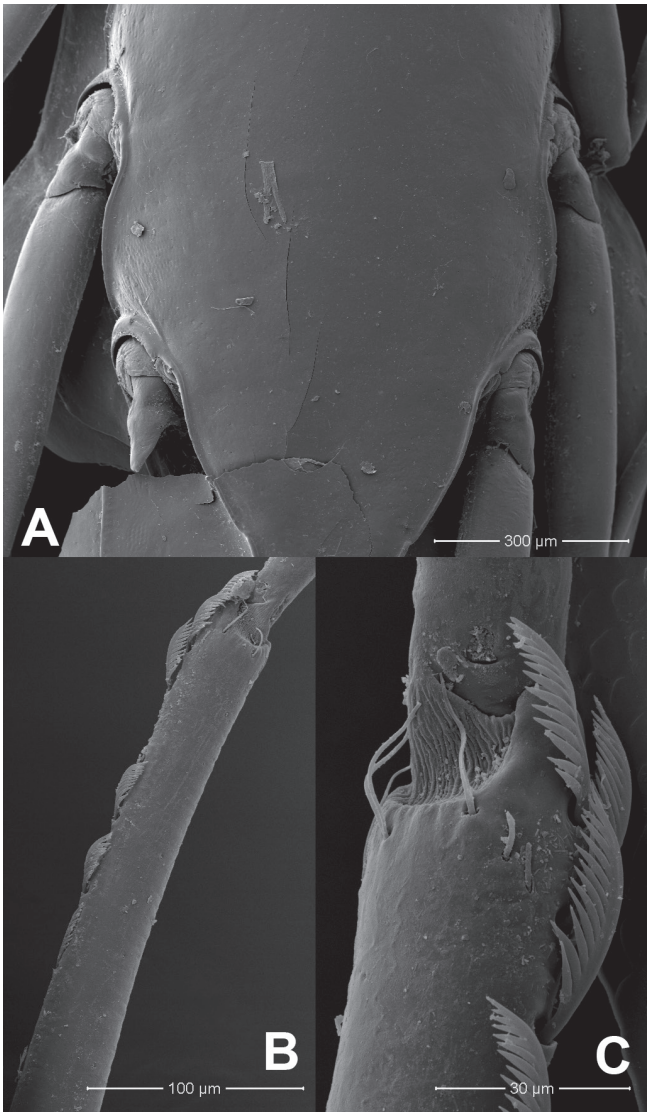

Figure 5. *Prosopistoma sinense*: **A** SEMs of sternal plate **B** ventral margin of fore tibia **C** pectinate setae.

Diagnosis. The larvae of *P. wouterae* can be distinguished from those of other congeners by the combination of the following characteristics: (i) apical segment of the maxillary palp shorter than 1/2 the length of segment II, (ii) mesonotum with five dark-brown patches connected by brown narrow stripes, (iii) apex of the ventral margin of the fore-tibiae with eight serrated spines and (iv) posterolateral spine of segments VII and VIII parallel to or bent inwards the body axis (Shi and Tong 2013).

Distribution. Songkhla province (S).

Remarks. *Prosopistoma wouterae* was originally described by Lieftinck (1932) from West Java. Parnrong et al. (2002) reported larvae of *P. wouterae* from the Songkhla province. In this study, we sampled in the same stream (Boripat Waterfall) but unfortunately, no specimens were found during our collection. This species seems to have a distribution limited only to the Sunda Islands and southern Thailand. Only four genes (16S, 18S, 28S rDNA, and H3) were sequenced for *P. wouterae* (Ogden and Whiting 2005), and no COI sequences were available for comparison.

***Prosopistoma carinatum* sp. n.**
http://zoobank.org/E4B47533-39E5-45D6-BFAA-BE6B5E681C7B
Figures 1D, 1F, 6, 7, 8, 9, 10, 12E, 12F, 14

Material examined. ***Holotype***. THAILAND; Holotype, 1 mature larva, Kanchanaburi province, Thong Pha Phum, Ban Pra Chum Mai, 14°35'01.4"N, 98°34'54.3"E, 233 m, 11.IV.2015, B Boonsoong leg. (ZMKU); ***Paratypes***. 1 larva same data as holotype (MZL, GBIFCH00657926); 6 larvae same data as holotype (ZMKU); 1 mature larva, 8 larvae, Kanchanaburi province, Ban Pra Chum Mai, 14°35'01.4"N, 98°34'54.3"E, 233 m, 26.IV.2016, B Boonsoong leg. (ZMKU).

Additional material. THAILAND; 1 larva, Nakhon Si Thammarat province, Lan Sa Ka, Khao Luang water fall, 8°28'08.30"N, 99°46'14.20"E, 533 m, 2.VII.2016, B Boonsoong leg. (ZMKU); 1 larva, Narathiwat province, Waeng district, Ai Sae, 5°47'45.9"N, 101°50'5.46"E, 64 m, 21.IV.2018, B Boonsoong leg. (ZMKU).

Distribution. Kanchanaburi province (W), Nakhon Si Thammarat province (S), Narathiwat province (S).

Diagnosis. The larvae of *Prosopistoma carinatum* sp. n. can be distinguished from those of other species by the combination of the following characteristics (Table 3): (i) carapace with two longitudinal ridges on each side of the midline on its surface (Fig. 1F), (ii) antenna 7-segmented, (iii) carapace with three pale-coloured depressions on each side, (iv) carapace with a very narrow flange width and strong convexity, (v) carapace with a typically brown colouration and a distally irregular (zig-zag) yellow pattern at 0.7 times the length of the carapace, (vi) carapace with circular scale-like structures, (vii) presence of three long serrated bristles at the base of the inner canine and (viii) ventral margin of the fore-tibia with nine pectinate setae.

Description (in alcohol). Body length 1.94–2.43 mm excluding caudal filaments.

Head. Head yellowish with median blackish ocellus between antennae (Fig. 8A), head width approximately 3 times length. Epicranial ecdysial sutures prominent, passing through the anterior margin of the lateral ocelli, and between the compound eyes and the antennal bases and continuing to the lateral margin of the head (Fig. 8B). Antenna 7-segments (Figs 6A, 8B, 8C), longer than the distance from antennal base to anterior margin of head; segment I usually retracts into head capsule; segment III the longest and shorter than combined length of segments IV–VII, antenna segment VII minute (Fig. 8C). Labrum (Fig. 6D) narrow, 3 times wider than long, anterior

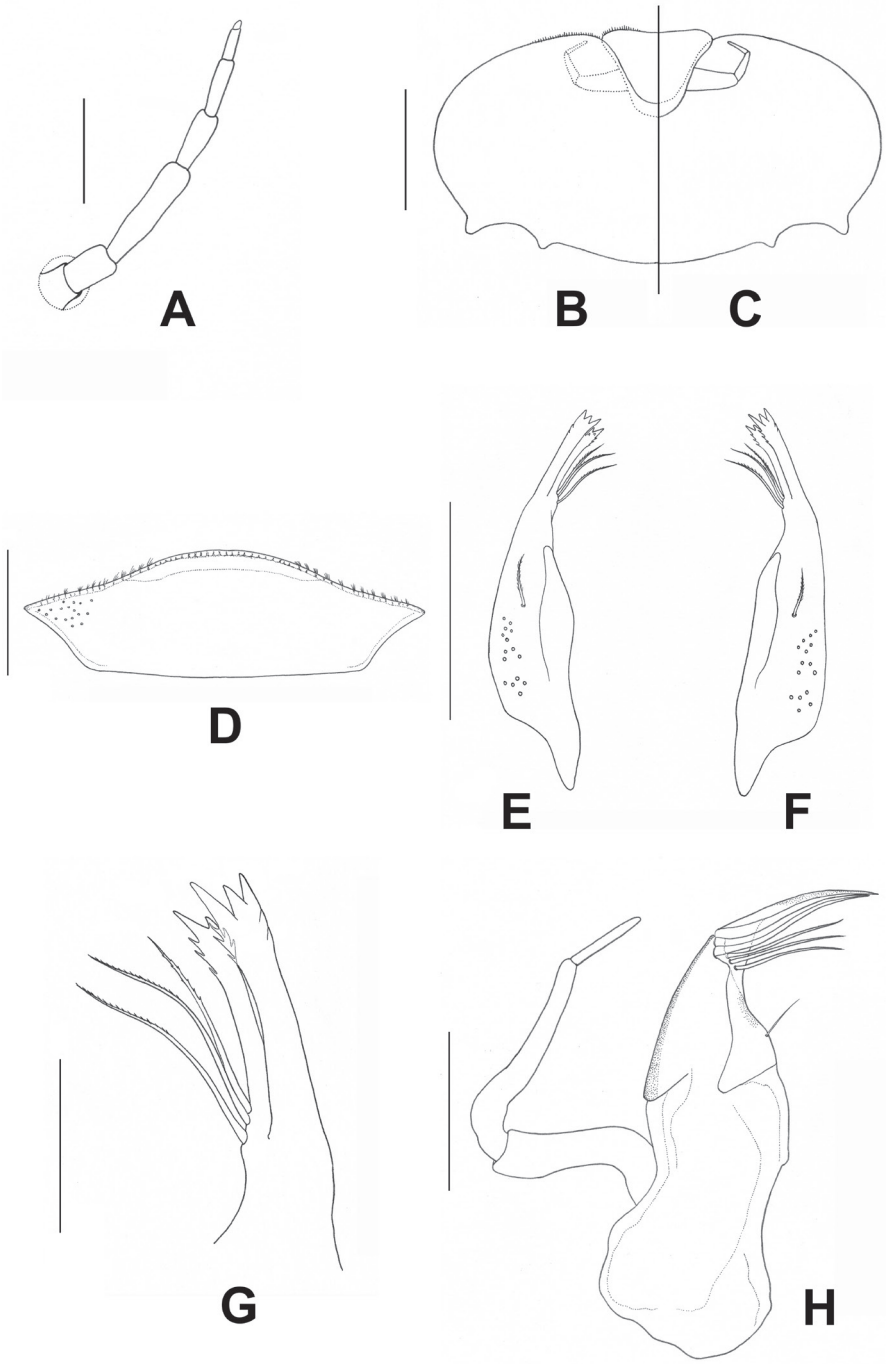

Figure 6. *Prosopistoma carinatum* sp. n.: **A** Antenna **B–C** Labium **B** ventral view **C** ventral view **D** Labrum, dorsal view **E–G** Mandible **E** Left mandible (ventral view) **F** Right mandible (ventral view) **G** Enlargement of canine of the right mandible, (**H**). Scale bars: 0.02 mm (**H**); 0.05 mm (**G**); 0.1 mm (**A, D, E, F**); 0.2 mm (**B, C**).

Table 3. Larval characters of *P. carinatum* sp. n. compared with Thai known species (Soldán and Braasch 1984, Sartori and Gattolliat 2003, Shi and Tong 2013).

	P. annamense	***P. sinense***	***P. wouterae***	***P. carinatum* sp. n.**
Distribution	Vietnam, Thailand	China, Thailand	Java, Sumatra, Thailand	Thailand
Antennae	5-segmented	5-segmented	6-segmented	7-segmented
Antenna with segment III to remaining segments	shorter	longer	shorter	shorter
Number of bristles on mandibles	3	4–6	3	3
Number of spines on foretibiae	4–6	6–8	8	9
Carapace flange width	wide	narrow	narrow	very narrow
Carapace ridges	no	no	no	2 ridges on each side
Distal end of carapace	incised notch	incised notch	incised notch	protruding notch
Length of inner canine to outer canine	shorter than outer canine	shorter than outer canine	subequal	subequal
Ratio length of carapace (along median suture):width	0.95–1.00 (n = 3)	0.96–1.02 (n = 3)	unknown	1.07–1.13 (n = 3)
Convexity: carapace depth:length	0.39–0.45 (n = 3)	0.30–0.49 (n = 3)	unknown	0.56–0.58 (n = 3)

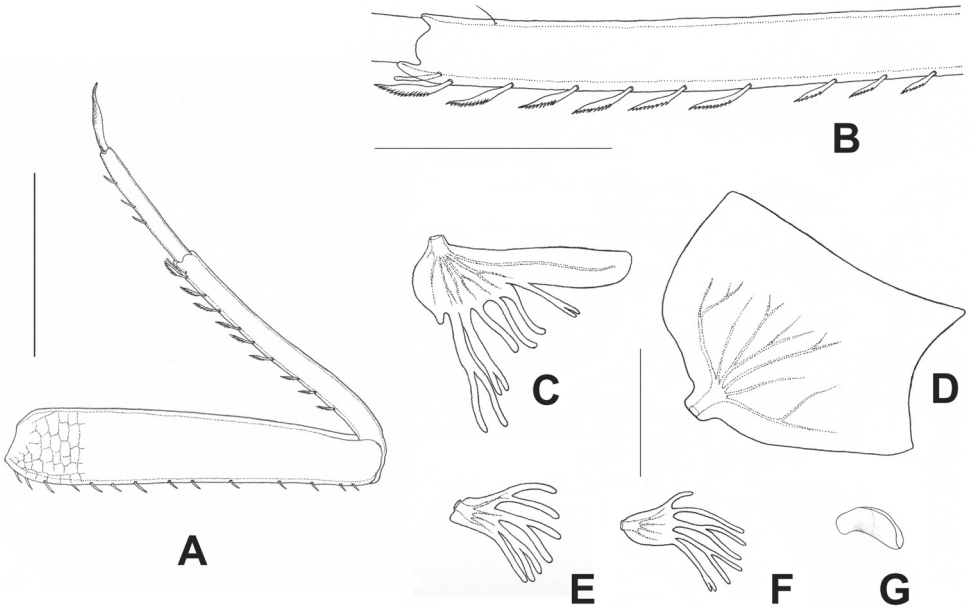

Figure 7. *Prosopistoma carinatum* sp. n.: (**A**) Foreleg, (**B**) Enlargement of part of the fore-tibia to show setation; (**C**) Gill I; (**D**) Gill II; (**E**) Gill IV; (**F**) Gill V; (**G**) Gill VI. Scale bars 0.1 mm (**B**); 0.2 mm (**A**); 1 mm (**C–F**).

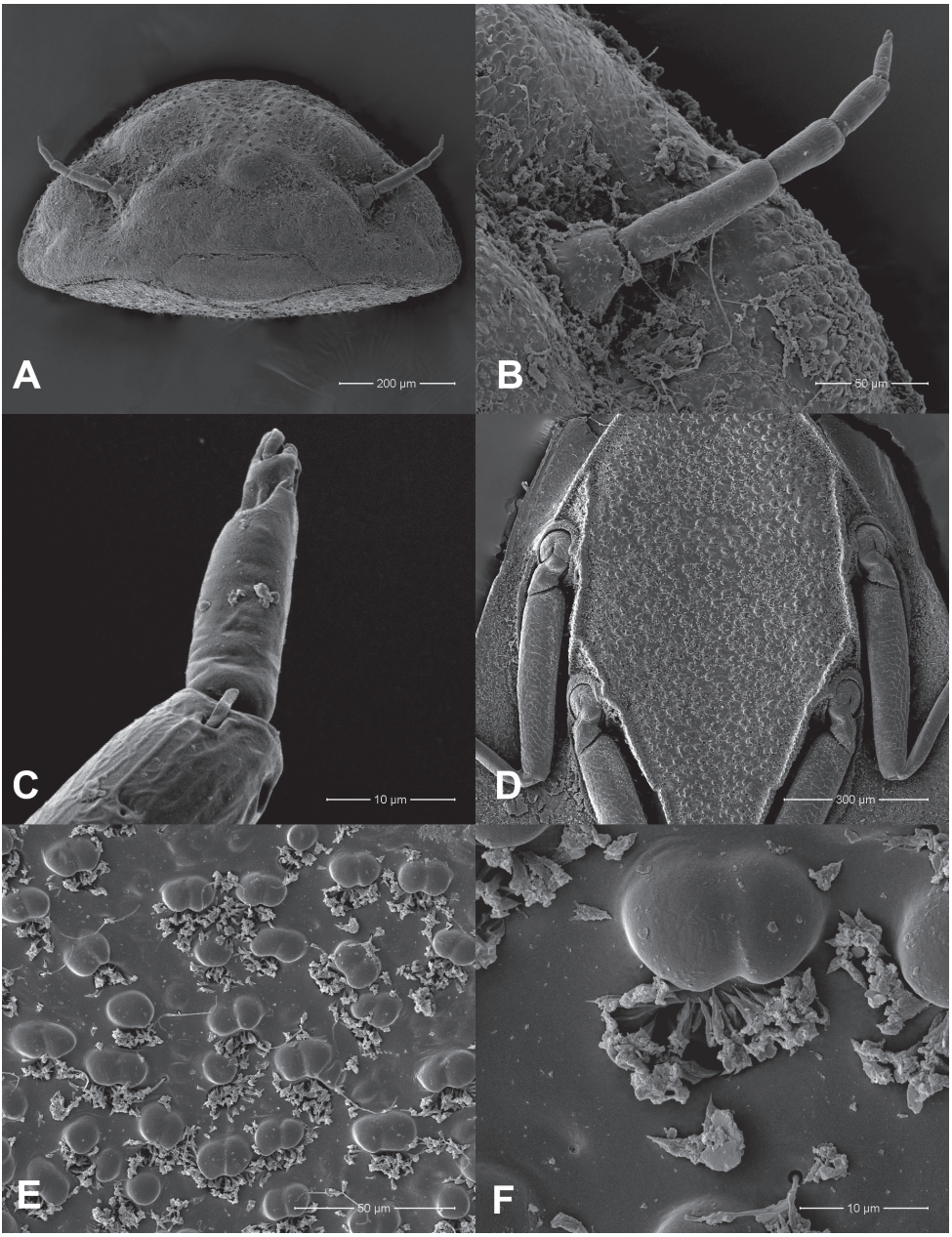

Figure 8. *Prosopistoma carinatum* sp. n.: **A** SEMs of head, frontal view **B** antenna, frontal view **C** tip of antenna **D** sternal plate and legs **E** closer view of surface of sternal plate **F** closer view showing details of scale-like structures.

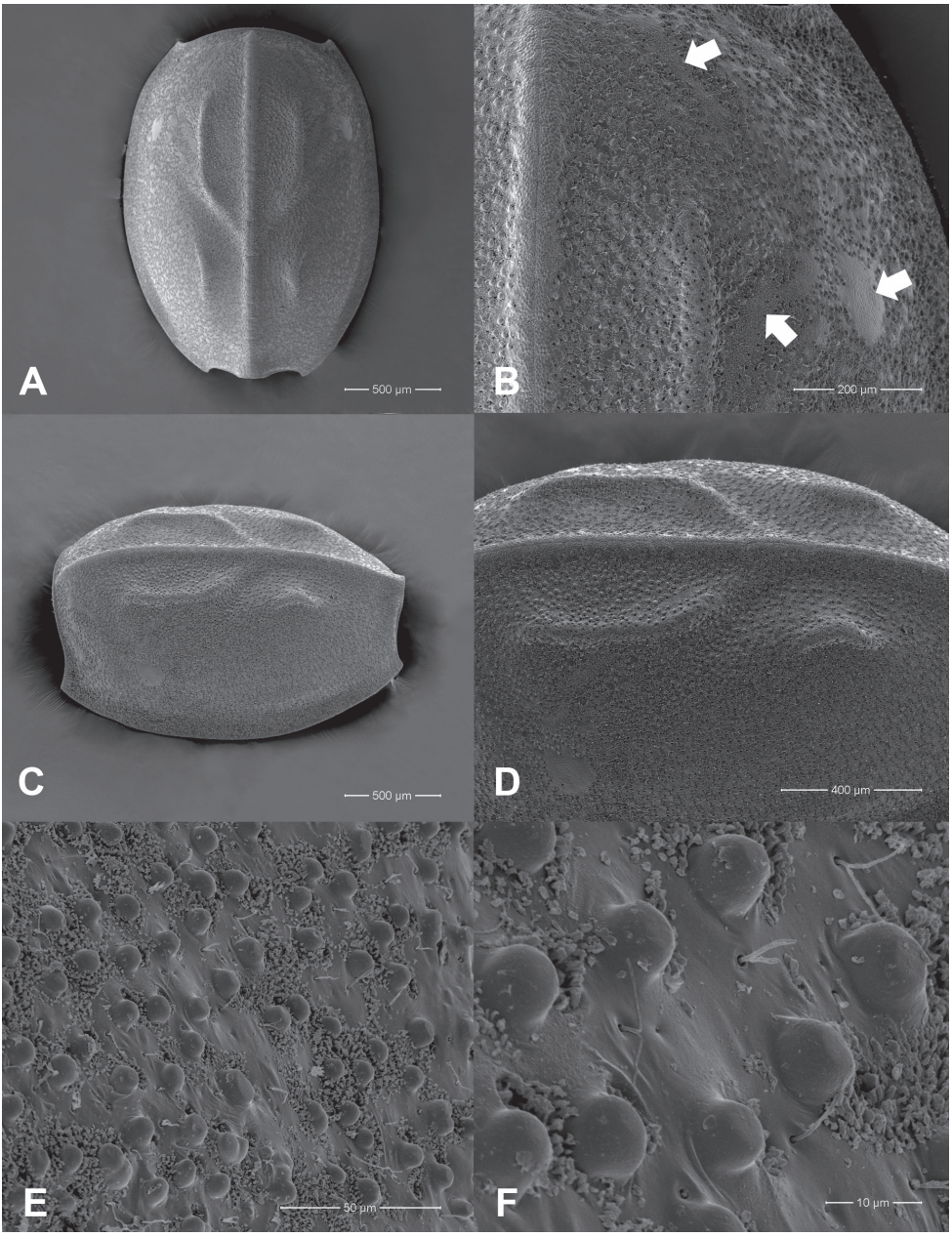

Figure 9. *Prosopistoma carinatum* sp. n.: **A** SEMs of notal shield, dorsal view **B** pale-coloured areas on carapace (arrows) **C** dorsolateral view of carapace **D** ridged longitudinal lines, dorsolateral view **E** scale-like structures **F** closer view showing details of scale-like structures.

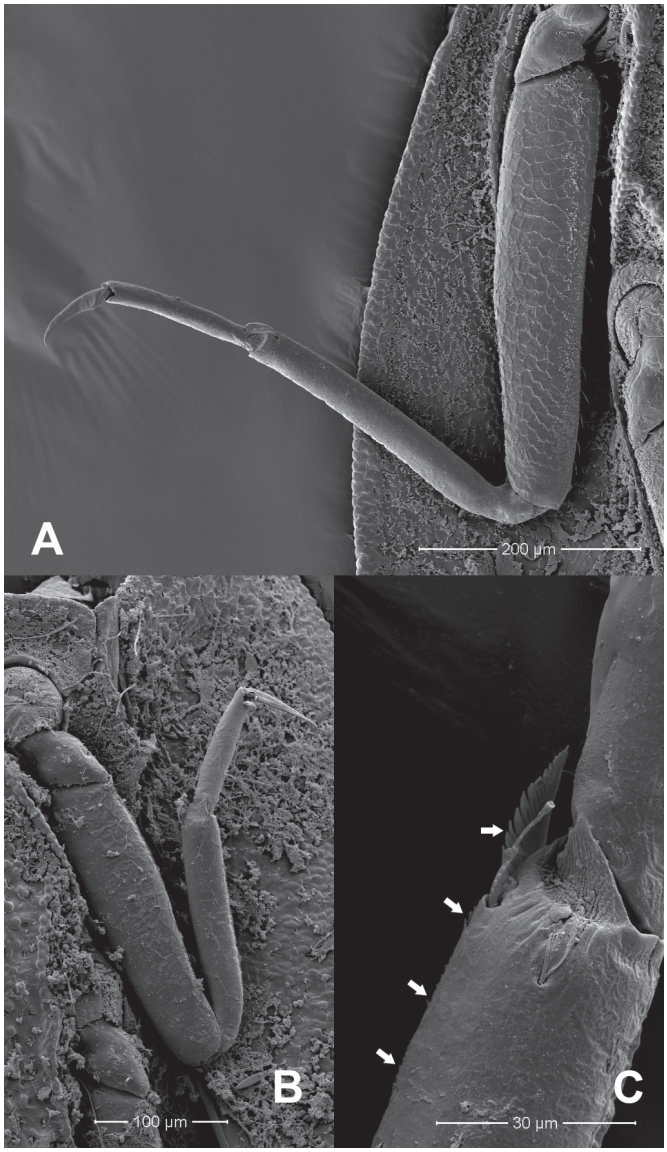

Figure 10. *Prosopistoma carinatum* sp. n.: **A** SEMs of middle leg showing scale-like pattern on femur, ventral view **B** ventral margin of fore tibia **C** pectinate setae (arrows).

margin fringed with dense fine setae. Left and right mandibles similar (Fig. 6E, 6F). Outer canine of mandibles subequal and broader than inner canine, with three apical teeth, a smaller outer tooth and a larger inner tooth with a serrated margin near the apex and three small spines; inner canine with two apical teeth, including a larger inner one with a serrated inner margin near the apex with three spines. Three long serrated

bristles arising from the base of the inner canine (Fig. 6G). A single stout feathered seta lateromedially on each mandible (Fig. 6E, 6F). Maxillae (Fig. 6H) crowned by a rigid canine and three subequal moveable dentisetae; three long-feathered stout bristles arising near the base of the apical canine and dentisetae on the galea-lacinia. A single unserrated bristle arising approximately 2/3 of the way down the sclerotised section of the galea-lacinia. Maxillary palpi 3-segmented, segment II the longest, length ratio of maxillary palp segments from basal one to apical: 1.9:2.2:1(Fig. 6H).

Carapace. Carapace general colouration dark brown, distally with an irregular (zig-zag) yellow pattern at 0.7 times the length of the carapace (Fig. 1D). Two longitudinal ridges on the anterior surface region, and two short ridges on the pale surface area (Figs 1D, 1F, 9A, 9C, 9D). Carapace with one pale-coloured circular depression on lateral side of the anterior region (Figs 1F, 9B) and two pale-coloured striped depressions at the midline. Carapace flange width very narrow. Cuticle of carapace coarsely pitted and interspersed with scale-like structures (Fig. 9E, F). Distal margin of the carapace protruding slightly over the exhalent notch (Figs 1D, 9A). In lateral view, carapace strongly convex, with a convexity (ratio of maximum carapace height to length along the posterior margin of the carapace) range 0.56–0.58. Sternum pitted, with coarse scale-like structures within the triangular sternal plate (Fig. 8D, F).

Legs. Dorsal margin of fore femur with 14 short simple setae (Fig. 7A); ventral margin of fore tibia with nine pectinate setae (Figs 7B, 10C). Anterior and posterior surface of femur covered with scale-like pattern (Figs 7A, 10A). Tarsal claws of all three pairs of legs sharp and without denticles.

Abdomen. Abdominal gills (Fig. 7C–G). Gill I with lamellate upper portion, margin serrated, lower portion divided into multiple filaments (Fig. 7C). Gill II expanded to form broad leaf-like lamella (Fig. 7D). Gills III-V with multiple branching filaments (Fig. 7E, F). Gill VI tiny, unbranched (Fig. 7G). Posterolateral projections of abdominal segments VII–IX broad, apex pointed. Caudal filaments small, retractile, short, feathered.

Subimago and Imago. Unknown.

Etymology. The name *carinatum* (Latin for carinate or keeled), refers to the prominent keels or ridge-like mesonotal convexity of the species.

Mitochondrial COI sequence analysis

The partial sequences of the mitochondrial COI gene (658 bp) of three species found in Thailand were analysed to investigate species delineation. Ten specimens of *Prosopistoma* were examined. In this study, we used *Baetisca laurentina* from GenBank (HM902945 and KR144660) as the outgroup since Baetiscidae is the sister family of Prosopistomatidae (Ogden et al. 2009). The consensus phylogenetic tree of ML analysis is shown in Figure 11. The tree clearly showed a monophyletic clade for the new species *(P. carinatum* sp. n.). Clade 2 includes *P. annamense* and *P. sinense*. The interspecific genetic distance ranged from 31 to 35% among the investigated species (Table 2).

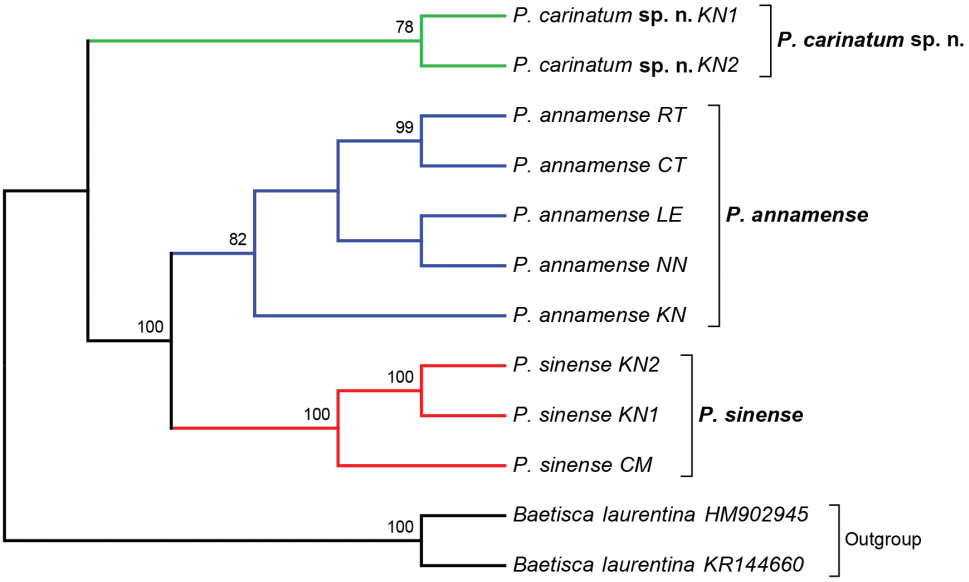

Figure 11. Consensus phylogenetic tree based on the maximum likelihood (ML) analysis of three Thai *Prosopistoma* species (the best model: T92 +G, parameter = 0.2619). The bootstrap consensus tree inferred from 1,000 replicates. Values above the branches are ML bootstrap values (> 70%). *Baetisca laurentina* from GenBank was used as the outgroup. There were a total of 658 positions in the final dataset. Abbreviations are the same as those found in Table 1.

Discussion

The molecular analysis revealed that *Prosopistoma carinatum* sp. n. is clearly separated from the other species. The molecular analysis suggests the morphological distinction between the three species. Morphologically, the new species differs from the two previously known species (*P. annamense* and *P. sinense*) by (i) longitudinal line ridges on the carapace, (ii) a strongly convex carapace, (iii) the sternal plate, (iv) the scale-like structures on the carapace, (v) 7-segmented antennae and (vi) nine pectinate setae on the ventral margin of the fore-tibiae. The larvae of *P. annamense* and *P. sinense* were placed in the same clade, and they share the characteristics of 5-segmented antenna and a smooth carapace. Moreover, the sternal plate of *P. annamense* and *P. sinense* has smooth surface (Figs 3A, 5A), while in *P. carinatum* sp. n. it bears distinctive scale-like structures (Fig. 8D–F). SEM examination on the carapace of the new species reveals a covering of circular scale-like structures scattered over the surface (Fig. 9E, 9F). The cuticle patterns of carapace of *P. annamense* is quite similar to *P. sinense* (Figs 2A–D, 4A–D), which are smoother than in the new species.

A comparison of the larvae of all Thai species is shown in Table 2. The irregular (zig-zag) pattern which occur on the carapace of *P. carinatum* sp. n. can also be found in *P. annamense* and *P. leftincki*. The comparison between the new species and other known Oriental species indicates close morphological similarity between *P. carinatum*

sp. n. and *P. someshwarensis* (from India) in terms of the presence of a longitudinal line that looks like a ridge (Roopa et al. 2017). However, the new species can be easily distinguished by its two distinct longitudinal ridges.

Ecology

The beetle-like mayfly larvae *Prosopistoma* inhabit shallow water under small stones in streams with a moderate to rapid current (Soldán and Braasch 1984, Sartori and Gattolliat 2003, Shi and Tong 2013). It is well documented that Prosopistomatidae are sensitive to pollution (Barber-James 2010). In this study, the habitats of the larvae were generally located in undisturbed upstream sites (forest streams), except *P. annamense*, which could be found in both disturbed and undisturbed sites. In addition, the larvae of *P. annamense* were also found in large rivers, including in the large urban river Xiangjiang in China (Yam 2015). In general, the larvae of *Prosopistoma* are rarely collected. In this study, most of the larvae were found from February through April in streams, with the exception of the southern region, in which they were found in July. *Prosopistoma*

Figure 13. Rearing chamber of *Prosopistoma annamense* larva.

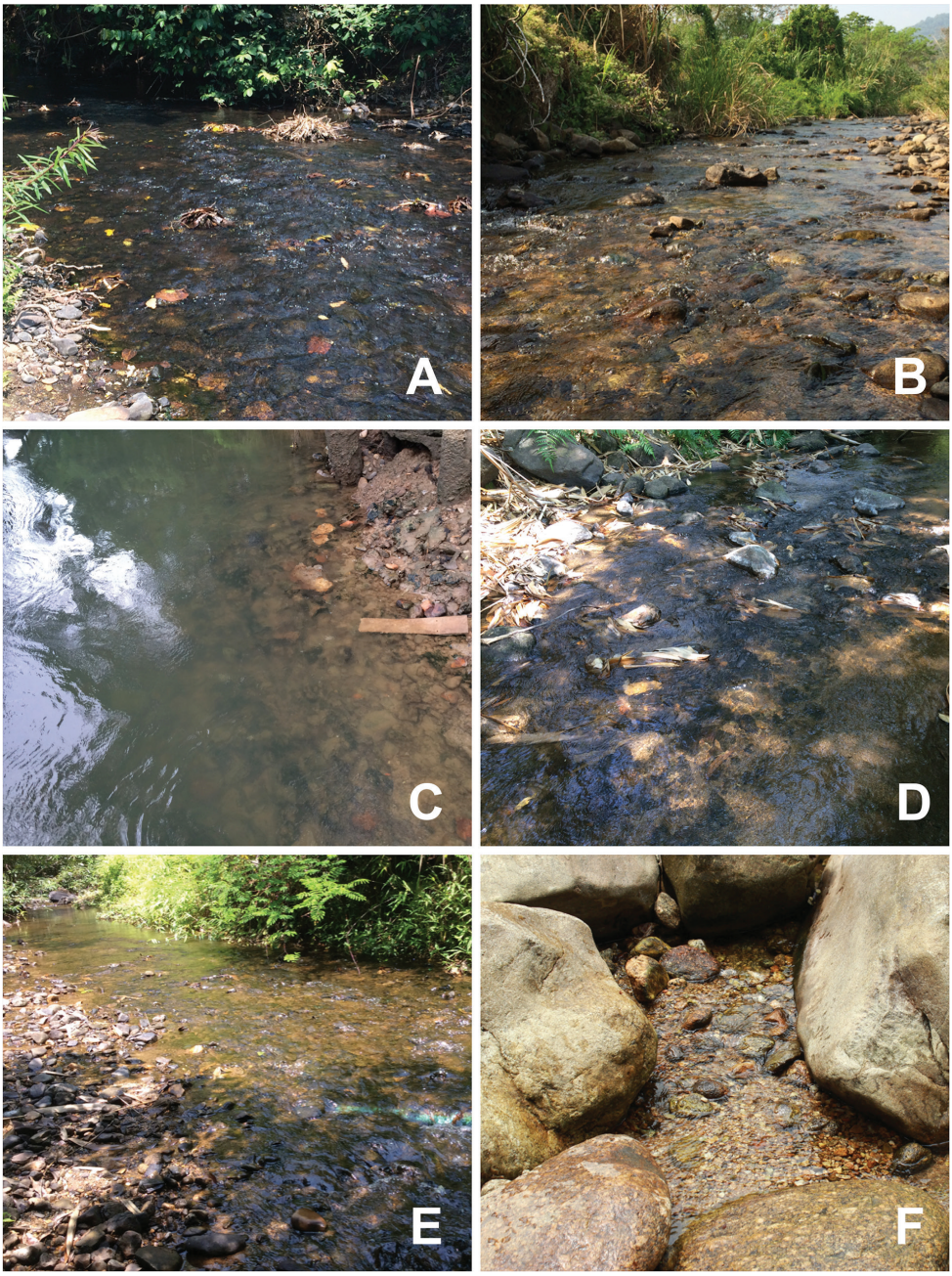

Figure 12. Habitats of *Prosopistoma* larvae: **A–C** *P. annamense* **A** = Loei province **B** = Nakhon Nayok province **C** = Kanchanaburi province (Khwae Noi River) **D** *P. sinense* (Kanchanaburi province) **E–F** *P. carinatum* sp. n. **E** = Kanchanaburi province **F** = Nakhon Si (Thammarat province).

annamense larvae were found in October in large rivers. The ecological aspects of Thai *Prosopistoma*, such as microhabitat, feeding, life history and season of larval maturity, should be explored in more detail. In this study, the larvae *P. annamense* were reared in an earthenware pot with aquatic plants without an extra air supply (Fig. 13). Under these conditions, the larvae can grow to maturity and survive for approximately one month. However, the fully-grown larvae did not moult to the subimaginal stage.

In Thailand, the Isthmus of the Kra region is a widely recognised as a biogeographic boundary (Hughes et al. 2003, de Bruyn et al. 2005, Jantarit et al. 2013). The distribution of the Prosopistomatidae in Thailand is shown in Figure 14. *Prosopistoma sinense*, which belongs to the '*P. variegatum*' clade (Barber-James 2009), is distributed only in the north and west of Thailand, whereas *P. annamense* is widely spread through northeast, central, and west Thailand. However, neither *P. annamense* nor *P. sinense* were found on the other side of the isthmus. The distribution of *P. carinatum* sp. n. seems to overlap the isthmus region, and this species apparently falls into the '*African*' clade. Barber-James (2009) examined the distribution of *P. wouterae* and suggested

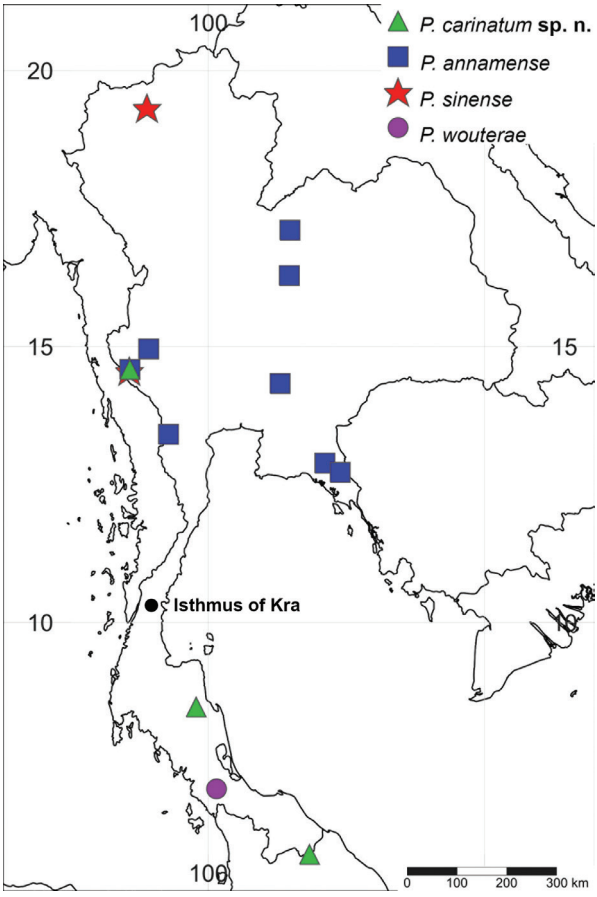

Figure 14. Distribution map of the four known Thai *Prosopistoma* species.

that there was a more recent dispersal from the Sunda Islands of this species after the sea level dropped. *Prosopistoma wouterae* seems to be restricted to the south of the Isthmus of Kra.

Acknowledgements

This research has been supported by the Centre of Excellence on Biodiversity (BDC) Office of Higher Education Commission (BDC-PG2-161004). We are most grateful to our colleagues for assistance during field trips. The authors would like thank the subject editor, Dr Helen Barber-James, and Dr Frederico Salles for their comments on the manuscript. We would also like to thank the Department of Zoology and the Faculty of Science at Kasetsart University in Bangkok for their assistance and use of their facilities.

References

Balachandran C, Anbalagan S, Kannan M, Dinakaran S, Krishnan M (2016) A new species of *Prosopistoma* Latreille, 1833 (Ephemeroptera: Prosopistomatidae) from South India. Zootaxa 4178(2): 289–294. https://doi.org/10.11646/zootaxa.4178.2.7

Barber-James HM (2009) A preliminary phylogeny of Prosopistomatidae (Ephemeroptera) based on morphological characters of the larvae, and an assessment of their distribution. Aquatic Insects 31: 149–166. https://doi.org/10.1080/01650420903020502

Barber-James HM (2010) Two new species of Prosopistomatidae (Ephemeroptera) from South Africa and Swaziland. African Entomology 18(1): 147–165. https://doi.org/10.4001/003.018.0112

Barber-James HM, Gattolliat JL, Sartori M, Hubbard MD (2008) Global diversity of mayflies (Ephemeroptera, Insecta) in freshwater. Hydrobiologia 595: 339–350. https://doi.org/10.1007/s10750-007-9028-y

De Bruyn M, Nugroho E, Hossain MM, Wilson JC, Mather PB (2005) Phylogeographic evidence for the existence of an ancient biogeographic barrier: the Isthmus of Kra Seaway. Heredity 94(3): 370–378. https://doi.org/10.1038/sj.hdy.6800613

Folmer O, Black M, Hoeh W, Lutz R, Vrijenhoek R (1994) DNA primers for amplification of mitochondrial cytochrome c oxidase subunit I from diverse metazoan invertebrates. Molecular Marine Biology and Biotechnology 3(5): 294–299.

Gattolliat JC, Cavallo E, Vuataz L, Sartori M (2015) DNA barcoding of Corsican mayflies (Ephemeroptera) with implications on biogeography, systematics and biodiversity. Arthropod Systematics & Phylogeny 73(1): 3–18. http://www.senckenberg.de/files/content/forschung/publikationen/arthropodsystematics/asp_73_1/01_asp_73_1_gattolliat_3-18.pdf

Hughes JB, Round PD, Woodruff DS (2003) The Indochinese–Sundaic faunal transition at the Isthmus of Kra: an analysis of resident forest bird species distributions. Journal of Biogeography 30: 569–580. https://doi.org/10.1046/j.1365-2699.2003.00847.x

Jantarit S, Satasook C, Deharveng L (2013) The genus *Cyphoderopsis* Carpenter (Collembola: Paronellidae) in Thailand and a faunal transition at the Isthmus of Kra in Troglopedetinae. Zootaxa 3721(1): 49–70. https://doi.org/10.11646/zootaxa.3721.1.2

Kumar S, Stecher G, Tamura K (2016) MEGA7: Molecular Evolutionary Genetics Analysis version 7.0 for bigger datasets. Molecular Biology and Evolution 33: 1870–1874. https://doi.org/10.1093/molbev/msw054

Lafon J (1952) Note sur *Prosopistoma foliaceum* Fourc. (Ephémoroptère). Bulletin de la Société Zoologique de France 77(5–6): 425–436.

Latreille M (1833) Description d'un nouveau genre de crustacés. Annales du Museum National, Paris 2: 23–34.

Lieftinck MA (1932) A new species of *Prosopistoma* from the Malay Archipelago (Ephemeroptera). Tijdschrift voor Entomologie (supplement) 75: 44–55.

Ogden TH, Whiting MF (2005) Phylogeny of Ephemeroptera (mayflies) based on molecular evidence. Molecular Phylogenetics and Evolution 37: 625–643. https://doi.org/10.1016/j.ympev.2005.08.008

Peters WL (1967) New species of *Prosopistoma* from the Oriental Region (Prosopistomatidae: Ephemeroptera). Tijdschrift voor Entomologie 110: 207–222.

Sartori M, Gattolliat JL (2003) First record and new species of the genus *Prosopistoma* Latreille, 1833 (Ephemeroptera, Prosopistomatidae) from Borneo (East Kalimantan, Indonesia). Mitteilungen der Schweizerischen Entomologischen Gesellschaft 76: 301–305.

Parnrong S, Buathong M, Sites RW (2002) New records of Behningiidae, Potamanthidae, and Prosopistomatidae (Ephemeroptera) from Thailand. ScienceAsia 28: 407–409.

Peters WL (1967) New species of *Prosopistoma* from the Oriental Region (Prosopistomatoidea: Ephemeroptera). Tijdschrift voor Entomologie 110: 207–222.

Roopa SR, Selvakumar C, Subramanian KA, Sivaramakrishnan KG (2017) A new species of *Prosopistoma* Latreille, 1833 and redescription of *P. indicum* Peters, 1967 (Ephemeroptera: Prosopistomatidae) from the Western Ghats, India. Zootaxa 4242(3): 591–599. https://doi.org/10.11646/zootaxa.4242.3.10

Shi W, Tong X (2013) A new species of *Prosopistoma (*Ephemeroptera: Prosopistomatidae) from China with a key to Oriental species. Zootaxa 3718: 89–096. https://doi.org/10.11646/zootaxa.3718.1.8

Soldán T, Braasch D (1984) Two new species of the genus *Prosopistoma* (Ephemeroptera: Prosopistomatidae) from Vietnam. Acta Entomologica Bohemoslovaca 81: 370–376.

Tong XL, Dudgeon D (2000) A new species of *Prosopistoma* from China (Ephemeroptera: Prosopistomatidae). Aquatic Insects 22: 122–128. https://doi.org/10.1076/0165-0424(200004)22:2;1-p;ft122

Tungpairojwong N, Boonsoong B (2011) New records of *Isonychia formosana*, *Prosopistoma annamense* and *Prosopistoma sinense* (Ephemeroptera) from Thailand. Ecological Research 41(2): 66–69. https://doi.org/10.1111/j.1748-5967.2011.00317.x

Yam RSW (2015) First record of the genus *Prosopistoma* Latreille, 1833 (Ephemeroptera, Prosopistomatidae) in Taiwan. ZooKeys 473: 147–156. https://doi.org/10.3897/zookeys.473.8787

Zhou CF, Zheng LY (2004) The genus *Prosopistoma* from China, with descriptions of two new species (Ephemeroptera: Prosopistomatidae). Aquatic Insects 26: 3–8. https://doi.org/10.1076/aqin.26.1.3.35375

ZooKeys 825: 145–152 (2019)
doi: 10.3897/zookeys.825.21872
http://zookeys.pensoft.net

RESEARCH ARTICLE

A peer-reviewed open-access journal
ZooKeys
Launched to accelerate biodiversity research

Redescription of *Arcifrons arcifrontalis* Ding & Yang, 1986 (Hemiptera, Fulgoromorpha, Delphacidae)

Hong-Xing Li[1,2], Lin Yang[1,2], Xiang-Sheng Chen[1,2]

1 *Institute of Entomology, Guizhou University, Guiyang, Guizhou, 550025, China* **2** *The Provincial Special Key Laboratory for Development and Utilization of Insect Resources, Guizhou University, Guiyang, Guizhou, 550025, China*

Corresponding author: *Xiang-Sheng Chen* (chenxs3218@163.com)

Academic editor: Mike Wilson | Received 26 October 2017 | Accepted 16 January 2018 | Published 27 February 2019

http://zoobank.org/0FF4E7A1-1C9E-4A95-95A2-19E7F69F9D4B

Citation: Li H-X, Yang L, Chen X-S (2019) Redescription of *Arcifrons arcifrontalis* Ding & Yang, 1986 (Hemiptera, Fulgoromorpha, Delphacidae). ZooKeys 825: 145–152. https://doi.org/10.3897/zookeys.825.21872

Abstract

The male of *Arcifrons arcifrontalis* Ding & Yang, 1986 (Hemiptera, Fulgoroidea, Delphacidae, Tropidocephalini) is redescribed. The female genitalia of the species here, is described and illustrated for the first time. The geographic distribution of the species and images of adult habitus are provided.

Keywords

Bamboo planthopper, distribution, female genitalia, Fulgoroidea, Homoptera, taxonomy

Introduction

The bamboo-feeding planthopper genus *Arcifrons* (Hemiptera, Fulgoromorpha, Delphacidae, Delphacinae, Tropidocephalini) (type species: *A. arcifrontalis* Ding & Yang, 1986), was established by Ding and Yang (1986). Until now, of only one described species in the genus, from China and with reported plant associations feed on bamboo (Ding and Yang 1986; Ding 2006). Members always collected on the genus *Phyllostachys* of bamboo in Yunnan Province, China (Ding 2006; this paper). This species was described and illustrated by the original authors, with the same illustrations recycled in Ding (2006). However, identification of species may be difficult because original species descriptions are inadequate in that many features are not evaluated

Copyright *Hong-Xing Li et al.* This is an open access article distributed under the terms of the Creative Commons Attribution License (CC BY 4.0), which permits unrestricted use, distribution, and reproduction in any medium, provided the original author and source are credited.

and included, especially the male genitalia. So it is necessary to add other more valid characters.

Herein, based on specimens of *A. arcifrontalis* collected from Yunnan Province, China by Chen and Yang in 15 August 2015, Li, Luo and Yang in 18 August 2018, we review the species, the male is redescribed and of the female genitalia is described and illustrated for the first time. The geographic distribution and images of adult habitus are given.

Material and methods

The morphological terminology and measurements follow Yang and Yang (1986) and the morphological terminology of female genitalia follows Bourgoin (1993). Body length was measured from apex of vertex to tip of tegmina. Dry male specimens were used for the description and illustrations. External morphology was observed under a stereoscopic microscope and characters were measured with an ocular micrometer. Color pictures for adult habitus were obtained by KEYENCE VHX-1000 system. Images of adult habitus were obtained by Canon Digital Camera EOS 5Ds. The genital segments of the examined specimens were macerated in 10% KOH and drawn from preparations in glycerin jelly using a Leica MZ 12.5 stereomicroscope. Illustrations were scanned with Canon CanoScan LiDE 200 and imported into Adobe Photoshop 6.0 for labeling and plate composition.

Specimens examined are deposited in the Institute of Entomology, Guizhou University, Guiyang, China (**IEGU**).

Taxonomy

Arcifrons Ding & Yang, 1986

Arcifrons: Ding and Yang 1986: 421; Ding 2006: 124.

Type species. *Arcifrons arcifrontalis* Ding & Yang, 1986, by original designation.

Differential diagnosis. The genus is readily distinguished from other genera in the tribe Tropidocephalini by the following features: frons distinctly sharply pointed at apex in dorsal view (Figs 1, 3, 5) and distinctly inclined anteriorly in lateral view (Figs 2, 4, 7), with median carina distinctly developed (Fig. 6); postclypeus with median carina distinct (Fig. 6).

Description. The distinctive characters used by Ding (2006) are modified as follows.

Head and thorax. Head including eyes narrower than pronotum. Vertex broad transversely, with basal compartment near trapezoidal (Fig. 5). Frons elongate, rectangular, longer in middle line than wide at widest part, lateral carinae subparallel, median carina distinctly developed, forked at base (Fig. 6), with distinctly sharply pointed at

Figures 1–4. *Arcifrons arcifrontalis* Ding & Yang, 1986. **1** male habitus, dorsal view **2** the same, lateral view **3** female habitus, dorsal view **4** the same, lateral view. Scale bars: 0.5 mm.

apex in dorsal view (Fig. 5) and distinctly inclined anteriorly in lateral view, with apical margin roundly convex (Fig. 7). Postclypeus with median carina distinct, lateral carinae absent, width at base slightly wider than frons at apex. Antennae short, cylindrical, reaching to frontoclypeal suture, with basal segment with length longer than width, shorter than second segment (Fig. 6). Pronotum longer than vertex, tricarinae distinct, lateral carinae reaching hind margin, with base curved inward, with posterior apex more closed anterior apex of lateral carinae of mesonotum. Mesonotum developed, tricarinae distinct, median carina complete, reaching tip of scutellum, lateral carinae reaching hind margin (Fig. 5). Spinal formula of hind leg 5-6-4. Hind tibiae with a lateral tooth basally and medially respectively. Post-tibial spur without teeth along hind margin, but with a small apical tooth, with inner side surface concave.

Male genitalia. Anal segment (Fig. 9) ring-like. Pygofer with ventral margin longer than dorsal margin in lateral view (Fig. 10), mediovental processes distinct (Fig. 9). Aedeagus (Fig. 11) with phallobase distinct. Genital styles (Figs 12, 13) simple, long.

Host plants. Bamboo.

Distribution. Oriental Region (China).

Remarks. This genus is similar to *Arcofaciella* Fennah, 1956 but differs from it by: frons with median carina distinctly developed, with lateral carinae subparallel (frons with median carina not delveloped, with lateral carinae arched in *Arcofaciella*); postclypeus with median carina developed (postclypeus with median carina absent in *Arcofaciella*); spinal formula of hind leg 5-6-4 (spinal formula of hind leg 5-8-5 or 5-9-5 in *Arcofaciella*); anal segment of male with two processes large and lamellate (anal segment of male with two processes short and spinous in *Arcofaciella*).

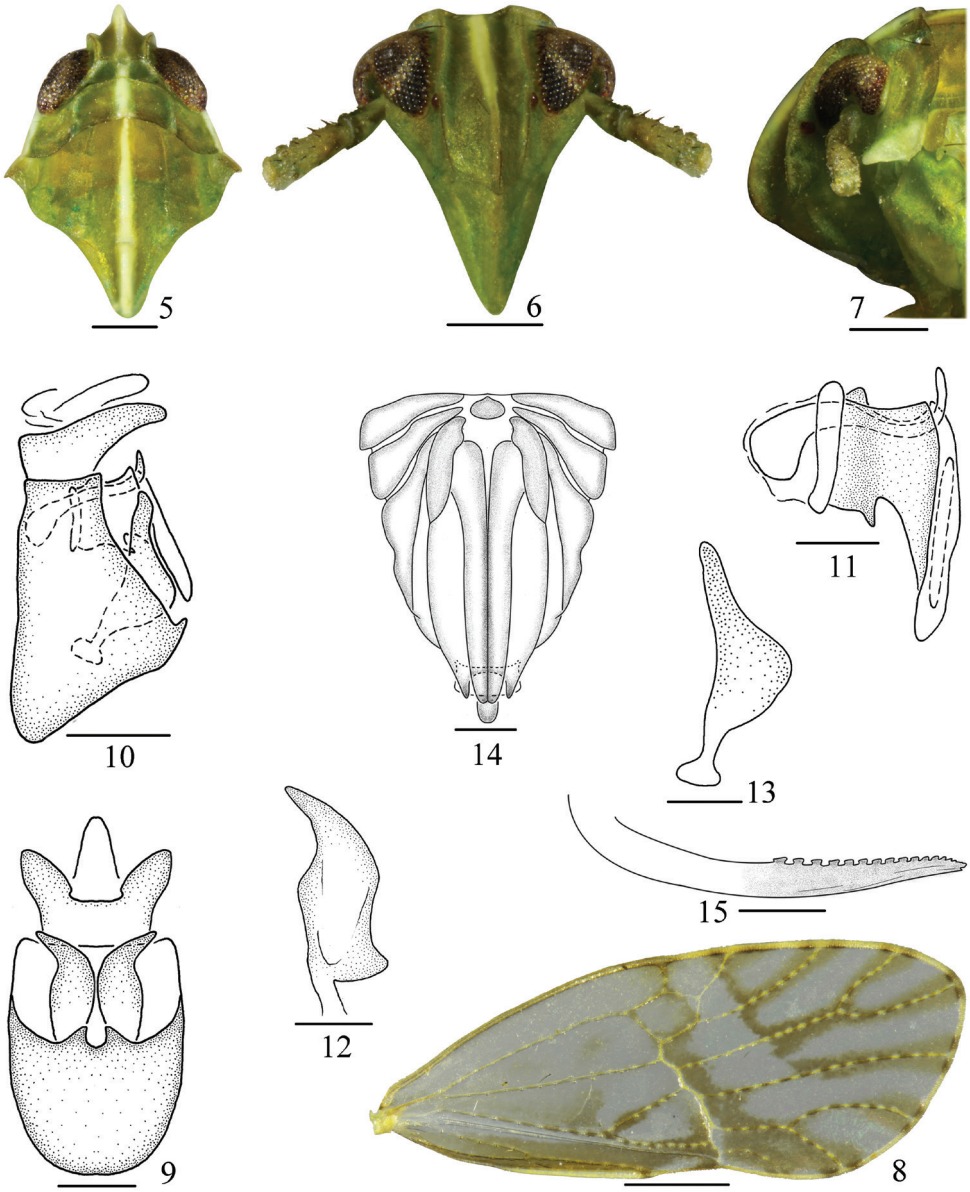

Figures 5–15. *Arcifrons arcifrontalis* Ding & Yang, 1986. **5** head and throad, dorsal view **6** frons and clypeus **7** the same, lateral view **8** tegmen **9** male genitalia, posterior view **10** the same, lateral view **11** aedeagus **12** genital style, posterior view **13** the same, left lateral view **14** female genitalia, posterior view **15** gonapophysis IX. Scale bars: 0.2 mm (**5–10, 14, 15**); 0.1 mm (**11–13**).

This genus is also similar to *Mucillnata* Qin & Zhang, 2010 but differs from it by: frons distinctly inclined anteriorly in lateral view (frons not distinctly inclined anteriorly in lateral view in *Mucillnata*); lateral carinae of the pronotum not diverging and attaining the hind margin (lateral carinae of the pronotum diverging and not at-

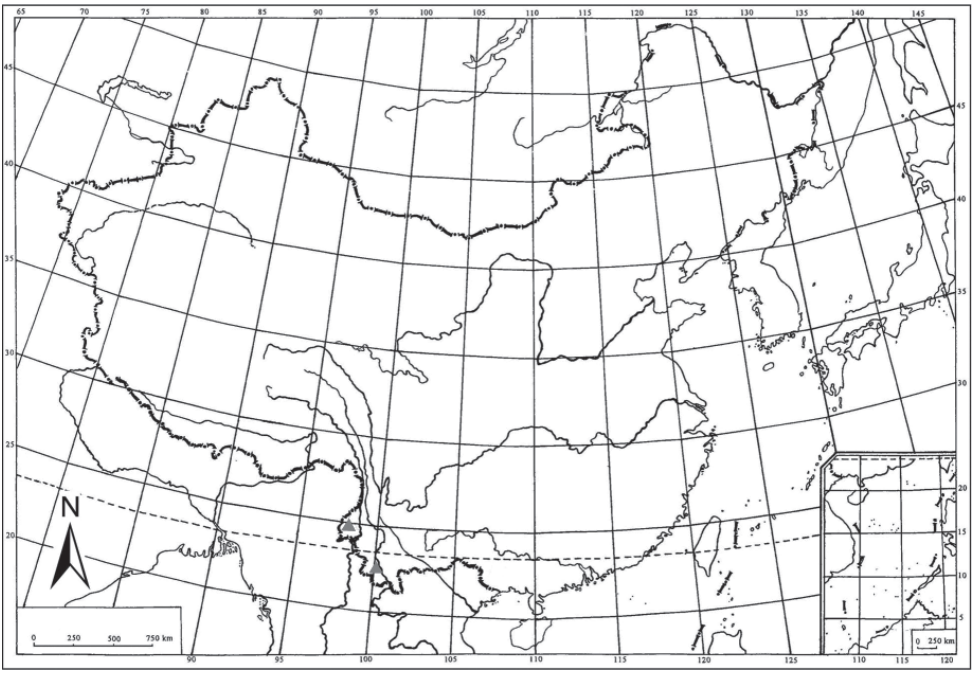

Figure 16. Geographic distribution of *Arcifrons arcifrontalis* Ding & Yang, 1986 in China (black triangle).

taining the hind margin in *Mucillnata*); pygofer of male with ventral margin with two processes (pygofer of male with a medioventral process in *Mucillnata*); anal segment of male with two lateral processes (anal segment of male with single process on the caudoventral margin on right side in *Mucillnata*).

Arcifrons arcifrontalis Ding & Yang, 1986

Figures 1–15, 17, 18

Arcifrons arcifrontalis: Ding and Yang 1986: 421; Ding 2006: 124.

Specimens examined. 17♂♂, 20♀♀, **China:** Yunnan, Yingjiang County (24°44N, 97°33E), on bamboo, 15 August 2015, Xiang-Sheng Chen and Lin Yang; 12♂♂, 18♀♀, Yunnan, Yingjiang County, on bamboo, 18 August 2018, Hong-Xing Li, Qiang Luo and Liang-Jing Yang.

Measurements. Body length (from apex of vertex to tip of tegmina): male 3.2–3.5 mm (N = 17); female 3.4–3.8 mm (N = 20); tegmen length: male 2.7–3.0 mm (N = 17); female 2.8–3.3 mm (N = 20).

Coloration. General color yellowish green (Figs 1–4). In dorsal view, a white large longitudinal stripe along median line from basal half of frons to the end of mesonotum (Fig. 5). Rostrum with apex dark brown. Eyes yellowish brown to blackish brown.

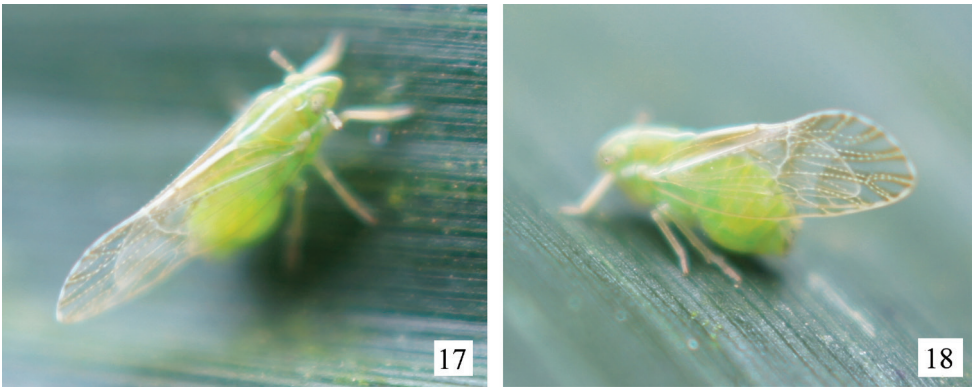

Figures 17, 18. Adult of *Arcifrons arcifrontalis* Ding & Yang, 1986 resting on leaf of bamboo. Photographed by Xiang-Sheng Chen.

Ocelli reddish brown. Pronotum with a white longitudinal band along lateral margin (Fig. 5). Tegulae yellowish white. Tegmina with white spots along longitudinal veins in apical half, along transverse vein and apical veins bordered yellowish brown stripes as figured (Fig. 8). Wings hyaline, with veins brown.

Head and thorax. Ratio width of vertex at base to length 2.9–3.2, to width at apex 1.3–1.5, lateral margin slightly keeled, Y-shaped carina distinct (Fig. 5). Frons with ratio length to width 1.5–1.8, the widest at near ocelli. Ratio length of rostrum to width 7.4–7.6. Basal segment of antennae with ratio length to width 1.3–1.6, to length of second segment 0.5–0.6 (Fig. 6). Pronotum with ratio length in midline to length of vertex 2.2–2.4, anterior margin straight, posterior margin concave. Mesonotum in midline 3.5–3.8 times longer than pronotum, 2.4–2.7 times longer than vertex and pronotum combined (Fig. 5). Tegmina (Fig. 8) amply exceeding the tip of abdomen, 2.5 times longer than wide, with apical margin broadly rounded; Sc+R and M with common petiole at base, and forked before midline; Sc and R with two branches respectively; M with three branches at apical, M_1 fused with Rs basally, and M_3 fused with Cu_1a basally; Cu with three branches; A with two branches fused at apical half.

Male genitalia. Anal segment short, with inverse collar-shaped in posterior view, with lateral processes large and lamellate, apical margin roundly convex (Fig. 9). Pygofer with mediovental processes paired, finger-like, directed each other, opening oval, longer than wide, with ratio length to width 1.5 (Fig. 9), in profile with dorsal margin longer than ventral margin (Fig. 10). Aedeagus (Fig. 11) with phallobase distinct. Phallus tubular, with basal third exceeding the phallobase cephalad, and with apical fifth exceeding phallobase caudad, directed dorsad. Phallobase with apical two thirds narrowing apically, directed ventrad, dorsal margin with a stout tooth-like process at base and ventral margin with another small tooth-like process at basal third, in posterior view ring-like, opening narrow. Genital styles in profile (Fig. 13) with ventral margin distinctly convex, and with dorsal margin slightly concave, in posterior view (Fig. 12) moderately long, flake-shaped, broad at middle, apex acute, reaching the base of anal segment.

Female genitalia. Anal style exceeded pygofer. Pygofer with gonocoxa VIII moderately large, basal third with inner lateral margin sinuate. Ovipositor longer than pygofer. Gonangulum small, with width wider than length, basal margin subangular convex in the middle, apical margin slightly convex, separated from gonocoxa VIII. Gonoplacs elongate, sword-like, with apex beyond apical margin of pygofer (Fig. 14). Gonapophyses IX (Fig. 15) slender, gradually narrowed apically, apex sharp, dorsal margin with apical half serrated.

Host plant. Bamboo (*Phyllostachys* sp.).

Distribution. Southwest China (Yunnan Province) (Fig. 16).

Discussion

The discovery of the species broadens our knowledge of the morphology and biogeography of the genus. Species of *Arcifrons* feed exclusively on bamboo and occur in Yunnan, China. This may be due to the climate warm and humid, subtropical monsoon climate of Yunnan, with minimal temperature changes. Members are collected on leaves of the genus *Phyllostachys* of bamboo. The genus *Phyllostachys*, with at least 51 species, has the highest species density in China (49 species). Many of the species are found in central and southern China (Wang and Stapleton 2006). Therefore, species of *Arcifrons* may be more widely distributed in China than hitherto reported, and that there may be many undescribed species in this genus. *Arcifrons arcifrontalis* Ding & Yang is of economic significance since the species has large population in the bamboo fields.

Acknowledgments

The authors are grateful to collectors for collecting specimens. We also wish to express our sincere thanks to Prof. J.C. Xin (Institute of Entomology, Guizhou University, China) for helpful suggestions on the revision of the early draft of the manuscript. This work is supported by the National Natural Science Foundation of China (No. 31472033, 31160163), the Program of Science and Technology Innovation Talents Team, Guizhou Province (No. 20144001), and the Program of Excellent Innovation Talents, Guizhou Province (No. 20154021).

References

Bourgoin T (1993) Female genitalia in Hemiptera Fulgoromorpha, morphological and phylogenetic data. Annales de la Société Entomologique France 29(3): 225–244.

Ding JH, Yang LF, Hu CL (1986) Descriptions of new genera and species of Delphacidae attacking bamboo from Yunnan Province, China. Acta Entomologische Sinica 29(4): 415–425. https://doi.org/10.16380/j.kcxb.1986.04.016

Ding JH (2006) Fauna Sinica. Insecta Vol. 45. Homoptera Delphacidae. Science Press, Beijing, 776 pp.

Liang AP, Guo MJ (2004) Discovery of the genus *Arcofaciella* Fennah (Hemiptera: Fulgoroidea: Delphacidae) in mainland China. Journal of the New York. Entomological Society 112(4): 221–226. https://doi.org/10.1664/0028-7199(2004)112[0221:DOTGAF]2.0.CO;2

Qin DZ, Zhang YL (2010) A key to the genera of Tropidocephalini (Hemiptera: Fulgoromorpha: Delphacidae) of China with description of *Mucillnata rava*, new genus and species. Zootaxa 2448: 61–68. https://doi.org/10.11646/zootaxa.2448.1.5

Wang ZP, Stapleton C (2006) *Phyllostachys* Siebold & Zuccarini. In: Wu ZY, Raven PH, Hong DY (Eds) Flora of China, Vol. 22 (Poaceae). Science Press, Beijing, and Missouri Botanical Garden Press, St Louis, Missouri, 163–180.

Yang JT, Yang CT (1986) Delphacidae of Taiwan (I) Asiracinae and the tribe Tropidocephalini (Homoptera: Fulgoroidea). Taiwan Museum Special Publication 6: 1–79.